IN VITRO MODELS FOR THE ASSESSMENT OF SKIN XENOBIOTIC METABOLISM

A thesis submitted in accordance with the conditions governing candidates for the degree of

DOCTOR OF PHILOSOPHY

To the University of Newcastle Upon Tyne

by

Christopher Jewell

B.Sc. (Hons) Chemistry (Glamorgan University, 1991)
M.Sc. Toxicology (Birmingham University, 1992)

1996

Department of Environmental and
Occupational Medicine,
The Medical School,
Framlington Place,
University of Newcastle Upon Tyne.
Newcastle Upon Tyne.
NE2 4HH.

Certificate

I hereby certify that the work embodied in this thesis is the result of my own investigations, except where reference has been made to published literature.

Signed C Jewell Candidate

Signed Director of Studies

Declaration

I hereby delare that this work has not already been accepted in any substance for any degree and is not concurrently submitted in canditure for any degree.

Signed C Jewell Candidate

Abstract

Skin subcellular fractions, keratinocytes, living skin equivalents (LSE) and percutaneous absorption using diffusion cells were examined as *in vitro* models for assessment of skin xenobiotic metabolism. Cytochrome P450 monooxygenase, esterase and glutathione-S-transferase (GST) activities were investigated in rodent, pig and human skin.

CYP1A1 activity was detected in rat and pig skin microsomes by ethoxyresorufin-*O*-deethylation. CYP2B activity was detected in rat skin microsomes by pentoxyresorufin-*O*-dependentylation. Neither were detected in human skin microsomes. Rat keratinocytes lost cytochrome P450 activity within several hours of being isolated from skin, and were not reliably induced following exposure to ß-naphthoflavone. Cytochrome P450 activities were detected in the LSE after induction by 3-methylcholanthrene.

Carboxylesterase activity was detected in skin, keratinocytes, and the LSE using 4-methylumbelliferyl heptanoate as the substrate. Induction of caboxylesterase activity by 3-methylcholanthrene was shown in the LSE but not keratinocytes. GST activity was shown in skin and keratinocytes, but induction was only shown in the LSE. The ability to induce xenobiotic metabolising activity suggests that enzyme induction may be linked to cell differentiation.

GST's were localised at the basal layer of the epidermis. During percutaneous absorption, DNCB was metabolised to the glutathione (GSH) conjugate, limited by the GSH available in the skin. GSH conjugation of DNCB is thought to be a detoxification pathway preventing the immune response illicited by DNCB.

Studies investigating the effect of age of rat on dermal xenobiotic metabolism revealed no differences between the neonate and mature rat with respect to cytochrome P450 monooxygenase activity or esterase activity. However, neonatal rat skin showed five fold lower GST activity and three fold higher reduced GSH levels.

Pig skin showed similar levels of xenobiotic metabolising activity to human skin and showed a similar metabolic profile for DNCB during percutaneous absorption, supporting its use as a better model for human than rodent skin. The LSE was a good model for studies of human dermal xenobiotic metabolism particularly with the influence of inducing agents.

Table of Contents

page

Title page .. 1
Certificate .. 2
Abstract .. 3
Table of contents .. 4
List of Figures .. 14
List of Tables .. 15
List of graphs .. 18
List of Plates .. 20
Acknowledgements .. 21
Abbreviations .. 22

Section 1 General Introduction

Chapter 1 The structure of skin

1.1 Introduction .. 23
1.2 Epidermis .. 23
1.3 Cells of the epidermis .. 27
1.4 Dermis .. 28
1.5 Cells of the dermis .. 28
1.6 Skin appendages .. 29
1.7 Species and site variables .. 29
1.8 An introduction to skin immunology .. 30

Chapter 2 Skin metabolism

2.1 Introduction .. 33
2.2 Phase I metabolism .. 33
a) Cytochrome P-450 monooxygenases .. 34
b) Esterases .. 37
c) Other phase I reactions .. 39
2.3 Phase II metabolism .. 39
a) Glutathione conjugation .. 39
b) Other conjugating reactions .. 43
2.4 Factors affecting xenobiotic metabolism .. 43
a) Species .. 43
b) Gender .. 44

page

c) Age 44
d) Inhibitors 45
e) Inducers 46

Chapter 3 Percutaneous absorption

3.1 Introduction 48
3.2 The barrier functions of the skin 48
3.3 Mechanisms of percutaneous absorption 49
3.4 Factors affecting percutaneous absorption 50

Chapter 4 Methods of studying percutaneous absorption

4.1 Introduction 52
4.2 In vivo studies 52
4.3 In vitro studies 53
a) Static diffusion cells 53
b) Flow-through diffusion cells 54
4.4 Diffusion cell conciderations 55
a) Receptor fluid 55
b) Skin viability 56
c) Skin storage 56
d) Preperation of skin for diffusion cells 57
e) Washing-in effect 57
f) Animal models 57

Chapter 5 Xenobiotic metabolism during percutaneous absorption

5.1 Introduction 59
5.2 In vivo percutaneous absorption and metabolism studies .. 59
5.3 In vitro percutaneous absorption and metabolism studies .. 59

Chapter 6 Keratinocytes and keratinocyte metabolism

6.1 Introduction 63
6.2 The development of keratinocyte cell culture 63
6.3 Isolation of keratinocytes 65
6.4 Factors influencing keratinocyte growth in culture 65

page

6.5 Keratinocyte metabolism in vitro 69
a) Cytochrome P450 monooxygenases 69
b) Esterases 71
c) Glutathione-S-transferases 71
d) Other enzyme reactions 72
6.6 Applications for cultured keratinocytes 72

Chapter 7 *Living skin equivalents*

7.1 Introduction 74
7.2 Epidermal differentiation 74
7.3 Construction of a living skin equivalent 75
7.4 Percutaneous absorption studies with living skin equivalents .. 77
7.5 Metabolism in the living skin equivalent 77
7.6 Applications for living skin equivalents 78

Chapter 8 *Dinitrochlorobenzene*

8.1 Introduction 80
8.2 Metabolism of dinitrochlorobenzene 81

Chapter 9 *Aims of the project* 83

Section 2 Materials and Methods

Chapter 10 *General Methods*

10.1 Chemicals 84
10.2 Buffers and Media 87
a) KCl Phosphate buffer 87
b) Glycerol buffer 87
c) Trisma buffer 87
d) Dulbeccos phosphate buffered saline 87
e) L-15 medium 88
f) MCDB153 medium 89
g) Dulbeccos modified Eagles medium 92
h) RPMI1640 medium 93

page

10.3 Tissue preparations
a) Origin 95
b) Removal and storage 95
c) Preparation of tissue subcellular fractions 96
d) Preparation of skin for diffusion cells 97
e) Tissue histology 97

Chapter 11 Analytical methods

11.1 Bicinchoninic acid (BCA) protein assay
a) Introduction 100
b) Assay procedure 100
11.2 Cytochrome P-450 monooxygenases
a) Introduction 101
b) Alkoxyresorufin-*O*-dealkylation 102
11.3 Esterases
a) Hydrolysis of 4-methylumbelliferyl heptanoate 102
b) Assay procedure 102
11.4 Glutathione-S-transferases
a) Glutathione conjugation of DNCB 103
b) Assay procedure 103

page

Section 3 Experimental studies

Chapter 12 Studies with subcellular fractions

12.1 Introduction 105

12.2 Enzyme kinetics 105

12.3 Aims of studies with subcellular fractions 107

12.4 Cytochrome P-450 monooxygenases 107

12.4.1 Methods of preparation 107

12.4.2 Effect of age on Cytochrome P-450 monooxygenase activity in skin and liver 107

a) Methods 108

b) Results 108

12.4.3 Species differences

a) Methods 112

b) Results 112

12.4.4 Induction study 113

a) Method 113

b) Results 114

12.4.5 Discussion 118

12.5 Esterase activity 121

12.5.1 Methods 121

a) Assay for 4-methylumbelliferyl heptanoate hydrolysis .. 121

b) Effect of age on 4-methylumbelliferyl heptanoate hydrolysis 122

c) Species differences 122

d) Effect of preinduction with ß-naphthoflavone, phenobarbital and ethanol 123

e) Characterisation of the esterase involved in 4-methylumbelliferyl heptanoate hydrolysis 123

12.5.2 Results

a) Assay conditions for 4-methylumbelliferyl heptanoate hydrolysis 124

b) Effect of age on 4-methylumbelliferyl heptanoate hydrolysis 124

c) Species differences 125

d) Effect of preinduction with ß-naphthoflavone, phenobarbital and ethanol 126

e) Characterisation of the esterase involved in 4-methylumbelliferyl heptanoate hydrolysis 128

page

12.5.3 Discussion 129
12.6 Glutathione-S-transferases 132
12.6.1 Methods 132
12.6.2 Results 133
12.6.3 Discussion 135
12.7 Reduced glutathione levels in skin 136
12.7.1 Method 136
12.7.2 Results 138
12.7.3 Discussion 138

Chapter 13 Keratinocyte studies

13.1 Introduction 139
13.2 Tissue culture of human keratinocytes 139
13.2.1 Methods 139
a) Preparation of skin for tissue culture of human keratinocytes .. 139
b) Isolation of human keratinocytes 140
c) Counting cells by trypan blue exclusion 140
d) Growth of human keratinocytes 141
e) Passage of human keratinocytes 142
f) Viability of cultured human keratinocytes 142
13.2.2 Results 142
13.2.3 Discussion 144
13.3 Tissue culture of rat keratinocytes 147
13.3.1 Methods 147
a) Preparation of skin for tissue culture of rat keratinocytes .. 147
b) Isolation of rat keratinocytes 147
c) Growth of rat keratinocytes 147
13.3.2 Results 148
13.3.3 Discussion 150
13.4 Metabolism studies with keratinocytes 151
13.4.1 Methods 151
a) Cytochrome P-450 monooxygenase activity in microsomes prepared from fresh and cultured keratinocytes 151
b) Cytochrome P-450 monooxygenase activity in freshly isolated keratinocytes 151
c) Induction and inhibition of cytochrome P-450 monooxygenase activity in cultured keratinocytes 152
d) Cytochrome P-450 monooxygenase activity in freshly isolated

keratinocytes from induced rats 152
e) Esterase activity in cultured keratinocytes 153
f) Glutathione-S-transferase activity in cultured keratinocytes .. 153
g) Reduced glutathione levels in cultured keratinocytes 153
13.4.2 Results 153
a) Results for cytochrome P450 monooxygenase activity in microsomes prepared from fresh and cultured keratinocytes .. 153
b) Results for cytochrome P450 monooxygenase activity in freshly isolated keratinocytes 154
c) Results for induction and inhibition of cytochrome P450 monooxygenase activity in cultured keratinocytes 155
d) Results for cytochrome P450 monooxygenase activity in freshly isolated keratinocytes from induced rats 156
e) Results for esterase activity in cultured keratinocytes 156
f) Results for glutathione-S-transferase activity in cultured keratinocytes 156
g) Results for reduced glutathione levels in cultured keratinocytes 156
13.4.3 Discussion 157

Chapter 14 Studies with living skin equivalents

14.1 Introduction 159
14.2 Tissue culture of human and rat dermal fibroblasts 159
14.2.1 Preparation of skin for tissue culture of human and rat dermal fibroblasts 159
14.2.2 Growth of human and rat dermal fibroblasts 159
14.2.3 Passage of human dermal fibroblasts 160
14.2.4 Results 160
14.3 Metabolism studies with dermal fibroblasts 162
14.3.1 Method 162
14.3.2 Results 162
14.4 Development of a Living Skin Equivelent (LSE) 162
14.4.1 Method for growing an LSE 162
14.4.2 Results 163
14.5 Metabolism studies with LSE's 167
14.5.1 Cytochrome P450 monooxygenase, esterase and GST activity in a LSE
a) Methods 168
b) Results 169

page

14.5.2 Induction of metabolising enzymes in a LSE
a) Methods 169
b) Results 170
14.6 Discussion 170

Chapter 15 Assessment of skin viability in vitro

15.1 Introduction 172
15.2 The skin absorption systems 172
15.2.1 The flow-through diffusion cell 172
15.2.2 The flow-through diffusion cell method 172
15.2.3 The static diffusion cell system 173
15.2.4 The static diffusion cell method 173
15.3 Viability of skin in the absorption system 176
15.3.1 The MTT assay 176
15.3.2 Reduced glutathione levels in skin 176
15.3.3 Esterase activity in skin 176
15.3.4 Glutathione-S-transferase activities in skin 177
15.3.5 Results 177
15.3.6 Discussion 185
15.4 Effect of absorption cell receptor medium on GST activities .. 187
15.4.1 Method 187
15.4.2 Results 187
15.4.3 Discussion 189
15.5 Storage of skin prior to absorption studies 189
15.5.1 Method 189
15.5.2 Results 190
15.5.3 Discussion 196
15.6 Immunohistochemistry of skin 196
15.6.1 Method 196
15.6.2 Results 197
15.6.3 Discussion 201

Chapter 16 Percutaneous absorption and metabolism of dinitrochlorobenzene

16.1 Introduction 202
16.2 Separation of DNCB and it's glutathione conjugate 203
16.2.1 Method 203

16.2.2 Results 204
16.2.3 Discussion 204
16.3 Percutaneous absorption and metabolism of dinitrochlorobenzene (DNCB) through mouse skin *in vitro*
16.3.1 Method 205
16.3.2 Results 206
16.3.3 Discussion 212
16.4 Percutaneous absorption and metabolism of DNCB through mouse skin in the flow-through system under occluded conditions 214
16.4.1 Method 214
16.4.2 Results 214
16.4.3 Discussion 215
16.5 Percutaneous absorption and metabolism of DNCB through the skin of buthionine sulfoximine (BSO) pretreated mice .. 216
16.5.1 Method 216
16.5.2 Results 216
16.5.3 Discussion 219
16.6 Depletion of glutathione in mouse skin *in vitro* 220
16.6.1 Method 220
16.6.2 Results 220
16.6.3 Discussion 222
16.7 Depletion of glutathione in mouse skin by diethyl maleate (DEM) after application of DNCB *in vitro* 223
16.7.1 Method 223
16.7.2 Results 223
16.7.3 Discussion 223
16.8 Percutaneous absorption and metabolism of DNCB through the skin of neonatal rat, 26 day old rat, pig and human 224
16.8.1 Method 224
16.8.2 Results 224
16.8.3 Overall discussion of studies with DNCB 228

Section 4 General discussion.

Chapter 17 Discussion 231
Chapter 18 Future work 238

Section 5 References and Appendices.

References 240
Appendices 261

List of Figures

		Page
1.1	The structure of skin	24
1.2	The cell layers of the epidermis	25
2.1	The cytochrome P-450 catalytic cycle	35
6.1	Effect of pH on human keratinocyte cell growth	68
12.1	A typical HPLC trace of glutathione derivitised with the fluorescent agent bromobimane	137
12.2	Standard curve of glutathione concentration vs. fluorescence	137
13.1	Cells were counted by trypan blue exclusion in the circled areas	141
16.1	Thin layer chromatogram for presence of glutathione in mouse skin	204

List of tables

		page
2.1	Glutathione conjugation in skin using the substrate dinitrochlorobenzene ..	41
2.2	Glutathione-S-transferase (GST) activity in rat, mouse and human skin cytosol for several substrates	41
2.3	The relationship between glutathione-S-transferase activity in rat skin cytosol and the age of the rat	42
2.4	GST activity in epidermis, dermis and whole skin of neonatal rat	42
2.5	Effect of inducers on retanoic acid metabolism to retanol in rat skin	47
5.1	Percentage of absorbed Sudan 1, SY7 and ANSC through mouse, guinea pig and human skin after application of $5\mu g/cm^2$ to skin in the flow-through cell ..	62
6.1	The metabolism of benzo[a]pyrene and 7-ethoxyresorufin in Balb/C mouse keratinocytes and epidermis	70
6.2	Effect of degree of confluence and differentiation on GST activity in cultured human keratinocytes	71
10.1	List of chemicals used in this project	84
10.2	Dulbecco's phosphate buffered saline (D-PBS) formulation.	87
10.3	Leibovitz-15 (L-15) formulation	88
10.4	Molecular, chemical and developmental biology of the University of Colorado cell culture medium number 153 (MCDB153) formulation .. .	89
10.5	Supplements to MCDB153 medium	90
10.6	Dulbecco's minimum essential medium (DMEM) formulation	91
10.7	Rosweel Park Memmorial Institure cell culture medium number 1640 (RPMI1640) formulation	92
12.1	Recovery of microsomal protein from rat skin and liver from three age groups ..	108
12.2	Ethoxyresorufin-*O*-deethylation and pentoxyresorufin-*O*-dependentylation activities in neonatal rat skin and liver microsomes	109
12.3	Ethoxyresorufin-*O*-deethylation and pentoxyresorufin-*O*-dependentylation activities in skin and liver microsomes of 26 day old rats	109
12.4	Ethoxyresorufin-*O*-deethylation and pentoxyresorufin-*O*-dependentylation activities in skin and liver microsomes of 9-10 week old rats	109
12.5	Recoveries of microsomal protein from control and induced rats	114
12.6	The ethoxyresorufin-*O*-deethylation and pentoxyresorufin-*O*-dependentylation activities of liver and skin microsomes from rats preinduced with ß-naphthoflavone, phenobarbital and ethanol, untreated and corn oil controls ..	115
12.7	Esterase inhibitors	123
12.8	Cytosolic protein recovery from rat skin and liver from three age groups	124
12.9	4-Methylumbelliferyl heptanoate hydrolysis by skin and liver cytosolic protein for rats age 4 days, 26 days and 9-10 weeks	124

page

12.10 Rates of 4-methylumbelliferyl heptanoate hydrolysis with either skin and liver cytosol, post mitochondrial or microsomal fractions .. 125

12.11 Hydrolysis of 4-methylumbelliferyl heptanoate in individual human post mitochondrial fractions 126

12.12 Hydrolysis of 4-methylumbelliferyl heptanoate activities in Wistar rat skin and liver after treatment with inducing agents 127

12.13 Hydrolysis of 4-methylumbelliferyl heptanoate activities in Wistar rat skin and liver after treatment with inducing agents 127

12.14 Inhibition of rat skin cytosolic 4-methylumbelliferyl heptanoate hydrolysis by different esterase inhibitors 128

12.15 Inhibition of mouse skin and liver post mitochondrial 4-methylumbelliferyl heptanoate hydrolysis by different esterase inhibitors 128

12.16 Inhibition of pig skin post mitochondrial and liver cytosolic 4-methylumbelliferyl heptanoate hydrolysis by different esterase inhibitor s 128

12.17 Inhibition of human skin post mitochondrial 4-methylumbelliferyl heptanoate hydrolysis by different esterase inhibitors 129

12.18 Inhibition of rat skin and liver microsomal 4-methylumbelliferyl heptanoate hydrolysis by different esterase inhibitors 129

12.19 GST activity per mg of protein for Balb/C mouse skin and liver, neonatal rat skin, adult rat skin and liver, pig and human skin post mitochondrial fractions and human liver cytosolic fraction .. 129

12.20 GST activity per gram of tissue for Balb/C mouse skin and liver, neonatal rat skin, adult rat skin and liver, pig and human skin post mitochondrial fractions and human liver cytosolic fraction 133

12.21 GST activity in individual human post mitochondrial fractions 135

12.22 GST activity in human liver cytosolic fraction 135

12.23 Glutathione content in rat, mouse, pig and human skin 138

13.1 Ethoxyresorufin-*O*-deethylation activity in freshly isolated keratinocytes over time, maintained at 4°C and 37°C 154

13.2 GST activity in cultured keratinocytes 156

14.1 Protein recoveries from living skin equivalents 169

14.2 Enzyme activities in living skin equivalents 169

14.3 Protein recoveries for living skin equivalents exposed to 3-methylcholanthrene .. 170

14.4 Enzyme activities in the living skin equivalent exposed to 3-methylcholanthrene .. 170

15.1 Viability of neonatal rat skin in flow-through diffusion cells, assessed by the MTT assay 177

15.2 Viability of neonatal rat skin in static diffusion cells, assessed by the MTT assay 177

15.3 Glutathione levels in neonatal rat skin in the flow-through diffusion cell 179

page

15.4 Glutathione levels in neonatal rat skin in the static cell 179

15.5 Esterase activity in neonatal rat skin in the flow-through diffusion cell 181

15.6 Esterase activity in neonatal rat skin in the static diffusion cell 181

15.7 GST activity in neonatal rat skin in the flow-through diffusion cell 183

15.8 GST activity in neonatal rat skin in the static diffusion cell 183

15.9 Effect of receptor medium on reduced glutathione levels in neonatal rat skin in the flow-through diffusion cell 187

15.10 Viability of skin stored at 32°C, 20°C, 4°C in air and 4°C on RPMI1640 medium, cut and uncut, as assessed by the MTT assay .. 191

15.11 Glutathione levels in skin stored at 32°C, 20°C, 4°C in air and 4°C on RPMI1640 medium, cut and uncut 191

15.12 Esterase activity in skin stored at 32°C, 20°C, 4°C in air and 4°C on RPMI1640 medium, cut and uncut 191

15.13 GST activity in skin stored at 32°C, 20°C, 4°C in air and 4°C on RPMI1640 medium, cut and uncut 191

16.1 Percentage of evaporative loss of DNCB from Balb/C mouse skin from static and flow-through diffusion cells 206

16.2 Disposition of dinitrochlorobenzene not absorbed into the receptor medium by 24 hours after application of 25μg in acetone 209

16.3 Disposition of dinitrochlorobenzene not absorbed into the receptor medium by 24 hours after application of 125μg in acetone 210

16.4 Disposition of dinitrochlorobenzene not absorbed into the receptor medium by 24 hours after application of 500μg in acetone 211

16.5 Amount of DNCB absorbed and metabolised through Balb/C mouse skin using acetone and propylene glycol vehicles at 24 hours 208

16.6 Reduced glutathione levels in skin untreated and treated with dinitrochlorobenzene (125μg/cm^2) in acetone over 12 hours 221

16.7 Viability of skin after exposure to DNCB and acetone as assessed by the MTT assay after 6 hours in the static cell 222

16.8 Disposition of unabsorbed dinitrochlorobenzene in a) neonatal rat skin, b) 26 day old rat skin, c) pig skin and d) human abdomen skin in the flow-through diffusion cell after application of 25μg/cm^2 and 125μg/cm^2 DNCB dissolved in acetone, conducted under unoccluded and occluded conditions 225

16.9 DNCB and conjugated DNCB recovered from the receptor medium 24 hours after application of 25μg/cm^2 and 125μg/cm^2 DNCB in acetone onto mouse, neonatal rat, adult rat, pig and human skin in the flow-through diffusion cell 228

List of graphs

		Page
11.1	A typical calibration graph for protein concentration determined using the bicinchoninic acid method	101
12.1	The effect of age of Wistar rats on ethoxyresorufin-*O*-deethylation (EROD) activities in liver and skin expressed as activity/min/mg microsomal protein	110
12.2	The effect of age of Wistar rats on ethoxyresorufin-*O*-deethylation (EROD) activities in liver and skin expressed as activity/min/g tissue	110
12.3	The effect of age of Wistar rats on pentoxyresorufin-*O*-dependentylation (PROD) activities in liver and skin expressed as activity/min/mg microsomal protein	111
12.4	The effect of age of Wistar rats on pentoxyresorufin-*O*-dependentylation (PROD) activities in liver and skin expressed as activity/min/g tissue	111
12.5	Liver weights of rats untreated and treated with corn oil, ß-naphthoflavone, phenobarbital and ethanol	114
12.6	Ethoxyresorufin-*O*-deethylation and pentoxyresorufin-*O*-dependentylation (PROD) activities in liver microsomes of rats untreated and treated with corn oil, ß-naphthoflavone, phenobarbital and ethanol	116
12.7	Ethoxyresorufin-*O*-deethylation and pentoxyresorufin-*O*-dependentylation (PROD) activities in dermatomed skin microsomes of rats untreated and treated with corn oil, ß-naphthoflavone, phenobarbital and ethanol	117
13.1	Ethoxyresorufin-*O*-deethylation activity in freshly isolated keratinocytes over time, maintained at 4°C and 37°C	155
15.1	Viability of neonatal rat skin in flow-through and static diffusion cells assessed by the MTT assay	178
15.2	Reduced glutathione levels in neonatal skin in flow-through and static diffusion cells (nmoles/cm^2)	180
15.3	Esterase activity in neonatal rat skin in flow-through and static diffusion cells (nmoles/min.mg postmitochondrial protein)	182
15.4	Glutathione-S-transferase activity in neonatal rat skin in the flow-through and static diffusion cell (nmoles/min.mg postmitochondrial protein) ..	184
15.5	Effect of receptor medium on the viability of neonatal rat skin in the flow-through diffusion cell	187
15.6	Viability of excised neonatal rat skin stored at 32°C, 20°C, 4°C in air and on RPMI1640 tissue culture medium at 4°C, cut and uncut, for 24 hours	192

Page

15.7 Reduced glutathione levels in excised neonatal skin stored at 32°C, 20°C, 4°C in air and on RPMI1640 tissue culture medium, and uncut skin stored on medium at 4°C for 24 hours 193

15.8 Esterase activity in excised neonatal skin stored at 32°C, 20°C, 4°C in air and on RPMI1640 tissue culture medium, and uncut skin stored on medium at 4°C for 24 hours 194

15.9 Glutathione-S-transferase activity in excised neonatal skin stored at 32°C, 20°C, 4°C in air and on RPMI1640 tissue culture medium, and uncut skin stored on medium at 4°C for 24 hours 195

16.1 Absorbed DNCB and metabolised DNCB in the receptor medium over 24 hours after application of 25μg DNCB/cm^2 in acetone and propylene glycol to Balb/C mouse skin in a) the flow-through diffusion cell and b) the static diffusion cell 209

16.2 Absorbed DNCB and metabolised DNCB in the receptor medium over 24 hours after application of 125μg DNCB/cm^2 in acetone and propylene glycol to Balb/C mouse skin in a) the flow-through diffusion cell and b) the static diffusion cell 210

16.3 Absorbed DNCB and metabolised DNCB in the receptor medium over 24 hours after application of 500μg DNCB/cm^2 in acetone and propylene glycol to Balb/C mouse skin in a) the flow-through diffusion cell and b) the static diffusion cell 211

16.4 Effect of occlusion on the appearance of DNCB and conjugated DNCB in the receptor medium over 24 hours after application of 25μg and 125μgDNCB/cm^2 in acetone to Balb/C mouse skin in the flow-through diffusion cell 214

16.5 Appearance of DNCB and glutathione conjugated DNCB through mouse skin in the flow-through diffusion cells. Mice pretreated with buthionine sulphoximine to depleat gluathione 217

16.6 Appearance of DNCB and glutathione conjugated DNCB through mouse skin in the static diffusion cells. Mice pretreated with buthionine sulphoximine to depleat gluathione 218

16.7 Depleation of glutathione levels in skin untreated and treated with dinitrochlorobenzene (125μg/cm^2) in acetone over 24 hours 221

16.8 Absorption and metabolism of DNCB through a) neonatal rat skin, b) 26 day old rat skin, c) pig skin and d) human abdomen skin in flow-through diffusion cells, unoccluded and occluded 227

List of Plates

		page
10.1	Cross section of neonatal rat skin x280	98
10.2	Cross section of dermatomed adult rat skin x140	98
10.3	Cross section of dermatomed pig skin x140	99
10.4	Cross section of dermatomed human skin x88	99
13.1	A small colony of human keratinocytes x140	145
13.2	A large colony of human keratinocytes x140	145
13.3	A confluent culture of human keratinocytes x140	146
13.4	Human keratinocytes at high magnification x445	146
13.5	Cultured rat keratinocytes at near confluence x140	149
13.6	Cultured rat keratinocytes at high magnification x 280	149
14.1	Human fibroblasts, a small colony x280	161
14.2	Human fibroblasts, confluent x280	161
14.3	Human fibroblasts grown on a porous membrane x280	164
14.4	An LSE at 24 hours x280	164
14.5	An LSE at 72 hours x280	165
14.6	An LSE at 2 weeks x445	165
14.7	An LSE x140	166
14.8	An LSE x280	166
14.9	An LSE x445	167
15.1	The flow-through diffusion cell	174
15.2	The flow-through diffusion cell system	174
15.3	The static diffusion cell	175
15.4	The static diffusion cell system	175
15.5	Balb/C mouse liver stained for π GST x310	198
15.6	Balb/C mouse liver stained for π GST (control, no antigen) x310	198
15.7	Balb/C mouse skin stained for π GST x310	199
15.8	Balb/C mouse skin stained for π GST (control, no antigen) x310	199
15.9	Balb/C mouse liver stained for GSH x310	200
15.10	Balb/C mouse skin stained for GSH x310	200

Acknowledgements

During my three years undertaking this research project in the Department of Environmental and Occupational Medicine at Newcastle University I have had a great deal of encouragement and moral support from the staff, technicians and fellow students to who I extend my deepest gratitude.

I would firstly like to thank Dr. Faith Williams, my supervisor, for her technical guidance and advice throughout my research. I would also like to give my thanks to Elaine Mutch, Drs. Séan Kelly, Ian Dick, Alan Langford and Sarah Crosbie for many words of wisdom.

A special thanks to Dr. Gail de Blaquière for her invaluable advice and criticism and for putting me up on my visits to Newcastle.

I would especially like to thank Carol Todd and Sylvia Kyne of the Department of Dermatology for their professional expertise and advise in tissue culture techniques.

I give my thanks to Dr. Jon R Heylings of Zeneca Central Toxicology Laboratory (CTL), my industrial supervisor, and to Helen M Clowes, also of Zeneca CTL for her expertise in *in vitro* percutaneous absorption methods.

I thank Ian Mounter for bearing the brunt of my frustrations and stress when things seemed hopeless.

Lastly, I could not finish without a special thanks to my Mum and Dad, with all my love, for always being there for me.

This project was funded by a joint collaborative award from the Medical Research Council and Zeneca Central Toxicology Laboratory.

Abbreviations

BSA	Bovine serum albumin
BPE	Bovine pituitary extract
BSO	Buthionine Sulfoximine
DMEM	Dulbecco's minimum essential medium
DMSO	Dimethylsulfoxide
DNCB	Dinitrochlorobenzene
DPBS	Dulbecco's phosphate buffered saline
EC	Ethoxycoumarin
ECOD	Ethoxycoumarin-*O*-deethylation
EGF	Epidermal growth factor
EOR	Ethoxyresorufin
EROD	Ethoxyresorufin-*O*-deethylation
FCS	Fetal calf serum
GSH	Reduced glutathione
GST	Glutathione-S-transferase
LSE	Living skin equivalent
3-MC	3-Methylcholanthrene
MCDB	Molecular, chemical and developmental biology of the University of Colorado
MTT	3-(4,5-dimethylthiozole-2-yl)-2,5 diphenyltetrazoliumbromide
MU	4-Methylumbelliferone
MUH	4-Methylumbelliferyl heptanoate
PB	Phenobarbital
POR	Pentoxyresorufin
PROD	Pentoxyresorufin-*O*-depentylation
RPMI	Roswell Park Memorial Institute

Section 1

General Introduction

Chapter 1

The structure and function of skin

The structure and function of skin

1.1 Introduction

The structure of skin is an important component of it's function. It is not only one of the most complex organs but is also the largest and heaviest organ of the body, with the average human male having an estimated skin area of 1.8-2.2m^2, accounting for about 10-15% body weight and receiving between 6-8% of cardiac output (Pinkis and Mehregan, 1981). The skin functions as a protective, waterproof layer which regulates body temperature, protects from pathogens, poisons and solar radiation, as well as acting as an extensive sensory organ. The skin has been regarded as an inert, flexible integument of the body, however, this highly specialised organ is very dynamic in nature and has tremendous regenerative potential, having a fast turnover of cells, which are continually proliferating and differentiating. The skin loses on average, 33grams of dead material each day, amounting to over 11 kilograms annually.

The three major layers of the skin are the hypodermis, dermis and epidermis. The hypodermis binds skin loosely to adjacent tissue and forms the superficial fascia. The epidermis is an avascular stratified layer of epithelial cells overlying the dermis, which is a connective tissue layer with a rich blood and nerve supply, providing the epidermis with physical and nutritional support. The continuous renewal of the stratum corneum, the outer most layer of the epidermis, maintains the skins integrity and its function as a barrier to the external environment. Numerous cell types make up the three major layers of the skin and appendage organs such as hair follicles, nails and sebaceous glands add to the heterogeneity of cells found in skin tissue. The structure of the skin is shown in diagram 1.1.

1.2 Epidermis

The epidermis is composed of several distinct layers of keratinocytes which differ in their state of terminal differentiation. Figure 1.2. diagrammatically details these layers and gives their nomenclature. In the basal layer, actively differentiating cells divide and move upwards. As they ascend to the outer surface of the skin they lose their capacity to replicate and terminally differentiate into the dead horny cells of the stratum corneum. The epidermis is composed of up to 50 layers of these cells depending on anatomical site, becoming more flattened towards the skin surface. Keratinocytes are the main cell type of the epidermis, amounting to 95% of epidermal cell mass. Less abundant cells of the epidermis are melanocytes, Langerhans' cells and Merkel cells. Human epidermis is replaced every 15-30 days depending on age and anatomical site.

The *stratum basale* consists of cuboidal germinative cells resting on the dermal-epidermal junction, the *basale lamina*, which separates the epidermis from the dermis. It is a layer characterised by intense mitotic activity for constant renewal of epidermal cells, as well as also having high metabolic activity. The cells are filled with cytoplasm rich in mitochondria and ribosomes and

Diagram 1.1. *The structure of skin*

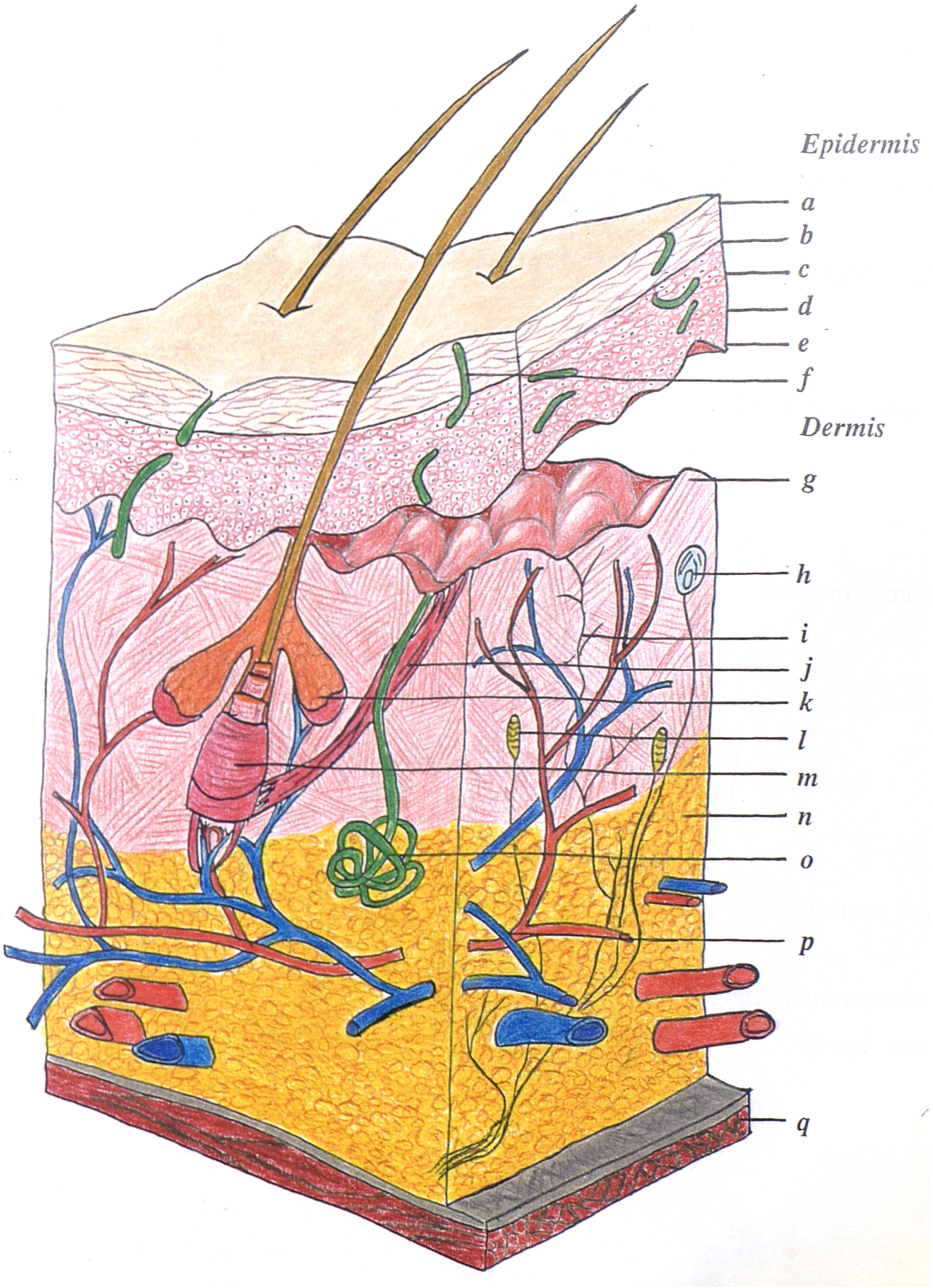

The structure of skin: a) Stratum corneum, b) Stratum lucideum, c) Stratum granulosum, d) Stratum spinosum, e) Stratum basale, f) pore, g) Dermal papillae h) Pacinian corpuscle, i) Free nerve endings, j) Arrector pili muscle, k) Sebaceous gland, l) Meissners corpuscles, m) Hair follicle, n) Fatty tissue, o) Sweat gland p) Vascular supply, q) Muscle tissue.

Figure 1.2. ***Layers of the epidermis***

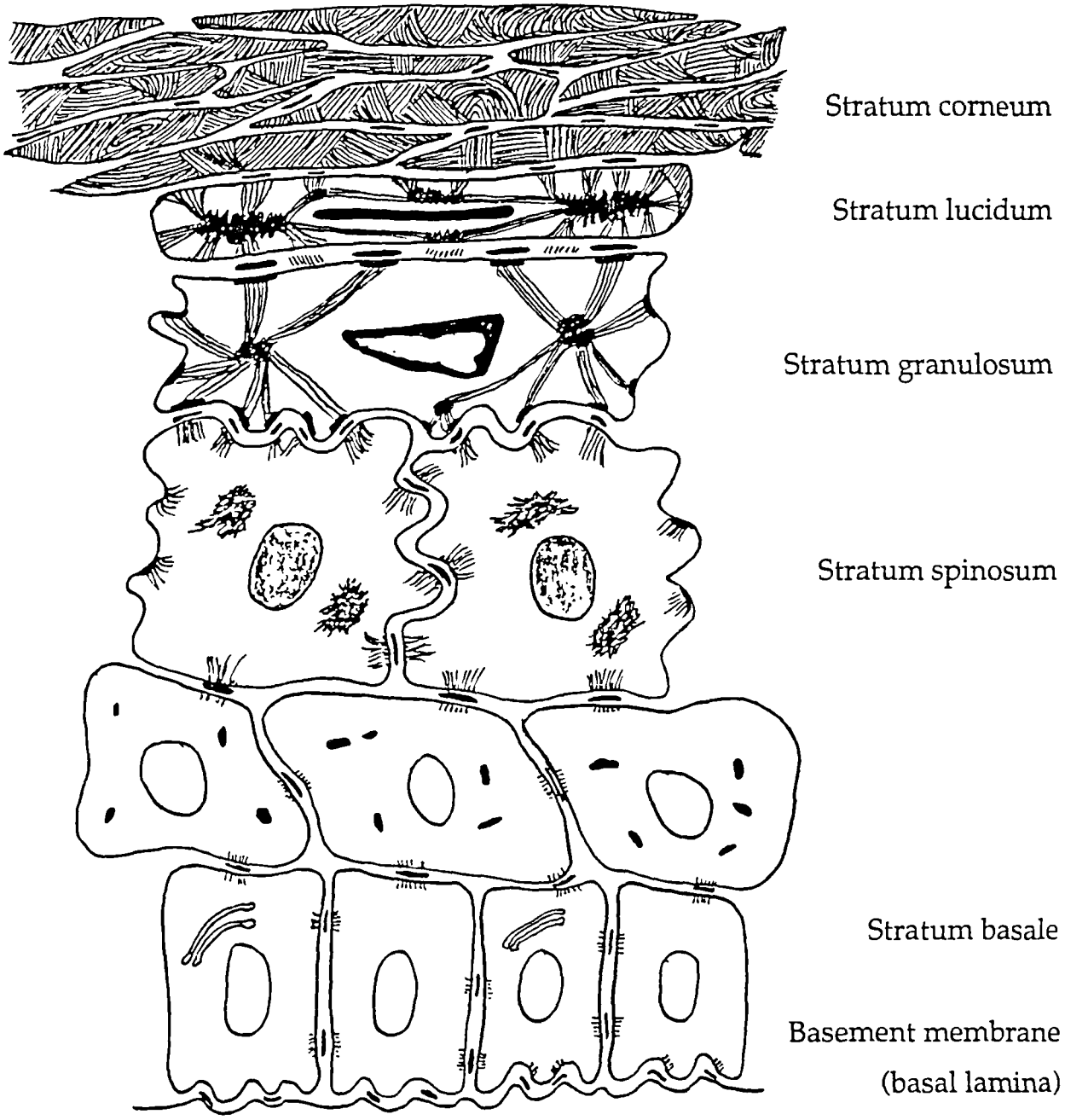

contain about 30% keratin. Basal cells lie between the basement membrane and *stratum spinosum* and possess a notable polarity. The cells are joined to the underlying dermis by hemidesmosomes and anchoring filaments extend into the basale lamina and beyond, into the dermal matrix. Cells adjacent and above are bound by numerous desmosomes. Physiologic communications between the cells of the basal layer and adjacent layers is achieved through gap junctions. Gap junctions are not found between keratinocytes and the non-keratinocytes of the epidermis.

The layer above the *stratum basale* is the *stratum spinosum*, sometimes referred to as the prickle cell layer and consists of slightly flattened cells that are filled with bundles of filaments. The filaments are closely associated with the many desmosomes of the cells and give the cells their characteristic prickly appearance. These desmosomes bind the cells together via bridges of tonofilaments bundled together into tonofibrils. The cells of this layer synthesis new keratins that are specific to the differentiation of the keratinocytes ascending from the basal layer, Mitotic activity still continues in this layer of the epidermis but at a slower rate than the basal layer. This region of the epidermis is thickest on the soles of the feet and palms of the hands where abrasion is the greatest.

The *stratum granulosum* consists of more greatly flattened cells, but still contain nuclei and cytoplasm. They also contain coarse basophilic granules called keratohyalin granules (KHG). These granules become larger as the cells ascend the layers of the *stratum granulosum.* In the cells of this layer, the protein filaggrin, subunits to profilaggrin, begin to aggregate and align keratin filaments. The keratin filaments become extensively bound with disulfide bridges and together with laminar granules form the barrier properties of the epidermis. Laminar granules synthesis and release lipids into the intercellular spaces which become a major composite of the *stratum corneum.* The lipids act as a cement between cells and add to the barrier properties of the epidermis.

The *stratum lucidium*, a layer a cells between the *stratum granulosum* and the *stratum corneum* is only really apparent in thick and hairless skin, organelles are no longer evident and the cytoplasm is filled with filaments.

The *stratum corneum* forms the final non-viable and virtually dehydrated horny layer that is responsible for the protection of the organism from the environment, being relatively impermeable to water and protects from extreme water loss, impact and frictional injury. It consists of 15-20 layers of non-nucleated keratinised cells where the cytoplasm has been replaced with keratin, amounting to 85% of the cell mass. The keratins are built up of at least 6 different polypeptides which have molecular weights between 40-70,000. The more differentiated the cell, the higher the polypeptide molecular weights become. The cells are surrounded by a thick lipid-protein envelope, reinforced by a near indestructible highly cross-linked protein. Between layers of these cells is a lipid lamellae matrix, derived from membraneous discs contained in the granules seen in the granular layer. These lipids consist of ceramides, cholesterol, free fatty acids and cholesteryl sulphate. Cornified keratinocytes have a much greater size than the basal keratinocytes they derived from. A cell of the

stratum corneum can be 30-40μm in diameter compared to a basal keratinocyte that has a diameter of 6-8μm. Cells of the *stratum corneum* also have ridges and villi which help them lock together. The desmosomes of these cells disappear towards the outer surface of the skin, allowing the outer cells to desquamate. (Montagna, 1974; Pinkis and Mehregan, 1981; Monteiro-Riviere, 1990).

1.3 Cells of the epidermis

Keratinocytes are the main cell type of the epidermis, contributing 95% of the total cellular mass. The primary structure of all keratinocytes is the presence of keratin intermediate filaments. They are organised into bundles that are found throughout the cytoplasm. These cells also contain rough endoplasmic reticulum, Golgi, ribosomes and mitochondria. The keratinocyte plasma membrane begins as a usual lipid bilayer cell membrane, but becomes thickened as the cell undergoes differentiation. Keratinocytes are discussed in more detail in chapter 6.

Melanocytes are notably different from keratinocytes. They have many Golgi regions, mitochondria, rough endoplasmic reticulum, but contain no keratin filaments. They possess many pigment containing melanosomes, though the numbers of these organelles differs considerably between individuals. Melanocytes are situated at the *stratum basale* and proliferate at the same rate as keratinocytes. These cells are not connected to keratinocytes by desmosomes, but are anchored to the *stratum basale* by hemidesmosomes. Melanocytes are evenly distributed throughout the epidermis and transfer pigment to the keratinocytes. They inject the pigment into the keratinocytes by a process called cytocrine secretion, which is a dendritic process. The melanin granules accumulate in the cytoplasm of the keratinocytes and protect the nuclei from the effects of solar radiation. The mechanism and regulation of melanin production is controlled by the keratinocytes (Thody, 1990).

Langerhans cells are another dendritic cell of the epidermis. They are typically found in the spinous region and are involved in the uptake, processing and presentation of antigens. Their cell structure consists of rough endoplasmic reticulum, Golgi, vacuoles and fine vimentin filaments (non-keratin filaments). They originate from precursor cells in the bone marrow. They pick up antigen in the skin and circulate it to the draining lymph nodes. After exposure to u.v. radiation, Langerhans cells become depleted and no immunological response is seen when the skin is challenged (Friedmann, 1981).

Merkel cells are neuroendocrine cells found within the epidermis and hair follicles. There are about 10-100 Merkel cells mm^2 of normal skin and are found in greater density in areas of high touch sensitivity. They possess membrane-bound granules (80-120nm diameter), characteristic of granules in neuroendocrine cells. The Merkel cell is affiliated, like a neural synapse, to an unmyelinated fibre, which extends from a sheath deficient neurite just below the basement membrane. (Pinkis and Mehregan, 1981).

1.4 Dermis

The dermis consists of loose connective tissue containing collagen, reticulin and elastin fibres and embedded in a glycosaminoglycan ground substance. Cell populations in the dermis are predominantly fibroblasts but also include macrophages, mast cells and lymphocytes. The thickness of the dermis varies with anatomical region and is thickest on the human back where it reaches up to 4mm.

The dermis can be divided into two regions, the upper papillary layer and the deeper reticular region. The papillary layer forms a region rich in collagen fibrils, which insert into the *basale lamina* and bind the dermis and epidermis together. The reticular layer contains collagen mainly of type I and having more fibres and less fibroblasts than the papillary layer. An extensive network of elastin fibres also make up the reticular region, giving skin it's characteristic elasticity. Fibres of the dermis and the ground substance are produced by one type of fibroblast, but the regulation of this process is not fully understood (Hashimoto, 1978).

The dermis is rich in vascular and lymph vessels. Blood vessels are involved in regulating body temperature, as well as providing nourishment to the skin. There is a rich supply of nerves in the dermis consisting of encapsulated nerve terminals, Meissner's and pacinian corpuscles, which are mechanoreceptors involved in tactile and pressure sensitivity respectively. These corpuscles decrease in number with age.

1.5 Cells of the dermis

Fibroblasts are the main cell type of the dermis. They are found among the collagen fibres, are motile and have mitotic capability. They excrete procollagen, proelastin and glycosaminoglycans. These are enzymatically converted to collagen and elastin extracellularly.

Mast cells vary in number depending on age and anatomical site. They tend to be found around the blood vessels of the dermis. They contain large granules which themselves contain histamine, heparin or seratonin.

Macrophages develop from monocytes and have a life span of 2-3 months. They contain several types of lysosomes with pinocytotic and phagocytotic vacuoles. Their function is to swallow up and destroy invading bacteria and foreign material and release antigens for presentation to the immune system.

1.6 Skin appendages

The skin also contains several appendages, these include nails, sweat glands, hair follicles, sebaceous glands and apocrine glands.

Hairs are elongated keratinized structures formed within the hair follicles. The keratinization process in hair formation differs from epidermis keratinization in that epidermal keratinocytes produce soft keratinized cells that adhere to each other slightly and easily desquamate, hairs are hard and compact keratinized structures. Epidermal keratinization is continuous and hair keratinization is intermittent.

Nails are plates of keratinized cells that form on a dorsal surface and the cells of this matrix divide distally and cornify, the nail plate then pushes forward over the nail bed.

Sebaceous glands are present in the skin at about $100/cm^2$. They are acinar glands with short ducts that open out into hair follicles. Undifferentiated epithelial cells rest on the basale lamina and as they differentiate they fill with a lipid mixture called sebum. The nuclei shrink and the cells eventually burst, sebum is then secreted to the skin surface. Sebaceous gland function is not fully understood, but it is thought sebum may act as a weak antibacterial.

Sweat glands are widely distributed over the skin, the fluid secreted is not viscous and consists of water, salt, urea and ammonia. These glands are involved in thermoregulation. Another type of sweat gland is the apocrine gland. These are found in small localised areas in the axillae and anogenital regions and are embedded in the hypodermis. The ducts open out into the hair follicles and secrete a viscous fluid that is initially odourless, but is broken down into its distinctive odour by skin bacteria (Jones, 1994).

Nails, sweat glands and hair follicles all derive from keratinocytes, which illustrates the diversity of keratinocyte characteristics. The term used to describe these keratinocytes is adnexal keratinocytes and they form all parts of the hair and hair follicle, the sebaceous ducts and sweat ducts. (Montagna, 1974; Pinkis and Mehregan, 1981; Monteiro-Reviere, 1990).

1.7 Species and site variables

The basic structure of mammalian skin is the same in all species, though differences do exist in thickness, the number of cell layers, the number of cell types and the density of the appendages. Monteiro-Riviere *et al* (1990) compared cell layers, epidermal and stratum corneum thickness between nine non-human species and five body sites. Their investigation showed that pig skin has the highest number of cells per epidermal layer and consequently the thickest epidermis and stratum corneum. Rats and mice have the lowest cell number per layer and the thinnest epidermis and stratum corneum. Rats and mice also have the lowest number of viable cell layers within the

epidermis, having only 1-2 layers. When the effect of varying body site was examined, the abdomen was generally the thinnest skinned, while buttocks were the thickest. Skin thickness can vary up to five fold between species and up to 1.5 times between sites on the same species. Scott *et al* (1991) compared human abdomen skin to the skin of the rat and monkey. Their investigation showed human skin to have thicker epidermis and stratum corneum than the rat or monkey skin. The results for human abdomen skin were in fact very similar to those of pig abdomen skin, as also found by Monteiro-Riviere *et al*, supporting the hypothesis that pig skin is structurally similar to human skin (Montagna and Yun, 1963). When hair follicle density was measured by Scott *et al* 1991, they found that human skin was 100 times less densely covered than rat skin and 10 times less densely covered than monkey skin. Rodent skin has 10-15 hairs per hair follicle, consisting of primary and secondary hairs. Pig skin hair follicle density is very similar to man.

Pig skin has the closest match to human skin in that it has a similar hair density, epidermal thickness, cell turnover, lipid composition, carbohydrate biochemistry and enzyme histochemistry. (Meyer *et al*, 1978, 1981, 1982).

1.8 An introduction to skin immunology

The skin is the first point of contact with most chemicals in the environment and the skin's barrier properties help prevent exogenous material entering the body. It is an organ that is clearly visible and therefore toxic reactions resulting from the exposure to chemicals have been described by morphological rather than functional changes.

The general response of skin to a wide variety of external stimuli, physical or chemical toxins, is acute inflammation followed by epidermal hyperplasia. Irritant and allergic contact dermatitis account for a majority of occupational skin disorders, with irritants accounting for 60-80% of contact dermatitis (Abel and Wood, 1986). An irritant on the skin is a substance that causes a local inflammatory response without the presence of an immunological reaction and generally cause itchiness or burning sensations. The remaining skin reactions are due to allergic contact dermatitis. This response is accompanied by erythema and oedema, vesiculation, scaling and epidermal thickening (Emmett , 1991; Kupper 1989).

Acute irritation is caused by a wide range of compounds, possessing various chemical and physical properties and a multitude of chemical structures. Many are highly reactive chemicals, solvents and strong acids and bases. So far there has been no reliable method of determining what chemicals will be irritants or which will cause allergic responses from their chemical structures. There has however been numerous attempts to predict the skin's response by using *in vivo* and *in vitro* assays. The most widely used test to date is the Draize test, first described by Draize *et al* in 1944. The method used by Draize required a test chemical to be applied to the surface of the skin of an albino rabbit. The skin is first prepared by clipping it free of fur, the test chemical is then applied to the surface (approximately 1 square inch) and surgical gauze placed over the test area. The test

area is assessed at 24 and 72 hours for any morphological changes and scored by degree of skin reaction to the test chemical. This method is generally considered to give reliable results in distinguishing strong irritants. However, there are limitations to this method, not only can mild or moderate irritants be misinterpreted but the scoring given to the rabbit skin reaction can differ due to subjectivity between test investigators. In these circumstances cumulative irritancy tests are seen to give better and more consistent results (Phillips *et al,* 1972). The Draize test still relies on morphological changes and the diverse mechanisms by which the irritants elicit their toxicity remain largely unclear.

Allergic contact dermatitis, a form of delayed-type hypersensitivity, is a type IV immune reaction. It is a response that is very specific to each chemical introduced to the immune system and can be triggered even by trace amounts of chemical. The skin contains all the essential constituents for an immunological response providing a defensive mechanism, complementing the skin's barrier properties. On first exposure to a chemical no reaction takes place, this is referred to as the refractory period. Over the next 1-3 weeks an induction period takes place in which develops a sensitisation to a chemical. On reexposure to the chemical, (the allergen), a response is elicited. Once induced, the sensitivity to the chemical persists and may last for the lifetime of the animal. Allergens usually have low molecular weights and the process which brings about an immunological reaction begins with the absorption of the allergen through the skin. During dermal absorption, the allergen binds to proteins in the skin forming a hapten-carrying complex. Binding may be to various reactive groups, such as $-NH_2$ and -SH (Parker *et al,* 1985). The antigen formed, binds to the surface of Langerhans cells or macrophages. These cells then process the antigen and carry it on the cell surface to be presented to T-lymphocytes. Either Langerhans cells or T-lymphocytes migrate through the skin and are transported to the draining lymph nodes. In the draining lymph nodes, immunoblasts proliferate and two types of sensitised T-lymphocytes are formed, these are effector T-lymphocytes and memory T-lymphocytes. Effector T-lymphocytes are carried back to the surface of the skin and memory T-lymphocytes will only proliferate to form new sensitised lymphocytes when reexposed to the antigen. Effector T-lymphocytes in the skin will activate on contact with the allergen and their response is to synthesis cytokines. The cytokines trigger the inflammatory response and result in the migration of macrophages to the effected site. Cytokines play an important role in inflammation, with each different cytokine involved in different stages of the immune reaction and participating in immune regulation. Tumour necrosis factor-α (TNF-α) stimulates the Langerhans cells to migrate from the epidermis to the draining lymph nodes via efferent lymphatics after exposure to allergens (Cumberbatch and Kimber, 1992). During migration, the Langerhans cells mature and transform into dendritic cells and possess high levels of antigen which in turn stimulate the T-lymphocyte response. TNF-α is also produced from keratinocytes during irritation and many other cytokines have been identified that are produced by keratinocytes, including interleukins 1α, 4, 6, 8 and 10, transforming growth factors α and ß (TGFα and ß), granulocyte/macrophage colony-stimulating factor (GM-CSF), monocyte chemotaxis and activating factor (MCAF), interferon-induced protein 10 (IP-10) and macrophage inflammatory protein 2 (MIP-2). (Barker, 1992; Enk and Katz, 1992; Kimber, 1993; Mckenzie, 1990). Interferon-γ (INF-γ) has an important function in controlling the cytokines released

during an immune response by regulating T-cell allergen receptors, macrophage phagocytosis and exerting antiviral activity (Talmadge *et al,* 1987).

There are many variables that influence irritancy and allergic contact dermatitis which include, site of exposure, vehicle, occlusion, concentration of the chemical, presence of hair, as well as marked differences between species. In man, variables extend to individual differences and not only do individuals vary in their response to an irritant, but an individual may react differently to different substances (Emmett, 1991). Therefore the sole use of the Draize test regarding it's relevance to man has been put into doubt. *In vitro* tests for predicting irritants have been investigated so that animals are not the exclusive means of evaluation. The *in vitro* tests utilise cell cultures, specifically keratinocytes and cultured skin models, also referred to as Living Skin Equivalents, LSE's. Irritancy in these models is evaluated by histological methods, cell death, change in pH, dye uptake into viable or non-viable cells, or release of inflammatory mediators such as interleukins and cytokines (Harvell *et al,* 1994). The use of *in vitro* models for skin irritancy testing probably will never replace the *in vivo* assay, as the complex mechanisms of the skin's reactions can not be imitated *in vitro.* Their use as a screening method is however more likely, as an aid to minimise animal testing and cut down production costs of new materials.

Chapter 2

Skin metabolism

Skin Metabolism

2.1 Introduction

Historically, skin was regarded as an inert integument of the body. However, this highly specialised organ has now been shown to possess metabolic capacity, including the capacity to metabolise drugs and foreign compounds. It inactivates many endogenous and exogenous compounds but also has the capacity to produce more biologically active ones (Bickers *et al*, 1982a/b). Exposure to exogenous chemicals from the environment is inevitable and drugs, agrochemicals and environmental pollutants can penetrate the skin. The liver is the main site of metabolism of these substances, but the potential of the skin to metabolise these compounds cannot be dismissed, especially when it is the primary route of exposure. The skin has low metabolising activity compared to the liver, but considering the size of the skin and its direct exposure to the environment, its metabolism is just as important. Cutaneous absorption through the skin acts as a portal of entry for many xenobiotics which can exhibit widely varying effects such as erythema from local toxicity or greater toxic insult which may lead to tumourgenesis (Maibach, 1976). Metabolism by the skin can also influence the percutaneous absorption of topically applied compounds (Kao *et al*, 1985). The study of the enzyme systems and their properties in dermal tissue has been limited for several reasons. Limitations have been mainly due to the lack of sensitive techniques for their measurement and often by the low performance of skin subcellular fraction, but also because skin is a tough tissue, making enzyme extraction and isolation a particularly difficult task.

Xenobiotic metabolism has been grouped into two phases, called phase I and phase II metabolism. Phase I metabolic pathways are the oxidation, reduction and hydrolysis of compounds whereas phase II metabolism involves the introduction of polar conjugating groups. Metabolism may involve phase I or both phase I and phase II in order to transform xenobiotics into excretable products. Although liver is the primary site of metabolism, skin has also been shown to metabolise xenobiotics by both the phase I and phase II metabolic pathways. Cytochrome P-450 monooxygenase, esterase, glutathione-S-transferase, sulfotransferase and glucuronosyltransferase activity are some of the enzyme systems that have been documented. Several general reviews on skin xenobiotic metabolism have been published which discuss the many techniques used in determining skin metabolism and the toxic and pharmaceutical implications (Martin *et al*, 1987; Kao and Carver, 1990 and 1991; Hotchkiss, 1992; Steinsträsser and Merkle, 1995).

2.2 Phase I metabolism

Phase I metabolism is usually by oxidation via the P-450 monooxygenase enzymes. These are found in the endoplasmic reticulum of cells and exist in most tissues. A simplistic definition of phase I metabolism is where a compound has a hydroxyl group added, which may form an alcohol group, though this may rearrange to form another product. Other phase I enzymes include the esterases and

the amidases. They hydrolyse groups such as esters and amides leaving the carboxylic acid, alcohol or amide as the metabolic product.

a) Cytochrome P450 monooxygenases

Cytochrome P-450's, are so called because in reduced form they bind to CO and exhibit a sharp spectral absorption at 450nm (Klingenburg, 1958). They are membrane bound enzymes found in the endoplasmic reticulum of most cells, but particularly those of the liver. Solubilisation of the membranes splits P-450 enzymes into their constitutive components, which are phosphatidylcholine, cytochrome P-450 reductase and the cytochrome P-450 *per se* (Lu *et al*, 1969). Separately, these components do not take part in metabolism, but together and in the presence of NADPH, they are involved in some very important metabolic reactions.

The name cytochrome P-450 is a general term that describes a family of isoenzymes, each of which have overlapping enzymatic specificity. Through purification of specific P-450 isoenzymes and use of inhibition, antibodies and genetic sequencing, over 150 individual cytochrome P-450's have been categorised in eukaryotic and prokaryotic species (Nebert and Gonzalez, 1987; Nebert *et al*, 1991; Nelson *et al*, 1993; Nelson *et al*, 1996). P-450 nomenclature has in the past been confusing, though now a system is used based on enzyme structure. The enzymes are first grouped into families, each of which share <40% structural homology. These are divided into subfamilies which share 40-75% homology. For example, 1A1 is the gene product, the gene family is '1' and the subfamiliy is 'A'. The name for the gene product is written in italic with the prefix CYP and is therefore *CYP1A1*. There are currently 27 gene families, 10 of which are mammalian. The families 1-4 are predominantly catabolic drug metabolising enzymes and the families 17, 19, 21 and 27 are steroid biosynthesis enzymes. Although each cytochrome P-450 enzyme catalyses specific metabolic reactions, there can be overlap of specificity with substrates, some substrates being metabolised by several P-450's, some by only 1. Coumarin is hydroxylated by both cytochrome P-450's 1A and 2B (Peters *et al*, 1991), while hydroxylation of progesterone to prenenolone is via cytochrome P-45021A2 only (Higashi *et al*, 1991).

The cytochrome P-450 catalytic cycle is shown in figure 2.1. The general reaction is:

$$RH + O_2 + NAD(P)H + H^+ \rightarrow ROH + H_2O + NAD(P)^+$$

The first step involves the binding of the substrate to the active site of the P-450. A change in the redox potential of the haem group facilitates the next step which is the reduction of the Fe(III) substrate complex to Fe(II). This is via the one electron transfer from NADPH and NADPH-dependent cytochrome P-450 reductase to the cytochrome P-450 protein. In the next step, molecular oxygen binds to the Fe(II) substrate complex, enabling the transfer of a second electron. Molecular oxygen is then split, generating an "active oxygen" species. Together with the uptake of two protons,

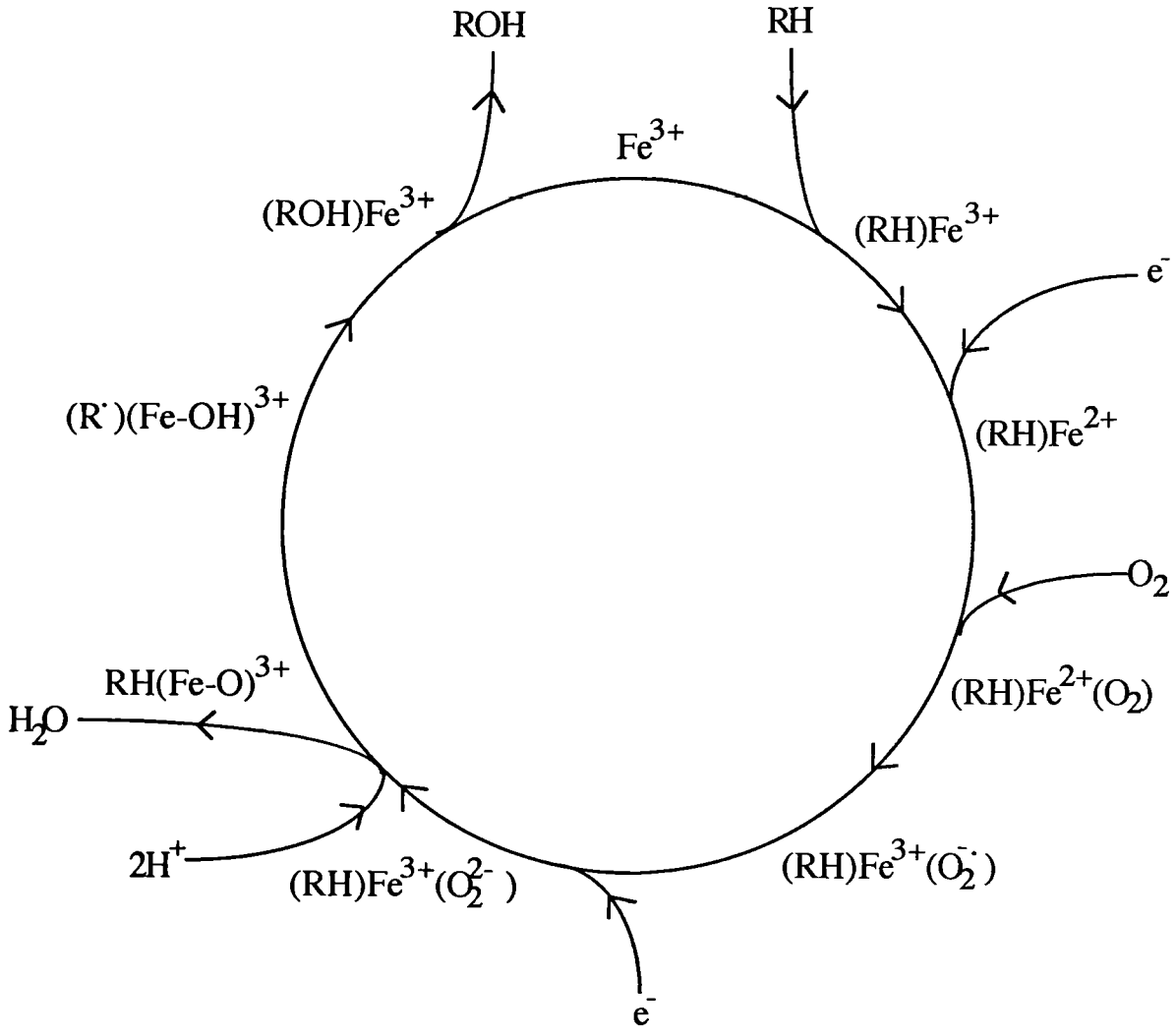

Figure 2.1 The cytochrome P450 catalytic cycle. Fe represents the haem atom at the centre of the P450 protein, RH represents the substrate and ROH the final product.

one oxygen atom is released to form a water molecule. The remaining active oxygen is inserted into the substrate resulting in the final ROH product and the haem group of the cytochrome P450 returns to it's Fe(III) state.

The P450 content in mouse skin was first measured by Bickers *et al* (1974), by difference spectroscopy. In control mouse skin, the levels of P450 were below the levels of detection but skin from Arachlor 1254 treated mice did show detectable levels. Benzo[a]pyrene was used as a model substrate for aryl hydrocarbon hydroxylase (AHH) activity and this showed an 800% increase in activity after Arachlor1254 administration. The induced level of activity in skin was only 10% of the activity found in uninduced liver. AHH activity is mediated by cytochrome CYP1A1 and cytochrome CYP1A1 has been extensively studied because of its role in the metabolism of procarcinogenic compounds, such as benzo[a]pyrene. The presence of CYP1A1/2 in skin was also shown by Raza *et al*, (1992) using specific antibodies to a protein showing 1A1-like activity in rat skin after ß-naphthoflavone induction. Though 1A2 is the predominant of the CYP1A isoforms in liver, 1A1 was shown to be the predominant isoform in skin.

AHH activity was measured in isolated skin cells from mouse by Coomes *et al* (1983). The different cell types were isolated from skin by trypsinisation and separated through use of centrifugation in a Percol gradient. AHH activity was localised to the cells of the basal layer (keratinocytes) and those lining the sebaceous glands (sebocytes). The AHH activity in sebocytes was 2.5 times greater than in keratinocytes. This difference was reduced to 1.5 times after topical pretreatment with ß-naphthoflavone.

Bickers *et al*, (1984) and Storm *et al*, (1990) measured AHH activity in human skin microsomes. They found activities of 62fmol min mg and 240fmol min/mg protein for dermatomed skin respectively, illustrating a wide variability in the human population. Storm *et al*, found that the human AHH activity was 10% of guinea pig skin activity and 7% of mouse skin activity, though the mouse skin was used at full thickness. AHH activity was measured in human and rat keratinocytes and fibroblasts by Kuroki *et al* (1982). The activity was found in all but human fibroblasts and the activity of the keratinocytes, but not the fibroblasts, was found to be inducible by 3-methyl cholanthrene.

Several compounds have been extensively used as substrates for specific P450 enzymes. 7-Ethoxycoumarin (7-EC) has been used as a substrate for CYP1A1/2 and CYP2B, the isoforms predominant in it's dealkylation. 7-Ethoxyresorufin and 7-pentoxyresorufin have been used for CYP1A1 2 and CYP2B respectively. 7-Ethoxycoumarin-*O*-deethylation (ECOD) in whole neonatal rat skin microsomes was found to be 0.36±0.04 pmoles/min/mg and inducible by Arachlor 1254 (Bickers *et al*, 1982a). ECOD was investigated in hairless mouse skin by Moloney *et al*, (1982) and found to be 24.3±2.5pmoles/min mg. ECOD has been measured in human liver microsomes with an activity of 108±10.6pmol min/mg (n=11) (Woodhouse *et al*, 1983), but Storm *et al*, (1990) failed to find any ECOD deethylase activity in human skin.

7-Ethoxyresorufin and 7-pentoxyresorufin were used to distinguish between CYP1A1/2 and CYP2B in the induced rat liver (Burke *et al*, 1985). 7-Ethoxyresorufin-*O*-deethylation (EROD) increased 51 fold after induction with 3-methylcholanthrene (3-MC) and 74 fold after induction with ß-naphthoflavone (ß-NF) with only 9 and 8 fold increases in 7-pentoxyresorufin-*O*-depentylation (PROD) activity on induction with 3-MC and ß-NF respectively. PROD increased 283 fold after induction with phenobarbitone with EROD showing only a 6 fold increase. These results show EROD and PROD to be a specific and sensitive method for measuring P450 activities. Guinea pig liver, Sprague-Dawley rat liver and Balb/c mouse liver each show an EROD activity of 1490±125, 513±63, 1580±125 pmoles min/mg microsomal protein respectively, showing a species variation in EROD activities (Aitio, 1978).

Pham *et al*, (1989) used 7-ethoxyresorufin, 7-pentoxyresorufin and 4A1 substrate, lauric acid, to investigate P450 activities in rat skin microsomes. EROD (CYP1A1) activitiy was 3.6±0.3pmoles resorufin/min mg microsomal protein in male rat skin, 1.5±0.2pmoles/min/mg in female rat skin. PROD (CYP2B) activity was 3.7±1.3pmoles min/mg for male rat skin and 1.8±0.1pmoles/min/mg for female rat skin. Compared to liver, the rate of EROD and PROD was 8-16 times less in skin. No CYP4A1 activity was detectable in rat skin and could not be induced by clofibrate treatment. EROD activity in Hairless mouse skin was shown to be 18.0±5.8pmoles min/mg by Moloney *et al* (1982), suggesting that mouse skin has higher CYP1A1 activity in the skin than rat skin.

CYP1A1 2, CYP2B1 2 as well as glutathione-S-transferases are concentrated in the epidermal basement membrane and the sebaceous glands of mouse rat and human skin as revealed by immunohistochemical staining (Pendlington *et al*, 1994).

CYP2B and low levels of CYP3A are known to be involved in the metabolism of the pesticide aldrin to its epoxide metabolite dieldrin. With the use of mouse skin microsomes and skin strips, Rettie *et al* (1986, 1987) showed detectable levels of aldrin metabolism. Rat skin has been shown to metabolise aldrin following topical application *in vivo* (Graham *et al*, 1991). Human skin has also been investigated for aldrin metabolism (Williams *et al*, 1985).

b) Esterases

Esterases are a group of phase I metabolising enzymes involved in the hydrolysis of not only ester bonds but also non-ester bonds. They are classified on the basis of their interaction with organophosphates (Aldridge, 1953). 'A' esterases metabolise paraoxon while 'B' esterases are inhibited by paraoxon. Some esterases have been found not to interact with paraoxon and these are termed the 'C' esterases (Bergmann *et al*, 1957).

The 'A' esterases were initially identified by their activity to hydrolyse paraoxon but were also found to metabolise phenyl acetate and were therefore also termed aryl esterases. However, later

evidence showed that there are distinct classes of aryl esterases that don't possess paraoxonase activity (Mackness *et al*, 1987). Therefore the 'A' esterases were reclassified as arylesterases (EC 3.1.1.2) and the paraoxonases, renamed as phosphoric triester hydrolase (EC 3.1.8.1). The phosphoric triester hydrolases can be further divided into two groups, the paraoxonases which hydrolyse paraoxon and other organophosphates and are calcium dependent and the DFPases (*O',O'*-diisopropylfluorylphosphatases, EC 3.8.2.1). DFPases require manganese or cobalt and hydrolyse organophosphates with P-F or P-CN bonds, for example mipafox. The 'A' esterases are inhibited by heavy metals, by reduction of thiol groups such as cysteine at the active site (Aldridge, 1989). 'B' esterases have serine groups at their active sites which bind phosphates and inhibit activity.

The 'B' esterases are subdivided into cholinesterases and carboxylesterases. They are both inhibited by organophosphates due to phosphorylation of the serine at the active site. The cholinesterases hydrolyse choline to the relevant acid and are further subdivided into acetyl cholinesterases (EC 3.1.1.7) and butyryl cholinesterases (EC 3.1.1.8). Acetyl cholinesterases are found primarily in neural tissue where they hydrolyses acetyl choline, but is also present in other tissues including plasma, erythrocytes and the placenta. The butyryl cholinesterases, found in most tissues, are not as specific as acetyl cholinesterases and will hydrolyse most choline esters. Carboxylesterases (EC 3.1.1.1) catalyse the hydrolysis of carboxylic acid esters to free acid anions and alcohol and have wide and overlapping substrate specificity (Junge, 1983). This esterase is found in most tissue types, though in man, microsomal carboxylesterase is mainly found in the liver (Junge, 1978).

Limited information is available on esterase activity in skin. A study by Meyer and Neurand (1976) showed esterase to be present in pig skin by histochemical staining techniques. Their results showed that carboxylesterase and acetyl cholinesterase are present in the epidermis and that butyrylcholinesterase was present to a lesser degree. Dermal layers however showed only low levels of carboxylesterase. Carboxylesterase staining was seen in the appendages of the skin, the hair follicles, sebaceous glands and apocrine glands. Clark *et al*, (1992) was also able to demonstrate the presence of esterases in rat, pig and human skin by histochemical staining, showing them to be present at the basal layer of the epidermis.

McCracken *et al* (1993), conducted studies in rat skin subcellular fractions to determine levels of paraoxonase, arylesterase, cholinesterase and carboxylesterase activities. The carboxylesterase activity was determined with the substrates fluazifop butyl and carbaryl and was found to be concentrated in the cytosolic fraction of the skin. Aryl esterase activity was also detected in the cytosol, but little cholinesterase and no paraoxonase activity was found.

Clark *et al* (1993) also used fluazifop butyl to study carboxylesterase activity in rat and human skin. Human skin postmitochondrial fractions were found to be 10 times less active than rat skin postmitochondrial fractions.

c) Other phase I reactions

Flavin monooxygenases or FMO's are endoplasmic reticulum bound enzymes that catalyse NADPH and oxygen dependent oxidation of many xenobiotics. They generally oxidise nucleophilic compounds that contain nitrogen or sulfur (Ziegler, 1990). Venkatesh *et al* (1992), has shown FMO activity in mouse skin at levels 10-20% as those found in the mouse liver. Immunohistochemical staining showed the FMO enzyme to be located in the epidermis.

Epoxide hydrolase (EC 3.3.2.3) hydrolyses polyaromatic hydrocarbon epoxides such as benzo[a]pyrene epoxides, thus acting as a detoxification mechanism and preventing the formation of DNA adducts. Epoxide hydrolase has been found in neonatal rat skin in both cytosolic and microsomal fractions (Bickers *et al*, 1982b, Pham *et al*, 1989).

Ethoxylates, such as phenoxyethanol, are a group of chemicals used in cosmetic products, paints and detergents as solvents, preservatives and surfactants. Phenoxyethanol is metabolised to the phenoxyacetic acid by skin post mitochondrial fractions and thought to be via enzymes similar to alcohol dehydrogenase (Roper *et al*, 1994).

2.3 Phase II metabolism

Some xenobiotics metabolised by phase I metabolism are excreted without the need for further modification, which includes products of hydrolysis. Other phase I metabolites need to be further metabolised to become excretable, for example polyaromatic hydrocarbons metabolised by the cytochrome P450's. These are metabolised by conjugation with more polar molecules and are classed as phase II reactions.

a) Glutathione conjugation

Glutathione (γ-glutamyl-cysteinyl-glycine, GSH) is found in the cells of all tissues where it is synthesised, though GSH is also transported around the body from the liver. Glutathione-S-transferases (GST's, EC 2.5.1.18) are dimeric enzymes which catalyse the reaction between electrophilic compounds and GSH. The GST's are found in the cytosol of a variety of tissues and their role is thought to be in the detoxification of substrates to prevent toxic insult. Examples of compounds that are conjugated by these enzymes include alkyl and aryl halides, lactones, epoxides, quinones, esters and alkenes. Glutathione conjugates are hydrophilic and are further metabolised before excretion. They are cleaved by γ-glutamyltranspeptidase and dipeptidase to the cysteine-S conjugate and then acetylated by renal *N*-acetyl-transferase to the corresponding *N*-acetyl-cysteine-S conjugate, also known as mercapturic acids, which are the final metabolites found in the urine (Koob and Dekant, 1991).

The structure and function of GST's has been reviewed by Wilce and Parker (1994). There are five known isoforms, α, μ, π, θ and microsomal and their classification has been based on substrate specificity, inhibition, antibody cross-reactivity and their primary protein structures. The α isoform is most reactive to cumene hydroperoxide, the μ isoform is most reactive to epoxides and the π most reactive to ethacrynic acid. All GST's are reactive to dinitrochlorobenzene (DNCB), except the θ isoform which conjugates *p*-nitrophenol in human liver. The glutathione conjugation of DNCB has been extensively studied (Habig and Jakoby, 1977) and it is widely used as a substrate for assessing GST activity.

Studies by Mannervik (1987) and Van Bladeren & Van Ommen (1991) have revealed the tissue distribution of the different GST isoforms in the rat. The π isoform is low in liver but is the predominant in skin as well as placenta, lung, kidney and small intestine. These tissues are also low in μ, where as testis are high in the μ isoform and low in the π isoform. Raza *et al*, (1991), showed that the π isoform of GST's is the predominant form in the skin of rodents and man and that rodent skin contains low levels of the μ isoform whereas human skin contains low levels of the α isoform. Human liver has minor amounts of π GST, whereas π GST is abundant in other tissue types, especially placenta, kidney, intestine and skin. Human GST's, their tissue distribution and activities are reviewed by Awasthi *et al*, (1994). Sprague Dawley rat skin cytosol exhibits a GST activity of 34.7±2.9nmol min mg for DNCB conjugation. The GST isoforms found were predominantly π, but some μ and a small but detectable amount of α was also found (Agarwal *et al*, 1992).

Human skin GST activities were assessed by Singhal *et al*, (1993). They showed that female human skin had a higher amount of GST activity than male skin (167±23nmol/min/mg vs. 104±16nmol min mg skin cytosolic protein using DNCB as substrate, n=6, $p<0.01$). Studies were conducted with leg skin, other anatomical sites were not compared. Their studies also showed that the π isoform was the predominant GST of human skin with small amounts of the α isoform detectable and that the π GST had a 40-50 times greater affinity for DNCB than the α isoform. Specific activities for π GST's in female and male skin were determined to be 41.5±9.5 and 32.6±5.7μmol min/mg GST protein respectively, n=3, $p<0.05$.

Several other substrates have been used to assess the activity of GST's, including bromobimane (Hulbert and Yakubu, 1983) as well as DNCB. Habig *et al*, (1974) made a detailed investigation in to GST's and studied their kinetic parameters and substrates. Table 2.1. summarises some of the GST activities evaluated in skin using the substrate DNCB.

Raza *et al*, (1991) conducted studies on the multiple forms of GSTs and activities in rodent and human skin. Microsomal GST activities were demonstrated to have less than 10% of the cytosolic GST activity. GST's were localised to sebaceous glands and hair follicles as revealed by immunohistochemical staining for all GST isoforms. In cultured human keratinocytes only the π isoform was found, this was also confirmed by the work of Blacker *et al*, (1991). GST activity towards *cis*-stilbene oxide in rat skin has been shown to be upto 50% of the rat liver activity (Pham

et al, 1989). Activity towards *cis*-stilbene oxide is also seen in human skin but at only 30% that of rat skin (Pham *et al*, 1990). Table 2.2. lists the GST activities in rodent and human for several of the substrates investigated by Raza and colleagues.

Table 2.1 Glutathione conjugation in skin using the substrate dinitrochlorobenzene (DNCB).

Skin preparation	Species	Specific activities	Reference
Whole skin cytosol	Mouse	54nmol min/mg protein	Das *et al*, 1985
Whole skin post mitochondrial fraction	Mouse, rat and human	2-90nmol/min/mg protein	Baars *et al*, 1981 Mukhtar *et al*, 1981
Epidermal cytosol	Rat	13nmol/min/mg protein	Mukhtar *et al*, 1984a
Epidermal post mitochondrial fraction	Rat	54nmol/min/mg protein	Summer and Göggelmann, 1980
Freshly isolated keratinocytes and sebaceous cells	Mouse	316nmol/min/mg DNA	Coomes *et al*, 1983
Freshly isolated keratinocytes	Mouse	399nmol/min/mg DNA	Coomes *et al*, 1983
Freshly isolated sebaceous cells	Mouse	1399nmol min/mg DNA	Coomes *et al*, 1983
Cultured skin fibroblasts	Human	30-90nmol/min/mg protein	Oesch *et al*, 1980

Table 2.2 Glutathione-S-transferase activities in rat, mouse and human skin cytosol for several substrates. (Raza *et al*, 1991).

	GST activities in skin cytosol, n≥3		
Substrate	Male Sprague-Dawley rat skin	Female SENCAR mouse skin	Human skin (breast or abdomen)
DNCB (nmol min mg)	59.30±3.91	54.07±4.52	25.82±1.95
Leukotriene A4 (pmole min mg)	27.33±2.80	12.32±1.13	5.90±0.42
Ethacrynic acid (nmol min mg)	3.05±0.22	15.50±1.50	5.02±0.41
Styrene-7,8-oxide(nmol min mg)	4.80±0.33	5.31±0.33	3.91±0.28

Investigations on the relationship between GST activity in rat skin and the age of the rat revealed that neonatal rat had almost as much activity as the adult (Table 2.3).

Table 2.3 The relationship between glutathione-S-transferase activity in rat skin cytosol and the age of the rat, assessed using the substrate DNCB (nmoles/min/mg). (Raza *et al*, 1991).

rat age (days)	GST activities in skin cytosol, n≥3
5	48.32±3.85
12	49.89±2.72
19	55.65±4.30
25	60.43±4.55
32	64.59±5.23
67	65.72±5.85

Raza *et al*, (1991), also conducted studies on the localisation of GST activities in neonatal rat skin. Their findings indicate that GST activity is found in both the dermis and epidermis, with approximately 50% greater activity in the dermis (Table 2.4.).

Table 2.4 Glutathione-S-transferase activity in the epidermis, dermis and whole skin of neonatal rat skin assessed using the substrate DNCB (nmoles/min/mg). (Raza *et al*, 1991).

neonatal rat skin	GST activities in skin cytosol, n≥3
Epidermis	27.59±2.83
Dermis	44.25±3.00
Whole skin	48.32±3.05

It must be noted that not all glutathione conjugations are detoxification pathways, glutathione conjugation of certain xenobiotics can lead to the formation of toxic metabolites. Xenobiotics which fall into this class include halogenated alkanes and alkenes, quinones and hydroquinones. The dihaloalkanes dibromochloropropane and tris-2,3-dibromopropylphosphate which are used in fire retardents form electrophilic sulphur mustards. These are capable of alkylation of nucleophilic sites in proteins and DNA. Hexachlorobutadiene forms a non-toxic glutathione conjugate, but is transformed to a toxic intermediate via cysteine conjugation and ß-lyase in the kidneys resulting in nephrotoxicity. Hydroquinones like benzoquinone form glutathione conjugates which are easily reversed back to the nephrotoxic quinone, therefore glutathione conjugation acts as a transport system for this toxic xenobiotic. Reversible glutathione conjugation also occurs with isothiocyanates. The kidney is the most susceptible organ for glutathione metabolites for several reasons. Kidneys represent only 0.5% of human body weight but receive 25% of cardiac output where the toxicants are filtered out and accumulated. Kidneys also possess γ-glutamyltranspeptidase and ß-lyase, enzymes involved in the biotransformation of glutathione conjugates to possible toxic metabolites. (Koob and Dekant, 1991).

b) Other conjugating reactions

Membrane bound uridine diphosphoglucuronosyl transferase (UGT, EC 2.4.1.17) conjugates UDP-α-D-glucuronic acid to the xenobiotic to form the glucuronide metabolite. The most common xenobiotics metabolised via this route are those which are first metabolised via the P450's. UDP-glucuronidation has been shown in rat skin and mouse skin using the substrates 1-naphthol and 7-hydroxycoumarin. The metabolism of 1-naphthol has also been shown to be inducible by pretreatment with 3-methylcholanthrene, whereas 7-hydroxycoumarin metabolism is not (Moloney *et al*, 1982a, 1982b). UDP-glucuronosyl transferase of the skin is located mainly in sebaceous glands and the basal cells of the epidermis as demonstrated by Coomes *et al*, (1983). The basal cell activity was inducible by ß-naphthoflavone, but not the sebaceous gland activity. Endogenous compounds are also metabolised by glucuronidation, including bilirubin.

Sulfotransferases (EC 2.8.2.1, 2, 4, 9, 14) are a group of enzymes which occur in the cytosol and utilise 3'-phosphoadenosine-5'-phosphosulfate (PAPS) as the donor of the sulfate conjugating group. This is generated from ATP and inorganic sulfate. Many sulfotransferases have been identified, 13 in rat and 3 in human (Faloney *et al*, 1991). They are classified according to substrate specificity, which may be phenol, or steroid sulfating groups. Sulfation in skin is very low but has been demonstrated. Many studies have used minoxidil as a substrate for sulfotransferases in the skin. This is mainly due to minoxidil being found to promote hair growth and the sulfate is thought to be the active drug. Activity has been demonstrated in rat skin by Wong *et al* (1993).

Carbaryl hydrolysis is followed by conjugation to the glucuronide and sulfate metabolites in rat skin. Carbaryl is hydrolysed to naphthol in skin at only 3% the rate of liver activity using postmitochondrial fraction. After 30 minutes incubation time in 10μM carbaryl, skin post mitochondrial fractions from 5mg wet weight tissue produce 2.67±0.4pmoles glucuronide and 5.2—1.6pmoles sulfate metabolites (MacPherson *et al*, 1991).

2.4 Factors affecting xenobiotic metabolism

There are several physiological and environmental factors which influence the metabolism of xenobiotics. It is important to consider these factors and their consequences when assessing the metabolism of a compound. The relevance of such factors are most evident when extrapolating animal data to the human population where the variables are particularly notable.

a) Species

There exists distinct differences in the way different species metabolise xenobiotics. By identifying these differences, the role of animals as models for human metabolism can be assessed. There are no animal models that can be used to accurately predict human metabolism for all

compounds, therefore animal models must be chosen carefully with full knowledge of their limitations.

Particular species are deficient in certain enzyme pathways. Rats cannot *N*-hydroxylate aliphatic amines, dogs cannot *N*-hydroxylate aromatic amides and also lack acetylation pathways, except slightly in beagles. Cats are unable to glucuronidate phenols and aromatic acids as they have very low levels of glucoside transferase. Fresh water fish are also unable to glucuronidate. Guinea pigs acetylate well, but have powerful deacetylating agents in their kidneys (Williams, 1975).

b) Gender

The rat has been the focus for many metabolic studies and therefore a greater knowledge of the differences in xenobiotic metabolism has been identified between the male and female rat. It must be noted that work on sex differences in skin metabolism has been poorly investigated.

P450 differences were demonstrated in the male and female rat by Elnarsson *et al* (1973) and Gustafsson *et al* (1974), who showed how the hormone levels of the different sexes affect the levels of P450 in the rat liver.

GST metabolites of hexachlorobenzene has been reported to be higher in male rats than female rats, explaining the greater toxicity of this compound to female rats (D'Amour and Charbonneau, 1992).

c) Age

Aging leads to a decrease in NADPH cytochrome P450 reductase and cytochrome P450 enzyme levels in male rats, but female rats do not show this. Levels of UDP-glucuronosyl transferase may increase, decrease or remain unchanged with age (Van Bezooijen, 1984). The degree of metabolism of benzo[a]pyrene in rat skin has been shown not to alter with increase in age (Williams and Woodhouse, 1995a). However, it has been shown that there is a decrease in NADPH cytochrome c reductase activity with age in the skin of C57B1/6J mice, which is not seen in the liver (Williams and Woodhouse, 1995b). This suggests that the ageing process may have a tissue specific affect in the monooxygenase system. Little information is available on the relationship between percutaneous absorption and metabolism with increase in age. In man, increase in age leads to an increase in the percutaneous absorption of salicylates (Merk, 1989) and a diminished percutaneous absorption of hydrocortisone, benzoic acid and caffeine (Roskos *et al*, 1989). In mice, the percutaneous absorption of phenol and heptoxyphenol is greater at 27 months old than 3 or 15 months, but acetamidophenol and cyanophenol show no differences (Hughs *et al*, 1994). Therefore differences in percutaneous absorption in aged skin is compound specific, and how metabolism effects percutaneous absorption is not yet known.

d) Inhibitors

Inhibition of metabolism is important for two reasons. Firstly, it has been important in elucidation and characterisation of biochemical pathways. Secondly, it is found to play an important role in many toxicological mechanisms.

Many drugs display inhibition pathways. For example, cimetidine and omeprazole inhibit cytochrome P-450's, though these are reversible (Chang *et al*, 1992; Andersson *et al*, 1990). Organophosphate insecticides inhibit "B" esterases and GST's are inhibited by ethacrynic acid and bromosulfophthalein.

Measurements have been conducted on the depletion of glutathione in rat skin exposed to DNCB. Control rat skin had GSH levels of 4.53±2.48nmoles/mg post mitochondrial protein where as skin treated with DNCB for 90 minutes contained 0.26±0.34nmoles/mg (n=5) (Summer and Göggelmann, 1980).

Chemical depletion of glutathione *in vivo* was reviewed by Plummer *et al*, 1981. There are three methods which can be employed:

i) Substrates of GST's that deplete the GSH levels.
ii) Thiol oxidants that convert reduced glutathione to the oxidised form (GSSG).
iii) Depletion of GSH by inhibition of its biosynthesis.

GST substrates that deplete GSH levels include the α,β-unsaturated carbonyl compounds which are weak electrophiles. This class of compound includes the widely used diethyl maleate (DEM). At a dose of 0.6-1.0ml kg i.p. in rat, DEM reduces hepatic GSH to 6-20% of control in 30 minutes for upto 4 hours. At 24 hours, levels of GSH are twice that of normal which then gradually drop to normal levels. Other compounds that deplete GSH acting as GST substrates are aliphatic halo compounds, such as iodomethane and aromatic halo compounds such as DNCB.

Thiol oxidants are mainly used *in vitro* to reduce GSH levels in cell preparations, e.g. methylphenyldiazinecarboxylate. The use of sodium tetrathionate as a thiol oxidiser has been used *in vivo* in rats. A dose of 860mg/kg reduces kidney, erythrocyte and liver GSH levels to 15%, 13% and 60% that of control in 5 hours, though this does have the side effect of producing nephrotoxicity.

Inhibition of GSH biosynthesis has been achieved by the use of sulfoximine (BSO), a specific inhibitor of γ-glutamylcysteine synthetase, the enzyme involved in the first step of GSH biosynthesis. Rats and mice can be given BSO i.p. at 32mmol kg single dose or multiple doses amounting to 72mmol kg over 72 hours, leading to GSH depletion and no side effects. Thereafter, the depleted levels of GSH can be maintained by administration of 4mmol kg every 1.5h or 20mM in drinking water. After 15 days treated mice have GSH levels in skeletal muscles, kidney, liver and

pancreas at 2,4,56 and 8% respectively that of control. (Griffith and Meister, 1979). Drew and Miners, 1984, showed that mice given BSO (1.6g/kg, i.p.) have a liver GSH level of 35% of control by 4 hours. Their study also showed that BSO did not interfere with the sulfation or glucuronidation pathways of paracetamol clearance.

Inhibition of GST's for regulating the metabolism of prostaglandins and leukotrienes was suggested by Van Bladeren and Van Ommen, (1991). They believed that by controlling GST metabolism then there would be potential in regulating allergic reactions, though this has never been investigated.

e) Inducers

Induction is where enzyme activity is increased by the presence of an agent, triggering the formation of more active enzyme to facilitate metabolism and therefore it's excretion. Inducers of cytochrome P-450's can be grouped into 6 classes (Soucek and Gut, 1992).

i) polyaromatic hydrocarbons (PAH's), which induce *CYP1A*
ii) barbiturates, which induce *CYP2B*
iii) ethanol, acetone, benzene and imidazoles, which induce *CYP2E* and *CYP4A*
iv) glucocorticoids, which induce *CYP3A*
v) clofibrate induces *CYP4A*
vi) macrolide antibiotics, which induce *CYP3A*

Mukhtar and Bickers (1981) showed AHH activity in neonatal rat skin using the substrate benzo[a]pyrene to be 1.1pmol min mg protein. After benzo[a]pyrene treatment, AHH activity in rats increased to 8pmol min mg. Activity in arachlor treated rats activity increased to 11pmol/min/mg. It was found that skin was more inducible than any other extrahepatic tissue and that skin homogenates showed 7, 16 and 28% AHH activity compared to liver in control, benzo[a]pyrene and arachlor treated rats respectively. 7-Ethoxyresorufin-*O*-deethylation in control rat skin was 0.36±0.06pmol min mg protein. After arachlor treatment this increased to 8.14±1.80pmol/min/mg. Glutathione-S-transferase activity in skin measured with the substrate styrene oxide showed 15% of liver activity in control rats. Liver GST activity increased 40-60% after arachlor induction by topical application, but skin GST activity did not increase. Therefore, it was shown that cytochrome P-450 monooxygenase activity in neonatal rat skin is inducible by arachlor, but GST activity is not.

Raza *et al*, (1992) characterised CYP1A1 in neonatal rat skin with the use of monoclonal antibodies. Topical treatment with ß-naphthoflavone resulted in a 2.6 fold increase in skin P-450 content and a 13 fold increase in AHH activity measured with benzo[a]pyrene as the substrate. Raza and Mukhtar, (1993) reported that i.p. treatment with ß-naphthoflavone also resulted in an increase in skin AHH activity and that EROD and ECOD activities also show a marked increase in activity. Interestingly, induction with ß-naphthoflavone, either topical or i.p.administration leads to a 3 fold

increase in GST activity, as measured with the substrate DNCB. Pickett *et al*, (1984) has shown that GST's are also inducible by phenobarbital and 3-methylcholanthrene. Phenobarbital has also been shown to induce esterase activity in the skin (McCracken *et al*, 1992).

Retinoic acid is formed in the epidermis from retinol to function in differentiation and proliferation of epidermal cells. Retinoic acid is not stored in the skin as it is readily transformed to its metabolites. The metabolism of retinoic acid is via the cytochrome P450's and has been shown to be inhibited by proadifen and inducible by phenobarbital (Schaefer, 1993). Skin microsomes from neonatal Wistar rats and Sprague-Dawley rats pretreated with acetone, retinoic acid, 3-methylcholanthrene and phenobarbital were used to study retinoic acid metabolism. Table 2.5. shows the microsomal metabolism of retinoic acid by each rat strain.

Table 2.5 Effect of inducers on retinoic acid metabolism to retanol in rat skin (Schaefer 1993).

	retinoic acid metabolism (fmol/min/mg±sem(n))	
rat pretreatment	Wistar rat	Sprague-Dawley rat
acetone	232±107 (5)	222±88 (4)
retinoic acid	760±247 (21)	862±287 (5)
3-methylcholanthrene	1058±157 (4)	1800±533 (3)
phenobarbital	532±84 (4)	360±21 (4)

Retinoic acid induces it's own metabolism, but is much more greatly induced by 3-methylcholanthrene. The Sprague-Dawley rat produces more of the metabolite 4-hydroxy retinoic acid than does the Wistar rat.

Topical application of Arachlor 1254 to neonatal rats lead to no increase in dermal GST activity, though liver activities increased by 50% (Mukhtar and Bickers, 1981). In the adult rat, administration of 3-methylcholanthrene also had no effect on inducing GST's in skin (Mukhtar and Bresnick, 1976). This data suggests that skin GST activity is unaffected by the inducing agents Arachlor 1254 and 3-methylcholanthrene.

Chapter 3

Percutaneous absorption

Percutaneous Absorption

3.1 Introduction

Percutaneous absorption of xenobiotics is one of the possible routes by which some chemicals may enter an organism and which may exhibit harmful effects. This chapter discusses how compounds can penetrate the skin and the factors which influence their absorption.

3.2 The barrier function of the skin

The skin forms a barrier between the organism and its environment, the major component of this barrier being the stratum corneum, with some resistance also shown by the epidermal and dermal layers. It was shown by Blank (1958) that by using the tape stripping technique of Wolf (1934) to remove the stratum corneum of human skin, that water permeability through it rapidly increased. The lipid composition and content of the stratum corneum was later identified as the major factor determining the skin's permeability (Elias *et al*, 1981).

The rate at which the process of percutaneous penetration takes place is called the flux. Absorption of a compound through the skin is by a passive mechanism, that is to say, the flux is linear and dependent on the concentration gradient of the penetrant. The process of percutaneous penetration can thus be described by Fick's law of diffusion:

$$J_s = k_p \Delta C_s$$

Where J_s is the flux of the penetrant, k_p is the permeability coefficient of the penetrant and ΔC_s is the concentration gradient across the membrane. This formula can be rearranged to give the permeability coefficient k_p:

$$k_p = \frac{KD}{\delta}$$

Where K is the stratum corneum/vehicle partition coefficient, D is the membrane diffusion coefficient and δ is the diffusion path-length (Schaefer and Jamoulle, 1988).

From these equations the flux of a penetrant is only dependent on K and D which are in turn subject to the lipophilicity and solute size of the penetrant respectively. The lipophilicity of a compound is often expressed in terms of its logP. The partition coefficient P of a compound is its ratio of equilibrium in a two phase system, usually octanol and water. High logP values are therefore an indication of greater lipophilicity (Eadswoth and Moser, 1983). Compounds which exhibit high

lipophilicitity are more able to penetrate the lipid rich stratum corneum and are absorbed. Although lipophilic compounds may be absorbed into this compartment of the skin, they may be not be absorbed through the lower layers of the skin as easily. Their lipophilicity may mean that they are retained in the stratum corneum and partition out into the skin's lower layers more slowly .

Potts and Guy (1992) were able to mathematically predict the skin permeability for a wide range of compounds based only on their molecular volume, molecular weight and the octanol-water partition coefficients. By using existing permeability data and physicochemical properties of compounds a strong correlation was made. They were able to show that skin permeation was dependant on permeant size and lipophilicity and that the barrier properties of mammalian skin can be characterised by the stratum corneum lipids.

Parry *et al*, (1990) studied the permeation of benzoic acid across isolated stratum corneum, stratum corneum with epidermis and split thickness human skin. It was demonstrated that the rate limiting barrier to percutaneous absorption was the stratum corneum alone.

The epidermis undergoes very high rates of lipid synthesis and this is regulated in response to its barrier requirements. For example, when exposed to acetone, the cholesterol, fatty acids and sphingolipids are removed and this compromises the barrier function of the skin. Increased cholesterol and fatty acid synthesis follows immediately after skin damage and sphingolipid synthesis begins later, in the course of barrier repair, illustrating the importance of dermal lipids to the skins barrier function (Elias and Feingold, 1992).

3.3 Mechanisms of percutaneous absorption

Potts *et al*, (1992) suggested a sequence of steps which a compound must take in order to penetrate through the skin. Firstly, the compound must partition from it's vehicle into the stratum corneum. The compound must then permeate into the stratum corneum. Following this, the compound then partitions from the stratum corneum into the epidermis, after which, it penetrates the upper dermis. Finally, it is taken up by the systemic circulation via the dermal blood supply. Wester and Maibach (1983), proposed 10 elements influencing the percutaneous absorption of chemicals. These were a) vehicle, b) absorption kinetics, c) excretion kinetics, d) cellular and tissue distribution, e) substantivity, (compound which is bound to the skin surface and lost through exfoliation), f) wash and rub resistance, g) volatility, h) binding, i)anatomical pathways and j) cutaneous metabolism. These will be discussed in greater detail in the following subsection.

The way in which a compound is absorbed through the skin from its surface to the systemic circulation may be transcellularly, through the cells of the skin, or paracellularly, through the intercellular matrix and via skin appendageal openings like hair follicles and sweat pores.

There is evidence to suggest that small molecular weight compounds such as water, acetone and volatile alcohols, permeate the skin via the paracellular route. Elias *et al*, (1981) showed that the lipid composition of the stratum corneum, rather than the thickness of the stratum corneum was the determining factor in absorption rate. Potts and Francoeur (1990) demonstrated that small polar molecules transverse the stratum corneum through 'holes' in the lipid matrix and that the rate of flux increased with increasing temperature. Lipophilic compounds are also shown to permeate the stratum corneum paracellularly. Rougier *et al*, (1988) demonstrated that the rate at which water and benzoic acid transverse the stratum corneum was inversely related to the size of corneocytes. Therefore, the larger the corneocyte, the longer the paracellular route and the slower the absorption rate.

Evidence also supports the percutaneous absorption of compounds via the skin appendages. Kao *et al*, (1988) conducted studies on the absorption of benzo[a]pyrene in haired and hairless mice and found the absorption rate to be greater in the haired strain. This was proposed as evidence for a transfollicular route of dermal absorption. Hueber *et al*, (1994) measured the percutaneous absorption of 4 steroids through human scar skin without hair follicles of sebaceous glands and adjacent normal skin. In all cases it was observed that the absorption through normal skin was significantly higher than through scar skin. Therefore hair follicles and sebaceous glands play a significant part in dermal absorption of steroids and probably other chemicals. Lauer *et al*, (1995) published a review discussing the various aspects of transfollicular xenobiotic absorption and its relevance to drug delivery, especially for skin diseases associated with the hair follicles.

3.4 Factors affecting percutaneous absorption

Percutaneous absorption may be affected by biological or physiochemical factors. The biological factors include such variables as age, anatomical site, sex and skin condition, while the physiochemical factors include the affects of vehicle, hydration and the penetrant binding to the skin.

Shah *et al*, (1987) studied the penetration of 14 pesticides through the skin of young and old rats and showed that age did not effect their absorption. Rougier *et al*, (1988) showed no evidence for age affecting absorption in human skin using water and benzoic acid up to 60 years, but between 65 and 80 years found a 4 fold decrease in dermal absorption. Dick and Scott, (1992) studied rats between 10 and 120 days old and although dermal thickness, hair follicle depth and number changed with age, the stratum corneum or the epidermal thickness did not and absorption was unaffected.

Feldman and Maibach, (1967) studied absorption of cortisol through human skin *in vivo* at different anatomical sites, the ventral forearm was assigned the standard rate of absorption and other sites of absorption expressed relative to this. The skin of the scrotum showed 42 times greater absorption, while the soles of the feet were the least permeable at 0.14 times the forearm absorption. High absorption rates were identified in the areas of the head, neck and axillae. Further studies by Maibach and Feldman (1971), measured the rate of absorption of parathion, malathion and carbaryl through human skin *in vivo*. It was observed that the abdomen and back of the hand had twice the

permeability of the forearm and skin rich with hair follicles had a four fold permeability. The axillae showed up to seven times greater penetration and the scrotum showed little barrier protection to these pesticides.

Human skin has not been shown to have any differences in absorption between the sexes (Rougier *et al*, 1988). There have been slight differences found between male and female rats for the absorption of benzoic acid (Bronaugh *et al*, 1983) and these differences have been related to hormonal control, after castrated rats were shown to have similar absorption rates to the females.

Damaged and diseased skin show high rates of dermal absorption and Scott *et al*, (1986) demonstrated this by damaging rat skin *in vivo* to four levels of severity and categorising the transepidermal water loss. It was shown that an increased permeability was associated with the increase in the skin damage.

Compounds which are applied to the skin are usually dissolved or diluted in a solvent, aqueous or organic which then acts as the vehicle. The vehicle may alter the rate at which a compound is absorbed through the skin, but this cannot usually be predicted on the chemical nature of the solvent alone. Ethanol tends to act as an enhancer of penetration and is thought to work by means of compromising the stratum corneum lipids (Guy *et al*, 1990). DMSO and oleic acid are also used as vehicles which increase percutaneous absorption and these are thought to work by solvation of the polar head groups of the stratum corneum lipids. The evaporation of volatile solvents can also increase the rate of dermal absorption by driving the compound through the skin.

Skin can become hydrated on long term exposure to water, or by occlusion from the atmosphere, at which point the tissue swells and becomes much softer. Wurster and Kramar, (1961) have shown that hydrated skin leads to greater percutaneous penetration of salicylic esters *in vivo*. The stratum corneum under normal conditions contains 5-15% water but after occlusion this can increase to 50%. The increase in hydration swells the corneocytes and promotes the uptake of water to within the intercellular lipids. Percutaneous penetration of many chemicals is enhanced, but occlusion does not always increase absorption. Hydrocortisone and certain para-substituted phenols are unaffected by occlusion (Bucks *et al*, 1992).

The percutaneous penetration of xenobiotics may be restrained by binding of the molecules to elements of the skin. Walter and Kurz, (1988) found binding of certain pharmaceuticals to proteins within the stratum corneum which include diazipam, ketoconizole, propanolol, phenytoin and warfarin. The skin may then acts as a reservoir for the penetrants.

In conclusion, if the skin were a simple membrane then absorption would be easily predicted and measured, but it is a living dynamic tissue with many variable factors. Therefore, when studying percutaneous penetration, the investigator needs to be aware of the unique qualities of skin and the degree to which absorption may be influenced by them.

Chapter 4

Methods for studying percutaneous absorption

Methods for studying percutaneous absorption

4.1 Introduction

The methods which have been developed to study qualitatively and quantitatively xenobiotic percutaneous absorption have taken two approaches, *in vivo* and *in vitro*. The *in vitro* systems will be discussed in greater depth as they are of more relevance to this thesis, but an overview of *in vivo* methods will be given first.

4.2 In vivo studies

Percutaneous penetration *in vivo* can be studied using the whole animal or by using skin flaps. Whole animal studies are the more widely used of the two since the skin flap method requires more complex procedures and a knowledge of surgical techniques.

Feldman and Maibach developed a method for assessing the percutaneous penetration of compounds through human skin *in vivo* by using radiolabelled steroids (1966), pesticides (1970) and herbicides (1974) and determining absorption by recovery of the compound in urine excretion. Due to concerns with the safety of using radiolabelled compounds these methods are no longer acceptable for human use, but due to be better extraction techniques and higher sensitivity with analytical equipment, dermal absorption through human skin can now be measured with non-radioactive compounds.

Carver and Riviere (1989), measured the absorption and metabolism of caffeine, benzoic acid, malathion, parathion, progesterone and testosterone through pig skin *in vivo* after intravenous and topical administration (200μg). Percutaneous absorption was determined from total urine and faecal excretion of the radiolabelled compound after topical application. This was corrected for incomplete excretion following intravenous administration. The percentage absorbed and excreted for each xenobiotic was calculated to be benzoic acid (25.7%), progesterone (16.2%), caffeine (11.8%), testosterone (8.8%), parathion (6.7%) and malathion (5.2%). The metabolism of the compounds investigated was not studied and therefore the contribution of metabolism to excretion is not known.

A direct correlation of application time and amount absorbed through skin was observed for theophylline, acetylsalicylic acid, nicotinic acid, benzoic acid, dexamethasone, hydrocortisone, testosterone, caffeine, mannitol and thiourea , in hairless rat skin *in vivo* (Rougier *et al,* 1983, 1985). The compounds showed a constant rate of absorption over time *in vivo*. The most important feature noted was that there was a direct correlation between the amount of compound found in the stratum corneum reservoir, 30 minutes after application and the amount that penetrated the skin by 96 hours. This relationship was only verified in the rat, but was suggested to be a good predictive tool for assessing the total absorption in 4 days. Dupuis *et al*, (1984) established an absorption correlation

with the stratum corneum reservoir effect in human skin *in vivo* with benzoic acid. Further studies by Dupuis *et al*, (1986) investigated the effect of vehicle on the stratum corneum reservoir using benzoic acid as the penetrant and the hairless rat. Even though the choice of vehicle did alter the rate of percutaneous penetration, there was still a direct correlation with the amount of compound in the stratum corneum at 30 minutes and the total amount absorbed in 4 days. Therefore vehicle effects can be predicted by measuring the amount of compound in the stratum corneum reservoir after 30 minutes exposure.

Moody *et al.* (1989) suggested the use of the rat tail for percutaneous absorption studies rather than the rat dorsal region and showed that absorption of lindane through tail and dorsal skin was similar. The advantages highlighted were that the tail was more accessible than dorsal skin and that this method removed the need to shave fur from the dorsal region, which may be damaged and lead to inaccurate absorption profiles.

The use of skin flaps is an alternative method by which *in vivo* absorption can be measured. The technique involves surgically isolating of a section of skin, usually dorsal skin, resulting in an independent blood supply, from which the absorption of a compound can easily be assayed. The method combines the *in vivo* conditions for skin, but also acting as an *in vitro* model for being isolated from other organs (Wester and Maibach, 1992). The disadvantage of this method is that a skin flap may take several weeks to prepare, but the advantage is that once prepared, a skin flap can be used for numerous experiments.

4.3 In vitro studies

In vitro methods allow the percutaneous absorption of chemicals to be assessed independently of the whole animal, therefore allowing absorption mechanisms to be studied. Many investigations have focused on the ability of *in vitro* models to predict *in vivo* absorption profiles, some of which will be discussed in this section. Most *in vitro* studies have used either static diffusion cells or flow-through diffusion cells, each method having it's own advantages and disadvantages, but both allowing finer manipulation of the experimental conditions than *in vivo* studies.

a) Static diffusion cells

The static cell has been used to examine the absorption of many compounds through skin. The cell design most frequently used is the Franz cell (Franz, 1975). Skin is placed on an open chamber in which receptor medium is deposited. The skin is clamped into place with a top chamber which is open to the atmosphere. The compound under investigation is dosed onto the surface of the skin and this may be left open to the atmosphere or occluded. Ethanol/water (50:50) has been used as the standard receptor fluid as it gives a close correlation to *in vivo* absorption, but tissue culture medium has also been used in an attempt to maintain tissue viability. The procedure for investigating

absorption is simple and provides data on the distribution of a compound in the skin as well as the rate of absorption.

Bronaugh *et al* (1982) measured the absorption of benzoic acid, acetylsalicylic acid and urea through rat skin *in vivo* and *in vitro* with using static diffusion cells containing 50:50 ethanol/water as receptor medium. After 5 days the percentage of absorbed dose *in vitro* (49%, 29%, 7% respectively)closely correlated with the absorbed dose *in vivo* (37% ,25% ,8%).

The disadvantage of the static cell are that they usually contain ethanol/water receptor medium which hydrates the skin, a factor which effects penetration (see chapter 3).

b) Flow-through diffusion cells

The flow-through diffusion system was developed in an attempt to mimic the blood flow under the skin. It uses a pump to provide a flow of receptor fluid under the skin in the diffusion cell. The advantages of the flow-through system include the ability to set up automatic sampling. The receptor medium is refreshed continually, avoiding the build up of concentration gradients. The system has the advantage over the static cell system in providing more physiological conditions and therefore maintaining greater skin viability (Bronaugh *et al*, 1989; Collier *et al*, 1989; Clark *et al*, 1991).

Hughes *et al*, (1993) compared the percutaneous penetration of eight *p*-substituted phenols through rat skin using static and flow-through cells. The whole range of phenols was absorbed well with up to 97% absorbed for phenol itself. It was found that significantly less compound was absorbed using the static cell system for five of the phenols, although the difference was less than 4%.

Permeability of hydrophilic compounds, water and mannitol, was investigated with rat, pig and human skin in flow-through cells by Clowes *et al*, (1994). Results for permeability were consistent with those found in the static cell. No difference was observed in the use of saline or tissue culture medium as receptor medium.

A comparison of *in vitro* and *in vivo* absorption of the insecticide isofenphos through human skin was conducted by Wester *et al* (1992). It was observed that *in vivo* 3.6±3.6% of a single applied dose was absorbed by 24 hours. *In vitro* absorption studies used the flow-through system with human cadaver skin and human plasma as the receptor medium. The absorbed isofenphos *in vitro* was 2.5±2.0% by 24 hours, thus similar to the *in vivo* results. Rat skin absorbed 47% of an applied dose in 24 hours, 12 times more than for human skin, showing the rat model could not be used to predict human percutaneous absorption of isofenphos.

Wester *et al,* (1993) measured the absorption of diazinon through human skin. There was no difference between the abdomen or the forearm in the amount absorbed. *In vivo*, the applied dose was 2$\mu g/cm^2$,of which 2.87±1.16% to 3.85±2.16% was absorbed. *In vitro* studies, used a dose of 0.25$\mu g/cm^2$ resulting in 14.1±9.2% being absorbed. The amount absorbed *in vivo* and *in vitro* was 0.035$\mu g/cm^2$, therefore agreeing with each other in the amount of potential systemic delivery.

4.4 Diffusion cell considerations

There are several factors which influence percutaneous absorption *in vitro* which must be considered when developing methods to evaluate the absorption profile of a compound.

a) Receptor fluid

The choice of receptor medium used in *in vitro* diffusion cells can alter the absorption profile of a compound. Penetration of hydrophilic compounds is hindered by the lipid rich stratum corneum, whereas for lipophilic compounds the greatest resistance to percutaneous penetration is the more aqueous epidermal layer. For a prediction of absorption into the systemic circulation, an absorbed compound must be able to partition into the dermal layer and then into the receptor medium. The nature of the receptor medium must ideally be characteristic of fluid in the underlying skin tissue *in vivo*. Absorption rates *in vitro* will therefore give a better reflection of the *in vivo* situation.

When choosing a receptor fluid, the experimental aim must be considered. If absorption rate data of a compound is all that is required, then a medium that will reflect *in vivo* data should be chosen, such as 50:50 ethanol/water (Scott, 1990). When maintenance of viability is important, tissue culture medium should be used.

Buffered salt solutions and cell culture medium are used as receptor medium to control pH (7.4) and osmolarity, but these do not favour the partitioning of lipophilic compound into the medium. Addition of surfactants, BSA, methanol and ethanol have been used to increase this partitioning. The absorption of benzo[a]pyrene (lipophilic) and estradiol (hydrophilic) were compared in the flow-through system using the receptor fluids Hepes buffered Hank's balanced salt solution (HHBSS), HHBSS + 4%BSA and 50:50 ethanol water flowing at a rate of 1.5ml/h for 24h. Use of HHBSS led to benzo[a]pyrene favouring to partition into the epidermis. Addition of BSA to the medium shifted partitioning into the medium by 3 to 13 times. When using 50:50 ethanol water, this increased to 200 times, but this receptor medium dehydrated the epidermal tissue and led to viability and metabolising function becoming compromised. Estradiol partitioned into all receptor medium (Collier and Bronaugh, 1989).

It was observed by Bronaugh *et al* (1989), that addition of 4% BSA led to an increase in viscosity of the receptor medium and this in turn led to a decrease in laminar flow in the diffusion cell. Therefore, the rate of diffusion of compounds across the skin also decreased. By stirring the

receptor medium in the diffusion cell chamber, the concentration gradient was decreased and absorption increased. The only restriction to percutaneous penetration was then the permeability of the compound.

b) Skin viability

The viability of skin *in vitro* is a key issue when investigating metabolism of dermally absorbed compounds. Clark *et al* (1991), measured the viability of Wistar rat skin in static and flow-through diffusion cells. Skin was dermatomed to 280μm and receptor medium was set at a flow rate of 1.5ml/h. Viability was assessed by phenylacetate esterase activity, NADPH cytochrome reductase activity and glucose utilisation. Five receptor media were tested for maintaining viability, these were phosphate buffered saline (PBS), Hank's balanced salt solution (HBSS), Eagles minimum essential medium (MEM), RPMI1640 and Dulbecco's MEM/F12 Ham medium. It was observed that greater viability was maintained with split-thickness skin than full thickness skin. Flow-through cells maintained viability longer than static diffusion cells and that the nutrient containing media prolonged viability more efficiently than salt based solutions.

MEM, HHBSS and Dulbecco's modified PBS were reported to sustain aerobic and anaerobic glucose utilisation and testosterone and estradiol metabolism for 24 hours in dermatomed fuzzy rat skin (Collier *et al*, 1988). PBS did not sustain viability or metabolic activity. FCS was not required to maintain viability, but was instead found to be a disadvantage, as it made extraction of metabolites from the receptor medium more difficult.

c) Skin storage

Skin may need to be stored before it can be used and this can be done in three ways, it can be frozen, freeze-dried or stored in medium at 4°C.

Swarbick *et al* (1982), compared the permeability of human skin that was stored frozen at -17°C with skin that was stored dried and fresh human skin. The frozen skin was thawed to room temperature and the dried skin rehydrated. It was observed that the permeability of fresh and dried skin to chromone acid was similar, whereas the permeability of frozen skin was significantly higher. This suggested that skin underwent structural damage during freezing that compromised its barrier function. Harrison *et al* (1984), studied the effect of freezing skin on it's permeability to water. Skin frozen up to 466 days showed no significant difference in permeability from fresh skin.

Freezing or freeze-drying skin may or may not lead to a decrease in the percutaneous penetration of a compound, as it is dependent upon the compound being investigated. If skin is to be stored, the affect of storage should be tested.

Viability of human skin stored in tissue culture medium was assessed by its ability to be grafted to nude mice and RPMI1640 medium was found to be a successful medium as well as MEM with Hepes buffer. Skin could be stored for up to 1 week without significant loss to structural integrity and viability (Reifenrath and Kemppainen, 1991).

d) Preparation of skin for diffusion cells

Skin can be used in the *in vitro* diffusion cells full thickness or split thickness. Split thickness skin can be prepared by dermatoming or by separating the epidermis from the dermis by chemical or mechanical methods. Most investigations into percutaneous penetration of compounds *in vitro* utilise split thickness skin. Full thickness skin is only used when the skin is already thin as in the mouse. Therefore skin from other species is split. Dermatoming removes the epidermis and a small amount of dermis from the full thickness skin, but skin can also be split at the dermal/epidermal junction by heat separation. Human skin will split after two minutes on a hot plate at 50°C or 30 seconds in hot water at 60°C, the epidermis is then pulled away with forceps. Only hairless skin can be separated this way as hairy skin leaves holes in the epidermis. Chemical separation of the skin can be achieved using dithiothreitol or EDTA, but both heat separation and chemical separation lead to a loss of skin viability. Skin may also be split by soaking in 2N sodium bromide (Scott *et al*, 1986), again, with loss of viability. Enzyme separation with dispase for 24h at 4°C leads to a split at the basal membrane leaving a viable epidermis. Collagenase has also been used to split skin, but viability is severely reduced. Therefore, for maximum viability of split thickness skin, preparation by dermatome gives the best result (Bronaugh and Collier, 1991).

e) Washing-in effect

Washing the skin with soap and water is the normal procedure to remove chemical contaminants which may come into contact with the skin. However, several studies have shown that instead of removing the contaminant, washing the skin can lead to an increase in the dermal absorption of a compound. Moody *et al*, (1994a) demonstrated the dermal absorption of DDT through rat, guinea pig, pig and human skin, using flow-through cells, was at a slow and constant rate until washing was introduced. Immediately after washing the rate of absorption increased up to 7 times and is termed the washing-in effect. A similar effect was also seen with the herbicide 2,4-dichlorophenoxyacetic acid (Moody *et al*, 1994b).

f) Animal models

When extrapolating absorption data from animal to man, a suitable animal model must be chosen that will best reflect human skin absorption. Therefore, many investigations have assessed the differences between species.

Dick and Scott (1990 and 1992) measured water permeability through Alderley Park rat and Sprague -Dawley rat skin from ages 10-120 days. There was no significant difference in age or strain on the permeability of skin. For human skin, Wester and Maibach, (1992) observed a wide variation in the permeability, therefore with human skin small sample numbers can give misleading results to permeability data.

For many compounds, absorption through non-living skin *in vitro* can give accurate absorption rates, but the use of fresh skin may be preferred as this can also give information on the formation of therapeutic and toxic metabolites during absorption. Human skin would be the ideal tissue to use for *in vitro* studies but it is scarce, especially when required fresh. Animal skin has it's limitations mainly because of the amount of hair compared to human skin. The use of hairless strains can sometimes compensate for this, though this skin is usually thinner and therefore more permeable (Bronaugh and Collier, 1991). Absorption of the hydrophilic compound diquat (Scott and Corrigan, 1990) and the lipophilic compound dinitrochlorobenzene (Scott *et al*, 1986), in the static diffusion cell with ethanol/water receptor medium, have shown that rodent skin is more permeable than human skin. The permeability of skin to diquat in different species was found to be in the order of guinea pig > rabbit > mouse > rat >> human. Rat skin was 4 times more permeable than human skin. Permeability of skin to dinitrochlorobenzene follows the order mouse > rat >> human, with rat skin 4 times more permeable than human skin.

Monkey and pig skin are used as animal models as their skin if structurally similar to that of human skin, but absorption rates may still differ (Bronaugh *et al*, 1982). Absorption studies comparing human, pig and rat by Bronaugh *et al*, have shown that acetylsalicylic acid was absorbed through all species at a similar rate, but benzoic acid was absorbed only half as quickly through pig skin as with human skin. Urea was absorbed through pig and human skin at similar rates. Bartek *et al*, (1972) investigated the absorption of cortisone, testosterone, caffeine and butter yellow through the skin of rabbit, rat, pig and human and found pig skin to have the closest permeability characteristics to human skin for these compounds.

Differences in dermal absorption *in vivo* and *in vitro* between species has also been investigated with the penetrant *N,N*-diethyl-m-toluamide (DEET), by Moody and Nadeau (1993). It was observed that *in vitro* permeability increased in species from hairless guinea pig, pig, rat human, to rhino mouse, with 11±1.4%, 18±0.8%, 21±2.2%, 28±4.4% and 36±27.5% (mean±error) of applied dose being absorbed respectively. *In vivo* data showed that the *in vitro* model underestimated the amount of dermal absorption for all species.

To summarise, a good animal model should give the same percutaneous absorption profile for a compound as human skin, but when such an animal model does not exist, then one that has an absorption profile consistently different from human skin should be used so that extrapolation to predict human absorption can be applied.

Chapter 5

Xenobiotic metabolism during percutaneous absorption

Percutaneous absorption and metabolism

5.1 Introduction

The absorption of xenobiotics through skin may be accompanied by metabolism. Skin metabolism occurs at a much lower rate compared to other tissues such as liver, but nevertheless, is extremely important, the relevance of which becomes more apparent when xenobiotics become activated into toxic compounds or carcinogens. The study of metabolism with skin homogenates does not take into account factors such as rate of absorption, accessibility to metabolising enzymes or binding to skin proteins and therefore does not give a true picture of skin metabolism during percutaneous penetration. Rapid penetration of compounds results in minimal metabolism, but slowly absorbed compounds reach the viable skin layer at a reduced rate which can result in greater metabolism. Characterisation of xenobiotic metabolism during percutaneous absorption is therefore essential for understanding the fate of compounds and the possible toxicological consequences.

5.2 In vivo percutaneous absorption and metabolism studies

Investigations into skin metabolism *in vivo* are extremely difficult. Differentiating the metabolism performed by the skin from the systemic metabolism is the major obstacle. Methodologies have therefore been developed to tackle this problem.

Benzo[a]pyrene metabolism to the 7,8-dihydroxy 9,10-epoxy-7,8,9,10-tetrahydrobenzo[a] pyrene by aryl hydrocarbon hydroxylase leads to the formation of DNA adducts. These occur locally after benzo[a]pyrene administration and therefore can be used as a measure of local metabolism. By this method benzo[a]pyrene metabolism has been demonstrated in neonatal rat skin, mouse skin and human skin and also shown to be inhibited by pretreatment with ellagic acid, an inhibitor of aryl hydrocarbon hydroxylase (De Tito *et al,* 1983; Huckle *et al,* 1986; Watson *et al,* 1988).

The metabolism of aldrin to dieldrin in rat skin has been measured *in vivo* by removal of the skin at time points after topical application of the pesticide. Thus a profile of skin metabolism could be followed with time. This was compared to metabolism at a non-application site to show that metabolism occurred at the application site alone (Graham *et al* 1991).

5.3 In vitro percutaneous absorption and metabolism studies

In vitro methods are more often employed in the study of absorption and metabolism of xenobiotics through skin as they allow the identification of metabolites without the interference from non-cutaneous metabolism. As described earlier, two systems have been used to study *in vitro* metabolism, the static and the flow-through diffusion cells. Keeping the skin viable is the major prerequisite in studying metabolism and several media have been reported to maintain viability for 24 hours, including MEM, RPMI1640 and Hanks buffered saline (Collier *et al*, 1989; Clark *et al*

1992, Van De Sandt *et al,* 1993; Moody *et al,* 1994). However, a problem with using medium is the inability of lipophilic chemicals to partition out into an aqueous receptor. This leads to an underestimation in the percutaneous penetration of lipophilic compounds. When simultaneously investigating metabolism, this can also lead to an overestimation of absorbed metabolites.

The major route of exposure to pesticides is through the skin and percutaneous absorption and metabolism of pesticides has received more attention than other xenobiotics for evaluation of their safety. Metabolism of aldrin was shown with mouse skin microsomes by Rettie *et al,* (1986), but metabolism was very low compared to the liver. The metabolism of aldrin during percutaneous absorption in rat skin *in vitro* using the static cell system was also shown to be very low (Macpherson *et al,* 1991). Another pesticide, carbaryl, has also been examined and although its metabolism to naphthol sulfate and naphthol glucuronide has been shown in skin homogenates, it could not be demonstrated in rat skin *in vitro* using static diffusion cells. It was suggested that slow percutaneous absorption and inaccessibility to metabolising enzymes account for the difference (Macpherson *et al,* 1991).

The absorption and metabolism of the pesticide butachlor, (2-chloro-2,6-diethyl-*N*-(butoxy methyl)acetanilide has been studied in human skin *in vitro.* A dose of 1μg applied to skin results in 5% being absorbed at 24 hours. Of the absorbed dose 0.19% is found in the skin as the metabolite 4 hydroxy butachlor and 3.4% as butachlor. Material found in the receptor medium consisted of 0.007% glucuronide, 0.04% cysteine and 0.013% glutathione conjugate (Ademola *et al,* 1993).

Van De Sandt *et al* (1993), measured the percutaneous absorption and metabolism of propoxur through rabbit, pig and human skin *in vitro.* The rate of absorption was similar in rabbit and human skin, but twice as fast through pig skin. Of the absorbed dose, 11-50% was metabolised. All three species showed phase I metabolism to the 2-isopropylphenol (IPP), though each species had a specific phase II metabolic profile. Rabbit skin further metabolised IPP to the glucuronide, human skin metabolised IPP to the sulfate while pig skin metabolised IPP to glucuronide and sulfate metabolites in equal amounts. Rabbit skin was shown to metabolise propoxur with doses up to 200μg/cm^2 while human skin metabolism became saturated by 100μg/cm^2.

Bronaugh *et al* (1990), studied the absorption and metabolism of DDT, acetylethyl tetramethyl tetralin (AETT), caffeine, butylated hydroxytoluene (BHT) and salicylic acid in the fuzzy rat using static diffusion cells for 24 hours with MEM and 10% FBS as receptor medium. It was observed that a majority of the applied caffeine and salicylic acid was absorbed into the receptor medium while DDT, AETT and BHT remained in the skin. AETT and BHT metabolites were found in the skin and the receptor medium. BHT was metabolised to 4-hydroxy BHT (6.6%), while AETT was metabolised to an unknown moiety (1.9%). DDT, caffeine and salicylic acid were not metabolised in detectable amounts. The results demonstrated that absorption could be small, especially with lipophilic compounds and in conjunction, that metabolism could be undetectable or

absent. The fact that metabolism was shown was important itself, for identifying the potential of toxicological pathways.

Nitroglycerin, used in the treatment of angina pectoris, is one of the most successful drugs administered by dermal absorption. It is metabolised to 1,2 and 1,3 glyceryldinitrate. Post mitochondrial mouse homogenates have demonstrated that 30% of nitroglycerin is metabolised to these metabolites when in the presence of glutathione, but only 5% when glutathione is absent. The percutaneous absorption of nitroglycerin from different formulations results in 63% of the absorbed dose being metabolised from aqueous solutions, 49% from dermal patches and 35% from ointments. Though less of the topically applied nitroglycerin is absorbed when in an aqueous formulation, more is metabolised, therefore the lower the absorption flux, the higher the rate of metabolism, possibly due to greater exposure time to the metabolising enzymes (Higo *et al*, 1992).

Kao *et al* (1985), studied the absorption and metabolism of benzo[a]pyrene and testosterone through rat, mouse, rabbit, guinea pig, marmoset and human skin *in vitro* with static diffusion cells containing MEM culture medium. Both benzo[a]pyrene and testosterone metabolism resulted in a full spectrum of metabolites. Frozen skin showed no metabolism and was used as a control. Mouse skin had the highest permeability and a significant difference in metabolic profiles was observed between species. The results also showed that enzyme inhibition with potassium cyanide led to a reduction in absorbed xenobiotic, therefore metabolism was shown to increase percutaneous penetration.

Also observed is the metabolism of phenanthrene during percutaneous absorption through hairless guinea pig skin (Ng *et al*, 1991). *In vivo* and *in vitro* absorption rates have been shown to be the same, but only when a receptor medium of Hepes buffered Hank's balanced salt solution with 4%BSA was used in the flow-through diffusion cells. With the use of the *in vitro* system the metabolites were recovered and identified. Approximately 7% of the applied dose was metabolised to the 1,2- ,3,4- and 9,10- diols.

The metabolism of retinyl palmitate to retinol is via esterase hydrolysis. Further metabolism by alcohol dehydrogenase leads to retinoic acid. Retinyl palmitate dissolved in acetone was applied to the skin of guinea pig and human in the flow-through cell. At 24 hours, 30% and 18% of the applied dose was absorbed into the guinea pig and human skin respectively, but less than 1% was found in the receptor medium. In human skin, 44% of the absorbed dose was found as retinol (Boehnlein *et al*, 1994).

Collier *et al*, (1993) investigated the percutaneous absorption and metabolism of azo dyes in Sencar mouse, guinea pig and human skin. The compounds phenylazo-2-naphthol (Sudan 1), phenylazophenol (SY7) and 5-(phenylazo)-6-hydroxynaphthalene-2-sulfonic acid (ANSC) were used. The metabolism by cytosolic and microsomal enzymes was also characterised. Table 5.1 summarises their results.

Table 5.1 Percentage of absorbed Sudan 1, SY7 and ANSC through mouse, guinea pig and human skin after application of 5μg/cm^2 to skin in the flow-through cell (Collier *et al*, 1993).

	Sudan 1	SY7	ANSC
Sencar mouse	32.8	64.1	< 5
Guinea pig	57.6	67.8	< 5
Human	26.4	36.1	< 5

The results showed that human skin was less permeable to the azo dyes than mouse or guinea pig skin. ANSC was poorly absorbed through skin of all species. Sudan 1 and SY7 was extensively reduced (29% and 26.5% respectively) after absorption through human skin. Greater than 50% of Sudan 1 and SY7 was reduced in mouse and guinea pig skin. It was also shown that SY7 was reduced by mainly cytosolic enzymes, whereas Sudan 1 was reduced by both cytosolic and microsomal enzymes.

Storm *et al* (1990), measured the absorption and metabolism of benzo[a]pyrene and 7-ethoxycoumarin through mouse, guinea pig and human skin *in vitro*. Skin was dermatomed, except for mouse which was used full-thickness and placed on flow-through diffusion cells with Hepes buffered Hank's balanced salt solution as receptor medium. Benzo[a]pyrene was absorbed into the skin but not found in the receptor medium due to its high lipophilicity. However, benzo[a]pyrene metabolites were found in the receptor medium and accounted for 6% of the absorbed dose for mouse, 3% for guinea pig and no detectable amount for human skin. 7-Ethoxycoumarin was absorbed by all species to between 50 and 80%. Being more hydrophobic this was found in the receptor medium. Metabolised 7-ethoxycoumarin amounted to less than 1% for mouse and guinea pig skin and less than 0.05% for human skin. Increasing the applied dose of 7-ethoxycoumarin did not lead to an increase in the amount of metabolite formed. Studies on the specific enzyme activities of ethoxycoumarin deethylase and arylhydrocarbon hydroxylase were shown to be very low. Thus it was demonstrated that for benzo[a]pyrene and 7-ethoxycoumarin the low degree of metabolism was associated with the low enzyme activity. Also, low enzyme activity becomes saturated at low doses and metabolism appears at a constant rate.

Chapter 6

Keratinocytes and keratinocyte xenobiotic metabolism

Keratinocytes and keratinocyte metabolism

6.1 Introduction

Keratinocytes are the main cell type of the epidermis, which features up to 50 layers of these cells, depending upon the anatomical site. The layer of cells which is of greatest interest in the epidermis is the stratum basale, where the keratinocytes are at their most undifferentiated, prolific and metabolically active.

The structure and function of keratinocytes has been of immense interest over the last three decades, not only for their role in the skin, but also in the elucidation of the mechanisms which control cellular proliferation and differentiation. Keratinocytes perform many functions in the skin, including protection of the organism from the environment, secretion of endogenous compounds, repair of damaged tissue and regeneration of the epidermis as it desquamates. Approaches have been taken to isolate keratinocytes and maintain their viability in culture in order to study their functions. It is the regulation of differentiation that has been of most importance in keratinocyte research and the driving force of many recent scientific investigations, so as to determine the underlying causes of many skin diseases, such as psoriasis. There has also been growing interest in the utilisation of keratinocytes as a model for skin metabolism, which has found use in the pharmaceutical industry for dermal drug development.

6.2 The development of keratinocyte cell culture

Epithelial cells of the skin have been cultured since the late 1960's, though a homogeneous culture of keratinocytes was more difficult to establish and was not achieved until the early 1980's. Many systems have been employed in the attempt to grow and cultivate keratinocytes. Their development has been motivated by the attempts to use sheets of these cultured keratinocytes for the use in skin grafts to treat severe burns and ulcerations (Pittelkow and Scott, 1986). Keratinocytes from human skin, human hair follicles (Lenoir *et al*, 1988) and from several other species, including canine keratinocytes (Flowers *et al*, 1987), rat keratinocytes (Vaughan *et al*, 1981; Birkedal-Hansen *et al*, 1981; Baden and Kubilus, 1983) and murine keratinocytes (Fusenig and Worst, 1975; Robine-Leon *et al*, 1981) have been successfully cultured.

In 1967, Briggaman *et al* successfully isolated epithelial cells from human skin. The cells were cultured in a medium composed of one part fetal calf serum (FCS) and two parts medium 199, to which penicillin and streptomycin were added to a final concentration of 1000 units/ml and 0.1mg/ml respectively. The viability of these cells was maintained only for several weeks and growth was slow. Since then there have been considerable advances in keratinocyte maintenance and growth, with the gradual improvement in the growth medium and its specificity for keratinocytes. This has helped characterise keratinocyte growth and development, maturation and properties such

as attachment and detachment and mechanisms of substrate movement across membranes. It was therefore important to have a defined culture medium in which to grow and observe keratinocytes in their proliferating and differentiating stages.

The tissue culture of epithelial cells was initially investigated by Kasarek (1966). Little growth was observed in culture and the chemical parameters that influenced proliferation were poorly understood. Initial media studies found minimal essential medium (MEM) to be the optimum choice and the pH was identified to be a determining factor of cell growth. Keratinocytes are highly sensitive to pH and conditions which are greater than 7.8 or less than 7.0 retard growth markedly.

Numerous attempts were carried out to cultivate keratinocytes as monolayers (Briggaman *et al*,1967: Yuspa *et al*, 1970; Karasek 1971; Fusenig 1971) with little success and subcultivation had poor results. The first reported serial cultivation of keratinocytes was by Rheinwald and Green in 1975, who used a technique in which cells were grown on a lethally irradiated feeder layer of murine 3T3 cells and a medium composed of Dulbecco's modified Eagles medium (DMEM), 20% fetal calf serum (FCS) and hydrocortisone (0.4mg/l). Under these conditions cell growth was achieved and the addition of epidermal growth factor (EGF) substantially increased cell proliferation and culture life span. Rheinwald and Green's technique of culturing keratinocytes on an irradiated cell feeder layer provided excellent short term growth but had disadvantages, the most notable being the presence of the feeder layer and the use of serum. The culture medium therefore contained chemically undefined components, which then stimulated the search for a serum-free medium of comparable effectiveness.

Keratinocytes have been grown in a variety of media. Fusenig (1975) used MEM with a 4x concentration of amino acids, vitamins and 20% FCS. Eisinger (1979) used MEM containing non-essential amino acids, 10%FCS and hydrocortisone (0.4μg/ml). Rheinwald modified his technique in 1980 with the use of DMEM with 10%FCS, hydrocortisone (0.4μg/ml) and EGF, on an irradiated mouse 3T3 cell feeder layer. In 1982 Dykes *et al*, effectively grew keratinocytes using DMEM and FCS as in the Rheinwald technique, but without a feeder layer of lethally irradiated 3T3 cells.

At the same time as Rheinwald was developing his techniques, Peehl and Ham (1980a) also found a method of culturing keratinocytes not requiring the feeder layer, by using a mixture of Ham's medium F12, 5mg/ml of dialysed FCS (dFCS) and hydrocortisone (10mg/ml). Additional components were later added for their ability to enhance colony growth of keratinocytes and a new formulation was derived, called MCDB150 (Peehl and Ham 1980a). MCDB is an acronym for molecular and chemical developmental biology of the University of Colorado and each new media developed was designated a new number. The amount of dialysed FCS was reduced and additional optimisation led to MCDB151 (Peehl and Ham 1980b). Culture conditions reached a point where fibroblast growth was inhibited and adenine and calcium levels were adjusted to support this. MCDB151 was optimised by Boyce and Ham in 1983 by the addition of trace elements and named MCDB153. Subsequently, MCDB153 was found to no longer require serum, with no loss in growth efficiency, therefore the medium now contained no undefined components. Tsao *et al*, (1982) added

several supplements including epidermal growth factor (EGF), hydrocortisone, transferrin, insulin, ethanolamine and phosphoethanolamine, which led to a completely defined serum-free medium. The calcium concentration was also a determining factor in the use of this medium. Low calcium concentrations (0.03mM) supported proliferation of keratinocytes and differentiation was suppressed. Raising the calcium concentration triggered keratinocyte differentiation. The specificity of the keratinocyte medium has led it to become the standard for maintaining keratinocyte cellular growth and function *in vitro*.

Epithelial cells were renowned for their difficulty to culture due to their slow growth and contamination by the much faster growing fibroblasts. With the use of MCDB153, the serum-free defined medium, these difficulties were overcome due to it's selectivity against fibroblast growth. The presence of serum which interferes with metabolic studies was eliminated and since then, the defined medium has become the desirable approach for characterising keratinocyte metabolism.

6.3 Isolation of keratinocytes

Several methods have been developed for isolating keratinocytes from skin. These include the explant method (Green,1975; Fischer *et al*, 1980), the trypsin method (Rheinwald, 1980) and the dispase (neutral protease) method (Kitano and Okada, 1983). The explant method is the least traumatic towards the cells of the skin, but is slow and leads to fibroblast contamination. Dispase is an enzyme from Bacillus *polymyxa* that digests specifically at the basale membrane, splitting the epidermis from the dermis. After splitting the epidermis from the dermis with dispase, the epidermis is incubated in trypsin at 37°C just long enough for the cells of the stratum basale to be detached. This method is most suited to isolating keratinocytes quickly, reducing trauma to cells on exposure to trypsin and minimising fibroblast contamination. From a sample of human foreskin ($1cm^2$), up to $3x10^6$ cells can be obtained for culturing (Watt, 1988). Trypsin used alone to isolate keratinocytes from skin, especially from human skin, may result in low yields of viable cells. Barton and Marks (1981) studied the changes to keratinocytes on short term exposure to trypsin and found invagination of desmosomes and vacuolation of the cells, therefore limiting the use of this enzyme. Trypsin is therefore used at low concentrations and short exposure times during the passaging of keratinocytes.

6.4 Factors required for keratinocyte growth in culture

The keratinocytes medium was developed for both primary and secondary cultures and contains specific growth factors which have been identified for optimum keratinocyte growth. A detailed description of each of the components is as follows:

Epidermal Growth Factor (EGF)

Epidermal Growth Factor (EGF) is an essential mitogen for human keratinocytes and improves proliferation by 20% and receptor sites have been found for EGF on these cells (O'Keefe *et al,* 1982). EGF has been shown to be a 60KD polypeptide, that acts as a mitogenic stimulant for epidermal and epithelial cells and can be used as a substitute for serum in conjunction with other additives and hormones like insulin and transferrin (Cohen, 1960). Added to cultures on a feeder layer, Rheinwald and Green (1977) showed that the keratinocyte colonies were less stratified, more evenly distributed and continued to grow exponentially until confluent in the presence of EGF. In the absence of EGF, passaged cells slowed down their rate of growth, but a concentration of 20ng/ml, EGF appears to exert it's optimum action. Higher concentrations can cause excessive flattening and decreased proliferation of keratinocytes (Green, 1979).

Hydrocortisone

Hydrocortisone is an established mitogenic compound (Gilchrest, 1981) and increases proliferation of keratinocytes both in the presence and absence of serum. Interestingly, topical application of hydrocortisone, or systemic administration inhibits proliferation, but in a defined culture medium it will stimulate cell growth. Hydrocortisone was first used by Peehl and Ham (1980) at above the physiological range of 100μg/ml. Tsao *et al,* (1982) showed that 10x this concentration had the greatest effect. Hydrocortisone also maintains regular epithelial appearance of passaged cultures, while increases colony size (Wille *et al,* 1984). Rat keratinocytes require at least 0.1μg/ml hydrocortisone for initial attachment and increasing the concentration to 50μg/ml also leads to an increase in cell proliferation (Vaughan *et al*, 1981).

Transferrin

Transferrin is an Fe^{2+} binding protein that stimulates growth. Transferrin can be omitted from growth medium if the concentration of zinc and iron are increased.

Insulin

Insulin promotes the uptake of glucose and amino acids and is added to cultures in the range of 100ng/ml to 500μg/ml. It is required for clonal growth and is a standard component of serum free medium. It is used at a supraphysiological concentration to exert its growth benefits and because it rapidly loses it's bioactivity (Shipley and Pittlekow,1987).

Amino acids

Amino acids, which include isoleucine, histidine, methionine, phenylalanine, tryptophan and tyrosine, are found to be a limiting factor in keratinocyte proliferation (Shipley and Pittlekow 1987). Supplementing MCDB153 medium with additional amino acids has been described by Pittlekow and Scott (1986). Isoleucine deficiency in rare clinical cases leads to a form of acral dermatitis, therefore its necessity in keratinocyte culture is not unexpected.

Bovine Pituitary Extract

Bovine pituitary extract is chemically undefined but is a very effective growth promoter especially in long term cultures and does not stimulate the proliferation of fibroblasts or keratinocyte differentiation (Boyce and Ham, 1983).

Trace elements

Trace elements are needed for keratinocyte growth and include calcium, selenium, manganese, molybdenum, silicon, tin, vanadium, copper and zinc, being mainly required for enzyme cofactors. Two key ions which dramatically effect keratinocyte growth are calcium and selenium. Calcium is mentioned separately due to its importance. Selenium has a marked effect on promoting clonal growth of keratinocytes (Tsao *et al*, 1982).

Ethanolamine and phosphoethanolamine

Phosphoethanolamine is a proliferation promoting factor isolated from rat pituitary gland extract. Ethanolamine has a similar action (Kano-Sveoka and Erric, 1981). The addition of ethanolamine and phosphoethanolamine as supplements to the medium have been shown to benefit the growth of keratinocytes. This is due to the incorporation of these compounds into the cell membranes of phospholipids of the cultured cells.

Oxygen

The effects of oxygen have been studied by Horikoshi (1986). Under conditions where oxygen concentration varied from 1-89%, with 5%CO_2, it was observed that 18% oxygen (a tension of 133mmHg) resulted in the optimum growth of human neonatal keratinocytes. Growth rate was retarded at oxygen concentrations above 20%. It was noted that when plating out keratinocytes into tissue culture flasks, an oxygen concentration of 2% facilitated plating efficiency and gradually increasing the oxygen to 18% lead to optimum growth conditions and keratinocyte harvest.

pH and temperature

Optimal growth was first shown to be at pH 7.2 to 7.4 by Karasek (1966), but proliferation was still effective as low as pH 5.8. Further studies on the influence of pH on keratinocyte growth by Hawley-Nelson *et al*, (1980) validated optimal growth rate at pH7.2 (Figure 6.1). Cells that were maintained between pH7.0-7.2 survived 5 passages while cultures at pH7.4 only survived 2 passages. Below and above pH7.0-7.4 cells could not be successfully subcultured. Studies on growth of keratinocytes at 36.5°C, 34°C and 31°C showed that growth rate was 2.4 times greater at 36.5°C than 34°C and 17 times greater than at 31°C. The ability to passage cells was also influenced by temperature, with cells at 36.5°C being passaged more successfully.

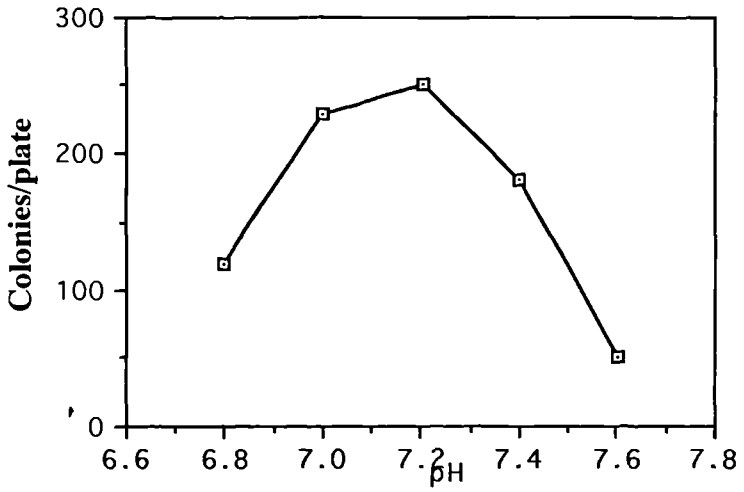

Figure 6.1 Effect of pH on human keratinocyte cell growth. Studied using medium199 with 10%FCS (Hawley-Nelson *et al*, 1980).

Calcium

The effects of calcium on keratinocyte growth were investigated by Dykes *et al* (1982) and Boyce and Ham (1983) and they found that not only could cell differentiation be controlled but that calcium was involved in cyclic nucleotide metabolism. At 0.3mM a maximum growth rate was obtained, fibroblast growth was retarded and differentiation was substantially reduced (Boyce and Ham, 1983). Human keratinocytes grown in MCDB153 with a calcium concentration of 70μM proliferate rather than differentiate and concentrations of 1.0mM and greater trigger keratinocytes to differentiate (Gillespie *et al*, 1989). Calcium at above 1.0mM increases the growth of fibroblasts, but by lowering the concentration fibroblast growth is reduced to give preferential growth to the keratinocytes. At a concentration of 0.1mM, calcium has been shown by Watt and Green (1982) to allow keratinocytes to produce involucrin, a protein subunit of cornified envelopes, indicating the terminal differentiation of these cells.

Rhodanile blue (MacConaill and Gurr, 1964) is a histological stain that can be use to differentiate between differentiated and undifferentiated keratinocytes. Differentiating keratinocytes produce keratin which stains violet to red, whereas undifferentiated cells stain blue.

6.5 Keratinocyte metabolism in vitro

Many biochemical pathways and enzymatic systems have been characterised in cultured keratinocytes. They have been shown to possess xenobiotic metabolising potential including phase I and phase II pathways and though these activities may be low compared to tissue such as liver, their significance may be of great importance as in the formation of toxic and carcinogenic metabolites.

a) Cytochrome P450 monooxygenases

Pendlington *et al*, (1994) measured P4501A1 and 2B activity in mouse, rat and human epidermal and sebaceous gland cells. Cells from each species were isolated by density gradient centrifugation and enzyme levels were measured using EROD and PROD. EROD and PROD could only be found in control mouse with increasing activity found in the different cell types from sebaceous cells < basal cells < differentiated keratinocytes. Activity was only detectable in rat cells after induced by ß-naphthoflavone for EROD and phenobarbital for PROD. Enzyme activities were not found in human skin cells. Antibodies raised to CYP1A1 and CYP2B and subsequent staining showed the distribution of enzymes was the same in all species in the epidermal cells and sebaceous cells, with higher amounts found in mouse than rat and low levels in human.

Similar investigations by Pham *et al*, (1990) also used 7-Ethoxyresorufin and 7-pentoxyresorufin to investigate P450 activity in cultured human keratinocytes and showed there were detectable levels of these enzymes. Their findings suggest that the substrates 7-ER or 7-PR are more sensitive than 7-EC for detecting these enzymes.

Raffali *et al*, (1994) demonstrated ECOD activity in human keratinocytes grown in Earles medium with 10% FCS. Activities varied widely between individuals and ranged from 5pmol/h/mg to 28pmol h mg. Although ECOD activity could be shown, no EROD or PROD was detectable, therefore indicating very low concentrations of P450. Induction of enzyme activity with 3-methylcholanthrene treatment (0.5μM) for 24 hours increased ECOD activity by 45 times and EROD 33 times.

Bickers *et al*, (1982), studied the metabolism of benzo[a]pyrene and 7-ethoxyresorufin in cultured Balb/C mouse keratinocytes and compared it to metabolism seen in the mouse epidermis. Keratinocytes were grown as monolayers in medium 199 with fetal calf serum for 3 days. Keratinocytes and epidermis were then treated with benzo[a]pyrene for 24 hours prior to metabolism studies. The metabolism of benzo[a]pyrene and 7-ethoxyresorufin was then measured and the results are shown in table 3.1. The P450 activity in keratinocytes was found to be 30% of that found in

epidermis of the same age, suggesting the need of a differentiated multilayered cell system for full enzyme activity to be expressed.

Table 6.1 The metabolism of benzo[a]pyrene to hydroxybenzo[a]pyrene and 7-ethoxyresorufin to resorufin in Balb/c mouse keratinocytes and epidermis. (pmole product/min/mg mean±sem).

	Keratinocytes		Epidermis	
	Control	Benzo[a]pyrene treated	Control	Benzo[a]pyrene treated
Benzo[a]pyrene hydroxylation	0.72 ±0.04	10.84 ±1.30	2.21 ±0.26	26.22 ±2.41
7-ethoxyresorufin deethylation	0.12 ±0.01	0.45 ±0.06	0.34 ±0.03	1.34 ±0.21

ECOD activity was also investigated in cultured monolayers of mouse keratinocytes grown in low calcium (0.04mM). Levels were determined to be 52.5±13.5pmol/h per 10^6 cells. After cells were exposed to a higher calcium concentration (1.2mM) for 12-24 hours, an increase in ECOD activity to 281±72.9pmol h per 10^6 cells was observed. EROD activity was only detectable in cells exposed to high calcium and had an activity of 4.4±1.1 pmol/h per 10^6 cells. The effect of calcium demonstrated the requirement for differentiation on enzyme activity (Reiners *et al*, 1990).

Guo *et al*, (1990) measured AHH activity in keratinocytes isolated form neonatal rat skin. Activity increased 2.5 times *in vivo* after exposure to benz(a)anthracene and 7 times after *in vitro* induction. Differentiated cells showed activity 7 times higher than undifferentiated cells in both noninduced and induced cells *in vivo* and *in vitro*. Immunocytochemical staining to P4501A1 showed binding to lower spinous cells of the epidermis and increased staining in induced cells. Therefore supporting the evidence that differentiated cells have higher capacity to metabolise than undifferentiated cells.

Levels of cytochrome P450 activity in isolated cells and cultured cells vary markedly between groups in the published literature. Where one group may find P450 activity in human cells, another may not. The diversity of culturing techniques and medium used to grow keratinocytes may account for some of the discrepancies, but not all. A greater knowledge in what factors that are required for keratinocytes to express P450 activity is needed. One area has already been identified, that is the level of cellular differentiation. Obviously the complexities of the skin cannot be reproduced in isolated cells or cultured monolayers, but their use does highlight some of the mechanisms behind enzyme activities.

b) Esterases

Esterases have attracted little attention in isolated keratinocytes and characterisation of these enzymes has not been approached. Stadler *et al*, (1989) utilised esterase activity in human keratinocytes to measure cellular proliferation in culture. Hydrolysis of 4-methylumbelliferyl heptanoate by non-specific esterases to the fluorescent metabolite 4-methylumbelliferone was used as a marker. Cell numbers were then quantified by the degree of fluorescence with time.

c) Glutathione-S-transferases

Glutathione, the major antioxidant defence of most tissues is also present in keratinocytes. All the components of the glutathione pathway, which include glutathione reductase, glucose-6-phosphate dehydrogenase and isocitrate dehydrogenase have been found in the skin and in isolated keratinocytes (Vessey and Lee, 1993; Yohn *et al*, 1991; Blacker *et al*, 1991). Vessey and Lee 1993 studied the soluble components of sonicated keratinocytes for enzyme assays. Measurements on Glutathione-S-transferases (GST's), selenium dependant and selenium non-dependant glutathione peroxidase, glutathione reductase, glucose-6-phosphate dehydrogenase and isocitrate dehydrogenase were measured to evaluate the effect of peroxides on cultured human keratinocytes. Hydrogen peroxide was found to be far less toxic than organic peroxides such as t-butyl hydroperoxide and cumene hydroperoxide due to the inhibition of enzymes in the glutathione pathway by organic peroxides.

Blacker *et al*, (1991) measured GST activities in the human keratinocyte cytosolic fraction and characterised the effect of confluence and differentiation on activity. Only the π isoform was found and as the keratinocytes proliferated and differentiated, the GST activity increased. Table 6.2. indicates the GST activity of keratinocytes at increasing stages of confluence.

Table 6.2 Effect of degree of confluence and differentiation on GST activity in cultured human keratinocytes (Blacker *et al*, 1991).

Degree of confluence	Activity (μmoles/min/mg protein)
10%	0.245±0.035
40%	0.348±0.005
65%	0.377±0.035
100%	0.626±0.052
3 days differentiation	0.718±0.095

d) Other enzyme reactions

Other possible metabolic activities which can be assessed are conjugations. e.g. minoxidil is transformed to minoxidil sulfate by sulfotransferases. Studies have used minoxidil as a substrate for sulfotransferases in the skin, especially in elucidating it's pharmacological property to promote hair growth. This activity has been shown to be detectable in human keratinocytes. Glucuronidation was also demonstrated in cultured human keratinocytes at levels 25-50% of that found in rat skin using 1-naphthol as a substrate. Human keratinocytes also displayed epoxide hydrolase activity at similar levels to rat skin (Pham *et al*,1990).

The metabolism of propanolol by split thickness human skin in organ culture and by keratinocytes has been seen to produce three metabolites, propanolol glycol, naphthoxyacetic acid and minor quantities of *N*-desisopropylpropanolol. Cultured fibroblasts also metabolise propanolol to form these metabolites, but to a much lesser extent. The metabolism has been identified to be via monoamine oxidase and P450 monooxygenases. Induction of the cultured keratinocytes by Ca^{2+} resulted in an increase in the *N*-desisopropylpropanolol metabolite (Cormier *et al*, 1991).

6.6 Applications of cultured keratinocytes

Human keratinocytes are cultured from the skin of burn victims for grafting on to injured epidermis. It is used as a method of generating large numbers of epidermal cells which are highly proliferative and undifferentiated, so that the healing of burn or ulcer wounds is facilitated (Green *et al*, 1979; Pittlekow and Scott, 1986). When a confluent sheet of keratinocytes has been grown, it is removed carefully by treatment with dispase, so as not to damage its integrity. The enzyme breaks hemidesmosomes, linking the basal layer to the flask, without breaking the desmosomes between cells. During detachment from the flask, the epidermal sheet contracts and thickens. The sheet is then placed onto a gauze, to allow it to be grafted on to the patient. (Green *et al*, 1979).

One particular area of interest is the use of cultured keratinocytes as models for toxicity studies. Local and systemic toxicity can be evaluated in simple *in vitro* tests by applying compounds to keratinocyte cultures and measuring the effect by the release of inflammatory mediators or expression of antigens. As keratinocytes are grown in a serum-free chemically defined medium, very low concentrations of inflammatory mediators such as interleukins and arachidonic acid metabolites, or toxic and carcinogenic compounds can be measured. This not only makes keratinocytes a useful cell culture for dermal irritation studies, but also as a cytotoxicity model. The advantages of models such as this is their use in screening large numbers of compounds for possible inflammatory and toxic effects, endpoints that can provide quantitative data and the *in vitro* studies cut down on animal studies. By using human keratinocytes in culture the extrapolation to man is more reliable.

Metabolism of xenobiotics maybe assessed using cultures of keratinocytes, which may then be followed up by further metabolic studies using whole skin. By comparing these systems, an early assessment of the toxicological properties of xenobiotics can be made by extrapolating data from cultures, to *in vitro* skin models and finally to the *in vivo* situation.

The dermal toxicity of surfactants was investigated by Gueniche and Ponec (1993), using cultured human keratinocytes and fibroblasts. Measurements included changes in cell morphology, inhibition of cell proliferation and modulation of interleukin-6 (IL-6) and their results were compared to *in vivo* skin irritancy data. Cell morphology and proliferation results correlated well with *in vivo* irritancy. IL-6 production was seen even before the concentration of surfactants was high enough to induce toxicity, therefore suggesting the measurement of IL-6 could be used as a sensitive test for dermal irritancy.

Cell cytotoxicity can be evaluated using several different markers. The fluorometric marker 4-methylumbelliferyl heptanoate can be used to evaluate viability of cells, which liberate the fluorescent metabolite 4-methylumbelliferone by intracellular esterase metabolism. The method was shown to be reproducible and highly sensitive (KrugerKrasakes *et al*, 1992). Hoh *et al,* (1987), used the Neutral Red (NR) uptake and MTT reduction assays as methods of evaluating cell viability (The MTT assay is where the yellow tetrazolium salt [3-(4,5-dimethylthiozol-2-yl)-2,5-diphenyl tetrazolium bromide] is metabolised by mitochondrial dehydrogenases to a purple formazan precipitate (Mosmann, 1983; Van De Sandt *et al*, 1993) There was a good correlation found (r=0.819) between NR50 values and *in vivo* irritancy data. The NR assay was found to be more sensitive than the MTT assay.

Although any one of the cell viability assays or irritancy tests can be used to assess the response of keratinocytes to potentially toxic compounds, their use is limited for screening out dermal toxicants. Each assay relies on certain biochemical pathways and several *in vitro* assays are usually performed in conjunction with one another to cover a broad range of possible toxicological endpoints. As only one cell type is being assessed for its reaction i.e. the keratinocyte, the full extent of a skin reaction may not be seen. The skin is far more complex and may show effects *in vivo* that are not seen *in vitro*. Therefore more complex culture systems may need to be employed to mimic these conditions. These are covered in the next chapter.

Chapter 7

Living skin equivalents

Living skin equivalents

7.1 Introduction

The living skin equivalent (LSE) is a fully proliferating and differentiating *in vitro* skin model, consisting of a coculture of dermal fibroblasts and differentiating keratinocytes. The aim of developing an LSE was to mimic the physical and chemical properties like of human skin so that it could be used in plastic surgery to aid the healing of burns and ulcerations. It has also provided an opportunity to study xenobiotic metabolism of skin *in vitro* without interference from other tissues. More importantly, the model has also been used as an alternative to animal skin for toxicological testing and penetration studies.

7.2 Epidermal differentiation

In order to construct a synthetic skin model by manipulation of isolated cells from skin *in vivo*, a knowledge of epidermal differentiation was first required. This characterised the way in which the cells of the epidermis function and form the barrier properties of skin. The following description is not intended to be a complete account of epidermal differentiation, but a brief overview of some of the steps which take place.

Only the keratinocytes of the basal layer have the capacity for DNA synthesis and mitosis. As the cells migrate to the surface of the skin they differentiate and produce dead, flattened cells. Basal cells are distinguishable by their network of keratin filaments, which are sparse and made up of keratin K5 (58kD) and K14 (50kD) in a ratio of 1:1. These cells also contain desmosomes which interconnect the cells. The first differentiating layers above the basal layer are spinous cells and contain new keratins K1 (67kD) and K10 (56.5kD) and can be used as markers of differentiation. Above these layers, the cells stop producing keratins and produce the proteins fillagrin and loricrin. Keratinocytes grown as monolayers reach confluence before they differentiate and when they do differentiate they only form a few layers, which do not express the keratins K1 or K10. Calcium is an essential factor in differentiation and the formation of these keratins. In the natural environment keratinocytes grow exposed to the air, sitting on a basement membrane being fed from the dermis below. The differentiating keratinocytes grown submerged in medium do not possess the spinous or granular cell types of epidermis *in vivo*, but growing the culture on a collagen containing matrix at the liquid-air interface alleviates this problem and the cells form a full epidermal tissue. Keratinocytes grown in calcium at a concentration of 0.05mM only grow as monolayers because desmosome assembly is inhibited. Higher calcium levels, 1.2mM leads to the formation of desmosomes and the cells are then able to stratify. Fuchs (1990) has published a review of epidermal differentiation and factors influencing the formation of an epidermis *in vitro*.

7.3 Construction of living skin equivalents

Bell *et al*, (1979), first developed a simple model of skin by using fibroblasts seeded into a collagen gel. This structure contracted to form a lattice matrix of collagen fibres which showed potential for use as a dermal model. In 1983, Bell *et al*, fabricated a more complex dermal equivalent with fibroblasts in a collagen matrix. This supported an epidermis derived from seeding keratinocytes onto the surface of the matrix. This model contained well developed skin structures such as desmosomes, hemidesmosomes and a basal lamina. These were formed within two weeks in a rat skin model and 3 weeks in a human skin model. The rat model was successfully grafted onto the dorsal skin of rats. In 1984 Bell parented a method for the preparation of a Living Skin Equivalent (LSE) (US Patent # 4,485,069.27 November) designed to meet the needs of research.

Lillie *et al*, (1980) grew rat lingual cells (method by Jepsen *et al*, 1980) on collagen rafts made from collagen extracted from guinea pig skin. They were grown at the liquid-air interface supported on stainless steel grids, in minimum essential medium with 20% fetal calf serum. Basal, spinous and keratinised cells were found and it was concluded that the high degree of organisation seen in this structure was a result of feeding the cells from the underside and exposing the surface of the model to the air.

By definition a dermal equivalent is fashioned by dispersing fibroblasts in a polymerised collagen lattice, whereas the LSE is then made by seeding keratinocytes onto the surface of the dermal equivalent. The LSE possesses a stratum corneum with similar properties to the human stratum corneum, but with greater permeability (Bell *et al*, 1991). These two methods are not the only ones which can be used to make a dermal model. Seeding keratinocytes onto the surface of deepidermised dermis leads to the formation of a fully differentiated epidermis that resembles human skin *in vivo* (Régnier *et al*, 1981). Prunieras *et al*, (1983) also grew a similar model with keratinocytes grown on dead deepidermised pig skin. This epidermis showed good morphology, especially at the granular layer. When exposed to the air the skin equivalent grown on deepidermised dermis and the LSE, possess a lipid composition which reflects that seen in human skin with only some slight differences. These are higher amounts of triglyceride and lower levels of linoleic acid, a major component of barrier function. These differences can also be seen in human skin maintained in organ culture and are therefore a result of not being part of the whole animal and being deprived of external factors and not a fault of the cell biology. Keratinocytes are capable of synthesising all the lipids present in *in vivo* tissue, but are formed at different rates. An improvement of culture conditions was suggested to be sufficient to lead to the correct lipid synthesis and composition of the epidermis (Ponec, 1991).

By 1991, Bell *et al*, had developed the LSE with standards high enough for meeting the requirements for commercial applications. These were adequate viability, percutaneous absorption and resistance to chemical damage. They were free of a broad range of viral pathogens and mycoplasma and where the collagen was extracted form a bovine source with high purity and

sterility. The LSE model resembled human skin after 14 days on exposure to the air and expressed a broad range of keratins including K1 at all epidermal layers and involucrin at the spinous and granular layers. Kp values for water through dry human skin ranges from 0.7×10^{-3} to 5.0×10^{-3} cm/hr. The usual for an LSE is 30.0×10^{3} cm/hr. Inadequate LSE's have Kp's of 10-50 times this value. Hydrocortisone has a Kp two orders higher than for human skin but is reproducible. This made it possible to create data tables for LSE's for reference and evaluations.

One of the most important aspects of a developing LSE is the cellular interactions at the epidermal-dermal junction. As keratinocytes proliferate and differentiate they form tonofilaments and desmosomes which form the structures between the cells. Hemidesmosomes anchor the basal cells to the underlying dermal matrix and form a basal lamina. This only occurs in the presence of a type IV collagen support. Fibroblasts grown within a dermal matrix provide not only the structural support, but also the necessary factors required, including type IV collagen, for the development and formation of the basal lamina (Contard *et al*, 1993).

Usually the collagen matrix was derived from growing dermal fibroblasts in a collagen gel, but a dermal model can also be fabricated by fibroblasts seeded onto a nylon mesh and grown until a dermal like structure is obtained. This leads to a matrix consisting of collagen proteoglycans and glycosaminoglycans as seen *in vivo*. Keratinocytes are seeded onto the dermal model and grown at the liquid/air interface until a differentiated epidermis and stratum corneum layers are formed. It has been shown that the epidermis contains the appropriate differentiation markers including keratin and involucrin (Slivka and Zeigler, 1993).

Slivka *et al*, (1993), characterised an LSE model where the fibroblasts were grown on a nylon mesh for 4 weeks to form a dermis, which was then frozen at -70°K in medium + 10%DMSO. Keratinocytes were grown on the resulting matrix for 3-7 days submerged in medium, the at the liquid-air interface for a further12-14 days. It was found that the dermal matrix was rich in collagens type I, III, IV and morphology of the final LSE epidermis was similar to human skin *in vivo*. The stratum corneum contained upto 8-10 layers and differentiation was confirmed by the presence of keratin K1 and involucrin.

Alternatively, keratinocytes have been grown on Millipore Millicell microporous membranes overlaid with a collagen gel. Differentiation of the epidermis lead to 20 cells in 5-7 days (Cook, *et al*, 1992).

Horiguchi *et al*, (1994) characterised the basal layer in two LSE models, one where keratinocytes were grown on a type I collagen gel and another where keratinocytes were grown on an extra cellular matrix gel derived from murine EHS sarcoma. Antibodies raised to collagen type IV, VII and keratins (68-kDa (LDA-1), 50-kDa, 58-kDa) were used to assay collagen and keratin expression in the skin models. The artificial epidermis grown on a collagen gel was only four to eight layers thick. The basal cells were small, desmosomes were sparse, hemidesmosomes were not

formed. The artificial epidermis grown on the dermal matrix showed a thick layer of keratinocytes, with cell layers appearing indistinguishable from human epidermis *in vivo*. There was a well developed network of tonofibrils desmosomes, hemidesmosomes. Expression of type IV and VII collagens, LDA-1 and laminin were only found in the LSE grown on a dermal matrix, factors that only belong to the lamina lucida of a well anchored and differentiated epidermis and therefore judged to have similar characteristics of the epidermis *in vivo*.

Therefore several key factors were recognised for the construction of an LSE. These were the need for a dermal matrix consisting of dermal fibroblasts, which express a broad range of collagen types to provide an anchor and a stimulus for the basal lamina and the epidermis. The medium needs to feed the LSE from the underside, while the surface of epidermis is exposed to the air. Finally, the medium needs to contain calcium for epidermal differentiation and the nutrients required for the growth of the cells. Interestingly, fibroblasts and keratinocytes lack MHC class 2 antigens on their cell surfaces, which are highly specific to each individual and allow the immune system to recognise foreign cells. Thus it is possible to construct an LSE with fibroblasts and keratinocytes from different sources, without the interference of rejection.

Already laboratory grown skin is being manufactured on the production line by several companies, for example, Advanced Tissue Sciences, California,. A decade ago, creating human tissue in the lab seemed like a wild dream, as there were too many obstacles to overcome, especially the complex cell-cell signalling that goes on in the tissue, but this was easier to overcome than was anticipated, as cells are able to achieve cell-cell signalling by themselves once an initial support was provided.

7.4 Percutaneous absorption studies with living skin equivalents

An LSE was found to be more permeable to testosterone than human abdominal skin by 4.3 times when in a water vehicle and 5.7 times in a petrolatum vehicle showing the LSE having only partial barrier function compared to human skin (Ernesti *et al*, 1992). Donnelly and King (1994) studied the permeability of their skin model grown on a nylon mesh with model substrates differing in lipid solubility. These were water, sucrose, urea, benzoic acid, caffeine, hydrocortisone and estradiol. Permeabilities of these compounds ranked in the same order as for human skin, although their permeability values were significantly higher.

7.5 Metabolism in the living skin equivalent

Pham *et al*, (1990) studied the metabolic profile in a reconstructed epidermal model, prepared from the cells of the outer root sheath of human hair follicles. The presence of cytochrome P-450 was strongly suggested by the activity of 7-ethoxyresorufin-*O*-deethylation, 7-pentoxyresorufin-*O*-dependentylation and 7-benzoxyresorufin-*O*-debenzylation resulting in the values of 0.55±0.07, 0.63±0.23, 1.47±0.28pmol/min/mg protein respectively. 1-naphthol was metabolised to the

glucuronide at a rate of 480±10pmol/min/mg protein. The arylsulfation of 4-methylumbelliferone and steroid sulfation of estrone were very low, but detectable and had values of 51.1±5.6nmol/h/mg and 3.26±1.6pmol/h/mg protein respectively.

Slivka, (1992) and Slivka *et al*, (1993) used Skin^{2}™ (Advanced Tissue Sciences, La Jolla, California, USA) to study the metabolism of testosterone. It was found to have a similar metabolic profile as found with neonatal foreskin. Metabolism of testosterone to dihydroxytestosterone and androstene-3,17-diol was inhibited by metyrapone, showing the P450 dependent metabolism. The mixture of polar metabolites also formed included androstane-3,17-dione and androsterone. This indicated that the LSE maintained the metabolic pathways that were present in the parent tissue.

The metabolism of testosterone was also studied with the commercially available LSE called Episkin™ (Imedex, Chapanost, France) by Roguet *et al*, (1994a, 1994b). They measured. ECOD and EROD values of 40pmoles/hour/mg and 16pmoles/hour/mg protein respectively, PROD was undetectable. After 3-methylcholanthrene (10μM) induction ECOD activity increased by 10 times while EROD activity increased by 17 times. Phenobarbital had no significant effect on ECOD or EROD activity. Testosterone permeated through the LSE at a linear rate for 6 hours at 8.33nmoles/hour. The metabolites also formed at a linear rate during penetration at 1.66nmoles/hour and were dihydrotestosterone (41%), androsterone (47%) with small amounts of 7αhydoxy-testosterone, 15ßhydoxytestosterone, 2αhydoxytestosterone and 2ßhydoxytestosterone. Ernesti *et al*, (1992) compared the metabolic profile of testosterone in fresh excised human skin from plastic surgery with an LSE. Testosterone (in acetone) was applied to the surface of the skin and the LSE and incubated for 24 hours at 37°C. A high proportion of the applied testosterone (36-55%) was metabolised and the same metabolites were observed in both human skin and the LSE.

The metabolic profiles shown by these groups illustrates that the LSE has the potential to reflect metabolism as seen *in vivo*. This implies that the LSE has a greater metabolic capacity than the use of keratinocytes alone and suggesting that keratinocytes need a dermal support, as well as to form a differentiated epidermis in order to express their full metabolic capabilities.

7.6 Applications for living skin equivalents

LSE's were initially developed as a medical tool, for covering large burns where natural grafts may be lacking, but the LSE model also provided an opportunity to study epidermal differentiation and wound healing. Applications for the LSE now extend to dermal irritation and toxicity assays and as a test model for topical drugs, cosmetics and wound dressings.

Until recently, most chemicals were only tested for skin toxicity and irritation by the method described by Draize *et al* (1944), but it is now preferable for the *in vivo* tests to be replaced by reliable, simple and inexpensive *in vitro* alternatives. These tests range from keratinocyte cultures to the more elaborate LSE. Organ cultures can also be used as a means of assessing dermal toxicity,

where discs of skin in culture are exposed to chemicals. Effects are evaluated by the cytotoxicity assays MTT and NR uptake (Van De Sandt *et al*, 1993). These are used as indicators of cell viability, while the release of cytokines and prostaglandin E2 and lactate dehydrogenase leakage can be used as signs of cell damage.

Gay *et al*, (1992) used the LSE Testskin™ (Organogenesis, Cambridge, Massachusetts, USA) as a model to evaluate its potential as an *in vitro* model irritancy test. Using the MTT assay as a means to measure cytotoxicity, the value which gave a 50% reduction in MTT conversion by the mitochondrial succinic dehydrogenases was used for comparative data. Eight irritants tested each ranked in the same order of toxicity as for human skin as well as having similar EC_{50} values. Nine chemicals that were classified as non-irritants were also tested and showed no inhibition of MTT conversion. Pro-inflammatory mediators, prostaglandin E2, prostacyclin and interleukin-1α were also detected in the LSE after exposure to the irritants morpholine and hydroxylamine sulfate. It was concluded that the LSE was a good in vitro model for assessing dermal irritancy. Roguet *et al,* (1994a), measured the release of interleukin 1α, a major proinflammatory cytokine and found a correlation with the degree of irritation observed *in vivo.*

As you build a model from cells, to cell suspensions, to monolayers of cells and then to cell layers you get more predictive response. There are still some limitations, as there is an absence of the influence of the whole body as in hormone effects, pharmacokinetics and metabolism. Compared to monolayers of keratinocytes, LSE's are more resistant to cytotoxic effects. Dykes *et al* (1991) used LSE for cutaneous toxicity studies. They studied histological morphology to show toxicological changes induced by benzoyl peroxide gel and found it could not completely mimic human skin *in vivo.* Their explanation was that the LSE could not respond like human skin as human skin contains many other cell types. The introduction of other cell types like melanocytes and Langerhans cells could lead to a more fully functional model with closer characteristics to human skin.

Chapter 8

Dinitrochlorobenzene

Dinitrochlorobenzene

8.1 Introduction

Dinitrochlorobenzene ($C_6H_3ClN_2O_4$), abbreviated to DNCB, has a structure as shown below and has a molecular weight of 202.56. It is obtained by nitrating *o*-nitrochlorobenzene and exists as small yellow crystals.

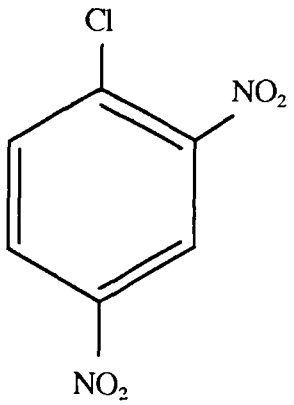

Dinitrochlorobenzene (Cas# 97-00-7) has many other synonyms which include 1-Chloro - 2,4-dinitrobenzene, 2,4-dinitro-1-chlorobenzene, 4-chloro-1,3-dinitrobenzene, 6-chloro-1,3-dinitrobenzene, chloronitrobenzene, dinitrochlorobenzol and DNCB.

The physical properties of DNCB are δ= 1.687, mpt 53-54°C and bpt 315°C. It is practically insoluble in water (8mg/l at 15°C), sparingly soluble in cold alcohol and freely soluble in hot alcohol. DNCB has a $\log P_{oct}$ of 3.38, characterising it as a moderately lipophilic molecule (Leo *et al*, 1971).

It is used as a reagent in the detection and determination of nicotinamide and other pyridine compounds. It is also used in the manufacture of azo-dyestuffs, fungicides, rubber chemicals and explosives. Medically it has been used as an immunostimulant in the treatment of leprosy and some forms of cancer, as well as in the treatment of alopecia and warts.

DNCB is a primary skin irritant and causes severe allergic dermatitis. It has an LD_{50} orally in rats, of 1.07g/kg , and i.p. 280mg/kg. (Smith,1962). DNCB is a strong direct mutagen as assessed with Salmonella typhimurium (Summer and Göggelmann, 1980).

8.2 *Metabolism of dinitrochlorobenzene*

DNCB is metabolised firstly by conjugation with glutathione (GSH), which leads to the formation of the *N*-acetylcysteine derivative. DNCB and other mono or dihalogenated dinitrobenzenes are further metabilised and excreted as mercapturic acids, principly in the urine but also in bile (Bray *et al*, 1958). It's metabolism has been shown to be time and dose dependent and human platelets exposed to DNCB are depleted of GSH with assossiated inhibition of GSH peroxidase activity.

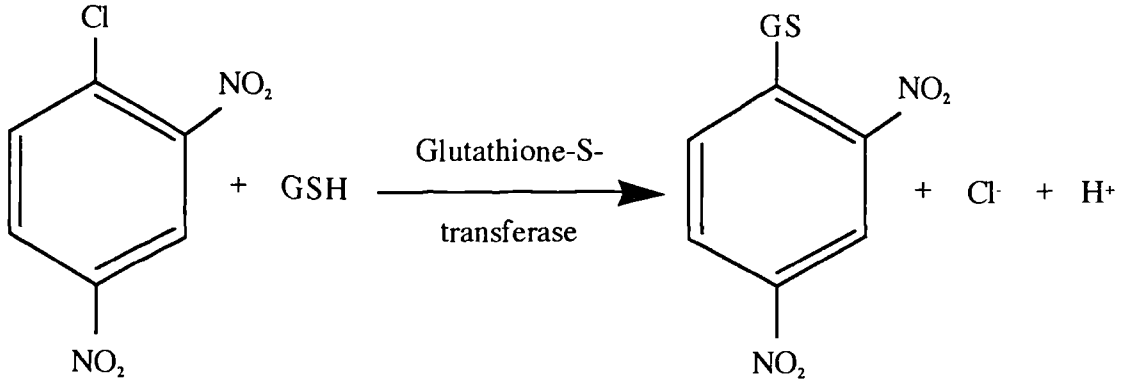

DNCB Glutathione conjugate

Maggs *et al*, (1986), have undertaken studies that show strong electrophiles like dinitrofluorobenzene and DNCB irriversibly bind to protein. It was also observed that in tissue with lower GSH levels, where less DNCB metabolism would occur, more protein binding took place. Incubation with glutathione lead to some release of tissue bound DNCB.

DNCB is a primary skin irritant and this response can be measured in mice by the local lymph node assay, in which the number of draining dendritic cells can be assessed (Kimber 1993). Topical application of 10% sodium dodecyl sulfate (SDS) with 0.1% DNCB causes a more vigorous proliferative response of draining lymph node cells than exposure to the sub-irritant concentration of 0.1% DNCB alone. SDS does not cause an increase in the percutaneous absorption of DNCB but augments the skin sensitising potential by increasing the release of Langerhans cells from the epidermis. This results in the arrival of more antigen-bearing dendritic cells to the draining lymph nodes (Cumberbatch *et al*, 1993).

A predictable log-dose relationship initiating a sensitising reaction has been characterised in man following dermal exposure to DNCB (Friedmann *et al*, 1983) and there is also a significant

difference in the susceptibility to develop contact hypersensitivity to DNCB between male and females. Females show a larger response than males to topically applied DNCB in acetone (30μg/ml, 24μl/cm^2, p = 0.008).

2,4-dinitrohalobenzenes generate oxidative stress in mouse skin. The consumption of NADPH and O_2 by skin microsomal fractions has been intrepreted as evidence that their metabolism is by a nitroreductase enzyme leading to the formation of potential free radicals. The reduction potentials of the dinitrohalobenzenes increase in the order DNIB < DNBB < DNCB << DNFB which also corrosponds to decreasing allergenicity. This provides additional evidence that dinitrohalobenzenes behave as prohaptens (Schmidt and Read, 1995).

Aims of the Project

The aim of the project was to define the xenobiotic metabolising potential of skin and to compare its activity in a series of skin models. Skin models, with increasing in complexity, were skin subcellular fractions, cultured keratinocytes, living skin equivalents and freshly excised skin mounted in diffusion cells.

Metabolism was assessed in skin subcellular fractions using model compounds as markers of specific metabolic pathways including cytochrome P450 monooxygenases, esterases and glutathione-S-transferases. Particular interest was applied to dinitrochlorobenzene (DNCB), a skin irritant and sensitiser, which is a substrate for glutathione-S-transferases. The influence of age on xenobiotic metabolism in skin was to be assessed in the rat.

Keratinocytes were grown in tissue culture from rat and human skin and used to determine the potential of these cells to metabolise xenobiotics, and to determine their usefulness as a model for human skin xenobiotic metabolism. The effect of induction and inhibition of xenobiotic metabolising enzymes in cell culture was also to be investigated.

A method was to be developed for constructing a living skin equivalent (LSE) to investigate the potential of a fully differentiated skin model for the metabolism of xenobiotics. The LSE was also to be evaluated for its usefulness as a model for human skin xenobiotic metabolism.

Studies were conducted to define viability and xenobiotic metabolising capacity of skin maintained in the flow-through diffusion cells. DNCB was used to define the importance of metabolism during percutaneous absorption and how this was related to the capacity to metabolise seen in other skin models. The aim was to also to assess metabolism of DNCB in skin during absorption to define it's degree of conjugation as a possible role in limiting DNCB toxicity.

Studies were to be conducted with human skin where possible and the results related to animal skin models using rat, mouse and pig. Results were to contribute to the evaluation of pig skin as a good model of human skin for the prediction of the fate of chemicals absorbed through skin in man.

Chapter 9

Aims of the project

Section 2

Materials and Methods

Chapter 10

General methods

10.1 Chemicals

Table 10.1 is a list of the chemicals used in this project, together with their source and their catalogue number. An asterisk(*) indicates tissue culture grade material.

Table 10.1 List of chemicals used in this project.

Chemical	Source	Catalogue #
Acetonitrile (HPLC grade)	Fisons	m/4056/17
Amphotericin B*	Sigma	A9528
Ascorbic acid*	Sigma	A4534
Bicinchoninic acid	Sigma	D8284
Biolute S	Zinsser Analytic	1310200
BisNitrophenyl Phosphate	Sigma	N1256
Bromobimane	Sigma	B4380
BW284c51 (1,5-bis(4-Allyldimethyl ammoniumphenyl)pental-3-one dibromide	Sigma	A9013
Calcium chloride*	Sigma	C7902
Dicumarol	Sigma	M1390
Dimethylsulfoxide	Sigma	D8779
[C14]-Dinitrochlorobenzene (1.5MBq/mg)	Amersham International	-
Dinitrochlorobenzene	Sigma	C6396
DispaseII	Borhenger Mannheim	165859
Dulbecco's Phosphate Buffered Saline	Sigma	D5652
Dulbecco's Modified Eagle's Medium	Sigma	D5523
EDTA*	Sigma	E6511
Eosin Y	Sigma	E4382
Epidermal Growth Factor*	Sigma	E4127
Eserine	Sigma	E8375
Ethanolamine*	Sigma	E0135
7-Ethoxyresorufin	Sigma	E3763
N-ethylmorpholine	Sigma	E0252
Formalin	Sigma	F1635
Gentamycin solution*	Sigma	G1272
Glycerol	BDH	101184K
L-Histamine*	Sigma	H9386
Hydrocortisone*	Sigma	H0888
Insulin*	Sigma	I1882

Isohexane	Fisons	H/0401/PB17
IsoOMPA (Tetraisopropyl pyrophosphor amide	Sigma	T1505
L-Isoleucine*	Sigma	I7383
L-15 Powdered Medium	Sigma	L4386
MCDB153 Powdered Medium	Sigma	M7403
Mercuric Chloride	Sigma	M6529
Methane Sulfonic acid	Sigma	M6391
Methanol (HPLC grade)	BDH	15250
L-Methionine*	Sigma	M2893
20-Methylcholanthrene (3-Methylcholanthrene)	Sigma	M6501
4-Methylumbelliferyl heptanoate	Sigma	M2514
MTT	Sigma	M5655
α–Naphthoflavone	Sigma	N5757
β-Naphthoflavone	Sigma	N3633
Paroxon (Diethyl p-nitrophenyl phosphate)	Sigma	D9286
7-Pentoxyresorufin	Sigma	P0928
L-Phenylanaline*	Sigma	P5030
Phenylmethylsulfonylfluoride	Sigma	P7626
Phenobarbital	Sigma	P1636
Phosphoethanolamine*	Sigma	P0503
Pituitary Extract, Bovine*	Advanced Protein Products	FB-155-TS
Protein Standard Solution (Precimat®)	Borhenger Mannheim	125601
RPMI1640 Powdered Medium	Sigma	R6504
Sodium bicarbonate*	Sigma	S5171
Sodium carbonate*	Sigma	S9140
Sodium tartrate	Sigma	S8640
Sucrose	Sigma	S1888
Transferrin*	Sigma	T2158
Trisma® 7.7	Sigma	T4378
Trypan blue solution	Sigma	T8154
Trypsin	Difco	0152-13-1
L-Tryptophan*	Sigma	T0271
L-Tyrosine*	Sigma	T1020
Umbelliferone	Sigma	U7626
Water (sterile)	Steripak	-

Advanced Protein Products ltd, Brierley Hill, West Midlands, UK.

Aldrich, Gillingham, Dorset, UK.

Amersham International, Newport, UK.

BDH Chemicals, Poole, UK.

Boehringer Mannheim, Lewes, UK.

Difco Laboratories, Detroit, Michigan, USA.

Fisons Scientific Equipment, Loughborough, UK.

Sigma Chemical Company, Poole, UK.

Steripak, Runcorn, UK.

Zinsser Analytic, UK.

10.2 Buffers and Medium

a) KCl/Phosphate buffer pH 7.4

Phosphate buffer for use in enzyme assays and cell homogenisation was prepared by dissolving K_2HPO_4 (100mM) and KCl (150mM) in double distilled water at room temperature. The pH of the buffer was adjusted to 7.4 with the use of HCl (0.1N) or NaOH (0.1N). Buffer was stored refrigerated at 0-5°C.

b) Glycerol Buffer

To maintain a high degree of cytochrome P-450 monooxygenase activity in frozen (-70°C) microsomal samples a glycerol buffer was used for preparation and storage. The buffer consisted of 10% glycerol, Trisma® 7.7 (50mM), KCl (0.1mM), EDTA (0.1mM) and sucrose (250mM) in double distilled water, prepared at room temperature. Buffer was stored refrigerated at 0-5°C. This buffer has a pH of 7.4 at 37 C.

c) Trisma buffer

Esterase activity in tissue homogenates was determined with Tris buffer. Trisma® 7.7 (50mM) and EDTA (0.1mM) was dissolved in double distilled water at room temperature and stored refrigerated at 0-5 C. This buffer has a pH of 7.4 at 37°C.

d) Dulbecco's phosphate buffered saline (D-PBS)

Dulbecco's phosphate buffered saline (D-PBS) is a physiological salt solution, maintaining pH and osmotic balance and is used for irrigating tissue specimens and cells. It is deficient in calcium and magnesium ions, factors which trigger keratinocyte differentiation. The powdered D-PBS was reconstituted into a solution by dissolving into sterile water at room temperature. The medium was then filter sterilised into sterile bottles using a membrane of 0.2μm porosity. When required, the pH was adjusted to 7.4 with sterile HCl (0.1N)or NaOH (0.1N). D-PBS was stored refrigerated at 0-5°C.

Table 10.2 D-PBS formulation.

Component	g/L
Potassium Chloride	0.2
Potassium Phosphate monobasic (anhydrous)	0.2
Sodium Chloride	8.0
Sodium Phosphate dibasic (anhydrous)	1.15

e) L-15 medium

L-15 medium (Leibovitz) is a general tissue culture medium developed for use in carbon dioxide deficient environments, relying on its complement of salts and free base amino acids for it's buffering capacity, thus not needing the addition of sodium bicarbonate. The medium was prepared by dissolving the powdered medium in 1L of sterile water at room temperature. Gentamycin sulphate (20μg/ml) and amphotericin B (5μg/ml) was added to the medium. The medium was then filter sterilised in to sterile bottles using a membrane of 0.2μm porosity. The pH of the medium was adjusted to 7.4 with sterile NaOH (0.1N) or HCl (0.1N) and stored refrigerated at 0-5°C.

Table 10.3 L-15 formulation.

Component	g/L
DL-Alanine	0.450
L-Arginine free base	0.500
L-Aspargine (anhydrous)	0.250
L-Cysteine free base	0.120
L-Glutamine	0.300
L-Glycine free base	0.200
L-Histidine free base	0.250
DL-Isoleucine	0.250
L-Leucine	0.125
L-Lysine free base	0.075
DL-Methionine	0.150
DL-Phenylalanine	0.250
L-Serine	0.200
DL-Threonine	0.600
L-Tryptophan	0.020
L-Tyrosine free base	0.300
DL-Valine	0.200
Choline Chloride	0.001
Folic Acid	0.001
Flavin Mononucleotide Sodium	0.0001
Myo-Inositol	0.002
Niacinamide	0.001
DL-Panthothenic Acid Ca	0.001
Pyridoxine HCl	0.001
Thiamine Monophosphate Chloride	0.001
Calcium Chloride.$2H_2O$	0.185

Table 10.3 continued.

Magnesium Chloride.$6H_2O$	0.2
Magnesium Sulfate (Anhydrous)	0.09767
Potassium Chloride	0.400
Potassium Phosphate (anhydrous)	0.060
Sodium Chloride	8.000
Sodium Phosphate dibasic (anhydrous)	0.190
Galactose	0.900
Phenol red Na	0.011
Sodium Pyruvate	0.550

f) MCDB153 medium

Specific tissue culture media have been developed for specific cell types and the culture of human keratinocytes has been greatly optimised by the development of the serum-free medium MCDB153 (Molecular, Cellular and Developmental Biology of the University of Colorado, number 153), which was developed by Boyce and Ham in 1983. The MCDB153 formulation used in this project to grow human keratinocytes is a modified MCDB153 medium as described by Pittlekow and Scott (1987). Table 10.4 lists the MCDB153 formulation available in powder form from Sigma.

Table 10.4 MCDB153 formulation.

Component	mg/L
L-Alanine	8.91
L-Argenine	210.7
L-Aspargine	15.01
L-Aspartic Acid	3.99
L-Cysteine.HCl.H_2O	4204
L-Glutamic Acid	1.471
L-Glutamine	877.2
Glycine	7.51
L-Histidine.HCl.H_2O	16.77
L-Isoleucine	1.968
L-Leucine	65.6
L-Lysine.HCl	18.27
L-Methionine	4.476

Table 10.4 continued.

L-Phenylalanine	4.956
L-Proline	34.53
L-Serine	63.06
L-Threonine	11.91
L-Tryptophan	3.06
L-Tyrosine.2Na.2H_2O	3.41
L-Valine	35.13
D-Biotin	0.0146
D-Pantothenic Acid Hemicalcium	0.238
Choline Chloride	13.96
Folic Acid	0.79
Myo-Inositol	18.02
Niacinamide	0.03663
Pyridoxine.HCl	0.06171
Riboflavin	0.03764
Thiamine.HCl	0.3373
Vitamin B_{12}	0.407
Adenine.HCl	30.88
DL-6,8-Thioctic Acid	0.2063
Putrecine.2HCl	0.1611
Thymidine	0.7266
Calcium Chloride.2H_2O	4.411
Potassium Chloride	111.83
Magnesium Chloride.6H_2O	122.0
Sodium Acetate	301.53
Magnesium Sulfate	0.000151
Molybdic Acid [NH_4]$_6$4H_2O	0.00124
Nickel Chloride.6H_2O	0.000119
Sodium Selenite	0.0038
Sodium Metavanadate	0.142
Stannous Chloride.H_2O	0.000113
Ammonium Metavanadate	0.000585
Sodium Chloride	7599.00
Sodium Phosphate dibasic (anhydrous)	284.088
$CuSO_4$.5H_2O	0.00275
FeSO4.7H_2O	1.39

Table 10.4 continued.

$ZnSO_4.7H_2O$	0.144
D-Glucose	1081.0
HEPES	6600.0
Phenol Red.Na	1.242
Pyruvic Acid.Na	55.0

The powdered MCDB153 was dissolved in 1L of sterile water at room temperature. The addition of the supplements in table 10.5 were made to the formulated MCDB153 tissue culture medium as described by Pittelkow and Scott 1986.

Table 10.5 Supplements to MCDB153 medium.

Component	Formulation	Amount added to medium mg/L	Total mg/L
Histidine	Powder	34.6	51.37
Isoleucine	Powder	98.4	100.3
Methionine	Powder	13.4	17.9
Phenylalanine	Powder	14.9	19.9
Tryptophan	Powder	9.2	12.3
Tyrosine	Powder	1.7	5.1
$CaCl_2.H_2O$	Powder	5.88	10.3
Ethanolamine	Liquid	6.1μl	6.1μl
Phosphoethanolamine	Powder	14.1	14.1
Hydrocortisone	0.5mg ml Absolute ethanol stock solution	0.181	0.181
Insulin	2.5mg/ml in 4mM HCl stock solution	5.0	5.0
Transferrin	5mg/ml in H_2O	5.0	5.0
Epidermal Growth factor	5.0μg/ml in H_2O stock solution	0.010	0.010
Amphotericin B	Powder	5.0	5.0
Gentamycin Sulfate	10mg/ml in H_2O stock solution	20.0	20.0

Stock solutions of hydrocortisone, Insulin, transferrin and epidermal growth factor were stored in aliquots at -20°C.

The pH of the modified MCDB153 medium was then adjusted to 7.4 with the use of sterile NaOH (4N). Sodium bicarbonate (1.176g) was then added to the medium, the colour of the medium at this point was orange/peach. The medium was then filter sterilised in to sterile bottles using a membrane of 0.2μm porosity and stored refrigerated at 0-5°C. Complete MCDB153 was used within 2 weeks of it's preparation. MCDB153 without hydrocortisone, insulin, transferrin and epidermal growth factor could be prepared and stored at 0-5°C for 6 months and supplements added when needed.

g) Dulbecco's Modified Eagles Medium (DMEM)

The tissue culture of dermal fibroblasts and the growth of Living Skin Equivalents (LSE) was achieved using Dulbecco's Modified Eagles Medium (DMEM). This formulation contains four times the level of amino acids than the usual Basal Medium Eagle (BME), plus a few non-essential amino acids. The powdered medium was dissolved in 1L of sterile water at room temperature. Ascorbic acid (10μg ml), gentamycin sulphate (20μg/ml) and amphotericin B (5μg/ml) were also added to the medium. Sodium bicarbonate (3.7g) was added and the pH of the medium was adjusted to 7.4 with sterile NaOH (0.1N) or HCl (0.1N). The medium was then filter sterilised in to sterile bottles using a membrane of 0.2μm porosity and stored refrigerated at 0-5°C.

Table 10.6 DMEM formulation.

Component	g/L
Calcium Chloride.2H_2O	0.265
Ferric Nitrate.9H_2O	0.0001
Magnesium Sulfate	0.09767
Potassium Chloride	0.400
Sodium Chloride	6.400
Sodium Phosphate monobasic	0.109
L-Argenine.HCl	0.084
L-Cysteine.2HCl	0.0626
L-Glutamine	0584
Glycine	0.030
L-Histidine.HCl.H_2O	0.042
L-Isoleucine	0.105
L-Leucine	0.105
L-Lysine.HCl	0.146
L-Methionine	0.030
L-Phenylalanine	0.066
L-Serine	0.042
L-Threonine	0.095

Table 10.6 continued.

L-Tryptophan	0.016
L-Tyrosine.2Na.2H_2O	0.10379
L-Valine	0.094
Choline Chloride	0.004
Folic Acid	0.004
Myo-Inositol	0.0072
Niacinamide	0.004
D-Pantothenic Acid (hemicalcium)	0.004
Pyridoxal.HCl	0.004
Riboflavin	0.0004
Thiamine.HCl	0.004
D-Glucose	1.000
Phenol Red.Na	0.0159
Pyruvic Acid.Na	0.110

h) RPMI1640 medium

RPMI1640 (Roswell Park Memorial Institute) medium was used as a receptor fluid for the static and flow-through diffusion cells. The medium uses a bicarbonate buffering system. It has been used as a growth medium and supports a wide range of cell types. The powdered medium was dissolved in 1L of sterile water at room temperature. Gentamycin sulphate (20μg/ml) and sodium bicarbonate (2.0g) was added to the medium and the pH was adjusted to 7.4 with sterile NaOH (0.1N) or HCl (0.1N). The medium was then filter sterilised in to sterile bottles using a membrane of 0.2μm porosity and stored refrigerated at 0-5°C.

Table 10.7 RPMI1640 formulation.

Component	g'L
Calcium Nitrate.4H_2O	0.100
Magnesium Sulfate (anhydrous)	0.04884
Potassium chloride	0.400
Sodium Chloride	6.000
Sodium Phosphate dibasic (anhydrous)	0.800
L-Argenine (free base)	0.200
L-Asparagine (anhydrous)	0.050
L-Aspartic acid	0.020
L-Cysteine.2HCl	0.0652

Table 10.7 continued.

L-Glutamic Acid	0.020
L-Glutamine	0.300
Glycine	0.010
L-Histidine (free Base)	0.015
Hydroxy-L-Proline	0.020
L-Isoleucine	0.050
L-Leucine	0.050
L-Lysine.HCl	0.040
L-Methionine	0.015
L-Phenylalanine	0.015
L-Proline	0.020
L-Serine	0.030
L-Threonine	0.020
L-Tryptophan	0.005
L-Tyrosine.2Na.2H_2O	0.02883
L-Valine	0.020
D-Biotin	0.0002
Choline Chloride	0.003
Folic Acid	0.001
Myo-Inositol	0.035
Niacinamide	0.001
p-Amino Benzoic Acid	0.001
D-Pantathenic Acid (hemicalcium)	0.00025
Pyridoxine.HCl	0.001
Riboflavin	0.0002
Thiamine.HCl	0.001
Vitamin B_{12}	0.000005
D-Glucose	2.000
Glutathione (reduced)	0.001
Phenol Red.Na	0.0053

All filter sterilisation was achieved using sterile Costar™ bottle filters with a 0.2μm pore size filter and facilitated by a venturi suction pump. The filter sterilisation was conducted in a laminar flow cabinet that was wiped down with 70% ethanol prior to use.

Formulation data for all media were taken from Sigma data sheets.

10.3 Tissue preparations

a) Origin

Animal skin and liver samples were obtained from several species. These were male Wistar rats aged either 4 days (neonatal), 26 days or 8-9 weeks old. Male and female Balb/C mice were aged 6-7 weeks and adult domestic pigs were approximately 6 months old. Rodent tissue was obtained from the animals housed at the Comparative Biology Centre, Newcastle University, or at Zeneca, Central Toxicology Laboratory (CTL), Alderley Park, Cheshire. Porcine tissue was obtained from Sunderland Abattoir, Sunderland, Tyne and Wear.

Human skin was obtained from plastic surgery either from the theatre at the Royal Victoria Infirmary (RVI) or the theatre at the General hospital, both located in Newcastle Upon Tyne. Skin was taken from breast (mastectomy or reduction mammoplasty) or abdomen (reduction abdominoplasty) which were removed for medical or aesthetic purposes. Use of human skin for this study had received approval from the Joint University and Health Authority Ethical Committee.

b) Removal and storage

Neonatal rats were sacrificed by inter-peritoneal injection of sodium pentabarbitone (1.5g kg). Older rats and mice were sacrificed by cervical dislocation. Pigs were killed by electrocution at the abattoir.

Skin from neonatal rat was removed by amputating limbs, cutting skin around the neck and peeling skin from the body. Subcutaneous fat was removed by gently scraping the underside of the skin with curved forceps. The skin was immediately placed in a petri dish and kept on ice in an ice bucket until used. Neonatal rat livers were carefully removed with forceps and scissors and placed in sterile universal tubes containing ice cold Dulbecco's phosphate buffered saline (D-PBS) and transported on ice.

Adult rats and mice were clipped of fur (Oster clippers) before removal of dorsal skin. Dorsal skin was removed from the rodent with scissors and subcutaneous fat removed by teasing away with tissue paper. Skin was then placed in a petri dish on ice in an ice bucket until used. Livers were removed with forceps and scissors and placed in sterile universal tubes containing ice cold D-PBS and transported on ice.

Pig ears and liver samples were cut from the pig by an abbatoir employee and were placed in a plastic bag to be transported in an ice packed cool box to the University for use in the laboratory. In the laboratory, pig liver samples were placed in universal tubes containing ice cold D-PBS. Pig ears were washed of dirt and blood with cold water and blotted dry with tissue paper. Hair was removed with a scalpel by gently stroking the surface of the skin with the blade. The skin of the

external ear was then cut away from the ear with a scalpel. Skin was placed in a petri dish on ice in an ice bucket until used.

Human skin was cleaned of subcutaneous fat by cutting away with scissors and scalpel. The surface of the skin was cleaned of blood with a tissue dampened with D-PBS. Tissue was then kept on ice until used.

c) Preparation of tissue subcellular fractions

1) Preparation of skin subcellular fractions.

Adult rat skin, pig skin and human skin was pinned out on a cork board and dermatomed into strips with a dermatome (setting 6, 350μm, on a Davis Miniplex Seven, Thackery, Leeds, UK.). Neonatal rat skin and Balb/C mouse skin was too thin to be dermatomed and was used full thickness. The dermatomed skin was weighed and finely minced with sharp scissors. The minced skin was placed in a large ceramic mortar and flash frozen with liquid nitrogen. The skin was then broken in to a fine powder with a pestle. The powdered skin was brushed into homogenisation tubes and 1ml of ice cold glycerol buffer (section 10.2b) was added per 100mg of tissue. Homogenisation tubes were kept on ice at all times. Homogenisation involved 3x10 second bursts at setting 6 with a homogeniser (Polytron PT10 35). Clumps of fatty tissue formed in the rotor of the homogeniser were removed with forceps between bursts and discarded. The homogenate was centrifuged for 10 minutes at 750g (3 000rpm) using a bench centrifure (Sorvall RC-5B) to remove cell debris. The supernatant was centrifuged for 10 minutes at 10 000g (12 500rpm), using an ultracentrifuge (Sorvall OTD65B) to remove mitochondria. The resulting supernatant was used either as post mitochondrial fraction in some experiments or further centrifuged to prepare cytosolic and microsomal fractions. Microsomes were prepared by centrifuging the supernatant for a further 70 minutes at 110 000g (44 000rpm). Supernatant (cytosol) was gently pippeted from the microsomal pellet, aliquoted into eppendorfs and stored at -70°C. The pellet was washed in buffer and resuspended in 1ml of buffer with a glass to glass homogeniser, aliquoted in eppendorfs and stored at -70°C. All homogenisation and centrifugation was done at 4°C.

Protein content of the post mitochondial, microsomal and cytosolic fractions was determined by the BSA method (see section 11.1). Recovery of microsomal protein was in the order of 0.02-0.07mg/g skin.

2) Preparation of liver subcellular fractions.

Livers were weighed and finely minced with sharp scissors. Minced liver was placed into homogenisation tubes and 1ml of ice cold glycerol buffer was added per 100mg of tissue. Homogenisation tubes were kept on ice at all times. Homogenisation involved 3x10 second bursts at

setting 6 with the homogeniser. Post mitochondrial, cytosolic and microsomal fractions were prepared by homogenising and centrifuging by the same procedure as used for the skin.

Protein content of the post mitochondial, microsomal and cytosolic fractions was determined by the BSA method (see section 11.1). Recovery of microsomal protein was in the order of 3mg/g liver for neonatal rats and 10-14mg/g liver for mature rats.

d) Preparation of skin for diffusion cells

Adult rat skin, pig skin and human skin was pinned out on a cork board and dermatomed into strips with a dermatome (setting 6, 350μm). Neonatal rat skin and Balb/C mouse skin was too thin to be dermatomed and was used full thickness. Skin from all species was then placed on to a cork board and cut in to discs with a cork borer with a 2cm diameter. The discs of skin were kept in a petri dish on ice until mounted onto diffusion cells.

e) Tissue histology

Samples of skin tissue were processed for histological examination. Tissue samples were fixed in formalin before processing and staining with Haemotoxylin and Eosin. Histolgy was undertaken in the pathology department at the Royal Victoria Infirmary, Newcastle Upon Tyne. Plates 10.1 to 10.4 show cross sections of full thickness neonatal rat skin (500μm thick) and dermatomed adult rat, pig and human skin (dermatomed at setting 6, 380μm). Cross sections of mouse skin can be found in chapter 15 section 15. "Immunohistochemistry of mouse skin".

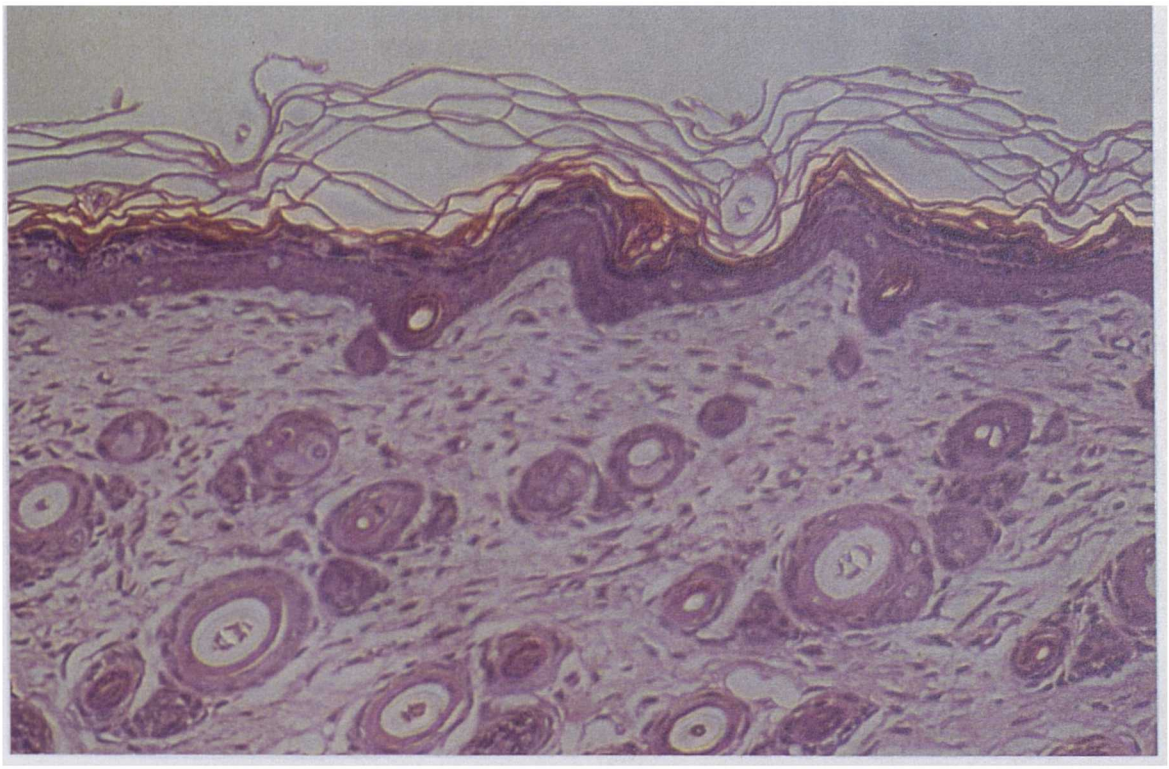

Plate 10.1 Cross section of full thickness neonatal rat skin, 500μm thick (x280) Stained with haemotoxylin and eosin.

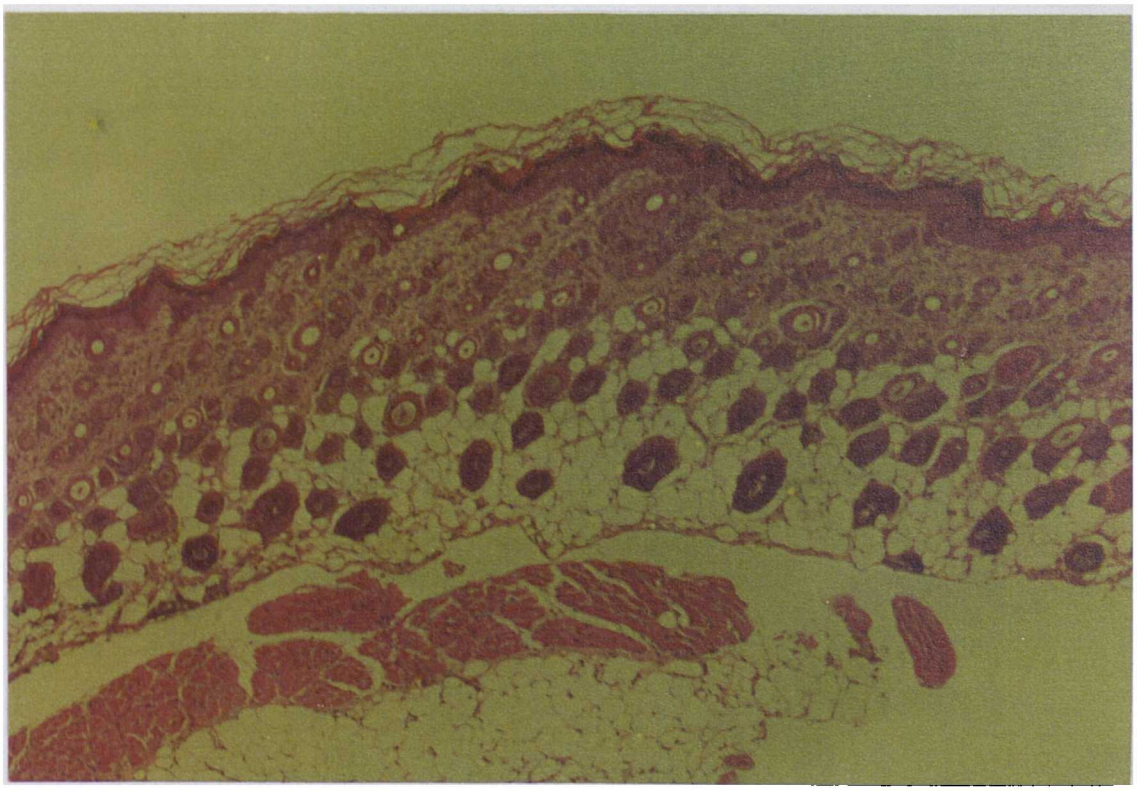

Plate 10.2 Cross section of adult rat skin dermatomed to 350μm (x140). Stained with haemotoxylin and eosin.

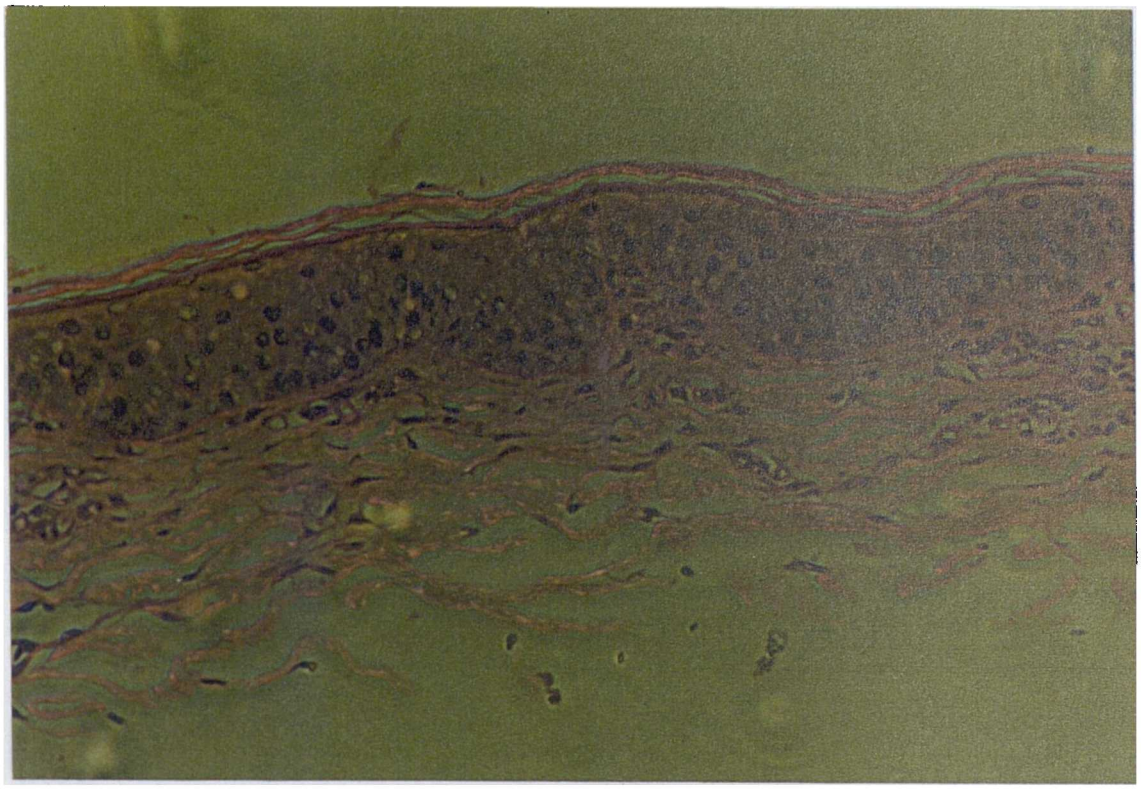

Plate 10.3 Cross section of pig skin dermatomed to 350μm (x140).
Stained with haemotoxylin and eosin.

Plate 10.4 Cross section of human skin dermatomed to 350μm (x88).
Stained with haemotoxylin and eosin.

Chapter 11

Analytical methods

Analytical methods

11.1 Bicinchoninic acid (BCA) protein assay

a) Introduction

The determination of protein concentration in biological samples was achieved using the method of Smith *et al,* (1985). The method utilises the formation of a protein-copper-bicinchoninic acid (BCA) complex giving an absorption reading that is dependant on the protein concentration. This method has several advantages over the more commonly used protein determination method described by Lowry (1958). The assay requires less protein sample and fewer steps in the procedure, which results in less experimental error. The BCA assay also has a greater tolerance to interfering agents than the Lowry assay and can be used with solutions containing EDTA (up to 10mM), sucrose (up to 40%), tris (up to 0.1M) and glycerol. This makes it a suitable assay for determining microsomal protein concentration in a glycerol buffer.

b) Assay procedure

i) For protein concentrations in the range (0.01-1.5mg/ml).

Two stock solutions were prepared and called reagent A and reagent B. Reagent A consisted of bicinchoninic acid (sodium salt) (1g/100ml), sodium carbonate monohydrate (2g/100ml), sodium tartrate (160mg 100ml), sodium hydroxide (400mg/100ml) and sodium hydrogen carbonate (950mg ml). The pH was adjusted to 11.25 using sodium hydroxide (50%) or solid sodium hydrogen carbonate. Reagent B consisted of copper sulfate pentahydrate (4g/100ml). Both reagents A and B are stable indefinitely. A working solution of BCA for the determination of protein consisted of reagents A and B mixed in a ratio of 50:1.

A calibration graph was constructed with Bovine Serum Albumin protein standards. Protein standards were made with concentrations of 0, 0.3, 0.6, 0.9, 1.2 and 1.5 mg/ml in distilled water. Samples of each standard (40μl) were added to 1ml ependorfs and 800μl of BCA reagent was added. A sample of homogenate (5μl), either postmitochondrial, cytosol or microsomal fraction and 35μl of distilled water was added to an ependorf and 800μl of BCA reagent was added. Samples were then incubated for 30 minutes at 37°C. Samples were measured at 562nm vs. a reagent blank, using disposable plastic microcuvettes (Elkay). All samples were done in triplicate.

ii) Micro-method, for protein concentrations in the range (0.5-10μg/ml).

Reagent A consisted of sodium carbonate monohydrate (8g/100ml), sodium hydroxide (1.6g/100ml) and sodium tartrate (1.6g/100ml). pH was adjusted to 11.25 with sodium hydrogen carbonate. Reagent B consisted of a solution of bicinchoninic acid.(4g/100ml) and reagent C

consisted of 1 volume of copper sulfate (4g/100ml) and 25 volumes of reagent B. Reagents A and B are stable indefinitely at room temperature. A working solution of BCA consisted of 1 volume of reagent A and 1 volume of reagent C.

A calibration graph was constructed with protein standards of 2, 4, 6, 8 and 10μg/ml. Sample or standard (400μl) was mixed with 400μl of BCA reagent for 60 minutes at 60°C. Samples were cooled and read at 562nm vs. reagent blank.

Graph 11.1. A typical calibration graph for protein concentration determination using the bicinchoninic acid method. Standards used were 0.3, 0.6, 0.9, 1.2 and 1.5 mg/ml. Each point represents the mean of triplicate determinations

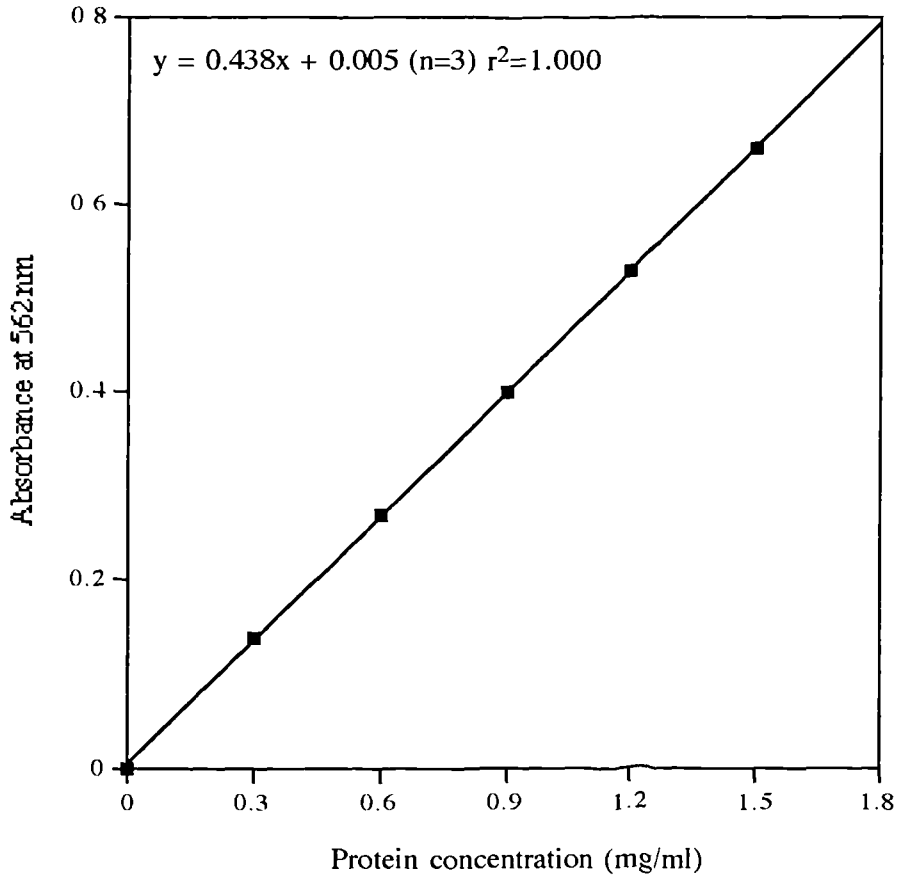

11.2 Cytochrome P450 monooxygenases

a) Introduction

Cytochrome P450 monooxygenase activity in liver and skin microsomal samples was determined using the markers ethoxyresorufin and pentoxyresorufin by a modification of the method

of Burke *et al*, 1985. Ethoxyresorufin-*O*-deethylation is primarily achieved with the cytochrome P450 monooxygenase CYP1A1 in normal skin and CYP1A2 in normal liver. Pentoxyresorufin-*O*-dependentylation is primarily achieved with the cytochrome P450 monooxygenase CYP2B of normal liver and skin.

b) Alkoxyresorufin-O-dealkylation

Determination of ethoxyresorufin-*O*-deethylation and pentoxyresorufin-*O*-dependentylation was conducted using a Perkin Elmer PE LS-5 fluorimeter with water jacketed cell holder set to 37°C. The fluorimeter was connected to an Amstrad PC2286/40 with a kinetics package. Fluorimeter settings were optimised for sensitivity and were set as follows. Excitation 530nm, emission 585nm, chart recorder speed 1cm/min, response 1, excitation slit width 10 and emission slit width 20.

A solution of NADPH (6mg/ml) in phosphate buffer (pH 7.4, 0.1M KH_2PO_4 and 0.15M KCl, pH adjusted when necessary with 4N NaOH) was prepared fresh and 500μl added to a microcuvette. Microsomal protein (50μg) was added to the cuvette and the volume made up to 1ml with phosphate buffer. The cuvette was incubated in the fluorimeter cell holder to bring the temperature to 37 C and 1μl of either ethoxyresorufin (EOR, 3mM in DMSO) or pentoxyresorufin (POR, 3mM in DMSO) was added to start the reaction. Data were collected by the computer and rate of increase in fluorescence plotted with time. The absorbance of 100pmoles of resorufin was used as a standard and determined by the addition of resorufin (1μl, 0.1mM in DMSO) to a cuvette containing 1ml buffer with microsomal protein.

Stock reagents of EOR, POR and resorufin were stored in the dark at room temperature.

11.3 Esterases

a) Hydrolysis of 4-methylumbelliferyl heptanoate

Measurements of non-specific esterase activity in the cytosol and microsomal fractions of skin and liver were evaluated with the substrate 4-methylumbelliferyl heptanoate. Activity was assessed by the formation of the fluorescent metabolite 4-methylumbelliferone.

b) Assay procedure

Determination of esterase activity in tissue cytosol or microsomes was conducted using a Perkin Elmer PE LS-5 fluorimeter with water jacketed cell holder set to 37°C (bath set to approx 44°C). The fluorimeter was connected to an Amstrad PC2286/40 with a kinetics package (ELMER). Fluorimeter settings were optimised for sensitivity and were set as follows: Excitation 345nm, Emission 435nm, Excitation slit 10, Emission slit 5, chart recorder 5cm/min, set scale to 1. Disposable microfluorimetric cuvettes were used for all determinations.

Stock solutions consisted of Trizma buffer pH 7.7 (50mM, 7.38g/L) containing EDTA (0.1mM, 38mg/L). Methylumbelliferyl heptanoate (17mM, MUH) in DMSO (4.9mg/ml). Methylumbelliferone (MU, 0.1mM) in DMSO (9.6mg in 5ml then dilute by 100). BSA solution (1.2mg/ml,20μl/ml distilled water).

Measurements of a standard were assessed with each determination. To a microcuvette was added 980μl of buffer and 20μl of BSA solution, placed in the fluorimeter and the fluorescence was set to zero. This was followed by the addition of 1μl of 0.1mM MU (100pmoles) to the cuvette and fluorescence was recorded. This was repeated in triplicate.

For enzyme activity 980μl of buffer was mixed in a cuvette with a sample of protein (cytosol or microsomes), approx 10-20μg protein. This was made up to 1ml with buffer. The cuvette was shaken and incubated for 5 minutes. The reaction was started by adding 3μl of MUH solution, which was mixed and replaced in to the cell holder immediately. Aquisition of data were started immediately and rate of reaction calculated. This was repeated in duplicate.

The following calculation was used to determine the activity:

$$\text{pmoles/ min / mg protein} = \frac{\text{change in fluorescence units min}}{\text{fluorescence units forlpmole MU}} \times \frac{1000}{\mu\text{g protein in reaction}}$$

Results are expressed as nmoles MU produced/min/mg protein.

11.4 Glutathione-S-transferases

a) Glutathione conjugation of DNCB

Glutathione-S-transferase activity was determined using the method of Habig *et al*, (1974).

b) Assay procedure

Determination of the glutathione conjugation of DNCB was conducted using a Kontron spectrophotometer with water jacketed cell holder set to 37°C. The spectrophotometer was set to a wavelength set to 345nm. Disposable plastic cuvettes were used for all determinations.

Stock solutions consisted of a phophate buffer (100mM, KH_2PO_4, pH6.5), glutathione in buffer (GSH, 30mM) and DNCB in ethanol (30mM).

To each of two 1ml microcuvettes, were added 30μl of GSH (30mM), 30μl of DNCB(30mM) and 750μl of buffer. The cuvettes were placed in the sample and reference

compartments of the spectrophotometer and incubated to 37°C. Initiation of the reaction was started by addition of 30μl of supernatant from the homogenised skin tissue, or 4μl of supernatant from the homogenised liver tissue under investigation and the reference cuvette balanced with buffer. Cuvettes were mixed rapidly and the increase in absorption at 345nm read for a 4 minute period.

The calculation to determine GST activity was as follows:

protein concentration in cuvette = [P]mg ml ^{1}
Extinction coefficient for glutathione adduct = 9.6mM ^{1}cm^{-1}
Absorbance change (345nm) per min = A

Specific activity = $\frac{A}{9.6 \times [P]}$ μmol product formed per minute per mg protein

Section 3

Experimental Studies

Chapter 12

Studies with subcellular fractions

Studies with subcellular fractions

12.1 Introduction

An important *in vitro* model for the assessment of xenobiotic metabolism is the use of tissue homogenates. These allow the study of the profile of metabolic reactions and eliminates the problem of accessibility of the xenobiotic to the reactive enzymes. Studies were conducted with tissue subcellular fractions of skin to assess their potential for metabolism. The skin and liver of rat, mouse, pig and human were assayed in parallel for direct comparison where possible.

12.2 Enzyme kinetics

For most enzyme catalysed reactions, the rate of catalysis υ varies with substrate concentration s in a saturable manner such that a plot of υ against s shows a hyperbolic curve. At a fixed concentration of enzyme, υ is linearly proportional to s when s is small, i.e. first order reaction kinetics. At high s, υ is independent of s, i.e. zero order reaction kinetics. Michaelis and Menten (1913) proposed a simple model to account for these kinetic characteristics thus:

$$E + S \Leftrightarrow ES \xrightarrow{k} P$$

where E is enzyme, S is substrate, ES is the enzyme-substrate complex and P is the product. The model assumes that the E + S = ES step is in equilibrium. Briggs and Haldane (1925) realised that this need not be the case and suggested the following adaptation of the Michaelis-Menten model:

$$E + S \underset{k2}{\overset{k1}{\Leftrightarrow}} ES \xrightarrow{k3} E + P$$

where substrate binding to enzyme is reversible, but not necessarily in equilibrium. This development enabled the equation known as the Michaelis-Menten equation to be formulated to describe the kinetics of enzyme catalysed reactions:

$$\upsilon = \frac{Vmax \,.\, s}{Km + s}$$

where υ is the reaction rate, s is substrate concentration, V_{max} is maximal reaction rate at enzyme saturation and K_m is the Michaelis constant.

K_m values range widely, for example the K_m for CO_2 binding to carbonic anhydrase is 8 x 10^{-3}M, while the K_m for ATP binding to pyruvate carboxylase is 6 x 10^{-5} M (Stryer, 1981). The K_m value for an enzyme has two applications, firstly the concentration of the substrate at which half the active sites are filled and secondly it reflects the affinity of an enzyme for a substrate where high K_m

shows low affinity. The Km is an intrinsic characteristic of the enzyme-substrate binding and within the conditions of an assay are often referred to as the apparent Km, which is unaffected by enzyme concentration or localisation.

The Vmax is a direct measure of the maximum rate of the catalysed reaction when all the enzyme active sites are filled and as such is dependent on the amount of enzyme present in the tissue under investigation. For most physiological pathways, substrate concentrations *in vivo* are usually well below those needed for Vmax conditions. In the case of xenobiotic metabolism, however, it is possible for substrate concentrations to reach these levels, such as metabolism of ethanol by alcohol dehydrogenase or paracetamol glucuronide conjugation in overdose. The Vmax can be used to determine the turnover rate of an enzyme if the enzyme concentration is known. The turnover number is equivalent to the rate constant k_3 in the above equation and is defined as the number of substrate molecules converted into product per unit time at fully saturable conditions. Like Km, turnover number can vary widely, carbonic anhydrase has a turnover number of $6 \times 10^5\ s^{-1}$, while glutathione-S-transferases have turnover numbers between 0.1 and $35 s^{-1}$.

Most methods for the calculation of Km and Vmax are from s and υ data and rely on linear transformations of the Michaelis-Menten equation. The most popular is the double-reciprocal plot described by Lineweaver and Burk (1934). This plots $1/\upsilon$ against $1/s$, the y-axis intercept is equivalent to 1/Vmax and the x-axis intercept is equal to -1/Km. However, this plot distorts the appearance of the experimental error in the primary observations of υ, especially at low substrate concentrations.

Other straight line transformations have been developed that eliminate the error of the double-reciprocal plot, but are still not entirely free of distortion. For example, a plot of υ against υ/s results in a straight line of slope -Km and x-axis intercept of Vmax, this is called the Eadie-Hofstee plot.

An alternative approach is the direct-linear plot described by Eisenthal and Cornish-Bowden (1974). Here, each observation at s is plotted as a straight line rather than a point, with Km and Vmax treated as the x and y variables respectively such that all possible pairs of values for Km and Vmax which satisfy each observation are shown. The point of intersection of the lines drawn provides the co-ordinates for Km and Vmax. In practice, the lines do not cross at one point due to experimental error. Each intersection point is therefore marked and the median Km and Vmax values are taken as the best estimate of each parameter.

Enzymes may exhibit competitive or non-competitive inhibition and this can be evaluated through the use of the Dixon plot, which calculates the enzyme inhibitor constant. A plot of $1/\upsilon$ against inhibitor concentration, at constant substrate concentration gives a straight line. When this is done at two or more different substrate concentrations, an intersection of the lines to the left of the

vertical axis indicates a competitive inhibitor. The intersection point is equivalent to -Ki, the inhibitor constant. If the lines are parallel, the inhibition is non-competitive.

12.3 Aim of studies with subcellular fractions

The aim of these studies was to investigate the metabolic profile of skin subcellular fractions with comparisons to liver and differences between species. The key question that was being addressed in these studies was how did metabolism with skin subcellular fractions of other species compare to man and could these be used as models to predict human *in vitro* data. The rat was used to investigate the effect of age on skin metabolism and also, how metabolism was affected by pretreatment with classical inducing agents. The metabolic pathways assessed included the cytochrome P450 monooxygenases using microsomal fractions, esterases using cytosolic fractions and glutathione-S-transferases using post mitochondrial fractions.

12.4 Cytochrome P450 monooxygenases

Cytochrome P450 monooxygenase activity was determined using the microsomal fraction of skin and liver with two substrates, ethoxyresorufin and pentoxyresorufin. The microsomal metabolism of ethoxy- and pentoxyresorufin results in the formation of resorufin, a fluorescent metabolite. As detailed in chapter 2, ethoxyresorufin is a substrate for CYP1A1 in skin (CYP1A2 is the main metabolising enzyme in uninduced liver). Pentoxyresorufin is a substrate for CYP2B in skin and liver.

12.4.1 Methods of preparation

The preparation of microsomal fractions from skin and liver are described in greater detail in section 10.3c. Briefly, skin from neonatal rat was used full thickness (as it is too thin, ≈500μm, to dermatome) and skin from 26 day old rats and 9-10 week old rats dermatomed at 350μm. The skin was then flash frozen in liquid nitrogen and ground to a powder. This was added to buffer for homogenisation (1g to 10ml buffer). Liver was also homogenised in buffer (1g to 10ml buffer). Cell debris was removed by centrifugation at 750g for 10 minutes. The supernatant was centrifuged at $10x10^3$g for 20 minutes to remove the mitochondrial fraction. Finally, the supernatant was spun at $110x10^3$g for 70 minutes to remove the microsomal fraction. Microsomes were prepared in a glycerol buffer to help maintain cytochrome P450 activity and were used fresh in all determinations of EROD and PROD activities.

12.4.2 Effect of age on cytochrome P450 monooxygenase activity in skin and liver

Wistar rats from three age groups were used to determine the effect of age on the metabolism of ethoxyresorufin and pentoxyresorufin. These were neonatal (4 days old), 26 days old and 9-10 week old rats. Neonatal rats were chosen for two reasons. Their skin was thin and free from

hair, making the tissue easier to homogenise for preparation of subcellular fractions and neonatal rat skin is most suitable for the preparation of rat keratinocytes. Rats at 26 days old were chosen as this age group was used for skin absorption studies, where the hair follicles are at their shortest in relation to the thickness of the skin. Rats at 9-10 weeks old were chosen as fully matured rats.

a) Methods

Four rats of each age group (neonatal, 26 days and 9-10 weeks) were used to prepare rat skin and liver microsomes as described earlier. The method for determining alkoxyresorufin-*O*-dealkylation is described in section 11.2b.

b) Results

The preparation of microsomal fractions only included one spin at 110 000g. It was found that a second spin following resuspension of the microsomal protein led to a large loss in the skin microsomal pellet. This was particularly noticeable when preparing human skin microsomes. It was also found that cytochrome P450 activity decreases rapidly in skin with time as indicated in the keratinocytes studies in chapter 13. It was therefore important to minimise the time spent preparing microsomes from skin in order to maintain maximum activity. Liver microsomes were prepared by identical procedures to allow direct comparisons. Protein recoveries for the microsomal fraction of rat skin and liver are shown in table 12.1.

Table 12.1 Recovery of microsomal protein from rat skin and liver from three age groups. (mg protein/g tissue. mean±sem, n=4).

	neonatal rat	26 day old rat	9-10 week old rat
skin	0.054±0.03	0.071±0.021	0.064±0.027
liver	3.50±0.67	9.51±1.59	14.17±3.22

Tables 12.2 to 12.4 show the data obtained for ethoxyresorufin-*O*-deethylation and pentoxyresorufin-*O*-dependentylation activities in rat skin and liver microsomes expressed as activity per mg of microsomal protein and as activity per gram of tissue. Levels were compared by ANOVA followed by paired t-test to evaluate statistically significant differences.

Table 12.2 Ethoxyresorufin *O*-deethylation (EROD) and pentoxyresorufin-*O*-dependentylation (PROD) activities in neonatal rat skin and liver microsomes (Mean±sem, n = 4).

	Skin		Liver	
	pmoles/min/mg protein	pmoles/min/g tissue	pmoles/min/mg protein	pmoles/min/g tissue
EROD	5.68±3.26	0.306±0.156	4.11±1.63	14.4±7.7
PROD	1.58±0.688	0.085±0 037	28.5±3.13	99.7±10.9

Table 12.3 Ethoxyresorufin-*O*-deethylation (EROD) and pentoxyresorufin-*O*-dependentylation (PROD) activities in skin and liver microsomes of 26 day old rats (Mean±sem, n = 4).

	Skin		Liver	
	pmoles/min/mg protein	pmoles/min/g tissue	pmoles/min/mg protein	pmoles/min/g tissue
EROD	3.79±1.32	0.306±0.111	103.0±26.6	980±253
PROD	2.68±0.548	0.216±0.044	19.1±3.07	181±29.2

Table 12.4 Ethoxyresorufin-*O*-deethylation (EROD) and pentoxyresorufin-*O*-dependentylation (PROD) activities in skin and liver microsomes of 9-10 week old rats (Mean±sem, n = 4).

	Skin		Liver	
	pmoles min/mg protein	pmoles min/g tissue	pmoles/min/mg protein	pmoles/min/g tissue
EROD	3.18±0.933	0.173±0.077	57.8±3.27	819±123
PROD	2.52±0.987	0.137±0.054	18.4±4.76	261±68.4

These tabulated results are illustrated graphically in graphs 12.1 to 12.4.

Graph 12.1. The effect of age of Wistar rats on ethoxyresorufin-*O*-deethylation (EROD) activities in liver and skin expressed as activity/min/mg microsomal protein (mean±sem, n=4).
(* indicates a significant difference from mature rats ($p<0.01$),
** indicates a significant difference from neonatal and 9-10 week old rats ($P<0.01$),
evaluated by ANOVA followed by paired t-test).

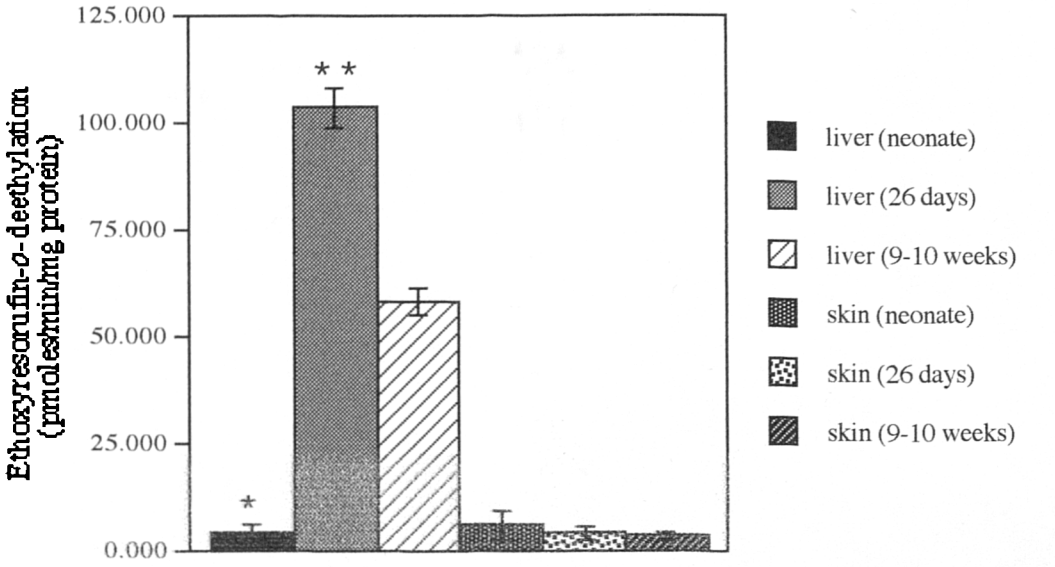

Graph 12.2. The effect of age of Wistar rats on ethoxyresorufin-*O*-deethylation (EROD) activities in liver and skin expressed as activity/min/g tissue (mean±sem, n=4).
(* indicates a significant difference from mature rats ($p<0.01$),
evaluated by ANOVA followed by paired t-test).

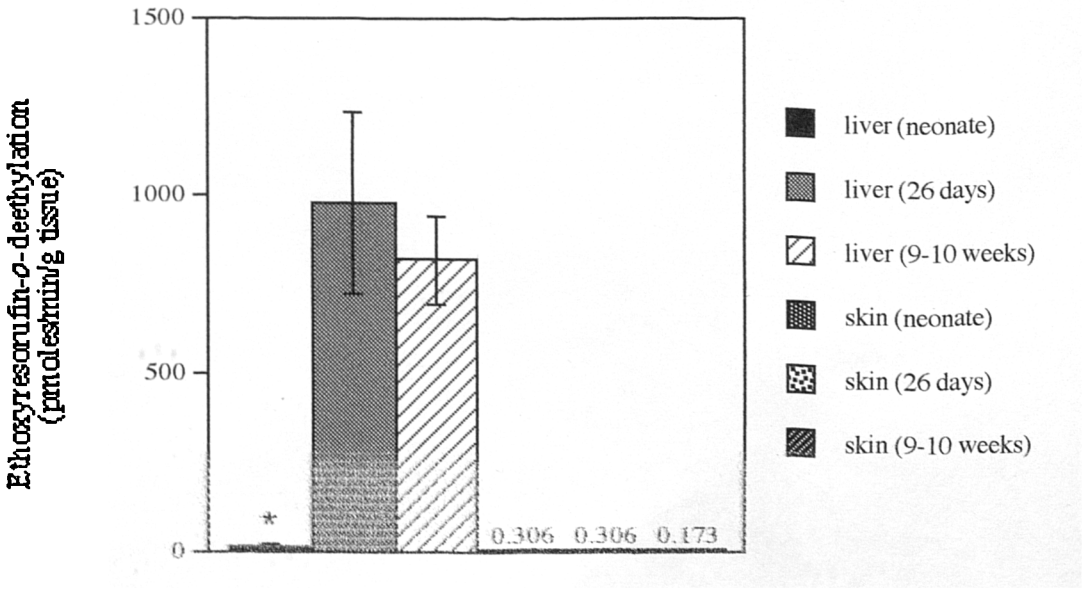

Graph 12.3. The effect of age of Wistar rats on pentoxyresorufin-*O*-dependentylation (PROD) activities in liver and skin expressed as activity/min/g tissue (mean±sem, n=4).
(* indicates a significant difference from mature rats ($p<0.01$),
evaluated by ANOVA followed by paired t-test).

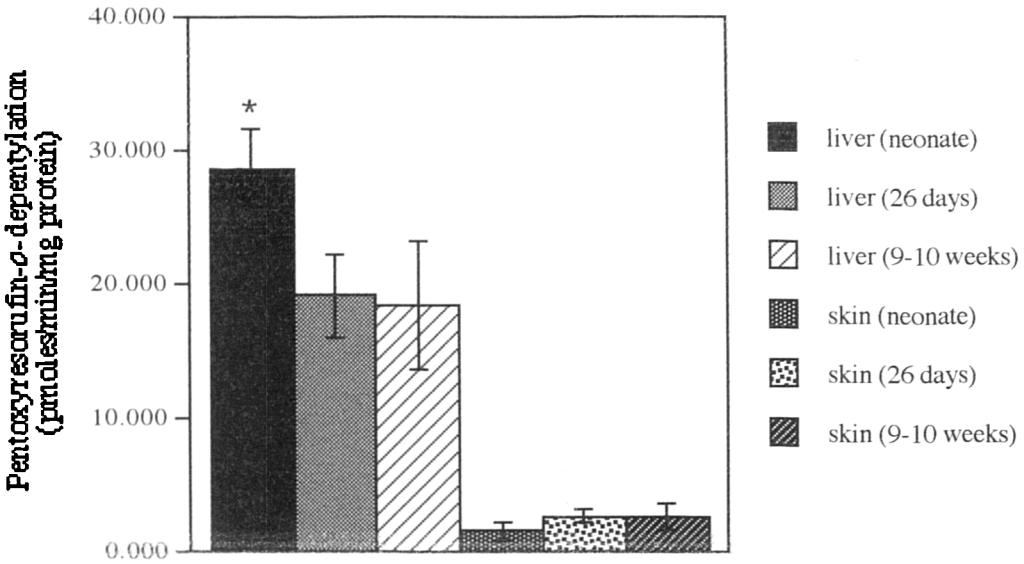

Graph 12.4. The effect of age of Wistar rats on pentoxyresorufin-*O*-dependentylation (PROD) activities in liver and skin expressed as activity/min/g tissue (mean±sem, n=4).
(* indicates a significant difference from mature rats ($p<0.01$),
evaluated by ANOVA followed by paired t-test).

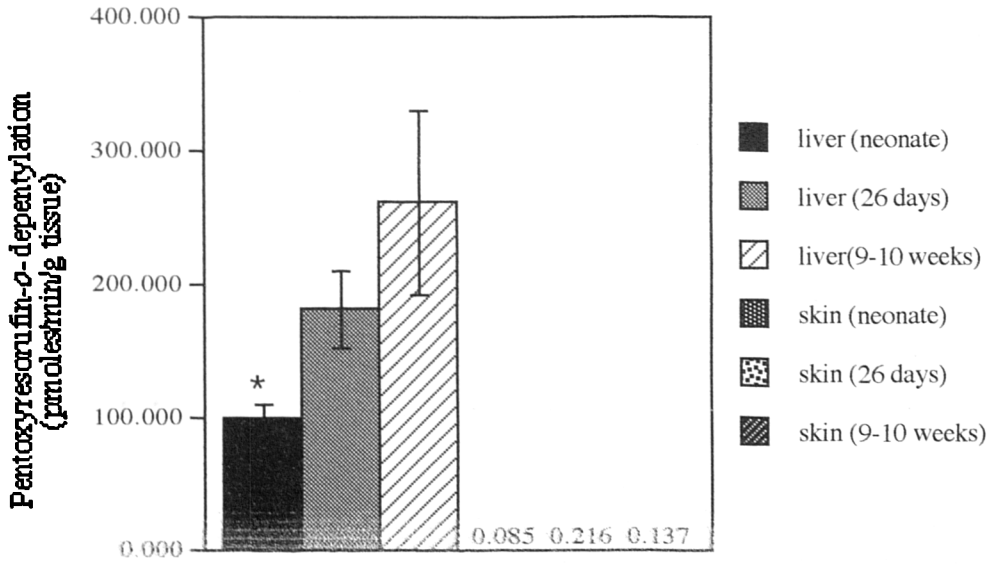

Ethoxyresorufin-*O*-deethylation (EROD) activity in neonatal rat liver was significantly lower than the mature rats ($p<0.01$). In terms of activity expressed per mg of microsomal protein, activity dropped from the 26 day old rat to the 9-10 week old rat, but in terms of activity expressed per gram of tissue, the 26 day old rat was not significantly different from the 9-10 week old rat ($p>0.05$). EROD activity in skin was not significantly different at any of the rat ages examined ($p>0.01$). In terms of activity per mg of microsomal protein, skin EROD was found to be similar to liver activity in the neonatal rat, 27 times lower in the 26 old rat and 18 times lower in the 9-10 week old rat. Due to the small amounts of microsomal protein found in skin compared to liver (0.05-0.07mg/g vs. 3-14mg/g), these comparisons become far greater when activity is expressed as per gram of tissue. Skin activities were 48, 3300 and 4700 times lower than liver for neonate, 26 day old and 9-10 week old rats respectively.

Pentoxyresorufin-*O*-dependentylation (PROD) activity in the neonatal rat was higher than the EROD activity. With respect to activity per mg of microsomal protein the 26 day and the 9-10 week old rat activities were much lower than neonatal rat ($P<0.01$). This could be due to other enzymes in the liver accounting for more microsomal protein as the rat ages. When expressed as per gram of tissue, liver PROD activity increases with the age of the rat, showing an increase of this enzyme per gram of liver with age. As with EROD activity, the levels of PROD activity in the skin remain fairly constant with relation to the age of the rat. Expressed as activity per mg of microsomal protein skin PROD shows 18, 7 and 7 times lower activity than liver. Expressed as per gram of tissue, skin shows 1160, 840 and 1900 times lower activity than liver.

12.4.3 Species differences

a) Methods

Microsomes were prepared in glycerol buffer from 9 dermatomed (350μm) human skin samples and 6 dermatomed (350μm) pig skin samples (from pig ears). EROD activity was measurable using only the freshly prepared microsomes, so that microsomal activity was as close to *in vivo* microsomal activity as possible.

b) Results

Recovery of human and pig skin microsomes were 0.021±0.007mg protein/g (n=9) and 0.019±0.004mg/g of dermatomed skin respectively. EROD activity was detectable in only one human skin sample out of the 9 samples tested. This was from female arm skin, obtained from reductive plastic surgery. Microsomes prepared from this skin showed an activity of 2.95 pmoles/min/mg protein. Pig skin EROD was detectable at low levels with an activity of 0.223±0.057 pmoles/min/mg microsomal protein (n=6). PROD was not detectable in human or pig skin.

12.4.4 Induction study

The effect of classical cytochrome P450 inducers on rat skin microsomal activity was determined. Rats were dosed with phenobarbital, ß-naphthoflavone and ethanol and the induction profile of liver was compared to the profile of skin.

a) Method

The following method utilised skin and liver tissue samples taken from rats used as part of an induction study by Sarah Crosbie (PhD student, University of Newcastle upon Tyne). 25 Male Wistar rats all aged 8 weeks old were divided into 5 groups. These 5 groups were then treated as follows:

Group 1: Corn-oil control. Rats were given corn-oil at a dose of 5ml/kg/day by gavage for three days and then sacrificed 24 hours after the last dose.

Group 2: ß-naphthoflavone treated. Rats were given 80mg/kg/day ß-NF in corn-oil by gavage for three days and then sacrificed 24 hours after the last dose.

Group 3: Phenobarbital treated. Rats were given 100mg phenobarbital in saline/kg/day by i.p. injection for 4 days and then sacrificed 24 hours after the last dose.

Group 4: Ethanol treated. Rats were given ethanol (15%) in their drinking water for 5 days and then sacrificed.

Group 5: Control. Rats given no treatment. Sacrificed on last day.

All rats were dosed and sacriced by animal house technicians. Rats were sacrificed by cervical dislocation and their fur clipped. Livers were excised and skins removed and both kept on ice. The skin was dermatomed to a thickness of 350μm. One strip of skin was used for isolating keratinocytes and determining activity in freshly prepared cells (see section 13.4). The remaining dermatomed skin was used to prepare microsomes. Microsomes from the livers and the skins were prepared freshly as previously described, in the general methods section 10.3c. EROD and PROD activities were determined with the freshly prepared microsomes from each tissue sample.

b) Results

Graph 12.5 illustrates the differences in liver weights between each group. Differences were statistically evaluated using ANOVA. There was no significant increase in liver weight for corn oil control and ß-naphthoflavone (dissolved in corn oil) treated rats. There was also no significant increase in liver weight between untreated and ethanol treated rats. There was however a significant increase in liver weight gain between untreated and corn oil control and also all groups with phenobarbital treated rats ($P<0.05$ as calculated from ANOVA followed by paired t-test).

Graph 12.5 Liver weights of rats untreated and treated with corn oil, ß-naphthoflavone, phenobarbital and ethanol (mean±sem, n=5). (* indicates significantly different from control untreated rats, ** indicates significantly different from all other groups, evaluated by ANOVA followed by paired t-test).

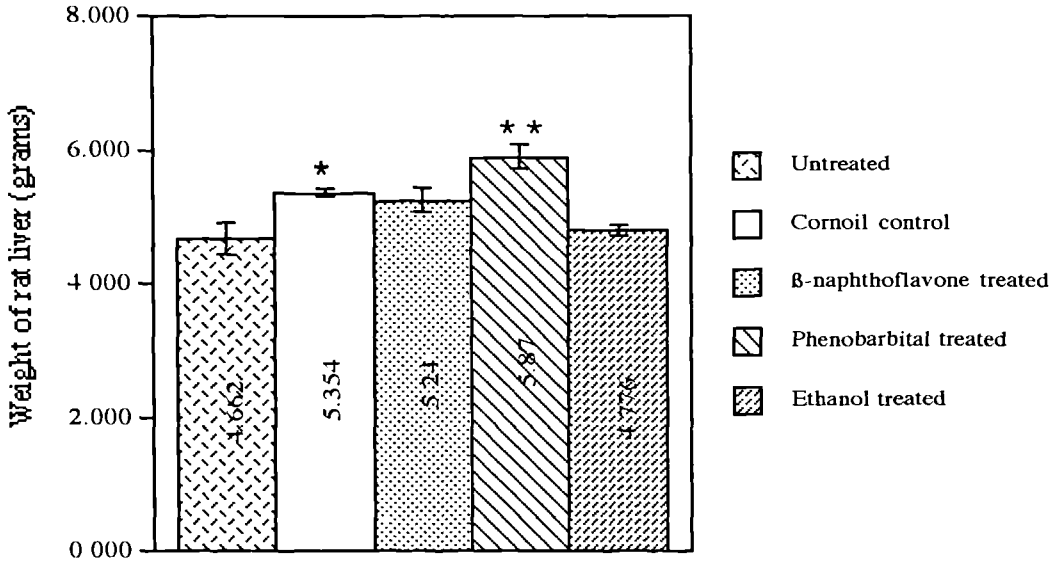

Table 12.5 Recoveries of microsomal protein from control and induced rats are shown in the following table. (* indicates significantly greater liver microsomal protein recovery, ** indicates significantly lower skin microsomal protein recovery, $P<0.01$, evaluated by ANOVA followed by paired t-test).

	Skin	Liver
No treatment	0.070±0.023	16.9±2.9
Corn oil	0.065±0.031	17.1±2.3
ß-naphthoflavone	0.082±0.026	16.8±1.1
Phenobarbital	0.085±0.028	19.4±1.5 *
Ethanol	0.046±0.019 **	16.3±2.1

The EROD and PROD activities of liver and skin microsomes were expressed per mg of microsomal protein and per gram of tissue. The data are tabulated in table 12.5 and illustrated in graphs 12.6 and 12.7.

Table 12.6 The ethoxyresorufin-*O*-deethylation (EROD) and pentoxyresorufin-*O*-dependentylation (PROD) activities of liver and skin microsomes from rats preinduced with ß-naphthoflavone, phenobarbital and ethanol, untreated and corn oil controls.

a) Liver activities pmoles/min/mg microsomal protein (mean±sem, n=5).

	Liver EROD	Liver PROD
No treatment	56.4±2.1	13.3±1.3
Corn oil	64.5±3.8	10.4±0.7
ß-naphthoflavone	368±28	16.9±1.1
Phenobarbital	445±39	841±39
Ethanol	81.8±6.9	14.2±2.6

b) Liver activities nmoles min/g liver (mean±sem, n=5).

	Liver EROD	Liver PROD
No treatment	0.955±0.047	0.224±0.021
Corn oil	1.101±0.059	0.175±0.015
ß-naphthoflavone	6.192±0.279	0.286±0.019
Phenobarbital	8.617±0.676	14.822±0.989
Ethanol	1.584±0.134	0.253±0.036

c) Skin activities pmoles min/mg microsomal protein (mean±sem, n=5).

	Skin EROD	Skin PROD
No treatment	3.34±0.24	2.31±0.17
Corn oil	2.80±1.09	2.09±0.33
ß-naphthoflavone	2.39±0.60	1.81±0.12
Phenobarbital	2.69±0.42	2.02±0.20
Ethanol	0.238±0.039	0.112±0.003

d) Skin activities pmoles/min/g dermatomed skin (mean±sem, n=5).

	Skin EROD	Skin PROD
No treatment	0.167±0.012	0.136±0.016
Corn oil	0.183±0.066	0.137±0.018
ß-naphthoflavone	0.197±0.046	0.144±0.008
Phenobarbital	0.239±0.027	0.168±0.014
Ethanol	0.011±0.002	0.009±0.0002

Graph 12.6 Ethoxyresorufin-*O*-deethylation and pentoxyresorufin-*O*-dependentylation activities in liver microsomes of rats untreated and treated with corn oil, ß-naphthoflavone, phenobarbital and ethanol (mean±sem, n=5).
(* indicates significantly different from control rats, P<0.01, evaluated by ANOVA followed by paired t-test).

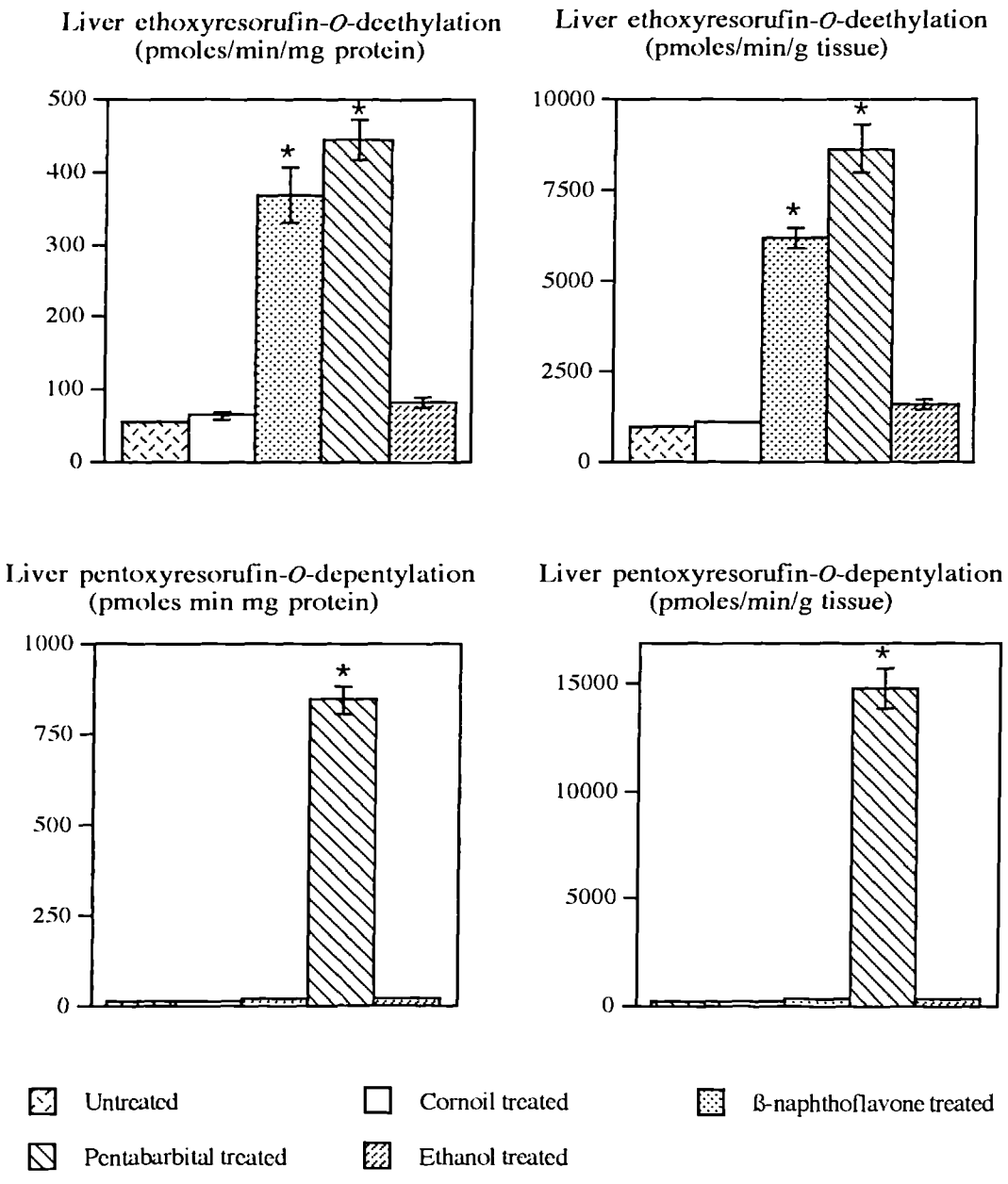

Graph 12.7 Ethoxyresorufin-*O*-deethylation and pentoxyresorufin-*O*-dependentylation activities in dermatomed skin microsomes of rats untreated and treated with corn oil, ß-naphthoflavone, phenobarbital and ethanol (mean±sem, n=5). (* indicates significantly different from all other groups, P<0.01, evaluated by ANOVA followed by paired t-test).

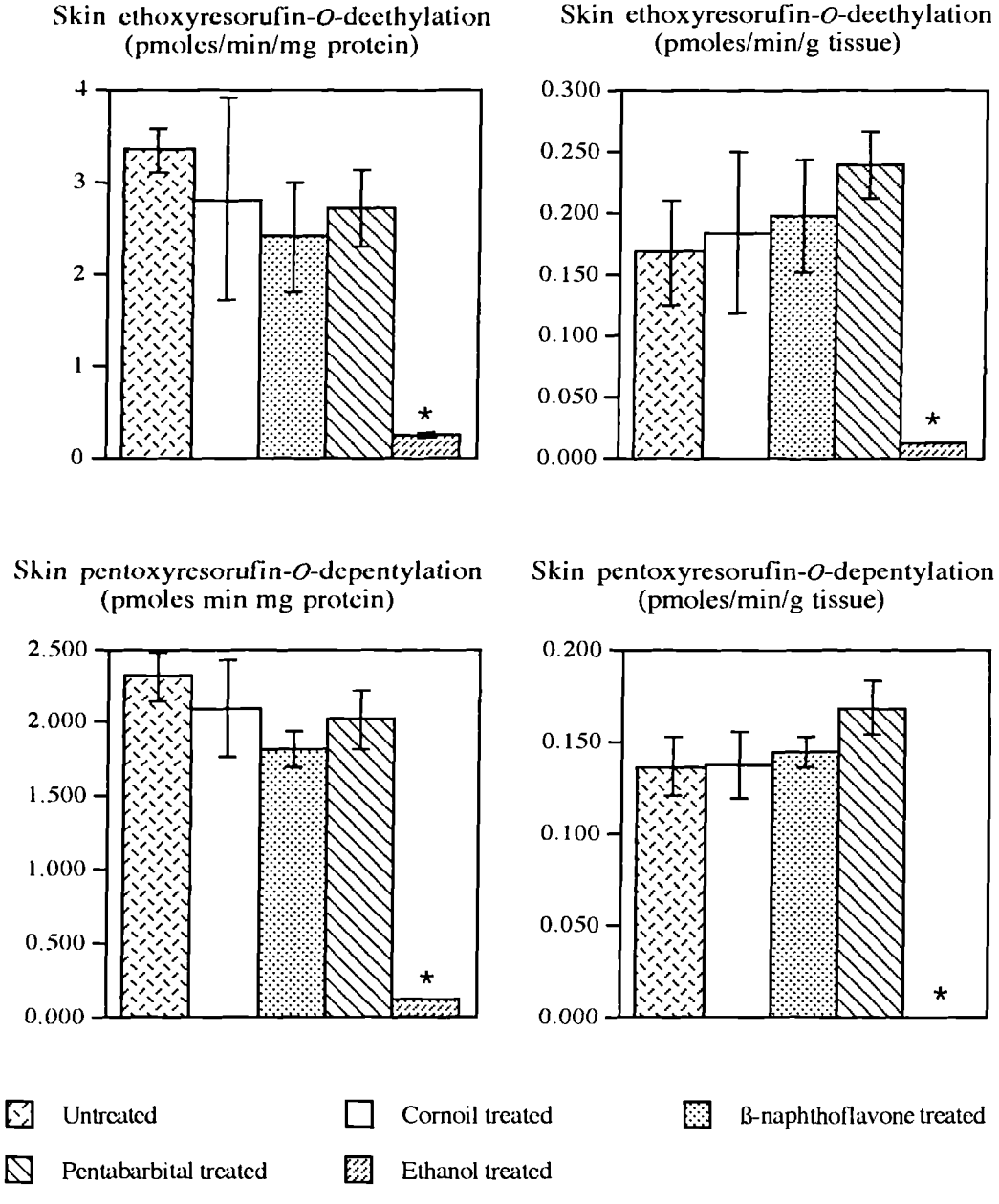

After induction, the livers of the rats were assessed for changes in weight and a significant increase in liver weight was found between the control rat and that of the phenobarbital treated rat ($p<0.01$). This difference in liver weight gain was also reflected in the microsomal protein recovery between the control rat and phenobarbital treated rat. The recovery of microsomal protein from the phenobarbital treated rat was significantly higher than the control rat ($p<0.01$), therefore indicating the induction of microsomal protein expression.

No statistical difference was found between the liver EROD and PROD activities in the untreated control, corn oil control and ethanol dosed rats. The EROD microsomal activity of the ß-naphthoflavone treated rats was induced to levels approximately 6 times greater than control rats ($p<0.01$), whereas PROD activity remained similar to control ($p>0.01$). The levels of EROD and PROD microsomal activities in the phenobarbitone treated rats were much higher and increased by 7.4 and 65 times respectively compared to control rats ($p<0.01$).

In terms of per gram of tissue weight, EROD activity in ß-naphthoflavone rats also increased 6 fold, while PROD activity was comparable to control. The levels of EROD and PROD in phenobarbital treated rats increased 8.6 and 75 times, showing not only an increase in activity in terms of microsomal protein, but also in activity per gram of liver.

EROD and PROD activities in the skin microsomes of ß-naphthoflavone and phenobarbital treated rats were not significantly different from control rats ($p>0.01$). Interestingly, EROD and PROD activities in ethanol treated rats were considerably reduced ($p<0.01$). This was also reflected by a significantly lower recovery of microsomal protein from the skin of rats treated with ethanol.

12.4.5 Discussion

The aim of this study was to determine the capacity of skin microsomes to carry out monooxygenase reactions. Few cytochrome P-450 isoforms have been characterised in skin. The ones which have include CYP1A1 and CYP2B. In the described experimental studies with skin homogenates CYP1A1 and CYP2B were measured with the markers ethoxyresorufin and pentoxyresorufin respectively.

Levels of cytochrome P-450 were found to be very low in skin compared to liver, therefore microsomes were prepared in a glycerol buffer, to minimise loss of activity. To measure activity as close as possible to *in vivo* microsomal activity, samples were used fresh in preference to those stored frozen at -70°C. This was to avoid any loss in activity during storage. Studies on the stability of cytochrome P-450 activity with isolated keratinocytes have revealed a substantial decrease in activity with time (see chapter 13). Therefore skin microsomal activity is unstable and rapidly lost. All possible delays in the preparation of microsomes from fresh skin were therefore avoided.

Measurements of EROD and PROD in rat skin of three different ages, neonate, 26 days old and 9-10 weeks old revealed that their activities did not change with age, unlike liver activity, which increased from the neonate to the adult rat. Therefore neonatal rat skin, which is much easier to use in the preparation of homogenates and keratinocytes, is suitable for use in metabolic studies involving CYP1A1 and CYP2B. However, it must be noted that skin EROD and PROD activities were measured in full thickness neonatal rat skin and dermatomed 26 day old and 9-10 week old rat skin. Therefore, activity expressed in terms of per gram of tissue may be misleading. Activity expressed in terms of full thickness skin for all age groups would lead to lower activity in the 26 day old and 9-10 week old rats. It has been demonstrated by immunohistochemistry, that cytochrome P450 monooxygenases are localised at the basal layer of the epidermis, in cells of the sebaceous glands and around hair follicles (Raza *et al*, 1992). By dermatoming skin, the epidermis (the active layer) is removed and the microsomal fraction more easily prepared. It may therefore be more appropriate to express EROD and PROD activity in skin in terms of per unit area.

Adult liver showed less EROD and PROD activity per mg microsomal protein than at 26 days. This may be due to other enzymes in the liver maturing in the adult rat and being responsible for increasing the level of protein in the microsomal fraction.

EROD and PROD activities in the skin of rats preinduced with ß-naphthoflavone or phenobarbital remain the same as in uninduced rats. Rat skin is therefore very slow to respond to induction after i.p. administration of inducing agents and may require longer induction periods. This was also found to be the case for keratinocytes, where exposure to ß-naphthoflavone often led to no cytochrome P450 induction (see chapter 13). It may also be that the inducing agents did not reach the skin in sufficient levels to increase xenobiotic metabolism. Studies have not been conducted to discover the concentration of inducing agents reaching the skin after oral or intraperitoneal administration. It was also seen that rats treated with ethanol, had greatly reduced levels of EROD and PROD activity. A clear reason could not be found for this result, but it has been reported in liver that ethanol may reduce enzyme activity by reducing the available oxygen to the cytochrome P450 enzymes (O'Shaughnessy and Sultatos, 1995). A similar effect may therefore have occurred in the skin.

The level of EROD activity in pig skin was low in comparison to rat skin and EROD activity was only detectable in one human skin sample. This one sample cannot be considered an indication of human skin EROD levels, as this may have been an erroneous result. Other human EROD activities were below the limit of detection. This indicates relatively low levels of cytochrome P450 in skin of man and pig. There are no reports in the literature of pig skin EROD and PROD activities. It was interesting to note that similar levels of microsomal protein were recovered from both human and pig skin. During the preparation of microsomes from human and pig skin, only very small amounts were obtained ($\approx 20 \mu g$/g skin), less than half that is found in rat skin. Therefore, the low levels of microsomal protein in human and pig skin may also contribute to the low enzyme activity. PROD activity was not detectable in either pig or human skin. CYP2B has been shown to be

responsible for PROD activity. CYP2B is also responsible for the metabolism of aldrin to the epoxide metabolite dieldrin. Rat skin has been shown to metabolise aldrin (Graham *et al*, 1991), but activity in human skin were shown to be at the limit of detection (Williams *et al*, 1985). Therefore, the low EROD and PROD activity of human skin microsomal protein is in part due to the low recovery of microsomal protein from skin and the lack of high sensitivity needed for the detection of these activities.

In summary, rat skin shows EROD and PROD activity which is not dependant on the age of the rat. Activity is not inducible by i.p. administration of ß-naphthoflavone or phenobarbital, (but is reduced after drinking ethanol). Pig skin showed detectable levels of EROD activity, but no PROD activity, while human skin showed neither detectable EROD or PROD activity. Both human and pig skin showed similar levels of microsomal protein, therefore, pig skin is more comparable to human skin than rat skin. Additional studies on skin metabolism and viability (chapter 15) have shown that esterase activity and glutathione content of pig and human skin are also similar, which suggests pig skin is a more suitable model for human skin than the rat. This has particular relevance to studies of metabolism during percutaneous absorption in which pig is used as a model for human.

12.5 Esterase activity

This section describes the characteristics of the hydrolysis of 4-methylumbelliferyl heptanoate (4-MUH), a non-specific esterase marker, to the fluorescent metabolite 4-methylumbelliferone (4-MU) by skin cytosolic fractions. The formula for the reaction is as follows:

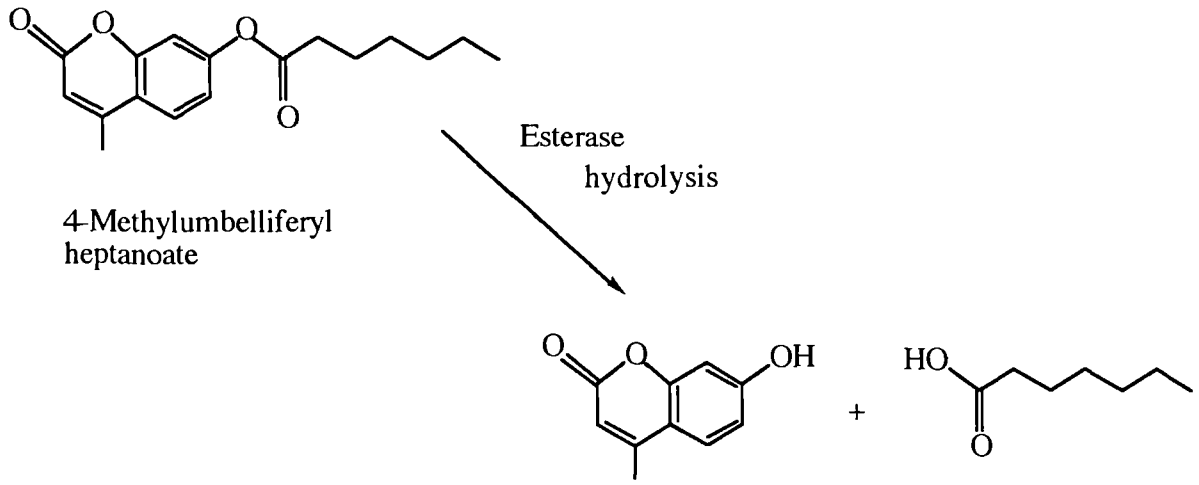

The aim of these studies was to measure the esterase hydrolysis of 4-MUH in the skin cytosolic fractions of the rat and to measure any differences with age. Species differences were measured between rat, mouse, pig and human skin. Comparisons were made with the liver of rat mouse and pig. The effect of the classical inducing agents ß-naphthoflavone and phenobarbital were also investigated. Characterisation of the esterase involved in the hydrolysis of 4-MUH was investigated by the use of broad range and specific esterase inhibitors.

12.5.1 Methods

The studies described here are subdivided into the effect of age on esterase 4-MUH hydrolysis in rat cytosol, differences in skin esterase activity between species, the effect of preinducing rats on 4-MUH hydrolysis and the characterisation of the esterase involved in hydrolysis.

a) Assay for 4-methylumbelliferyl heptanoate hydrolysis

The general assay for determining 4-MUH hydrolysis in skin cytosolic and post mitochondrial fractions is described in section 11.3. Briefly, determination of esterase activity in tissue cytosol or microsomes was conducted using a water jacketed fluorimeter set to 37°C. The fluorimeter was set to an excitation wavelength of 345nm and an emission wavelength of 435nm. Stock solutions consisted of Trizma buffer pH 7.7 (50mM) containing EDTA (0.1mM). 4-MUH (17mM) in DMSO. 4-MU (0.1mM) in DMSO and BSA solution (1.2mg/ml).

Measurements of a standard were assessed with each determination. To a microcuvette was added 980μl of buffer and 20μl of BSA solution, placed in the fluorimeter and the fluorescence was set to zero. This was followed by the addition of 1μl of 0.1mM 4-MU (100pmoles) to the cuvette and fluorescence was recorded. This was repeated in triplicate.

The concentration of 4-MUH in the incubation was assessed to ensure saturation of the enzyme. Increasing concentrations of cytosolic protein (5μg, 10μg, 25μg, 50μg and 100μg/ml) were measured with a fixed concentration of 4-MUH to determine the concentration giving the fastest rate of reaction. Then using a fixed concentration of cytosolic protein at a point below the fastest rate of reaction, several different concentrations of 4-MUH (8.5μM, 17μM 34μM, 51μM, 68μM and 85μM) were used to determine the concentration of substrate saturating the enzyme. The concentration of substrate was evaluated for both skin and liver of all species.

For enzyme activity 980μl of buffer was mixed in a cuvette with a sample of protein (cytosol or microsomes), approx. 10-20μg protein. This was made up to 1ml with buffer. The reaction was started by adding 3μl of 4-MUH solution, which was mixed and replaced in to the cell holder immediately. Acquisition of data was started immediately and rate of reaction calculated. This was repeated in duplicate.

Activity was calculated as follows:

$$\text{pmoles min mg protein} = \frac{\text{change in fluorescence units min}}{\text{fluorescence units forlpmole MU}} \times \frac{1000}{\mu\text{g protein in reaction}}$$

Results are expressed as nmoles MU produced min/mg protein.

b) Effect of age on 4-methylumbelliferyl heptanoate hydrolysis

The rats used in this study were neonatal (4 days old), 26 days old and 9-10 weeks old (4 from each age group). All skin and liver cytosolic fractions were prepared during the preparation of the microsomal fractions, which were used in the previous section to determine microsomal monooxygenase activity. Samples were stored frozen at -70°C before use.

c) Species differences

Cytosolic protein was prepared from the skin and liver of Wistar rats only. For Balb C mouse (nine animals), preparation of skin and liver subcellular fractions was conducted at Zeneca central toxicology laboratory, where facilities were only available for the preparation of post mitochondrial fractions. Pig skin (4 samples) and human skin (14 samples) post mitochondrial fractions were prepared and pig liver (4 samples) and human liver (5 samples) cytosolic fractions were prepared at the University of Newcastle. All fractions were used to determine 4-MUH

hydrolysis. Additionally, rat skin and liver microsomes were also assessed for 4-MUH hydrolysis activity.

d) Effect of preinduction with ß-naphthoflavone, phenobarbital and ethanol

Skin and liver cytosolic fractions from rats preinduced with ß-naphthoflavone, phenobarbital and ethanol were prepared during the preparation of microsomes for studies in section 12.4.4. These were used to evaluate the effect of exposure to these classical inducers on the hydrolysis of 4-MUH.

e) Characterisation of the esterase involved in 4-methylumbelliferyl heptanoate hydrolysis

The effect of a range of different esterase inhibitors on 4-MUH hydrolysis was investigated in order to characterise which form(s) of esterase was involved in the reaction. The inhibitors used are listed in table 12.7.

Table 12.7 Esterase inhibitors.

Inhibitor	Form of esterase inhibited	mwt.
Paraoxon	Carboxylesterase, acetylcholinesterase and cholinesterase inhibitor. Inhibitor of enzymes with serine groups.	275.2
BNPP (bis-(p-nitrophenyl)-phosphate)	Differential carboxylesterase inhibitor.	362.2
BW284c51 (1,5 bis(4-allyldimethylammonium phenyl)pentan-3-one dibromide)	Acetylcholinesterase inhibitor.	566.4
IsoOMPA (tetraisopropylpyrophosphoamide)	Cholinesterase inhibitor.	342.4
Mercuric Chloride	Inhibitor of aryl esterases, paraoxonases and DFPases.	271.5
PMSF (phenymethylsulfonyl fluoride)	Carboxylesterase, acetylcholinesterase and cholinesterase inhibitor. Inhibitor of enzymes with serine groups.	174.2

Inhibitors were incubated with cytosolic or post mitochondrial protein for 4 minutes before addition of the substrate 4-MUH. Inhibitors were added in a range of concentrations (20μM, 50μM and 100μM). Inhibition was then calculated as a percentage decrease in 4-MUH hydrolysis.

12.5.2 Results

a) Assay conditions for 4-methylumbelliferyl heptanoate hydrolysis

A concentration of the substrate 4-MUH for enzyme saturation was found at 51μM and this was suitable for all skin and liver cytosolic and post mitochondrial fractions for all species, with incubations containing 10-20μg protein. Therefore, this concentration was used in all experimental investigations.

b) Effect of age on 4-methylumbelliferyl heptanoate hydrolysis

The recovery of cytosolic protein from the skin and liver of neonatal, 26 day old and 9-10 week old rats is shown in table 12.8.

Table 12.8 Cytosolic protein recovery from rat skin and liver from three age groups (mg protein g tissue. mean±sem, n=4).

	neonatal rat	26 day old rat	9-10 week old rat
skin	20.5±3.5	17.5±2.9	22.9±2.9
liver	26.9±2.6	27.9±0.9	31.1±2.2

The activities measured are shown in table 12.9 expressed as activity per mg of cytosolic protein and per gram of wet weight tissue.

Table 12.9 4-Methylumbelliferyl heptanoate hydrolysis activities by skin (full thickness neonatal and dermatomed 26 day old and 9-10 week old rat skin) and liver cytosolic protein from neonatal, 26 days and 9-10 weeks old Wistar rats (mean±sem, n=4).

Age of rat	Skin		Liver	
	nmoles/min/mg protein	nmoles/min/g tissue	nmoles/min/mg protein	nmoles/min/g tissue
neonate	6.32±0.26	129.3±6.2	4.48±0.18	120.8±21.8
26 day old	7.07±0.29	123.8±17.2	7.89±0.24	220.8±45.4
9-10 week old	6.64±0.35	152.1±15.7	8.59±0.42	267.2±39.0

With respect to cytosolic protein or per gram of tissue, esterase activity as determined by 4-methylumbelliferyl heptanoate hydrolysis was not significantly different in skin with increase in age of rat. The liver activity was significantly lower in neonatal rat per mg cytosolic protein and per gram of tissue than in the older rats. As recovery of cytosolic protein from neonatal rats was similar to older rats, absolute esterase activity was therefore lower in neonatal rat liver.

c) Species differences

The rate of 4-MUH hydrolysis was measured in the cytosolic fraction of skin and liver of neonatal rat and adult rat. Measurements were also conducted with mouse skin and liver post mitochondrial fractions, pig and human skin post mitochondrial fractions and pig and human liver cytosolic fractions. Additionally, 4-MUH hydrolysis was measured with adult rat skin and liver microsomal fractions. Table 12.10 details their activities per mg of protein.

Table 12.10 Rates of 4-Methylumbelliferyl heptanoate hydrolysis with either skin and liver cytosol, post mitochondrial or microsomal fractions from neonatal rat, 26 day old rat, Balb/C mouse, pig and human. (nmoles/min/mg ±sem, * = post mitochondrial fractions).

	Neonatal Rat (n=4)	Adult Rat (n=5)	Mouse (n=9)	Pig (n=4)	Human	Adult rat microsomes (n=4)
Liver	4.48±0.18	7.89±0.24	16.73±2.44*	2.47±0.15	1.92±1.90 (n=5)	17.62±2.08
Skin	6.32±0.26	7.07±0.29	14.73±1.90*	19.73±0.26*	18.49±3.42* (n=14)	14.72±1.89

The rate of hydrolysis of 4-MUH in adult rat skin and liver cytosol was similar. The rate of neonatal rat skin cytosolic 4-MUH hydrolysis seemed to be similar to adult rat skin, but was statistically significantly lower ($p<0.01$). As previously determined, the rate of neonatal rat liver cytosolic 4-MUH hydrolysis was significantly lower than in 26 day old rat liver cytosol ($p<0.01$).

The rate of 4-MUH hydrolysis in mouse skin and liver post mitochondrial fractions was insignificantly different ($p>0.01$), as was the rate of hydrolysis between rat skin and liver microsomal fractions ($p>0.01$).

Human and pig skin post mitochondrial fractions showed similar levels of 4-MUH hydrolysis. Human and pig liver cytosolic fractions also showed a similar level of activity.

Table 12.11 shows the 4-MUH hydrolysis activities for each individual human skin post mitochondrial fraction., to illustrate the spread of activity in the human population The table also list the age and anatomical site for each human skin sample so that any differences in activities between age and anatomical site could be identified.

Table 12.11 Hydrolysis of 4-methylumbelliferyl heptanoate in individual human skin post mitochondrial fractions (nmoles/min/mg).

Human skin sample	Age	sex and site	nmoles/min/mg post-mitochondrial fraction
1	22	Female breast	12.423
2	23	Female breast	15.198
3	25	Female breast	11.574
4	21	Female breast	14.020
5	68	Female breast	16.580
6	22	Female breast	9.405
7	26	Female breast	15.232
8	-	Abdomen	18.724
9	21	Female breast	32.168
10	35	Female breast	11.427
11	-	Abdomen	12.450
12	42	Female breast	17.714
13	-	Abdomen	13.319
14	-	Female breast	58.629

Generally, rates of 4-MUH hydrolysis by human skin post mitochondrial fractions were between 9.4 and 18.7nmoles/min/mg protein, and no difference was seen between age or anatomical site. There were two exceptions in the samples studied (samples 9 and 14), both were female breast skin, and both were much higher than the other samples.

d) Effect of preinduction

After exposure to ß-naphthoflavone, phenobarbital and ethanol, cytosolic fractions were prepared from the rat skin and liver. The cytosolic fractions were then assayed for 4-MUH hydrolysis. Tables 12.12 and 12.13 represent the data obtained from the study in terms of activity per mg of cytosolic protein and per gram of tissue respectively.

Table 12.12 4-MUH activities in Wistar rat skin and liver after treatment with inducing agents. nmoles/min/mg cytosol (mean±sem, n=5)

Induction treatment	Dermatomed skin	Liver
No treatment	6.51±0.40	8.99±0.15
Corn oil	6.56±0.17	9.89±0.16
ß-naphthoflavone	6.45±0.22	9.79±0.45
Phenobarbital	6.06±0.29	9.74±0.48
Ethanol	5.71±0.51	10.45±0.72

Table 12.13 4-MUH activities in Wistar rat skin and liver after treatment with inducing agents. nmoles/min/g tissue (mean±sem, n=5)

Induction treatment	Dermatomed skin	Liver
No treatment	162.49±10.03	599.2±9.5
Corn oil	164.45±4.21	615.8±10.6
ß-naphthoflavone	160.68±5.52	643.0±29.8
Phenobarbital	150.99±7.70	640.1±18.3
Ethanol	147.30±12.76	652.6±21.1

The results showed that rats treated with ß-naphthoflavone, phenobarbital or ethanol did not lead to any significant change in activity compared to control rats ($p>0.01$), indicating no induction of the esterase activity associated with 4-MUH hydrolysis (results statistically evaluated with ANOVA).

e) Characterisation of the esterase involved in 4-methylumbelliferyl heptanoate hydrolysis

Tables 12.14 to 12.18 show the results obtained for the inhibition of 4-MUH hydrolysis with a broad range of esterase inhibitors for rat, mouse, pig and human skin and liver homogenates expressed as percentage inhibition.

Table 12.14 Inhibition of rat skin and liver cytosolic 4-MUH hydrolysis (mean of two determinations from the same sample).

	% inhibition							
	skin				liver			
inhibitor concentration	BNPP	Paraoxon	PMSF	IsoOMPA	BNPP	Paraoxon	PMSF	IsoOMPA
20μM	65.52	84.70	31.72	5.77	46.34	57.46	11.81	4.22
50μM	73.43	87.50	55.57	10.57	47.46	66.23	29.82	21.87
100μM	83.27	89.95	73.93	-0.07	56.47	67.08	53.07	28.87

Table 12.15 Inhibition of mouse skin and liver post mitochondrial 4-MUH hydrolysis by different esterase inhibitors (mean of two determinations from the same sample).

	% inhibition							
	skin				liver			
inhibitor concentration	BNPP	Paraoxon	PMSF	IsoOMPA	BNPP	Paraoxon	PMSF	IsoOMPA
20μM	22.10	86.12	14.92	0.24	ND	ND	ND	ND
50μM	35.73	87.10	50.86	7.55	ND	ND	ND	ND
100μM	67.75	91.42	64.40	17.33	98.98	99.25	92.99	66.72

Table 12.16 Inhibition of pig skin post mitochondrial and liver cytosolic 4-MUH hydrolysis by different esterase inhibitors (mean of two determinations from the same sample).

	% inhibition							
	skin				liver			
inhibitor concentration	BNPP	Paraoxon	PMSF	IsoOMPA	BNPP	Paraoxon	PMSF	IsoOMPA
20μM	64.28	72.65	72.52	61.26	72.18	79.42	77.03	1.87
50μM	68.43	76.25	72.74	69.57	75.42	81.06	81.98	3.27
100μM	78.65	83.72	75.72	73.95	82.22	84.90	80.57	7.24

Table 12.17 Inhibition of human skin post mitochondrial 4-MUH hydrolysis by different esterase inhibitors (mean of two determinations from the same sample).

	% inhibition			
inhibitor concentration	BNPP	Paraoxon	PMSF	IsoOMPA
20μM	6.11	22.90	17.52	9.59
50μM	12.29	21.00	13.70	0.93
100μM	38.02	41.20	24.75	2.85

Table 12.18 Inhibition of rat skin and liver microsomal 4-MUH hydrolysis by different esterase inhibitors (mean of two determinations from the same sample).

	% inhibition							
	skin				liver			
inhibitor concentration	BNPP	Paraoxon	PMSF	IsoOMPA	BNPP	Paraoxon	PMSF	IsoOMPA
20μM	58.98	78.66	56.92	1.67	71.93	95.89	62.22	1.56
50μM	72.74	82.13	74.06	-2.15	79.65	95.69	74.61	4.51
100μM	77.18	85.84	82.31	0.73	88.36	96.49	86.10	5.02

The inhibitors mercuric chloride and BW284c51 were ineffective at inhibiting 4-MUH hydrolysis in rat, mouse, pig or human skin or liver subcellular fractions. Rat microsomal fractions were also uninhibited. Therefore neither 'A' esterases nor acetylcholinesterase are involved in the hydrolysis of 4-MUH.

BNPP, paraoxon and PMSF were very effective inhibitors of 4-MUH hydrolysis and at 100μM could almost totally inhibit the reaction. IsoOMPA did not effectively inhibit rat liver or skin, mouse skin, pig liver or human skin 4-MUH hydrolysis in post mitochondrial fractions, though pig skin and mouse liver did display some degree of inhibition.

12.5.3 Discussion

The hydrolysis of 4-MUH in rat skin does not change with age. Therefore skin from neonatal rats was found to be a suitable model for further metabolism studies with keratinocytes and percutaneous absorption studies in the flow-through diffusion cell.

The absolute activity expressed in terms of protein and wet weight of tissue in rat gave similar profiles of 4-MUH hydrolysis, which also seems to apply across species with respect to

subcellular fractions. Hewitt *et al*, (1996) showed that fluoroxypyr methyl ester hydrolysis had a similar cross species spread. The high rate of 4-MUH hydrolysis seen in the post mitochondrial fractions compared to the cytosolic fractions indicates a high involvement of microsomal esterases. Addition of rat cytosolic and microsomal esterase activity in a ratio proportional to the protein per gram of tissue (cytosolic:microsomal is 2:1) would lead to an estimate of post mitochondrial activity similar to mouse liver and skin activity and human and pig skin activities. Human and pig skin have similar levels of esterase activity with respect to 4-MUH hydrolysis. This makes pig skin a good model for compounds involving esterase metabolism. Together with the similar level of cytochrome P450 monooxygenase activity established in earlier studies, pig skin seems to closely resemble the human skin metabolic profile.

No effects of induction of rat cytosolic esterase could be found in liver or skin. It has been previously shown that there was no effect of the induction regimen on cytochrome P450 monooxygenases in the skin, so this is consistent with those results. Specific monooxygenases were induced by ß-naphthoflavone or phenobarbital, in particular the phenobarbital induction of PROD in the liver microsomes. Experimental studies by McCracken *et al*, (1993b) have shown that phenobarbital induces microsomal carboxylesterase in rat liver, responsible for hydrolysing fluazifop butyl, carbaryl and phenyl valerate. The aryl esterases and the paraoxonase were also induced. However, the effects of induction by phenobarbital were microsomal specific and not seen in cytosolic esterases, therefore consistent with these studies.. This is probably due to the different composition of cytosolic esterases. Therefore 4-MUH may also be a substrate for different esterase isoforms than fluazifop butyl and carbaryl, although 4-MUH is a relatively non-specific substrate. Unfortunately the rate of 4-MUH hydrolysis with microsomes from the induced rat, was not investigated in this study. It is postulated that some degree of induction may have been seen with the microsomal fraction in parallel with the studies of McCracken *et al*, (1993b).

Mercuric chloride failed to inhibit any 4-MUH hydrolysis, therefore eliminating the involvement of aryl esterases and acetylcholinesterase. On the basis of the degree of BNPP, paraoxon and PMSF inhibition seen in these results, the esterase involved in the hydrolysis of 4-MUH is clearly a carboxylesterase. Rat microsomal esterase inhibition displayed a similar profile to cytosolic and post mitochondrial esterase inhibition, therefore carboxylesterase in microsomes is also responsible for 4-MUH hydrolysis. Lack of inhibition by isoOMPA, suggested little involvement of cholinesterase, except in mouse liver and pig skin. An explanation for this is not available from these studies, but the concentration of isoOMPA in these reactions may have been too high to be specifically a cholinesterase inhibitor and carboxylesterase may have been effected. Heymann *et al*, (1993) showed that liver and skin cytosol contains at least 4 types of carboxylesterase, two of which are sensitive to paraoxon (serine active centres) and two which are insensitive to organophosphate inhibition. It is possible that one or more forms of carboxylesterase could be sensitive to isoOMPA inhibition. Little information is available in the literature on pig skin esterases. Further investigations classifying pig skin esterases may reveal a different pattern of esterases compared to other species. In human skin, only 60% of activity was inhibited by paraoxon.

This may also suggest that the forms of carboxylesterase in human skin are not as sensitive to paraoxon as other species, or that forms insensitive to paraoxon make up more of the esterase in human skin.

The data for esterase metabolism in skin and liver are comparable with those of McCracken *et al*, (1993c) who investigated the hydrolysis of fluazifop butyl and carbaryl and identified a major role for carboxylesterase in the microsomes and liver of rat skin and liver. It could be suggested from these results that the metabolism of xenobiotics via esterase hydrolysis may also take place during percutaneous penetration. This was evident in studies by Clark *et al*, (1993) who showed metabolism of fluazifop butyl by esterases during percutaneous absorption through rat and human skin and by Boehnlein *et al*, (1994) who showed the involvement of esterases in the metabolism of retinyl palmitate during percutaneous absorption through guinea pig and human skin. However, Macpherson *et al*, (1991) demonstrated that carbaryl can be metabolised by skin homogenates but not by skin during percutaneous penetration. However, the studies by Macpherson were undertaken using the static diffusion cell where viability of the skin was not efficiently maintained.

12.6 Glutathione-S-transferases

Skin glutathione-S-transferases can metabolise dinitrochlorobenzene (DNCB), a skin irritant and sensitiser, to the hydrophilic glutathione conjugate (Raza *et al*, 1991; Singhal *et al,* 1993). The aim of these studies was to determine the capacity of skin from several species including man, to metabolise DNCB using post mitochondrial homogenates.

12.6.1 Methods

Post mitochondrial fractions were prepared from the skin and liver of 6-7 week old Balb/c mouse (9 male and 9 female). Post mitochondrial fractions were also prepared form neonatal rat skin and liver (6 animals), 26 day old Wistar rat skin (6 animals) and domestic pig skin (from ears of 6 animals). Human skin (19 samples) from plastic surgery were also used to prepare post mitochondrial fractions.

Post mitochondrial fractions were prepared by a modification of the method previously described in section 10.3c. Dermatomed adult rat skin, pig skin and human skin and full thickness neonatal rat skin and Balb/C mouse skin was weighed and finely minced with sharp scissors. The minced skin was flash frozen with liquid nitrogen and ground to a fine powder in a mortar and pestle. The powdered skin was brushed into homogenisation tubes and 1ml of ice cold D-PBS buffer (section 10.2d) per 100mg of tissue. Homogenisation tubes were kept on ice at all times. Homogenisation involved 3x10 second bursts at setting 6 with a homogeniser (Polytron PT10/35). Clumps of fatty tissue formed in the rotor of the homogeniser were removed with forceps between bursts and discarded. The homogenate was centrifuged for 10 minutes at 750g (3 000rpm) using a bench centrifuge (Sorvall RC-5B) to remove cell debris. The supernatant was centrifuged for 10 minutes at 10 000g (12 500rpm), using an ultracentrifuge (Sorvall OTD65B) to remove the mitochondrial fraction. Livers were weighed and finely minced with sharp scissors. Minced liver was placed into homogenisation tubes and 1ml of ice cold buffer was added per 100mg of tissue. Homogenisation tubes were kept on ice at all times. Post mitochondrial fractions were then prepared by homogenising and centrifuging by the same procedure as used for the skin.

Differences in GST activities were assessed between male and female Balb/C mice and GST activities were compared with liver. Activities were determined by a modification of the method of Habig (Gibson and Skett, 1989). The procedure for the determination of GST activity is described in section 11.4.

12.6.2 Results

The results for GST activities with male and female Balb/C mouse skin and liver post mitochondrial fractions, neonatal rat, adult rat, pig and human skin post mitochondrial fractions are shown in table 12.19.

Table 12.19 Glutathione-S-transferase activities per mg of protein for Balb/C mouse skin and liver, neonatal rat skin, adult rat skin and liver, pig skin and human skin post mitochondrial fractions and human liver cytosolic fraction using the substrate DNCB. (* indicates cytosolic fraction).

	Skin nmoles/min/mg protein (mean±sem)	n	Liver nmoles/min/mg protein (mean±sem)	n
Male Balb/C mouse	106±12	9	975±104	9
Female Balb/C mouse	94±9	9	746±51	9
neonatal rat	52±5	6	ND	-
26 day old rat	247±6	6	513±19	6
domestic pig	129±10	5	ND	-
human	451±21	19	887±81*	10

Table 12.20 Glutathione-S-transferase activities per g of tissue for Balb/C mouse skin and liver, neonatal rat skin, adult rat skin and liver, pig skin and human skin post mitochondrial fractions and human liver cytosolic fraction using the substrate DNCB. (* indicates cytosolic fraction).

	Skin nmoles/min/g tissue (mean±sem)	n	Liver nmoles/min/g tissue (mean±sem)	n
Male Balb/C mouse	2.16±0.24	9	31.45±3.35	9
Female Balb C mouse	1.92±0.18	9	24.06±1.65	9
neonatal rat	1.04±0.10	6	ND	-
26 day old rat	4.33±0.11	6	14.31±0.53	6
domestic pig	4.3±0.3	5	ND	-
human	9.00±0.42	19	60.2±4.7*	10

There was no statistical difference between male and female Balb/C mouse skin GST activity ($p>0.01$). Male and female liver GST activity was however statistically significantly different, with females showing a lower activity ($p<0.01$). Adult rat showed a five fold increase in activity in skin compared to neonatal rat skin in terms of post mitochondrial protein, though only four fold in terms of per gram of tissue. Pig skin GST activity was statistically much lower than human GST activity ($p<0.01$). Human skin showed the highest GST activity in skin of all species

examined in terms of post mitochondrial protein and per gram of tissue. Table 12.21 shows the individual human skin GST activities, displaying the range of activities between 306-642nmoles/min/mg post mitochondrial protein or 76-137μmoles/min/g tissue. Table 12.22 shows the range of human liver GST activities, which were between 553-1230nmoles mg cytosolic protein or 41-80nmoles/min/g tissue. Although the small sample size for human skin GST activities can't be used to determine any age or anatomical site differences, it does show a spread of GST activities seen in the human population.

12.6.3 Discussion

In previous experiments on enzyme activities in skin, cytochrome P450 monooxygenases and esterase activity in pig and human skin were similar. However, the results show a three fold difference between pig and human skin GST activities. Human skin post mitochondrial fractions showed the highest GST activity of any of the species investigated, but this may not mean that the skin has the capacity for greater GST metabolism *in vivo*. For conjugation to proceed, there is a requirement for the cofactor glutathione, the availability of which will determine the degree of metabolism possible. Therefore the following study to determine the level of glutathione in the skin of each species will help conclude the capacity of skin to metabolise by glutathione conjugation.

Table 12.21 Glutathione-S-transferase activities in human post mitochondrial fractions.

Human sample	Age	sex and site	nmoles/min/ mg protein	μmoles/min/g skin
1	22	Female Breast	493	93.67
2	23	Female Breast	642	137.64
3	25	Female Breast	334	80.59
4	21	Female Breast	343	83.18
5	68	Female Breast	306	76.19
6	22	Female Breast	552	97.09
7	26	Female Breast	342	82.73
8	-	Abdomen	436	86.72
9	21	Female Breast	539	75.14
10	35	Female Breast	462	128.39
11	-	Abdomen	532	128.37
12	42	Female Breast	589	117.80
13	-	Abdomen	421	90.26
14	-	Female Breast	440	90.90
15	-	-	469	114.06
16	47	Male	452	125.61
17	71	Male leg	550	135.91
18	60	Female face	351	83.36
19	-	Female face	325	93.44

Table 12.22 Glutathione-S-transferase activity in human liver cytosolic fractions from different individuals (Results from studies undertaken by E.Mutch, Department on Environmental and Occupational Medicine, University of Newcastle Upon Tyne, Unpublished).

Human Sample number	Activity (nmol/min/mg protein)	Activity (nmol/min/g tissue)
1	859	72
2	553	41
3	568	45
4	1230	49
5	1120	81
6	1190	72
7	892	61
8	910	63
9	978	76
10	570	42

12.7 Reduced glutathione levels in skin

The metabolism of DNCB to the glutathione conjugate not only requires the glutathione-S-transferases but also the presence of reduced glutathione (GSH). The concentration of GSH determines the degree of metabolism possible, therefore the levels of GSH were determined in skin.

12.7.1 Method

Reduced glutathione binds readily to the labelling reagent bromobimane. Bromobimane itself is a fluorescent reagent, but becomes strongly fluorescent at a different wavelength to the parent compound when reacted with reduced thiol groups (Kosower and Kosower, 1987). This makes the detection and quantitation of different thiols possible.

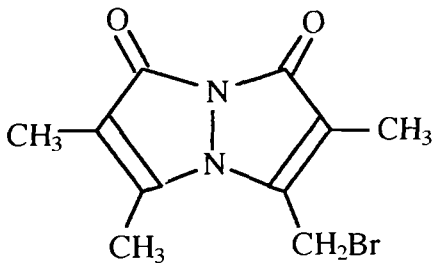

Bromobimane

Total reduced glutathione levels were measured in skin by a modification of the method of Cotgreave and Moldeus (1986). GSH in skin is primarily located at the basal layer of the epidermis (see histological staining in chapter 15.6), therefore, to minimise the effect in differences of skin thickness and protein content per sample, results were expressed as nmoles of GSH/cm^2 skin. Discs of skin (0.5cm^2), were homogenised in 900μl of monobromobimane (0.5mg/ml) in n-ethylmorpholine buffer (0.05M, pH 8). After 30 minutes in the dark, 100μl of 10% methane sulfonic acid was added to precipitate the protein and the homogenate was centrifuged for 10 minutes at 2000g. Supernatant was assayed for glutathione content by HPLC with fluorometric detection (Kontron instruments). The monobromobimane/thiol complex was detected at an excitation wavelength of 350nm and an emission wavelength of 477nm. The HPLC mobile phase was a freshly prepared solution of 5.7% acetonitrile in 0.025% acetic acid (pH3.70). This mixture was run for 10 minutes at a rate of 1.3ml/min and followed by 100% acetonitrile for 5 minutes to remove the excess bromobimane from the column. The column used was a 3μm C18 ODS, 150mm x 4.6mm and 20μl of each sample was injected on column. A standard curve was constructed with AUC data from the HPLC data collection program. Standards of reduced glutathione (reacted with bromobimane) were 10μM, 20μM, 30μM, 40μM, 50μM and 100μM. Figure 12.1 illustrates a typical HPLC trace of bromobimane derivitised GSH and figure 12.2 shows a typical standard curve.

Figure 12.1 A typical HPLC trace of glutathione derivatised with the fluorescent agent bromobimane. Peak 1 is bromobimane derivitised with cysteine and peak 2 is bromobimane derivatised with glutathione. Peaks 3, 4 and 5 are residual peaks from the bromobimane in buffer.

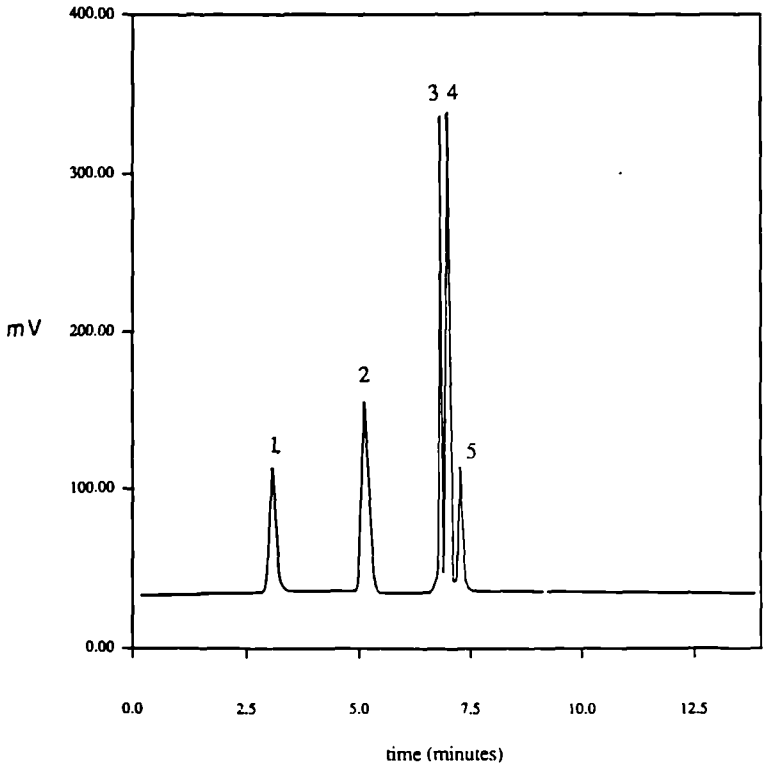

Figure 12.2 Standard curve of glutathione concentration vs. fluorescence. (Each point is a mean of 3 determinations).

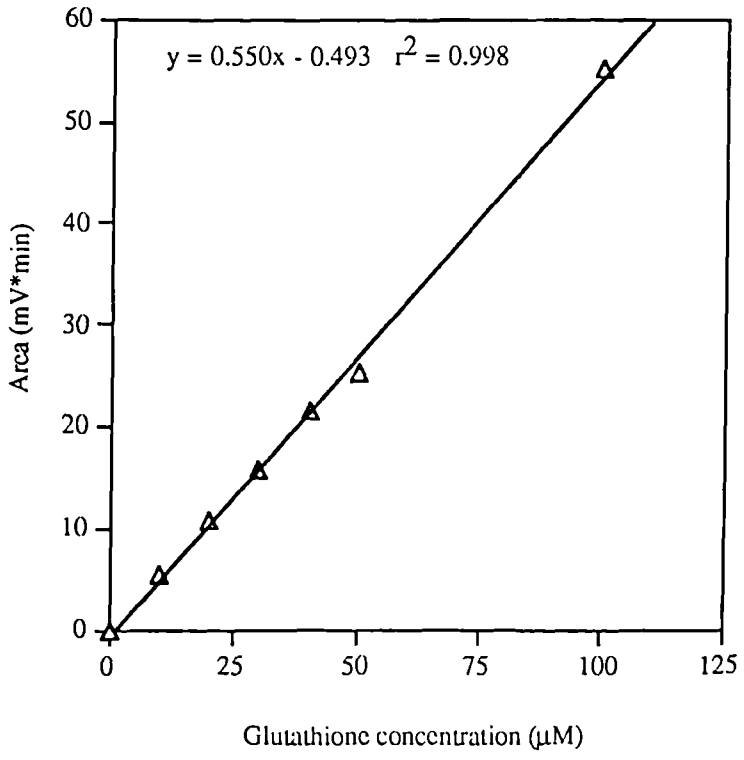

12.7.2 Results

Levels of reduced glutathione varied considerably between species. Due to the varying thickness of skin between species representing the data per gram of skin or per mg of protein is unsatisfactory. Therefore, using the knowledge that the majority of glutathione in the skin is concentrated in the basal layer of the epidermis, glutathione data was represented per unit area of skin (Table 12.23).

Table 12.23 Glutathione content in neonatal rat, 26 day old rat, mouse, pig and human skin (nmoles/cm^2 skin).

Species	nmoles glutathione/cm^2 (mean±sem)	n
Neonatal rat	91.31±3.82	6
26 day old rat	30.31±2.49	6
Balb/c mouse	151.20±6.89	4
Pig	18.62±1.50	7
Human	18.94±0.99	5

Glutathione concentrations in the skin of Balb/C mouse was much higher than in the other species examined ($p<0.01$, evaluated by ANOVA). Neonatal rat skin had higher GSH than 26 day old rat skin ($p<0.01$). Pig and human skin were shown to have statistically similar levels of GSH ($p>0.01$).

12.7.3 Discussion

Glutathione-S-transferase conjugation of xenobiotics cannot take place without the presence of the cofactor reduced glutathione. Therefore the level of glutathione may dictate the degree of xenobiotic metabolism that can take place *in vivo*. Mouse skin was shown to have highest levels of GSH of the species examined, but was also shown to have the lowest GST activity. During percutaneous absorption of DNCB, its degree of metabolism will therefore be influenced by the amount of GSH available for conjugation, and the rate at which conjugation takes place. Pig and human skin have similar levels of GSH, but human skin was shown to have greater GST activity than pig skin. If levels of GSH are the determining factor in the degree of DNCB metabolism during percutaneous absorption, then pig and human skin should show similar metabolic profiles. This was investigated in the studies on metabolism of DNCB during percutaneous absorption, detailed in chapter 16.

Chapter 13

Keratinocyte studies

Keratinocyte studies

13.1 Introduction

Keratinocytes exist in a range of morphological forms, from the completely undifferentiated cells of the basal layer of the epidermis, to the fully differentiated cells of the stratum corneum. The techniques for growing keratinocytes in tissue culture involve many stages, beginning with the isolation of the basal keratinocytes. During the culturing stage, the correct nutritional media for their growth must be provided, proliferation and differentiation must be controlled, as well as pH and temperature and all must be carried out in completely sterile conditions.

When growing keratinocytes for use in metabolism studies, the viability of the cell culture is of great importance. The usual method for evaluating cell viability is by dye exclusion e.g. trypan blue, as well as visual inspection of the cultured cells for normal morphology. Other common methods for assessing cell viability include dye uptake e.g. neutral red, measurement of enzyme leakage such as lactate dehydrogenase, or measurement of thymidine incorporation into cellular DNA. Assertaining the number of viable cells in a population then allows the contribution to xenobiotic metabolism from these cells to be determined.

Variations in tissue culture procedures exist between all laboratories but the end results are basically the same. Monolayers of keratinocytes can be grown successfully and used in a wide variety of applications which range from the study of cellular mechanisms, to skin grafts in the treatment of burns.

The following chapter details the procedures used in this project to culture keratinocytes and ascertain their potential for *in vitro* metabolic studies. As well as studying keratinocyte metabolism, the stability of the xenobiotic metabolising enzymes in cultured keratinocytes were investigated. The ability to induce the enzyme activities in these cells was also examined.

13.2 Tissue culture of human keratinocytes

The historical development of the culture of human keratinocytes has already been described in chapter 6. Details of the procedure as developed for use in this project are detailed in this chapter.

13.2.1 Methods

a) Preparation of skin for tissue culture of human keratinocytes

The preparation of human skin for the tissue culture of keratinocytes was conducted within a laminar flow cabinet under sterile conditions at all times. The laminar flow cabinet and all equipment used were cleaned with 70% ethanol before use. Fresh human skin was collected

immediately after surgery and was washed on the outer surface with tissue paper dampened with sterile saline. It was then cleaned of subcutaneous fat by cutting it away with scissors and a scalpel. When the skin sample was large enough, usually from abdominoplasty, it was also dermatomed, using setting 6 on the dermatome (350μm). The skin was then thoroughly washed in several changes of Dulbecco's PBS containing gentamycin (10μg/ml) and amphotericin B (5μg/ml). The skin was then placed in a petri dish dermal side down and cut into strips 2-3mm wide with a scalpel.

b) Isolation of human keratinocytes

Strips of human skin were placed in sterile universal tubes (20ml volume) and the tubes filled with L-15 medium containing dispase II (4mg/ml) (Kitano and Okada, 1983). The tubes of skin were then incubated at 4°C for 24 hours. The incubated skin was then warmed for 20 minutes in the tissue culture cabinet, thereafter the strips of skin were removed from the medium and gently washed in prewarmed Dulbecco's PBS. They were placed in a petri dish and with the use of two fine pointed forceps the epidermis was peeled away from the dermis. The dermis was discarded or placed in Dulbecco's PBS to be used to culture dermal fibroblasts (see chapter 14). The epidermis was transferred to a fresh universal tube containing Dulbecco's PBS (10ml) with trypsin (50μg/ml) and EDTA (20μg ml) and incubated at 37°C for 15 minutes. After 15 minutes, the tube was agitated vigorously to loosen the keratinocytes from the basal layer of the epidermis. Fetal calf serum (FCS, 50μl) was then added to neutralise the trypsin. The epidermis was removed from the solution with forceps and discarded, leaving a suspension of keratinocytes. Cells were spun down into a pellet at 600g for 10 minutes and then re-suspended in MCDB153 culture medium. The procedure for preparing MCDB153 medium is detailed in section 10.2f.

c) Counting cells by trypan blue exclusion

A total viable cell count was conducted for all cell suspensions by the trypan blue exclusion method. A sample of cell suspension (50μl) was mixed with trypan blue solution (50μl) in an ependorf. Using a haemocytometer, viable cell counts were calculated by taking the average non-stained cell count from 5 different regions of the haemocytometer grid as indicated in figure 13.1.

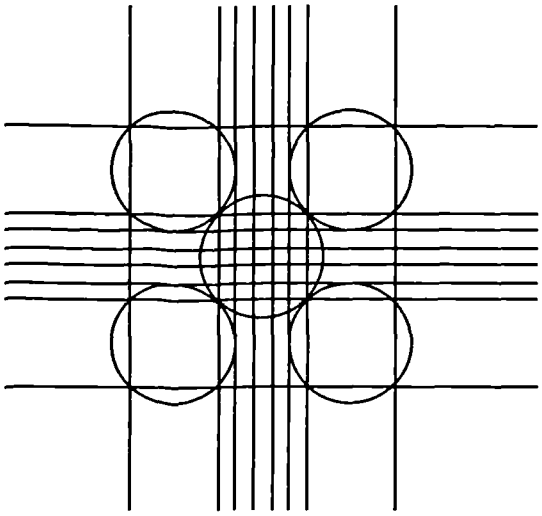

Figure 13.1. Cells were counted by trypan blue exclusion in the circled areas.

The number of cells in suspension were calculated as:

Average number of cells per region x 10000 x 2(dilution factor) = number of cells per ml of suspension.

Percentage cell viability was calculated as:

% viability = Total cells unstained / Total cells unstained and stained.

d) Growth of human keratinocytes

Cells were plated out into tissue culture flasks (Falcon® 25cm^2 Cat#3013 or 75cm^2 Cat# 3084 with cantered necks) at a density of 15000 viable cells /cm^2 in a volume of 0.2ml MCDB153/cm^2. Flasks were placed in a humidified tissue culture cabinet set at 37°C and gassed at 5% CO_2. The flask screw cap was left loose to allow gaseous exchange with the air of the tissue culture cabinet. Tissue culture medium was changed every two to three days with fresh prewarmed MCDB153 medium. Exhausted medium was seen when the colour changed from peach to pale yellow due to a change in pH, at which time the medium was changed or cell death was inevitable.

To all primary cultures of human keratinocytes, initial seeding of the cells was accompanied by the addition of 1-2% FCS. This was to encourage the cells to attach to the tissue culture flask. Serum was omitted on subsequent feeding of the cells.

e) Passage of human keratinocytes

Cells were grown to 70-80% confluence before passaging. The monolayer of cells in the tissue culture flasks were gently washed twice with Dulbecco's PBS (prewarmed to 37°C to avoid temperature shock). A solution of trypsin (50μg/ml) and EDTA (20μg/ml) in Dulbecco's PBS was added to the flask to cover the surface of the cells. The cultured cells were then incubated at 37°C for 10 minutes and the keratinocytes were detached by gently tapping the flask. The cells were washed out of the flask with a little more Dulbecco's PBS into a universal tube and FCS (50μl) was added to neutralise the trypsin. Cells were spun down into a pellet at 600g for 10 minutes and resuspended in fresh prewarmed MCDB153 culture medium. Cells were counted by trypan blue exclusion and reseeded into fresh tissue culture flasks.

f) Viability of cultured human keratinocytes

The viability of keratinocytes in the tissue culture flask was assessed firstly by visual inspection of the cells. Flasks were removed from the tissue culture cabinet and the screw cap tightened to contain the sterile environment. Cells were viewed using an inverted microscope at a magnification of 320x. Healthy keratinocytes were regular in size and shape, giving the appearance of crazy-paving. The cell membranes were smooth and the cell nucleus clearly defined. Secondly, cell viability was assessed by trypan blue exclusion. A tissue culture flask of keratinocytes was washed gently with prewarmed Dulbecco's PBS and trypan blue (100μl) was added. The dye was washed around the flask and left for 5 minutes in the tissue culture cabinet. The cells were then viewed under the microscope and assessed for viability. Cells which stained blue were considered dead or unhealthy, as their cell membranes allowed trypan blue to permeate into the cell. Unstained cells were considered to be healthy and viable. The flask of keratinocytes exposed to trypan blue was discarded as it could not be used for further studies. Only flasks from the same batch of keratinocytes were used for further experiments.

13.2.2 Results

Establishing cultures of keratinocytes was a lengthy and demanding process and many problems were encountered during the development of the above procedures. After cleaning the skin in preparation for isolating the keratinocytes, the skin was cut into strips of 2-3mm in width and this was adequately thin enough for the dispase to work effectively in splitting the epidermis from the dermis. The dispase solution was made up in L-15 medium, because it was found to maintain the pH at 7.4. Dulbecco's minimum essential medium and RPMI1640 did not maintain the pH and became acidic over the 24 hour incubation period. The result of the pH lowering was that far fewer viable cells were isolated from the skin. Warming the tissue for 20 minutes after the incubation period in dispase, allowed the epidermis to be more easily peeled from the dermis than if done cold. It was also found that freshly made solutions of dispase were more effective than ready made stock solutions that were stored frozen.

The percentage viability of keratinocytes that were in the cell suspension, after being trypsinised from the epidermis, varied considerably between samples (2%-80%) and depended primarily on the number of squamous cells that contaminated the keratinocyte cell suspension. When trypsinising the epidermis to isolate the keratinocytes it was found that cell viability also depended upon the trypsin used. Trypsin from Sigma was too harsh and cell viability was low. Even when there was a good yield of viable cells, they would not successfully attach to the tissue culture plastic. Trypsin from Difco was tested as it was a more crude preparation of the enzyme. This was found to be more suitable, resulting in a much better yield of cells, which were viable and readily attached to the tissue culture plastic. Cell suspensions containing less than 10,000 viable human keratinocytes were not used for culturing as the numbers were generally found to be too low for effective cell growth.

The size of the skin tissue used for isolating cells ranged from foreskin with an approximate area of $4cm^2$, to breast or abdomen tissue with an approximate area of 20-$25cm^2$. The number of viable cells that were obtained from these samples would range from $2x10^6$ to $15x10^6$. When large cell numbers were isolated it was best not to allow the cell suspension to become too dense, or cell aggregation would occur.

A persistent problem was maintaining cultures free of bacterial and fungal infections. Increasing the concentration of antibiotic and antifungal supplements resulted in very slow cell growth and sometimes no growth at all. Therefore concentrations of gentamycin and amphotericin B were kept at a low level and sterile conditions and aseptic techniques were strictly adhered to. By routinely sterilising equipment, wearing latex gloves and restricting access to the tissue culture cabinet, bacterial and fungal infections were controlled. Infections still occurred, but only occasionally and only in batches of keratinocytes that were derived from one skin sample. Therefore all flasks of the same batch were discarded.

Keratinocyte cell growth varied between individual samples. Keratinocytes from foreskin grew the fastest, forming very regular colonies and reaching confluence in 8-10 days. These cells could be passaged 3-4 times before cell morphology began to change and their growth rate decreased. Keratinocytes from abdomen and breast skin grew much more slowly than foreskin keratinocytes and confluence often took up to 4 weeks to be reached. The colonies contained many more cells that spontaneously differentiated and some keratinocytes were larger than others. Passaging keratinocytes derived from abdomen and breast skin was not as successful as with foreskin keratinocytes. They could be passaged twice at most, thereafter growth often deteriorated rapidly. Cells became much larger and contained many vacuoles and the cell membranes would become blebbed. Cultures at this stage would stain with trypan blue and were discarded.

Passage of cultured keratinocytes which had reached confluence were more difficult to detach from the tissue culture plastic and required longer exposure to the trypsin. Consequently, the viability of the keratinocytes was impaired and the following cultures took longer to initialise and

grow. Cultures which were passaged when about 80% confluent, needed less exposure to trypsin, detached more easily from the tissue culture plastic and the following cultures grew more readily. When leaving confluent cultures to continue to grow, more keratinocyte layers would appear and the cells would became more compact. Following this, the cells would begin to detach from the tissue culture plastic and the remaining cells vacuolated and blebbed and eventually died.

Plate 13.1 shows a small human keratinocyte colony. This was seen 2 or 3 days after the initial seeding of the cells into the tissue culture flask. Many of these small colonies would be seen growing over the entire flask surface and to the naked eye appeared as opaque speckles on the tissue culture plastic. The clear round cells which have a bright ring around them are cells that have spontaneously differentiated. The number of these cells in culture varied from batch to batch, but occurred more often in samples from abdomen and breast skin and increased with the age of the sample.

Plate 13.2 shows a larger keratinocyte colony. Usually seen during days 10-14 of culture, these colonies could be seen with the naked eye as opaque patches on the tissue culture plastic. A few cells which had spontaneously differentiated can be seen. At this stage, passaging the cells usually followed.

Plate 13.3 shows a confluent culture of keratinocytes. The time taken to reach this stage varied depending upon the skin site the keratinocytes were obtained from. At this time passaging the cells was more difficult and subsequent cultures were more difficult to establish.

Plate 13.4 shows keratinocytes at high magnification. Cell organelles are clearly visable and desmosomes can be seen between the cells.

13.2.3 Discussion

Culturing keratinocyes required time and patience. Foreskin was not as readily available for growing keratinocytes as breast or abdomen skin due to the demand for foreskin samples in the dermatology department. Therefore keratinocyte culture conditions and techniques were optimised for the more readily available breast and abdomen skin. Due to the long period of cell growth, generally 3-4 weeks, cultures were staggered to create a continuous supply of keratinocytes ready for metabolism studies. Occasional bacterial or fungal infections were usually isolated to cultures originating from the same skin sample, which suggested they had contamination that was not controlled by the antimicrobial agents. Therefore the whole batch was disposed of before contaminating other batches.

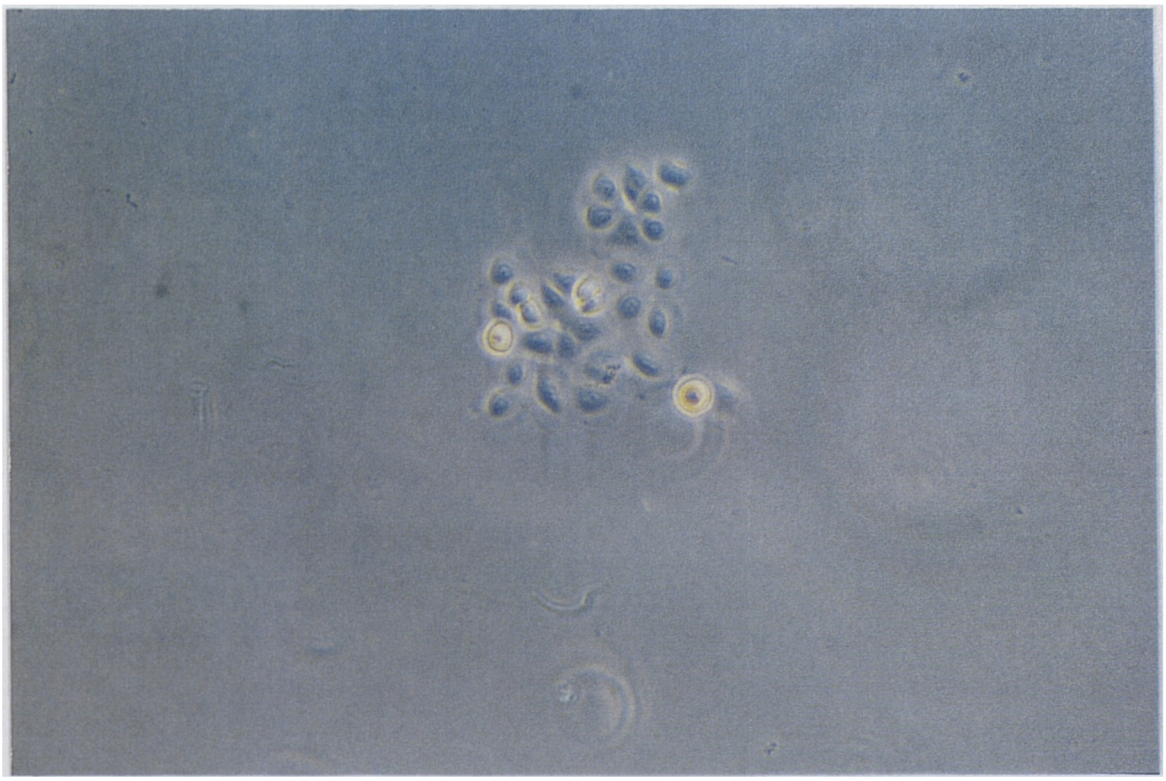

Plate 13.1 A small colony of human keratinocytes (x140).

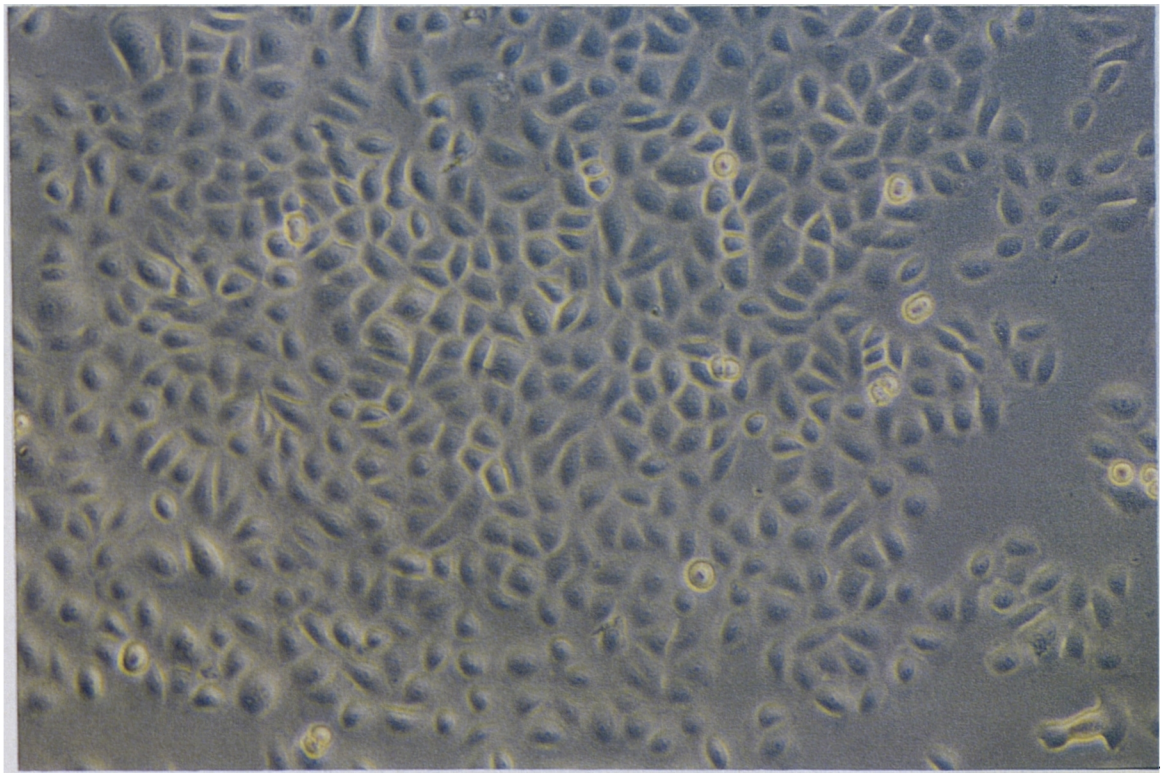

Plate 13.2 A large colony of human keratinocytes (x140).

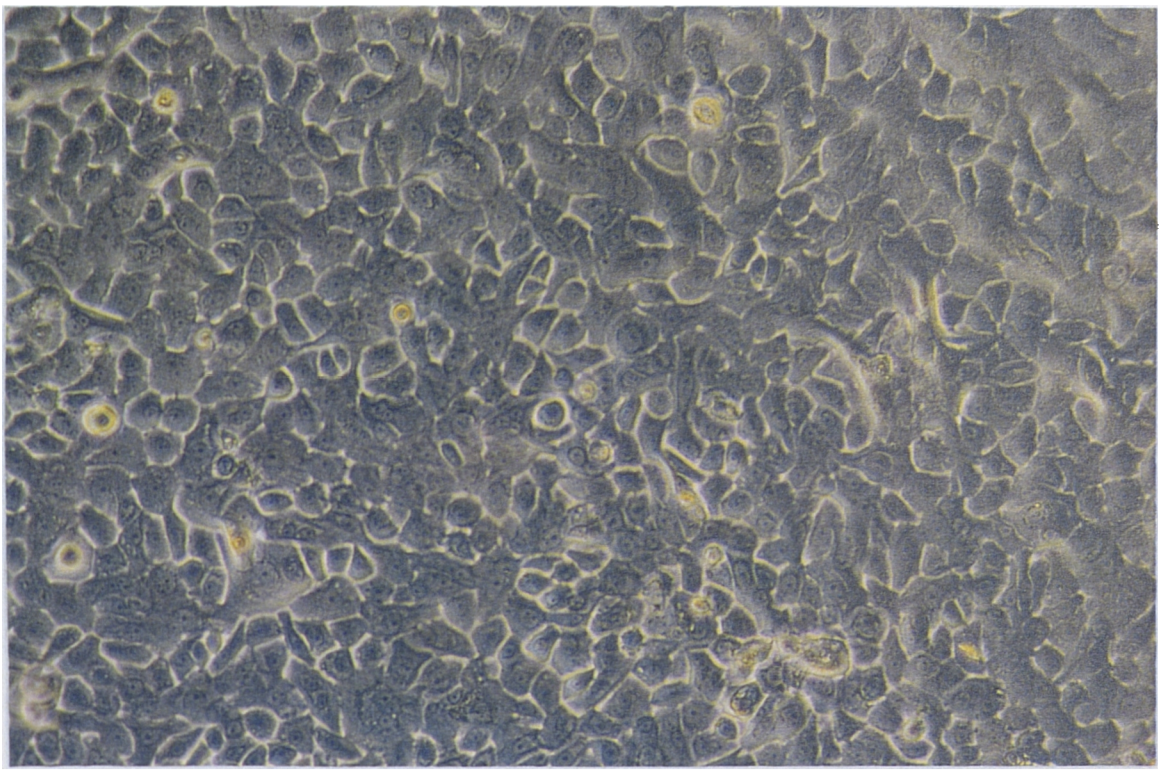

Plate 13.3 A confluent culture of human keratinocytes (x140).

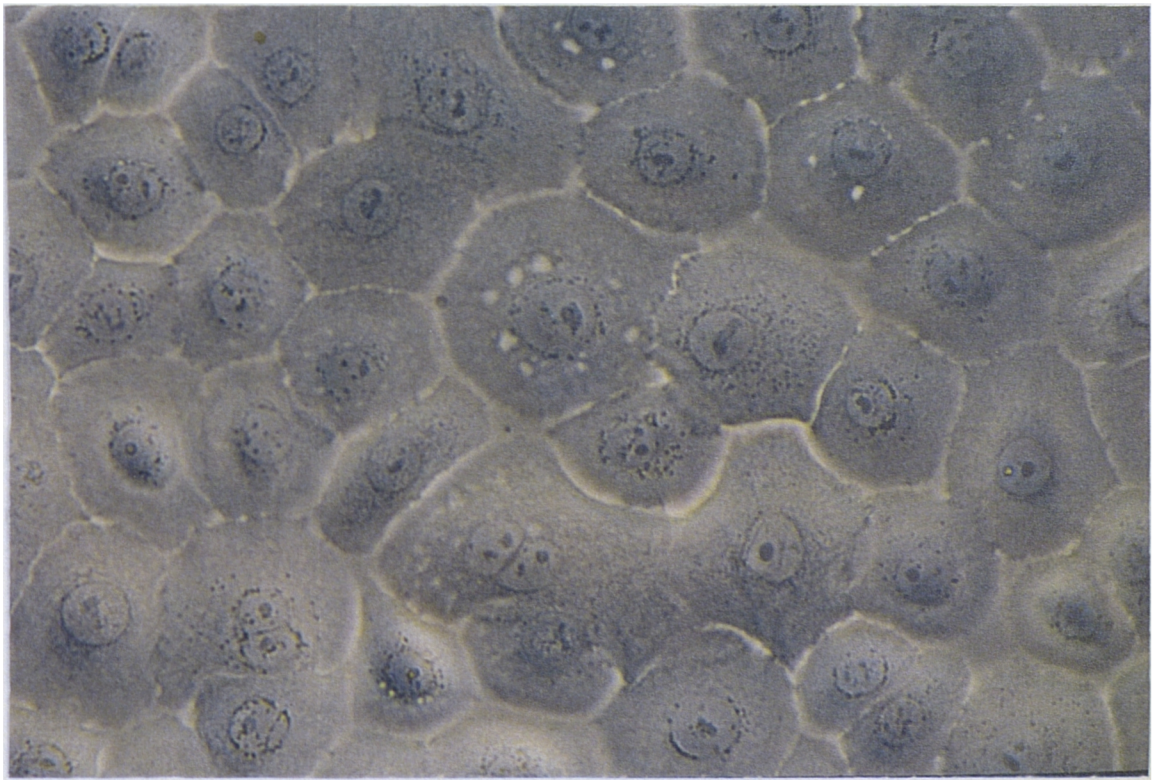

Plate 13.4 Human keratinocytes at high magnification (x445).

The cell cultures which were grown had the characteristics to those described by Boyce and Ham (1983), Karasek, (1983) and Pittlekow and Scott (1987). Although all these groups generally used foreskin as their source of keratinocytes the cells had the same appearance and growth patterns. The differences that were noted were the time periods for cell growth.

13.3 Tissue culture of rat keratinocytes

The tissue culture of rat keratinocytes followed a very similar method to the culture of human keratinocytes. There were however some modificatons allowing for the differences between human and rat skin.

13.3.1 Methods

a) Preparation of skin for tissue culture of rat keratinocytes

Neonatal Wistar rat skin was used for a source of rat keratinocytes. It had a minimal amount of hair and was quick to remove and isolate, reducing the risk of contamination by microorganisms. The skin of neonatal rats was removed as described in the general methods section 10.3b. Preparation of rat skin for tissue culture was conducted in the same way as for human skin.

b) Isolation of rat keratinocytes

Strips of rat skin were placed in sterile universal tubes (20ml volume) and the tubes filled with L-15 medium containing dispase II (2mg/ml) (Kitano and Okada, 1983). The tubes were then incubated at 4 C for 16-24 hours. After incubation, the strips of skin were removed from the medium and gently washed in Dulbecco's PBS. They were then placed in a petri dish and the epidermis was peeled away from the dermis. The epidermis was transferred to a fresh universal tube containing Dulbecco's PBS(10ml) and agitated vigorously to loosen the keratinocytes from the basal layer of the epidermis. The epidermis was removed from the solution and discarded leaving a suspension of rat keratinocytes. Cells were spun down into a pellet at 600g for 10 minutes. The cells were then re-suspended in MCDB153 culture medium which contained no epidermal growth factor, as this inhibited rat keratinocyte growth. Cells were counted and seeded into flasks as described for human keratinocytes.

c) Growth of rat keratinocytes

Cells were plated out into tissue culture flasks at a density of 10000 viable cells /cm^2 in a volume of 0.2ml MCDB153 (EGF deficient)/cm^2. Flasks were placed in a humidified tissue culture cabinet set at 37°C and 5% CO_2 with the screw cap slightly loose. Tissue culture medium was changed every two to three days as with human keratinocytes. No FCS was required for the growth of rat keratinocytes or to facilitate attachment to the tissue culture plastic..

13.3.2 Results

Neonatal rat skin is much thinner than human skin in terms of epidermis and full thickness. Therefore the concentration of dispase used to split rat skin was only 2mg/ml verses the 4mg/ml needed to split human skin. After incubation in dispase neonatal rat skin became much more fragile and the dermis became gel-like in texture. The keratinocytes of rat skin need only to be shaken off the basal layer of the epidermis without the need for a further incubation with trypsin.

Rat keratinocytes were grown in a MCDB153 medium without epidermal growth factor (EGF) as needed by human keratinocytes. Rat keratinocyte growth was inhibited with the use of EGF. Rat keratinocytes could not be passaged as they were found to be sensitive to trypsin and the cells died on exposure to the enzyme regardless of concentration or time of exposure.

Plate 13.5 shows cultured rat keratinocytes at near confluence and plate 13.6 shows a high magnification of the same cells. Note the smaller size of the rat keratinocytes compared to the human keratinocytes. Rat keratinocytes also appear more elongated than human cells and are more densely packed.

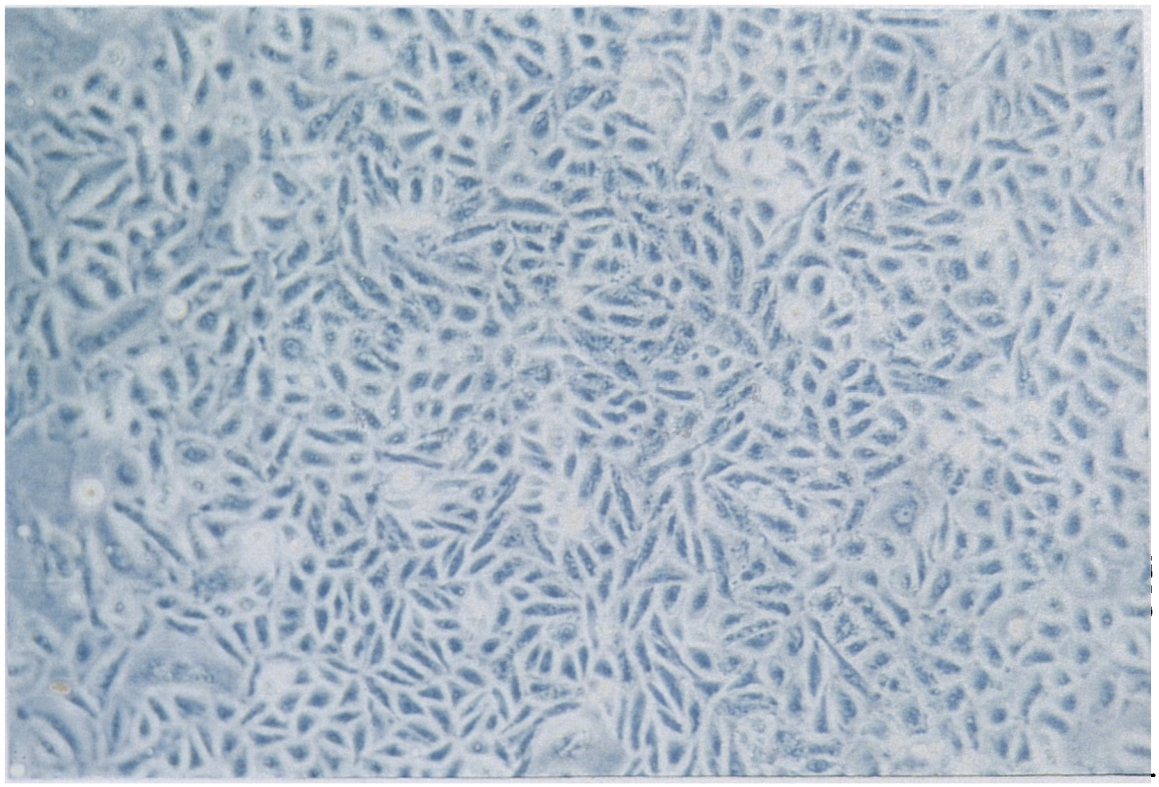

Plate 13.5 Cultured rat keratinocytes at near confluence (x140).

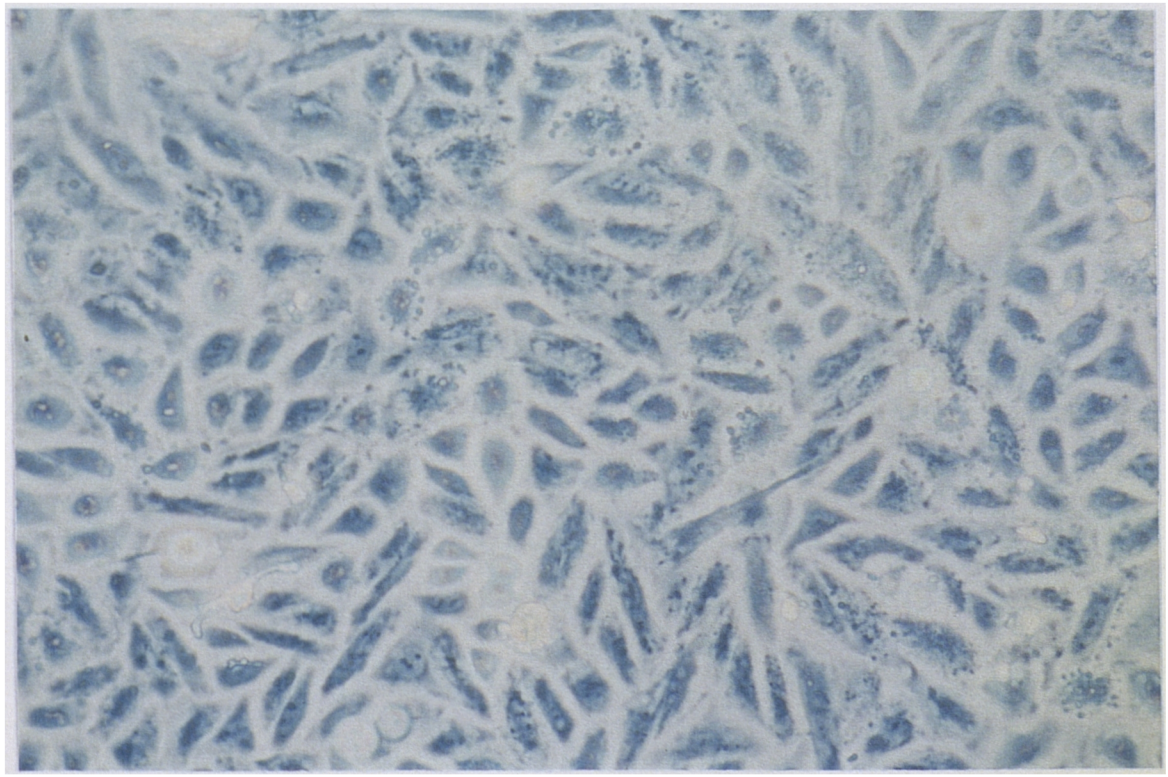

Plate 13.6 Cultured rat keratinocytes at higher magnification (x280).

13.3.3 Discussion

Rat keratinocytes were more easy to culture than human keratinocytes. They were more rapidly proliferating and did not require FCS or epidermal growth factor, an expensive supplement in human keratinocyte culture medium. They did however have the disadvantage of being sensitive to trypsin and any exposure to this proteolytic enzyme lead to immediate cell blebbing and quickly leading to cell death. Therefore they could not be passaged as human keratinocytes. All rat keratinocytes that were used for metabolism studies were therefore primary cultures.

13.4 Metabolism studies with keratinocytes

Several enzyme activities of human keratinocytes were investigated. Ethoxyresorufin-*O*-deethylation (EROD) and pentoxyresorufin-*O*-dependentylation (PROD) activities were assessed in microsomes isolated from cultured keratinocytes. The EROD activity in freshly isolated cells in a culture medium suspension was examined together with activity stability with time. These activities were also examined in cultured cells after exposure to inducing agents and in keratinocytes isolated from rats which had been induced by ß-naphthoflavone, phenobarbital and ethanol. Other enzyme activities examined in keratinocytes were esterase activity using 4-methylumbelliferyl heptanoate hydrolysis and glutathione-S-transferase activity using DNCB. The levels of reduced glutathione in cultured keratinocytes were also measured.

13.4.1 Methods

(a) Cytochrome P450 monooxygenase activity in microsomes prepared from fresh and cultured keratinocytes

The preperation of microsomes from keratinocytes was as follows: Keratinocytes were obtained fresh from the skin of four neonatal rats and six individual human breast skin samples. Keratinocytes were also obtained from confluent cultures of rat and human cells. Fresh keratinocytes were resuspended in D-PBS (5ml) and the cultured keratinocytes were scraped from the tissue culture flask into 2.5ml D-PBS. Both cell suspensions were placed in a cryovial and kept in ice. Samples of the cell suspensions were taken and the number of viable cells were counted. The cell suspensions were sonicated, followed by centrifugation at 750g for 5 minutes to remove cell debris. The supernatant was spun for a further 10 minutes at 10,000g to remove the mitochondrial fraction and then at 100,000g for 1 hour. The resulting pellet was kept on ice and resuspended in D-PBS (1ml). Protein concentration was measured by the BCA method (section 11.1) and EROD and PROD activities were determined by the method described in section 11.2, using 100μl of the microsomal protein solution.

(b) Cytochrome P450 monooxygenase stability in freshly isolated keratinocytes

Male Wistar rats of 4 days old, were sacrificed by i.p. administration of sodium phenobarbital (0.1ml). The skin was then removed and washed in D-PBS, cut into strips and placed in a solution of dispase. After 24 hours, cells were isolated and maintained in suspension ($1x10^6$ cells/ml) in MCDB153 culture medium. Cell number and viability was assessed by the trypan blue exclusion method. The cell suspension was then treated in two ways:

1. The cell suspension was incubated at 37°C and at timed intervals aliquots (0.5ml) were taken and the activity of ethoxyresorufin-*O*-deethylation was determined.

2. The cell suspension was kept on ice, (4°C) and at timed intervals aliquots were taken and ethoxyresorufin-*O*-deethylation activity was determined.

At each time interval, a sample of cell suspension was taken and viable cell numbers determined by the trypan blue exclusion method. EROD activity was measured using a freshly prepared buffer consisting of D-PBS pH 7.4 with dicoumarol (0.1mM), to inhibit the breakdown of resorufin by DT-diaphorase in viable cells and EDTA (0.1mM). This was used to make a stock solution of NADPH (1.2mg/ml). The suspension of isolated keratinocytes in D-PBS was kept on ice immediately before assay. To a micro-fluorometric cuvette was added 0.5ml of cell suspension and 0.5ml of NADPH solution. The cuvette was placed in a water jacketed cell holder set at 37°C and incubated for 1 minute. Ethoxyresorufin (2μl) was added to the cuvette, the solution mixed well and placed back in the cell holder and activity was measured. The reaction was quantitated by measuring the protein quenching. Resorufin (1μl 100pmoles) was added to the cuvette and the additional fluorescence measured. The results were calculated to express the activity as pmoles of resorufin produced/minute million cells.

(c) Induction and inhibition of cytochrome P450 monooxygenase activity in cultured keratinocytes

Cultures of rat and human keratinocytes were exposed to ß-naphthoflavone or 3-methylcholanthrene (CYP1A inducers) at 1μM, 2μM, 5μM and 10μM for 24 hours. Cultures were then washed with prewarmed D-PBS and then either trypsined to make a cell suspension for assessment of EROD activity, or refed with tissue culture medium for a further 24 hours before being assayed for EROD. Freshly isolated rat keratinocytes ($0.5x10^6$ cells/ml) were also preincubated in tissue culture medium, with α-naphthoflavone (CYP1A inhibitor) at 10μM for 30 minutes. These cells were then assayed for EROD activity.

(d) Cytochrome P450 monooxygenase activity in freshly isolated keratinocytes from induced rats

Wistar rats were induced by the protocol described in section 12.2.4. Strips of dermatomed skin were taken from each rat and washed in D-PBS, cut into strips and placed in a solution of dispase at 4°C for 24 hours. The skins were washed in D-PBS and the epidermis was carefully peeled away from the dermis using forceps. The epidermis was then placed in a universal tube containing 10ml D-PBS. The epidermis was shaken to loosen the keratinocytes and the remaining epidermis was removed. The cell suspension was kept on ice while cell number and viability was assessed by the trypan blue exclusion method. Cells were then assessed for EROD activity by the method described above.

e) Esterase activity in cultured keratinocytes

Confluent cultures of keratinocytes were scraped from the tissue culture flask with 2.5ml D-PBS into a cryovial and kept in ice, a sample of the suspension was taken and cells were counted. The cell suspension was sonicated followed by centrifugation at 750g for 5 minutes to remove cell debris. The supernatant was spun for a further 10 minutes at 10,000g to remove mitochondrial fraction. Esterase activity was determined using the method described in section 11.3.

f) Glutathione-S-transferase activity in cultured keratinocytes

A postmitochondrial fraction from keratinocytes was prepared as for the determination of esterase activity and glutathione-S-transferase activity determined by the method described in section 11.4.

g) Reduced glutathione levels in cultured keratinocytes

Cultured keratinocytes were washed twice with prewarmed D-PBS. A solution (2.7ml) of bromobimane (0.5mg/ml n-ethylmorpholin buffer, 0.05M, pH 8) was added to the flask and cells scraped into a suspension. The cells suspension was sonicated with a sonic probe, then left for 30 minutes in the dark. Methane sulfonic acid (300μl of a 10% solution) was added to the suspension and the precipitate removed by centrifugation for 10 minutes at 2000g. The supernatant was assayed for GSH levels by the method described in section 12.5.1.

13.4.2 Results

a) Results for cytochrome P450 monooxygenase activity in microsomes prepared from fresh and cultured keratinocytes

Microsomes were prepared from rat and human keratinocytes with great difficulty. At least 20 flasks of confluent keratinocytes were needed to obtain sufficient microsomal protein (30-40μg) for EROD and PROD activity studies. Freshly isolated keratinocytes from rats resulted in a slightly greater yield of microsomal protein (40-45μg microsomal protein from keratinocytes obtained from each neonatal rat. No EROD or PROD activity could be measured with the microsomes.

(b) Results for cytochrome P450 monooxygenase stability in freshly isolated keratinocytes

Table 13.1 shows the stability of EROD in freshly isolated rat keratinocytes maintained in tissue culture medium at 4°C and 37°C and graph 13.1 illustrates these data. When freshly isolated keratinocytes were incubated at 37°C the activity of EROD rapidly decreased with time and was undetectable within 5 hours. When the keratinocytes were kept on ice, the activity was maintained for longer and was still detectable 24 hours later, though viability of the keratinocytes had greatly reduced.

Table 13.1 Ethoxyresorufin-*O*-deethylation activity in freshly isolated rat keratinocytes over time, maintained at 4°C and 37°C (pmoles/min/10^6 cells, mean±sem, n=4).

4 C	
time (minutes)	mean activity pmoles/min/10^6 cells n=4
0	8.3±0.158
15	8.3±0.101
30	7.735±0.236
45	7.45±0.211
195	5.905±0.145
230	6.102±0.155
1500	0.780±0.284
2880	0.000±0.000

37°C	
time (minutes)	mean activity pmoles/min/10^6 cellsn=4
0	7.640±0.156
15	7.120±0.127
30	6.655±0.038
45	6.025±0.149
180	6.260±0.248
240	0.545±0.127
300	0.110±0.052
400	0.000±0.000

Graph 13.1 Ethoxyresorufin-*O*-deethylation activity in freshly isolated keratinocytes over time, maintained at 4°C and 37°C (mean±sem, n=4).

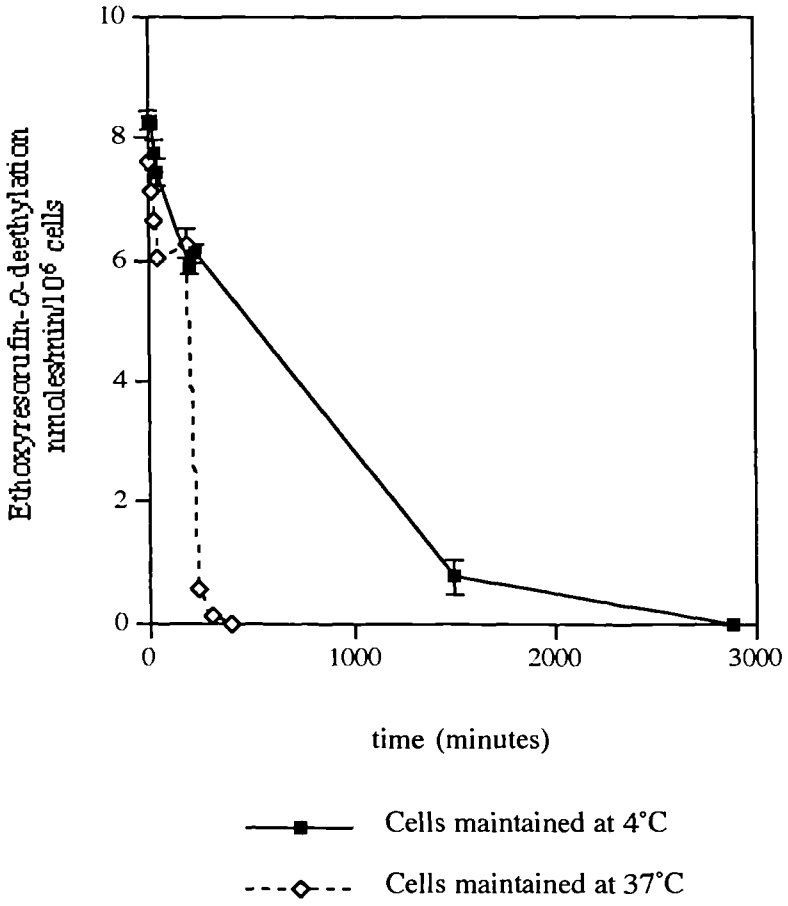

(c) Results for induction and inhibition of cytochrome P450 monooxygenase activity in cultured keratinocytes

Freshly isolated neonatal rat keratinocytes showed an EROD activity of 10.86±2.03 pmoles min 10^6 cells (mean±sem, n=6). Preincubation of the keratinocytes with α-naphthoflavone gave 100% inhibition of EROD activity. Absence of NADPH in the buffer resulted in a 33% reduction in activity and measurements in the absence of dicumarol gave a 56% reduction in activity. PROD activity of rat keratinocytes was 5.68±0.87 pmoles/min/10^6 cells. No detectable EROD or PROD activity could be found in freshly isolated human keratinocytes.

EROD activity measured directly in keratinocytes after 24hr exposure to ß-naphthoflavone or 3-methylcholanthrene did not produce consistant results at any concentration of inducer. Measurements varied from no detectable activity to 1442 pmoles/min/10^6 cells. There was no trend seen in the different concentrations of inducer used.

(d) Results for cytochrome P450 monooxygenase activity in freshly isolated keratinocytes from induced rats

No detectable EROD or PROD activity was found in keratinocytes freshly isolated from adult rats preinduced with ß-naphthoflavone, phenobarbital or ethanol.

e) Results for esterase activity in cultured keratinocytes

Esterase activity was detectable in both neonatal rat and human keratinocyte postmitochondrial fractions. Esterase activity in neonatal rat keratinocytes was 7.75±2.68 nmoles/min/10^6 cells (mean±sem, n=6) and activity in human keratinocytes was 7.20±0.91 nmoles/min/10^6 cells (mean±sem, n=8)

f) Results for glutathione-S-transferase activity in cultured keratinocytes

Glutathione-S-transferase activity (using DNCB as substrate) was also detectable in both neonatal rat and human keratinocytes (table 13.2). There was also a measurable increase in GST activity with degree of confluence of the cell culture.

Table 13.2 Glutathione-S-transferase activity in cultured keratinocytes.

keratinocyte source	nmoles/min/mg protein (mean±sem)
Rat keratinocytes (confluent)	112.5±1.6 n=6
human keratinocytes (50% confluent)	292.6 mean of 3
human keratinocytes (confluent)	676.3±28.7 n=6

g) Results for reduced glutathione levels in cultured keratinocytes

Reduced glutathione levels in rat keratinocytes were undetectable. Human keratinocytes had a reduced glutathione content of 0.628±0.080 nmoles/cm^2 or 0.146±0.023 nmoles/10^6 cells (mean± sem, n=6) or approximately 0.34 nmoles/mg cellular protein.

13.4.3 Discussion

Ethoxyresorufin-*O*-deethylation (for CYP1A1) or pentoxyresorufin-*O*-dependentylation (for CYP2B) could not be measured in microsomal preparations from keratinocytes, either freshly isolated or from culture. The small amount of keratinocyte microsomal protein (30-40μg microsomal protein from 20 75cm^2 flasks) made it difficult to provide enough protein for the measurements. Even the use of pooled microsomal protein from many preparations of keratinocytes failed to give any EROD or PROD activity.

However, the direct measurement in freshly isolated rat keratinocytes to evaluate EROD and PROD did lead to measurable activity, which in turn was inhibited by α-naphthoflavone and was dependant on NADPH. These results were only possible with the use of neonatal rat keratinocytes, as EROD or PROD was not measurable in human or adult rat keratinocytes. Investigations by Pham *et al*, (1990) reported that EROD and PROD activity was detectable in cultured human keratinocytes, though the levels of activity were not given. Additionally, the isolation of keratinocytes, from the adult male rats that were preinduced with ß-naphthoflavone, phenobarbital and ethanol presented problems. The cell suspension was heavily contaminated with dead squames and hair follicles and viable cell numbers were low. This was unavoidable and illustrated the advantages of using neonatal rat skin for preparation of keratinocytes. The use of skin homogenates in the previous chapter showed that EROD and PROD activity were similar in neonatal rats and adult rats, therefore, adult rat keratinocytes suspensions were not used in further studies.

The activity of P450 enzymes in freshly isolated keratinocytes showed that activity decreased markedly in the first few hours, especially when incubated at 37°C. This indicated that P450 enzymes involved in EROD are unstable when isolated from whole skin and activity is easily lost. Keeping the cells at 4°C did help to slow down the rate at which P450 activity was lost, but only helped maintain the activity for a few more hours.

Preparation of the subcellular fractions from rat keratinocytes was accompanied by a large loss of activity compared to enzyme activity in "freshly" isolated cells. As P450 activity in keratinocytes was lost rapidly after isolation from the skin, it is of no surprise that P450 activity was not found in cultured cells that had been isolated fom the skin for several days. This information can then be also applied to human keratinocytes. These cells had lower microsomal protein than rat keratinocytes and therefore it would be expected that EROD activity could also be lower. The loss in EROD from the skin obviously would begin after the skin is removed from the animal. Isolation of keratinocytes from the skin requires 24 hours incubation in dispase, in which time P450 activity is being lost. Human skin is transported from the operating theatre to the laboratory. Due to the lower levels of activity in human skin compared to rat, any delay in preparing human skin for microsomes or keratinocytes only leads to more loss in activity.

Each batch of cultured keratinocytes gave variable EROD activities after exposure to inducing agents, but often showed no activity. The results suggested that induction of keratinocyte enzymes was achievable, but it was not controllable. Other external factors may be involved in the induction of keratinocytes and that these may not be present in the cultures. The activity of cytochrome P450 could be restored to measurable levels possibly from protein induction. However, there was always a high degree of variability. It appears to be related to the length of time at which the cells are exposed to an inducing agent, or the length of time after exposure at which the enzymes are measured. Keratinocytes induced for 24 hours, refed with fresh medium for a further 24 hours and then measured seemed to yield more cultures of cells with measurable activity, but were still highly variable. Therefore a more rigorous study of the induction regimen is needed. Investigations by Reiners *et al*, (1990) using mouse keratinocytes demonstrated the need for calcium in the culture medium to facilitate the induction of P450 activities. Calcium triggers the differentiation of keratinocytes, therefore differentiation may be the key to P450 expression. Further studies investigating this question are explored in the following chapter on the living skin equivalent.

Esterase and GST activities were measurable in both rat and human keratinocytes. GST activities increased with degree of confluence of the cell culture, suggesting that an intact epithelial sheet triggers induction of this enzyme. Similar results were also shown by Blacker *et al*, (1991). Glutathione was not found in rat keratinocytes and only in low concentrations in human keratinocytes. This indicates that keratinocytes can not synthesize GSH in culture. It may also be that glutathione in cultured cells existed in the oxidised form, GSSG. Cofactors such as glutathione may therefore need to be added to the culture medium to stimulate the cells to boost their own glutathione levels.

In summary, keratinocytes can be grown in culture to form monolayers of cells that have the potential to be used for xenobiotic metabolism studies. However, cytochrome P450 monooxygenases were found to be unstable and activity was rapidly lost. Esterase and GST activity are both present, with GST activity being greatest when cultures were confluent. The conditions in which cells are cultured play an important role in the manifestation of many enzymes. One such factor, the influence of cellular differentiation is investigated in the following chapter.

Chapter 14

Studies with living skin equivalents

Studies with living skin equivalents

14.1 Introduction

An *in vitro* skin model with reproducible metabolic activity can be useful for studying the metabolism of various compounds by skin, both endogenous and exogenous. A skin model can be used as an alternative to animal skin for toxicology testing and penetration studies. A three dimensional skin model consisting of keratinocytes and fibroblasts, generally derived from human foreskins can be constructed and is called a living skin equivalent (LSE). To produce a dermal model, fibroblasts are seeded onto a collagen gel or on a nylon mesh and grown until a dermal like matrix is obtained, consisting of collagen, proteoglycans and glycosaminoglycans. Keratinocytes seeded onto the dermal model are grown at the air/liquid interface until a morphologically differentiated epidermis consisting of basal, spinous, granular and stratum corneum layers is formed. It has been shown that the model epidermis contains the appropriate differentiation markers including specific keratins and involucrin (Slivka and Zeigler, 1993). This chapter describes the development of an LSE, it's histology and some initial studies into LSE metabolism of xenobiotics.

14.2 Tissue culture of human and rat dermal fibroblasts

The development of the LSE began with the culture of dermal fibroblasts. Fibroblasts are the main cell type of the dermis. They form a network of collagen fibres which maintain the structure of the dermis. They can be isolated and grown in tissue culture and passaged many times. In comparison to keratinocytes, fibroblasts are easy to culture and the following section describes the procedure used in this study.

14.2.1 Preparation of skin for tissue culture of human and rat dermal fibroblasts

Dermis from either human or rat skin was obtained after removal of the epidermis for the preparation of keratinocytes . It was bathed in DMEM containing 10%FCS at 37°C for 2 hours and then placed into a petri dish. With a pair of fine scissors the dermis was cut into small pieces about $1mm^3$.

14.2.2 Growth of human and rat dermal fibroblasts

Tissue culture flasks (Falcon® $25cm^2$ Cat#3013 with cantered necks) were scratched on the internal surface with the point of sterile scalpel blade. Pieces of dermis to be used as explants were blotted dry on tissue paper and placed onto the scratches in the flasks with forceps. Approximately 6-8 pieces of dermis were placed into each $25cm^2$ flask. The flasks were placed in a humidified tissue culture cabinet set at 37°C and 5% CO_2 for 20 minutes to allow the dermis to attach to the tissue culture plastic. DMEM containing 10%FCS was then carefully added to the flasks

(0.2ml/cm^2). Tissue culture medium was changed every three days. Fibroblasts migrate from the tissue onto the tissue culture plastic after 2-3 weeks, from which confluence is reached in 2-3 days.

14.2.3 Passage of human dermal fibroblasts

Dermal fibroblasts were grown to 90-96% confluence before passaging. The cells in the tissue culture flasks were washed twice with D-PBS (prewarmed to 37°C to avoid temperature shock). A solution of trypsin (50μg/ml) and EDTA (20μg/ml) in D-PBS (1ml) was added to the flask. The cultured cells were then incubated at 37°C for 5-10 minutes and the fibroblasts easily detached from the plastic. The cells were washed out of the flask with D-PBS into a universal tube and FCS (50μl) was added to neutralise the trypsin. Cells were spun down into a pellet at 600g for 10 minutes and resuspended in fresh DMEM culture medium containing 10%FCS. Cells were counted by trypan blue exclusion and reseeded into fresh tissue culture flasks at a density of 5000cells cm^2.

14.2.4 Results

Fibroblasts were grown from rat dermis and from the dermis of various human anatomical sites including foreskin, ear, breast and abdomen. All had the same characteristic appearance. The dermal fibroblasts were easily passaged and they detached easily with trypsinisation. They underwent 4-5 passages and displayed no signs of stress or blebbing. Plate 14.1 shows foreskin dermal fibroblasts shortly after migrating from the skin onto the tissue culture plastic. Plate 14.2 shows a confluent culture of fibroblasts.

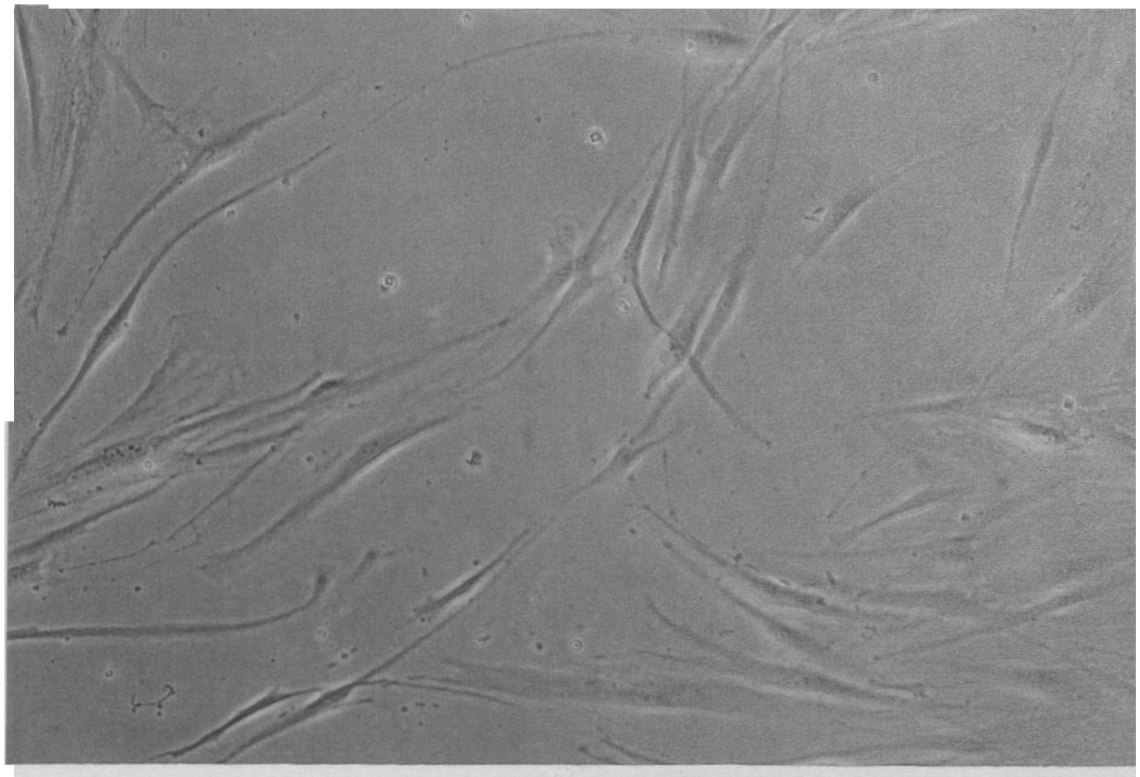

Plate 14.1 Human dermal fibroblasts, shortly after migrating from the skin onto the tissue culture plastic (x280).

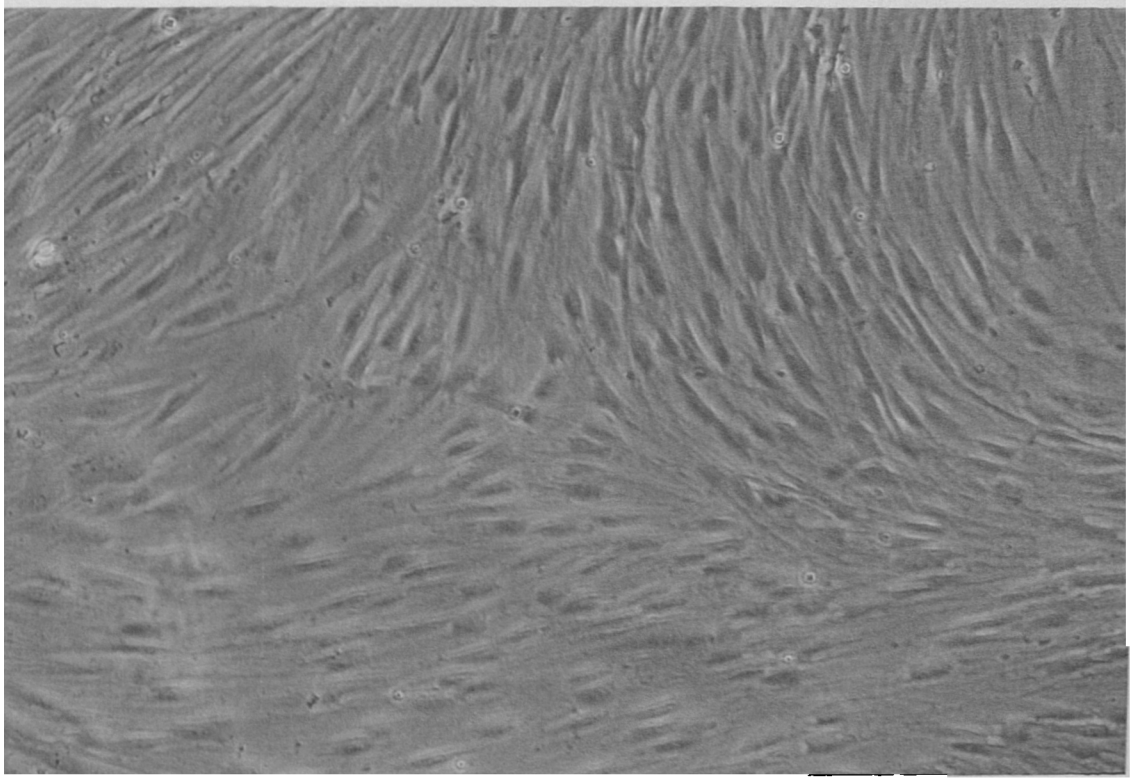

Plate 14.2 Human fibroblasts at confluence (x280).

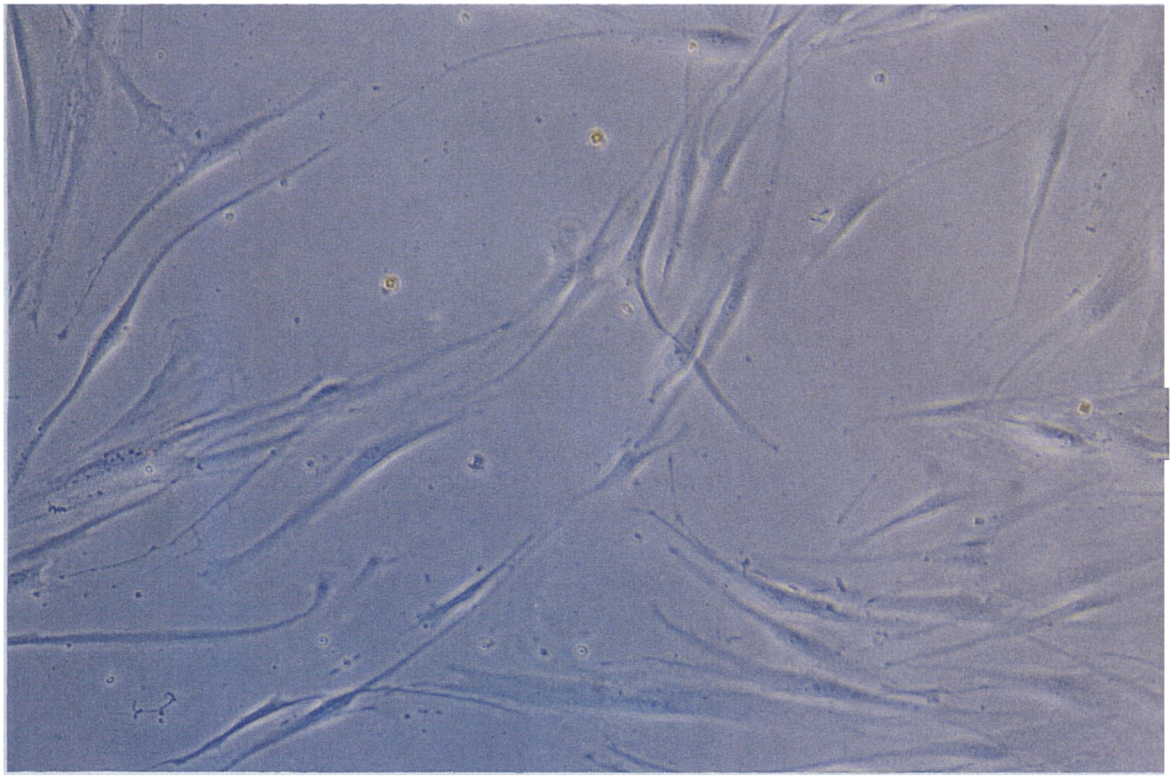

Plate 14.1 Human dermal fibroblasts, shortly after migrating from the skin onto the tissue culture plastic (x280).

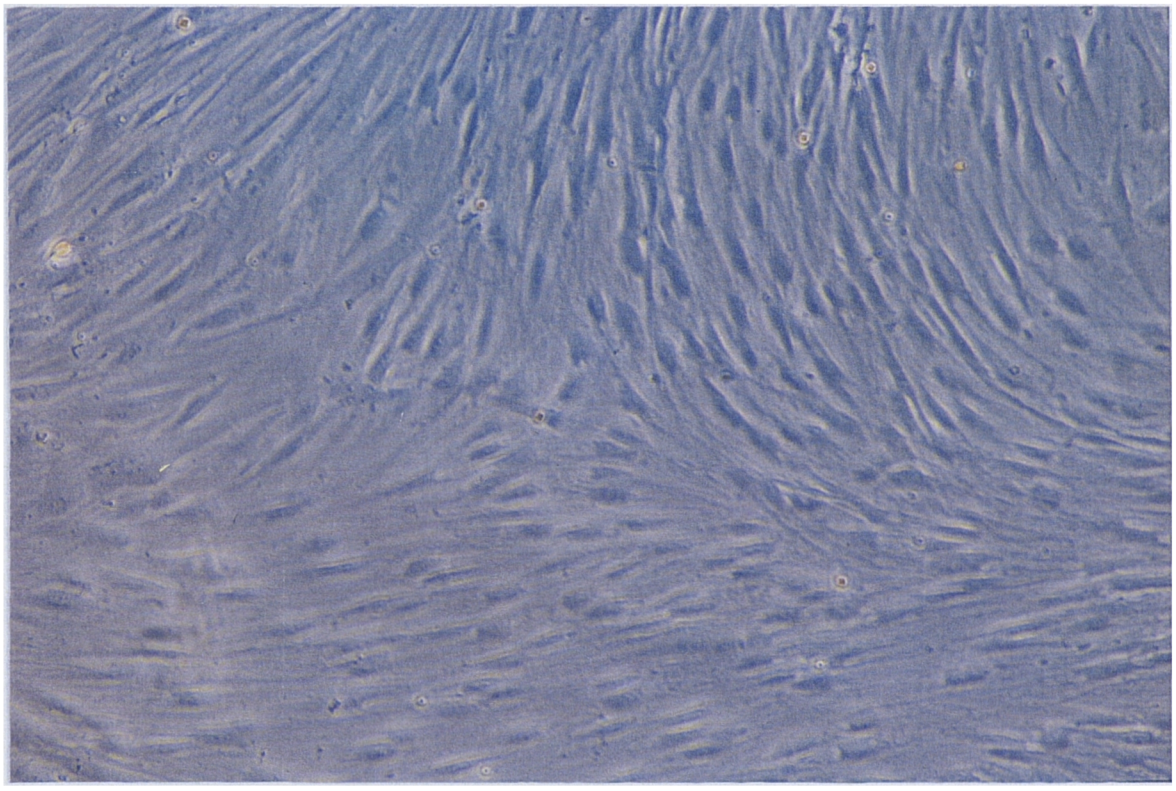

Plate 14.2 Human fibroblasts at confluence (x280).

14.3 Metabolism studies with dermal fibroblasts

14.3.1 Method

Fibroblasts were assayed for cytochrome P450 monooxygenase activity, esterase activity and glutathione-S-transferase activity. The same analytical methods were used to assay cultured dermal fibroblasts as were used for assaying keratinocytes (see section 13.4).

14.3.2 Results

No detectable levels of ethoxyresorufin-*O*-deethylation or pentoxyresorufin-*O*-dependentylation activity were found in either human or rat dermal fibroblasts. Esterase activity was found in both human and rat dermal fibroblasts at activities of 2.7 and 6.51 nmoles/min/10^6 cells or 6.41 and 15.17 nmoles min mg post mitochondrial protein (means of 3 determinations). Glutathione-S-transferase activity in rat fibroblasts was 1.02±0.04 nmoles/min/mg protein (n=6) and human fibroblasts was 21.5±4.8 nmoles/min/mg protein (n=6).

14.4 Development of a Living Skin Equivalent

Falcon® cell culture inserts (cat#3103) contain a tissue culture treated polyethylene teraphthalate membrane with an area of 0.8cm^2, containing 1.0μm pores, amounting to approximately 1.6x10^6 pores/cm^2. The membranes are translucent, strong and do not curl when cut from the insert. Due to these specifications, the Falcon® cell culture inserts were chosen as a base on which to grow an LSE. Due to demands on time, only the human living skin was fully developed.

14.4.1 Method for growing a living skin equivalent

Human fibroblasts that had grown to confluence were detached from the culture flask with a solution of trypsin (50μg/ml) and EDTA (20μg/ml) in D-PBS (1ml). After detachment from the tissue culture plastic 5ml D-PBS containing 100μl of fetal calf serum was added to wash out the cells and neutralise the trypsin. The cells were washed twice with fresh D-PBS prewarmed to 37°C to avoid temperature shock and spun down into a pellet at 600g for 10 minutes. The cultured cells were then resuspended in DMEM (3ml). Cells were seeded into the cell culture inserts at a density of 10,000 cells cm^2. Additional DMEM containing 10%FCS and gentamycin (10μg/ml) and amphotericin B (5μg ml), was placed in the insert well so that the level of medium outside the insert was just above the line of the membrane. The inserts were placed in a tissue culture cabinet at 37°C, gassed with 5% CO_2 and 95% air. Medium was replaced every two days with fresh medium for a period of two weeks.

After two weeks, the DMEM was removed from the insert and the surface of the membrane carefully washed with MCDB153. A fresh suspension of human keratinocytes in MCDB153 was

seeded onto the surface of the insert at a density of 15,000 cells/cm^2. Additional MCDB153 containing gentamycin (10μg/ml) and amphotericin B (5μg/ml) was placed in the insert well to a level above the line of the membrane. After 24 hours the medium was changed and added to a level equal to the surface of the culture insert membrane, to allow the living skin equivalent to be at the liquid/air interface. Medium was changed every two days.

14.4.2 Results

Beginning with freshly excised human skin as a source of fibroblasts and keratinocytes, a living skin equivalent took four to five weeks to develop. During this time, the medium was changed regularly, not only to provide the nutrients required for growth but also to maintain concentrations of the antibiotic and antifungal which lose efficacy with time.

Firstly, fibroblasts were grown on the tissue culture membrane for two weeks. Plate 14.3 shows the appearance of the fibroblasts forming a dermal matrix during this time, stained with haemoxylin and eosin for visualisation. The fibroblast matrix is very fragile and loosely attached to the membrane. After two weeks, keratinocytes were seeded on to the surface of the fibroblast matrix. In plate 14.4 it can be seen that the dermal matrix has a more compacted structure but the presence of the keratinocytes are not yet discernible. By 72 hours, the dermal matrix had become far more analogous with dermal tissue *in vivo*, and the keratinocytes are far more apparent (plate 14.5). At two weeks the structure of the living skin equivalent shows histological similarities with *in vivo* skin (plate 14.6). There is a clear division between the dermal and epidermal layers. The lower half of the epidermal layer shows layers of keratinocytes morphologically similar to the granulosum layer of *in vivo* epidermis. The outer layers of the living skin equivalent are composed of more flattened cells typical of keratinocyte differentiation. Plate 14.7 shows a wider view of the living skin equivalent. The dermal layer is more darkly stained than the epidermal layer. Increasing in magnification (plate 14.8) the cells at the dermal epidermal junction are quite distinct, typically cuboidal and possessing a nucleus. At higher magnification (plate 14.9) these cells are far more visible and the presence of desmosomes can be seen between the cells. Some of the cells at the surface of the epidermis have lost their nucleus, indicating the beginnings of the formation of a stratum corneum, though the presence of a stratum corneum is not yet seen in these tissue cultures.

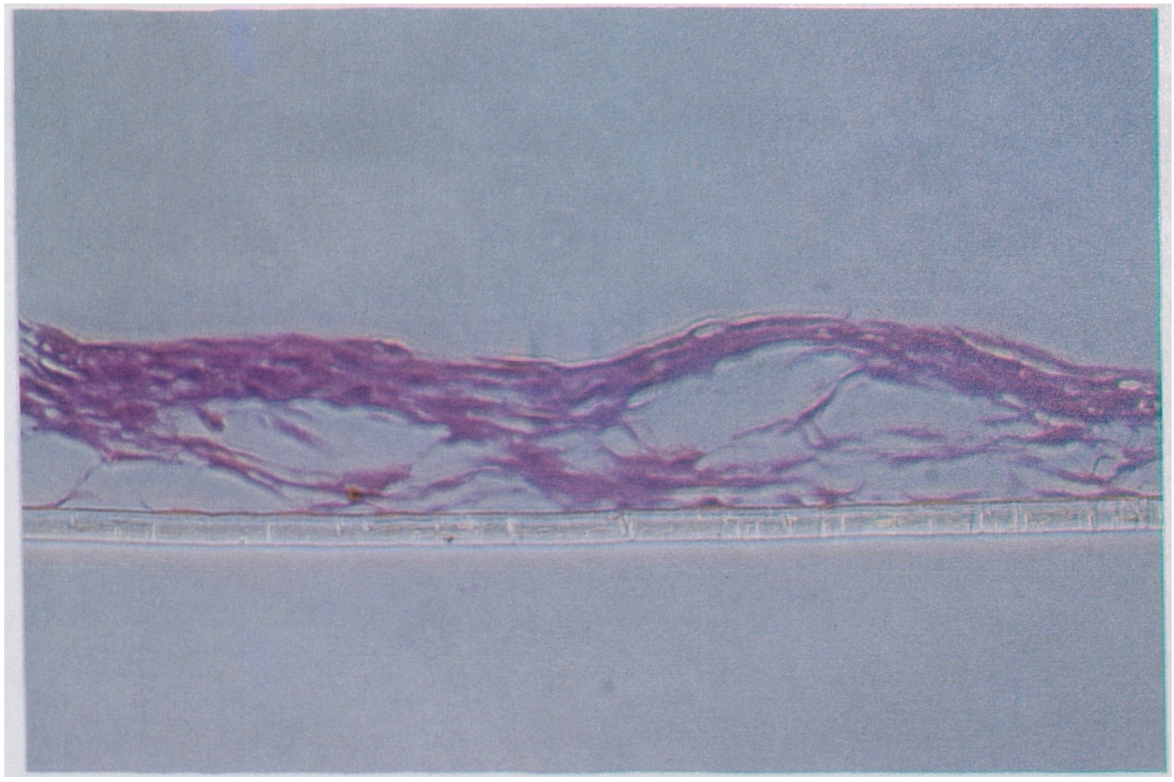

Plate 14.3 Fibroblasts grown on a porous polyethylene teraphthalate membrane with 1.0μm pores (x280).Stained with haemotoxylin and eosin.

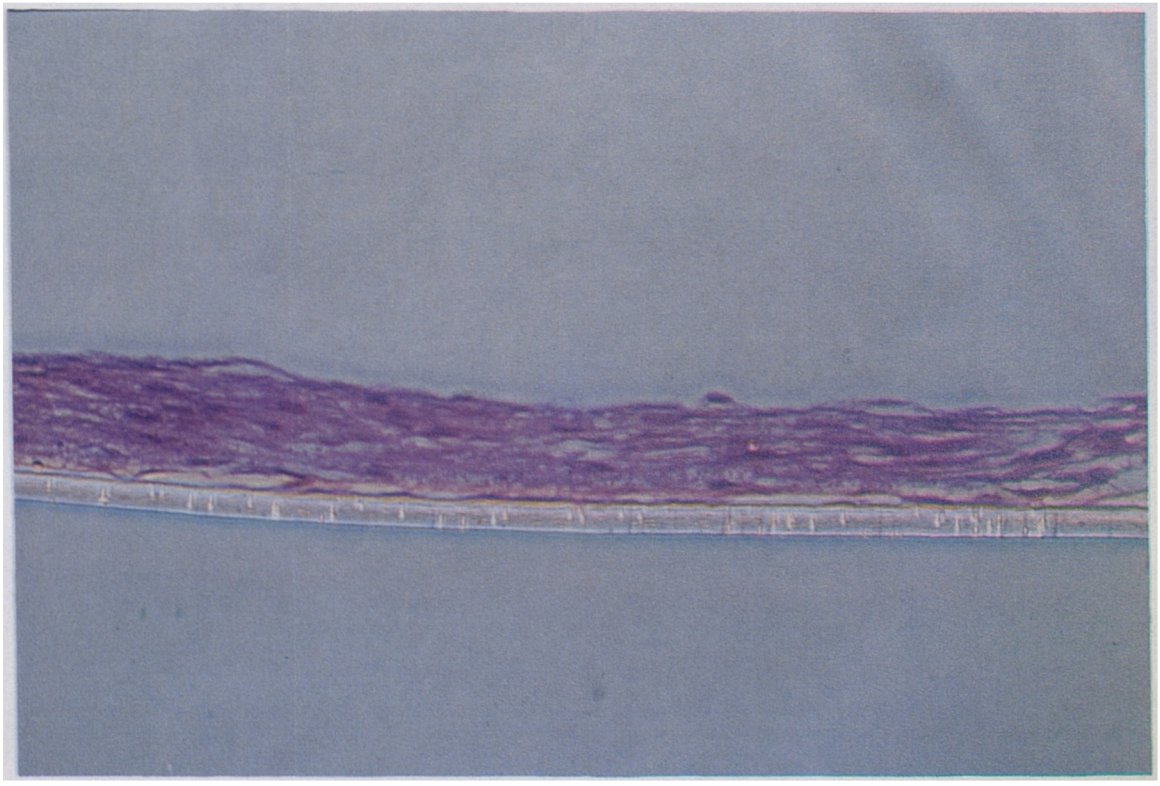

Plate 14.4 A living skin equivalent 24 hours after seeding keratinocytes onto the surface of the fibroblasts (x280).Stained with haemotoxylin and eosin.

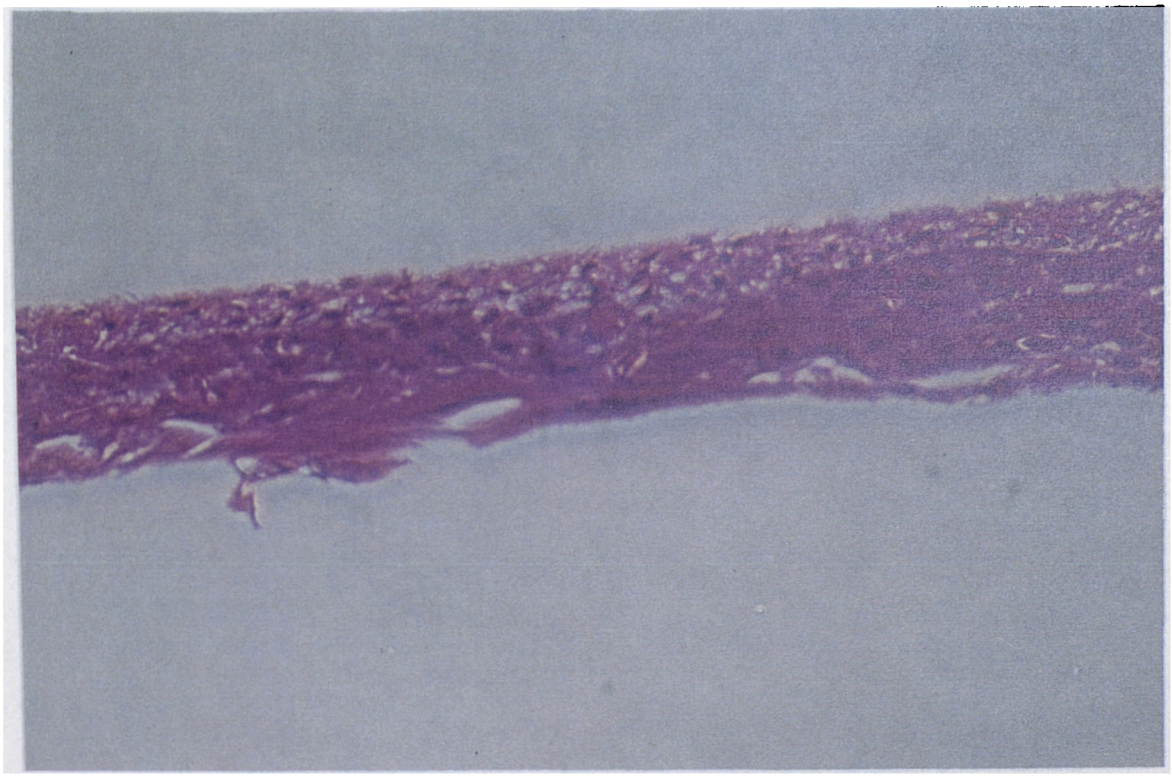

Plate 14.5 A living skin equivalent 72 hours after seeding keratinocytes onto the surface of the fibroblasts (x280). Stained with haemotoxylin and eosin.

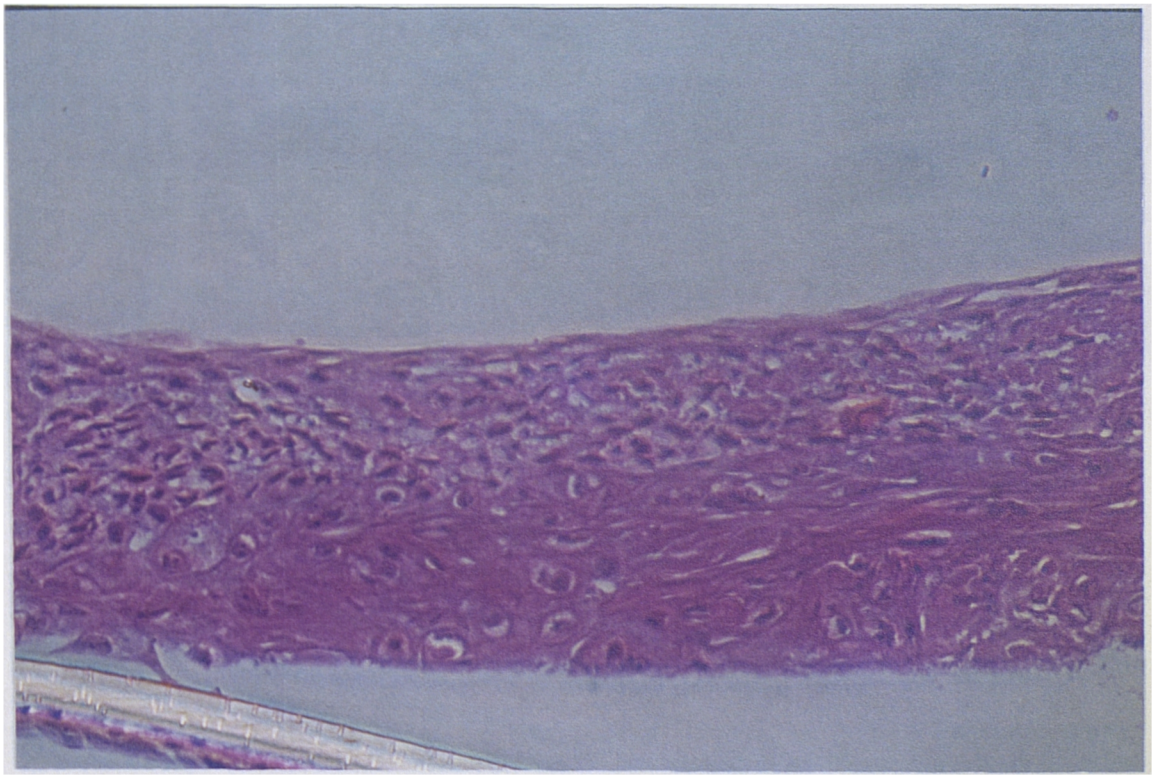

Plate 14.6 A living skin equivalent two weeks after seeding keratinocytes onto the surface of the fibroblasts (x445). Stained with haemotoxylin and eosin.

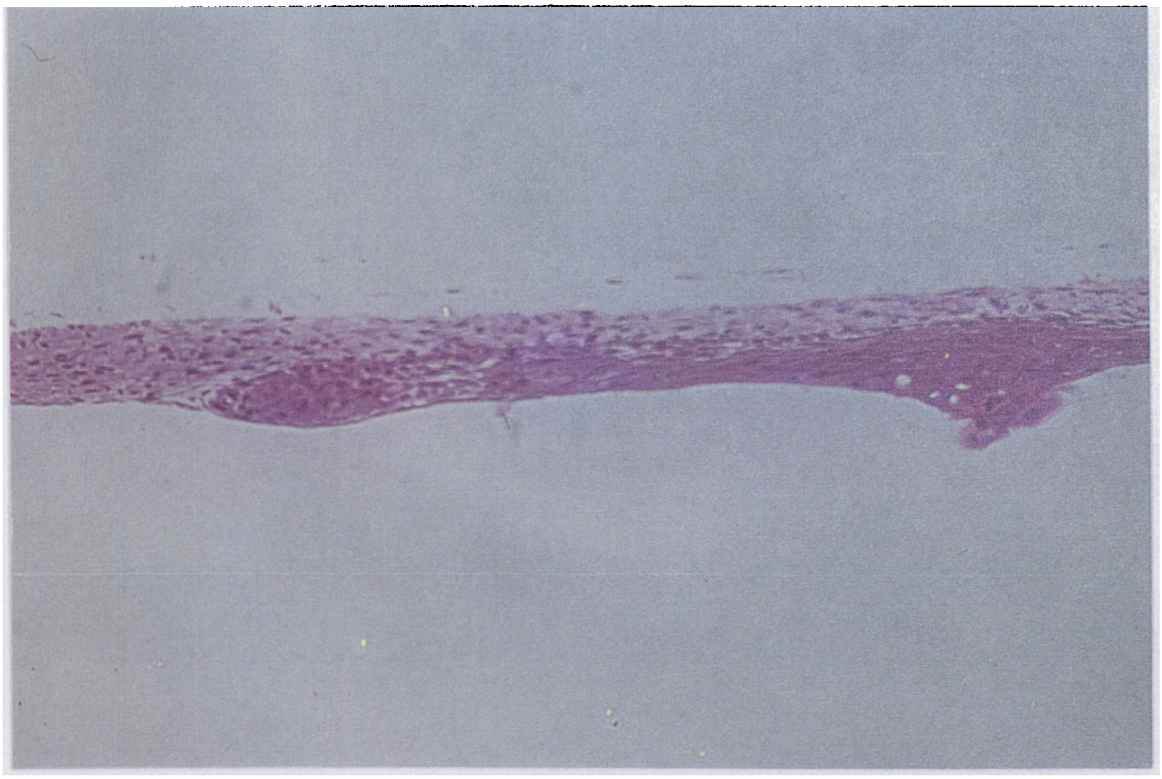

Plate 14.7 A living skin equivalent at a magnification of x140.
Stained with haemotoxylin and eosin.

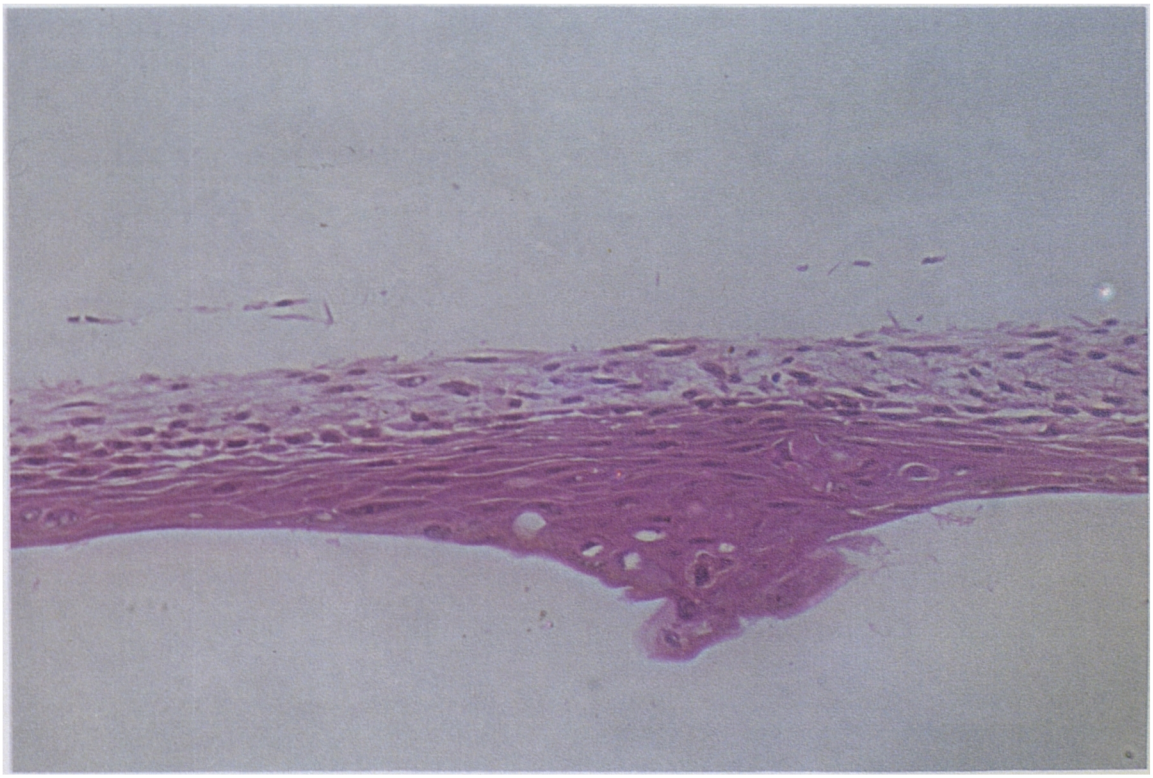

Plate 14.8 A living skin equivalent a magnification of x280.
Stained with haemotoxylin and eosin.

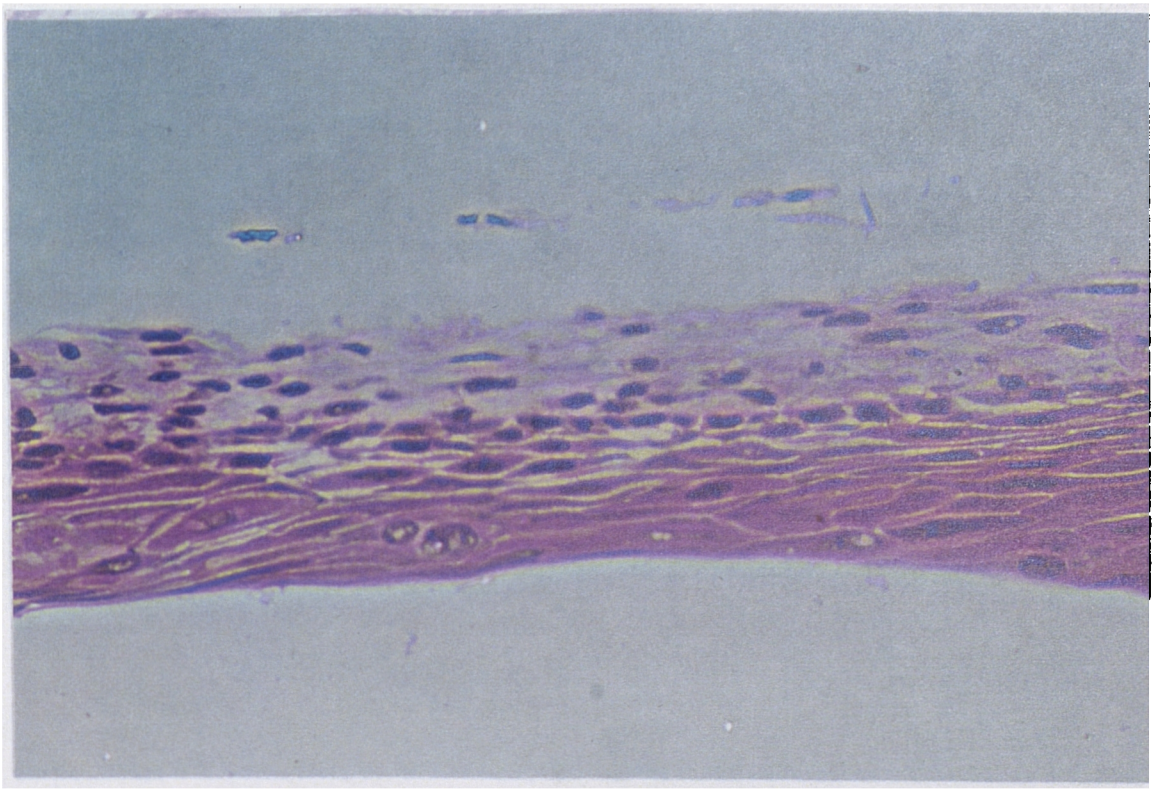

Plate 14.9 A living skin equivalent at a magnification of x445. Stained with haemotoxylin and eosin.

14.5 Metabolism studies with living skin equivalents

In chapter 13, cell suspensions and monolayers of undifferentiated human keratinocytes were used to determine the capacity of isolated cells from skin for metabolism and their use for metabolism studies. The results from those studies indicated that metabolic capacity of these cells was unstable and cytochrome P-450 monooxygenase activity quickly lost after isolation from the skin. The next approach was therefore to establish whether enzymes in the living skin equivalent containing keratinocytes in a fully differentiating tissue were more functional than in keratinocytes alone, and to determine if xenobiotic metabolism in the living skin equivalent was inducible by classical inducing agents.

14.5.1 Cytochrome P450 monooxygenase, esterase and GST activity in a living skin equivalent.

a) Methods

LSE's were grown as outlined in section 14.4. After 5-6 weeks in culture, LSE's were washed with ice cold D-PBS and carefully removed from the tissue culture insert by teasing away with a pair of forceps. Three tissue samples were placed in a cryovial containing ice cold glycerol buffer (1.5ml). The tissue was then homogenised with 3x10 second bursts using a polytron homogeniser (PT10 35, at setting 6). The homogenate was centrifuged for 10 minutes at 10 000g (12 500rpm), using an ultracentrifuge (Sorvall OTD65B) to remove mitochondria and cell debris. The resulting supernatant was used as post mitochondrial fraction for determining GST activity or further centrifuged to prepare cytosolic and microsomal fractions for esterase and cytochrome P-450 monooxygenase activity respectively. Microsomes were prepared by centrifuging the supernatant for a further 70 minutes at 110 000g (44 000rpm). All homogenisation and centrifugation was done at 4 C.

b) Results

Due to the length of time and cost of growing LSE's, the number of samples that were grown was limited. Due to their small size (0.8cm^2), three LSE's were pooled for each subcellular fraction preparation. Enzyme assays were measured using three of these preparations, from a total of 9 LSE's. Protein recoveries for the subcellular fractions of each living skin equivalent are detailed in table 14.1. Subcellular fractions were assayed for GST activity, esterase activity and cytochrome P450 activity using the substrates DNCB, 4-MUH and 7-ethoxyresorufin respectively. Results are shown in table 14.2.

Table 14.1 Protein recoveries from living skin equivalents.

Fraction	protein recovery from separate living skin equivalent
post mitochondrial fraction	0.466mg
cytosolic fraction	0.451mg
microsomal fraction	No microsomal fraction recovered

Table 14.2 Enzyme activities in the living skin equivalent (mean of three separate samples).

Enzyme	Substrate	Activity
GST activity	DNCB	412 nmoles/min/mg post mitochondrial protein
Esterase activity	4-MUH	22.1 nmoles/min/mg cytosolic protein
Cytochrome P450 activity	7-Ethoxyresorufin	None detectable

14.5.2 Induction of metabolising enzymes in a living skin equivalent

a) Methods

LSE's were grown as described above. 24 Hours before metabolism studies, the tissue culture medium was replaced with fresh medium containing 3-methylcholanthrene (10μM). The tissue was then removed and subcellular fractions prepared as described above.

b) Results

Only 9 LSE's were available for induction with 3-methylcholanthrene. Subcellular fractions were prepared by pooling 3 LSE's, therefore 3 samples were available for assays. Table 14.3 details the protein recovery from LSE's induced with 3-methylcholanthrene. Because of the low microsomal recovery, the whole protein fraction from each sample was used to determine 7-ethoxyresorufin-*O*-deethylation activity.

Table 14.3 Protein recoveries from living skin equivalents exposed to 3-methylcholanthrene..

Fraction	protein recovery from each living skin equivalent
post mitochondrial fraction	0.441mg
cytosolic fraction	0.412mg
microsomal fraction	0.008mg

Table 14.4 Enzyme activities in the living skin equivalent exposed to 3-methylcholanthrene (mean of three separate samples).

Enzyme	Substrate	Activity
GST activity	DNCB	678 nmoles/min/mg post mitochondrial protein
Esterase activity	4-MUH	31.4 nmoles/min/mg cytosolic protein
Cytochrome P450 activity	Ethoxyresorufin	1.75 pmoles/min/mg microsomal protein

14.6 Discussion

Growing an LSE was time consuming and expensive, in equipment and in tissue culture medium. After successful growth, metabolism was shown in the LSE subcellular fractions, although only small sample numbers were available for assay. The LSE showed both GST activity and esterase activity with similar levels to subcellular fractions prepared from fresh human skin. However, microsomal protein was not found in the samples. This was contradictory to studies by Pham *et al*, (1990) who showed a 7-ethoxyresorufin-*O*-deethylation activity in uninduced LSE's at 0.55±0.07 pmoles/min/mg protein.

Exposure of the LSE to 3-methylcholanthrene led to the recovery of microsomal protein. The microsomal fraction from each pooled sample of LSE's was small and only provided enough protein for one determination of 7-ethoxyresorufin-*O*-deethylation. This was enough to establish that CYP1A1 activity had been induced in the samples to give an activity of 1.75 pmoles/min/mg microsomal protein. Further more, the induction of CYP1A1 in a living skin equivalent derived from

cells isolated from human skin, shows that human skin does indeed have low but detectable levels of cytochrome P450 monooxygenase activity, showing the capacity to express the protein. This is especially important as this activity could not be shown in microsomal fractions prepared from human skin in earlier studies. Not only was cytochrome P450 activity found in the induced LSE, but GST and esterase activity were found to have increased from the uninduced LSE's. GST activity has increased by 65% and esterase activity by 41% suggesting some degree of induction.

It therefore appears that maintenance of xenobiotic metabolising enzymes in skin is dependent on the whole tissue rather than on isolated cells. The process of keratinocyte differentiation and the presence of a dermal support seems to improve the expression of xenobiotic metabolising enzymes. Other published work also shows xenobiotic metabolism in the LSE, including studies by Slivka (1992) and Slivka *et al*, (1993). Studies by Roguet et al, (1994a; 1994b) have also shown that metabolism of testosterone in the LSE has a similar profile to metabolism in human skin.

The studies with the LSE were only preliminary, but show that the application of the LSE for evaluating xenobiotic metabolism in human skin has great potential. Not only are enzymes expressed with similar activities to human skin, but levels of expression can be influenced by induction. Studies with inducers cannot be conducted in man *in vivo*, for ethical reasons.

Chapter 15

Assessment of skin viability in vitro

Assessment of skin viability

15.1 Introduction

Maintaining skin viability *in vitro*, is an essential factor when investigating the potential of skin to metabolise xenobiotics during percutaneous absorption. The aim of the following experiments were to measure the viability of freshly excised skin under different conditions, using various markers over 24 hours. Two *in vitro* diffusion cell systems were examined, the flow-through diffusion cell system and the static diffusion cell system.

15.2 The skin absorption systems

15.2.1 The flow-through diffusion cell

In an attempt to mimic the blood flow under the skin the flow-through system uses a peristaltic pump to provide a flow of receptor medium under the skin in the diffusion cell. The flow-through system has an advantage over the static cell system in providing physiologically similar conditions and therefore helping to maintain greater skin viability (Clark *et al*, 1992). The flow-through system used in the laboratory at the University of Newcastle Upon Tyne was designed by R. Scott and I.P. Dick at the Central Toxicology Laboratories, ICI, Alderley Park, Cheshire in 1990. This design was brought to the Department of Environmental and Occupational Medicine, in The Medical School at the University of Newcastle Upon Tyne by I.P. Dick. and was constructed by the University workshop technician. The flow-through diffusion cell consists of a stainless steel chamber to which skin is held and secured by a stainless steel donor ring and screws (Plate 15.1). There are inlet and outlet tubes for the flow of receptor medium through the diffusion cell chamber, which also contains a magnetic stirring bar. The skin in the flow-through diffusion cell has an exposure area of 0.64cm^2 to which a test compound can be applied.

15.2.2 The flow-through diffusion cell method

Neonatal Wistar rats (4 days old,11-12g) were sacrificed (i.p. 20mg sodium pentobarbitone in 0.1ml saline) and the freshly excised skin was cut into pieces of approximately 1.5cm in diameter with a cork borer. A magnetic stirring bar was placed in the diffusion chamber and the skin was carefully positioned on the cell. The skin was clamped into place with the cell donor and screwed firmly together. Six neonatal rats were sufficient for setting up 12 diffusion cells.

A water bath was filled with distilled water and heated to a temperature of 32°C (skin temperature). The water was pumped through the flow-through system manifold (positioned on a magnetic stirring pad) by a water bath pump. Receptor medium (RPMI1640, section 10.2h) used for the study was placed in the water bath to incubate to skin temperature. A gas tube was placed in the medium bottle and a steady stream of 5% CO_2 was gassed over the medium surface to maintain its

pH of 7.4. Peristaltic pump tubing (Elkay #116-0549-020) was connected from the medium to the peristaltic pump, then on to the diffusion cell. Finally, PTFE tubing channels medium leaving the diffusion cell to receptor vials which receives the samples. This tubing was found to be the most suitable for samples leaving the diffusion cell because of its inertness. Some compounds, especially lipophilic molecules, bind to polyethylene tubing but this is eleviated by the use of PTFE. Medium was pumped through the system at a flow rate of 1.5ml/hr. (Plate 15.2).

Experiments were run over 24 hours. At the end of each experiment, all tubing was thoroughly washed with 70% ethanol followed by distilled water. Tubing was flushed dry and removed from the peristaltic pump. Cells and stirring bars were soaked in Decon solution and washed thoroughly with distilled water.

15.2.3 The static diffusion cell system

The static cell has been used to investigate the absorption of many compounds through skin. It provides data on the distribution of a compound in the skin as well as rates of absorption. Ethanol water (50:50 v v) has been used as the standard receptor fluid as it gives a close correlation to *in vivo* absorption profiles (Bronaugh and Stewart, 1982), although tissue culture medium has also been used in an attempt to maintain the tissue viability. Static diffusion cells that were used in these experiments were first described by Scott (1989). (Plate 15.3). The diffusion cells consist of two glass chambers between which the skin is placed and the chambers are held together with a spring loaded clamp. The lower chamber is filled with receptor medium via the receptor arm (approximately 1.5ml) and a magnetic stirring bar added. The exposed area of skin in the upper chamber is $0.7cm^2$ to which a test compound can be applied.

15.2.4 The static diffusion cell method

Neonatal rat skin was prepared in the same manner as for flow-through cells. Skin was placed on the cells and clamped together, they were filled with RPMI1640 medium, then placed on a magnetic stirring pad, in a water bath set at 32 $^{\circ}$C, (Plate 15.4). Samples of medium can be taken via the receptor arm and the volume replaced with fresh medium. Experiments were run over 24 hours. Equipment was cleaned by soaking in decon solution and rinsing with distilled water.

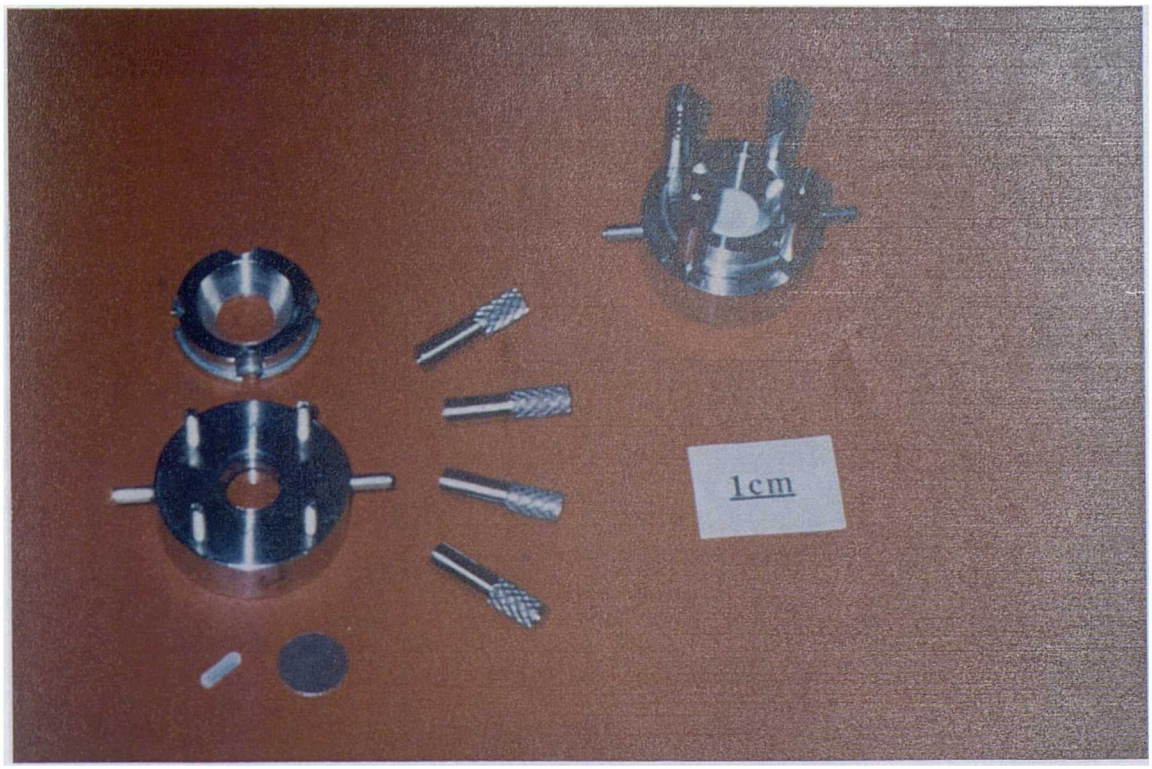

Plate 15.1 The flow-through diffusion cell.

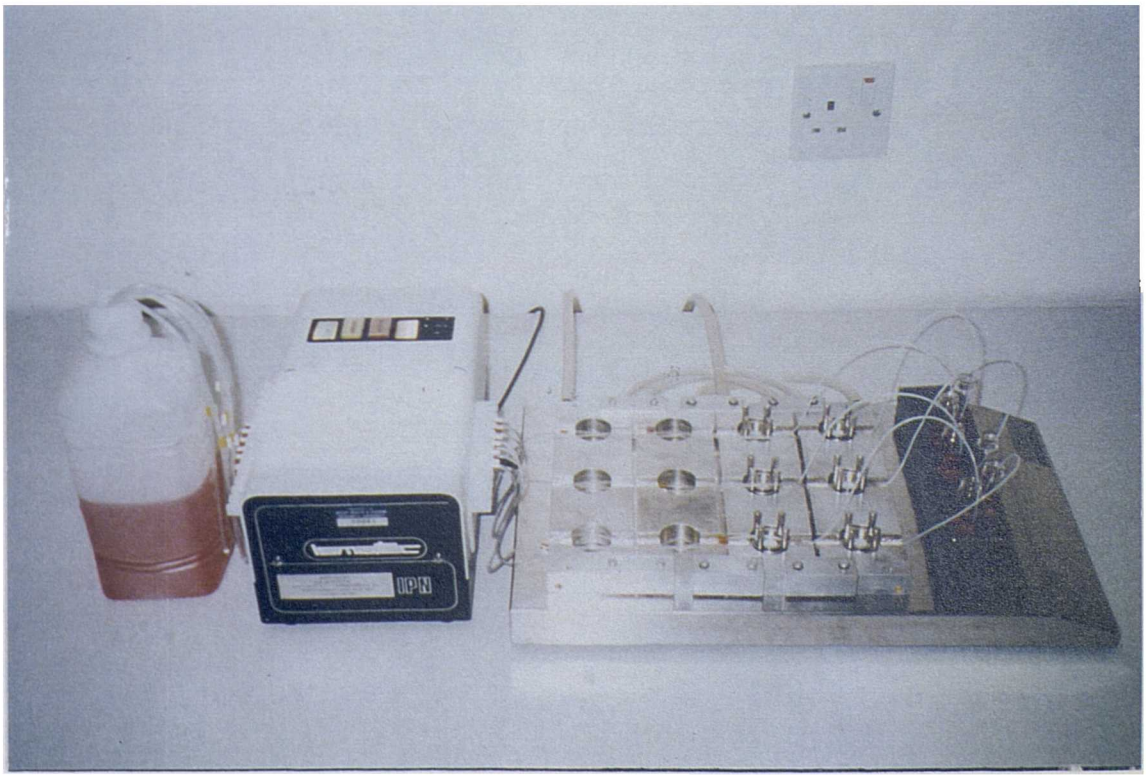

Plate 15.2 The flow-through system.

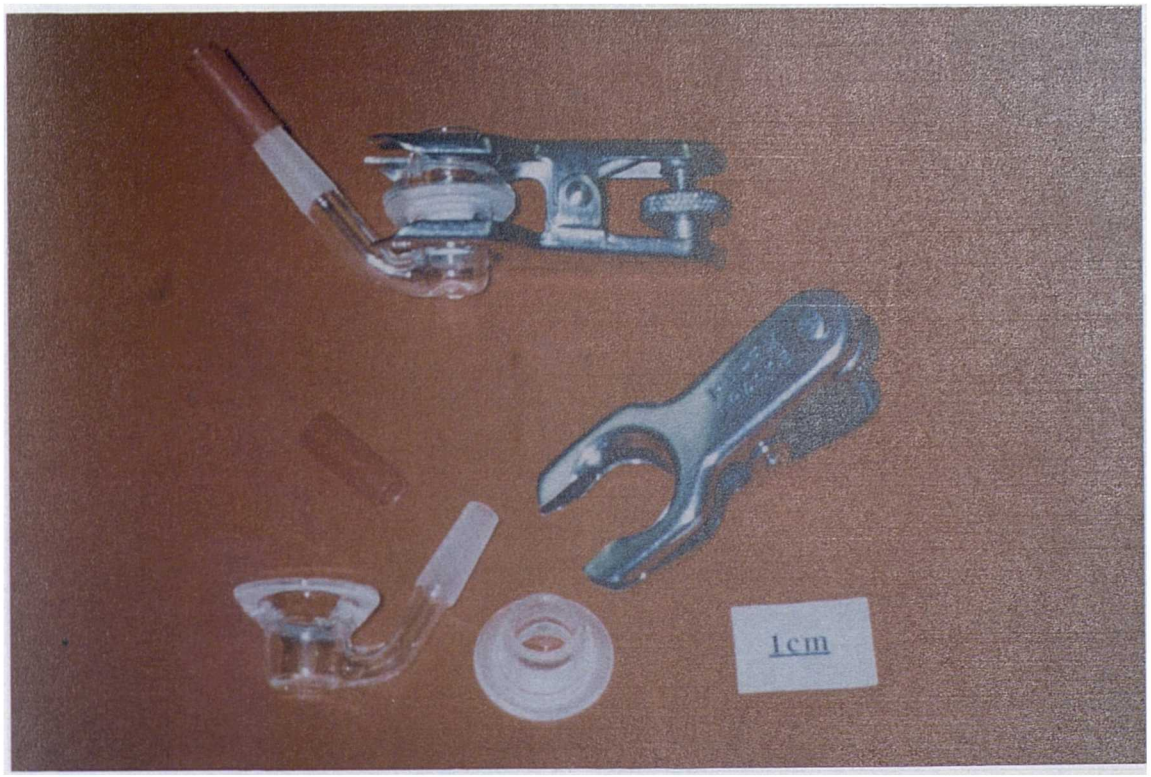

Plate 15.3 The static diffusion cell.

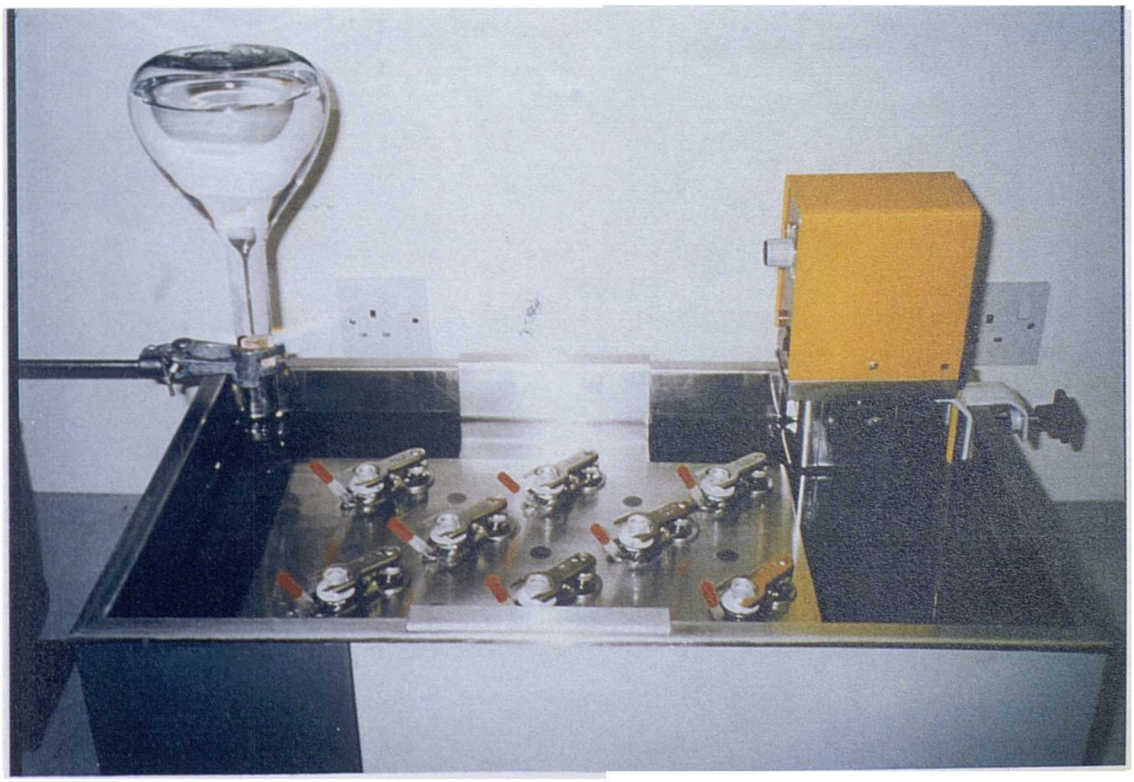

Plate 15.4 The static diffusion system.

15.3 Viability of skin in the absorption system

At time points over a 24 hour period, diffusion cells from the flow-through cell system and the static cell system were taken and the skin removed from the cell. A section of the exposed area of skin (0.5cm^2) was cut out with a cork borer and immediately assayed for it's viability. The viability was assessed by the following four markers: Mitochondrial dehydrogenase activity using the MTT assay, reduced glutathione levels using the thiol derivitising agent bromobimane, esterase activity using 4-methylumbelliferyl heptanoate and glutathione-S-transferase (GST) activity using dinitrochlorobenzene (DNCB),

15.3.1 The MTT assay

Viability of skin in the diffusion cells was evaluated by the MTT assay, which is a yellow tetrazolium salt [3-(4,5-dimethylthiozol-2-yl)-2,5-diphenyltetrazolium bromide] metabolised by mitochondrial dehydrogenases to a purple formazan precipitate, (Mosmann, 1983, Van De Sandt *et al*, 1993). Discs of skin (0.5cm^2), cut from the diffusion cells were incubated at 37°C for precisely 1 hour in freshly prepared MTT solution (2ml, 2mg/ml in RPMI1640 medium). The discs were then washed in sodium chloride solution (0.9%) and the formazan dye extracted into isopropanol (4ml). The absorbance of the solution was read at 570nm and viability expressed as a percentage of fresh skin at time zero.

15.3.2 Reduced glutathione levels in skin

The method for measuring total reduced glutathione (GSH) levels in skin is detailed in section 12.7. Briefly, discs of skin from the diffusion cells (0.5cm^2), were homogenised in 900μl of bromobimane (0.5mg ml) in n-ethylmorpholine buffer (0.05M, pH 8). After 30 minutes in the dark, 100μl of 10% methane sulfonic acid was added to precipitate the protein and the homogenate was centrifuged for 10 minutes at 2000xg. Supernatant was assayed for glutathione content by HPLC with fluorometric detection (Kontron instruments). GSH in skin is primarily located at the basal layer of the epidermis, therefore, to minimise the effect in differences of skin thickness and protein content per sample, results were expressed as nmoles of GSH/cm^2 skin.

15.3.3 Esterase activity in skin

Esterase activity was measured with the substrate 4-methylumbelliferyl heptanoate (4-MUH). Discs of skin (0.5cm^2), cut from the diffusion cells were homogenised in D-PBS buffer (2ml). The homogenate was centrifuged at 2000xg for 20 minutes and the supernatant was assayed for protein concentration and esterase activity by the method described in section 11.3.

15.3.4 Glutathione-S-transferase (GST) activities in skin

GST activity was measured with DNCB as the metabolic substrate by the method of Habig (1974). Discs of skin (0.5cm^2), cut from the diffusion cells were homogenised in DPBS buffer (2ml). The homogenate was centrifuged at 2000xg for 20 minutes and the supernatant was assayed for protein concentration and GST activity by the methods described in section 11.4.

15.3.5 Results

In both the flow-through diffusion cell and the static diffusion cell, neonatal rat skin showed no significant decrease in viability by 8 hours as measured by the MTT assay ($p>0.01$). By 12 hours, skin in both diffusion cell systems had fallen to approximately 65% of that of fresh skin, but there was still no significant difference between the cell systems ($p>0.01$). However, by 24 hours, skin in the flow-through cells had fallen to 63.59% in viability and the skin in static cells had fallen to 50.05% in viability compared to fresh skin, marking a significantly difference between diffusion systems ($p<0.01$). Details of the data are in tables 15.1 and 15.2. Graph 15.1 illustrates the decrease in viability over 24 hours assessed by this assay.

Table 15.1 Viability of neonatal rat skin in flow-through diffusion cells, assessed by the MTT assay. Viability expressed as a percentage of control at t_0. (mean±sem, n=6, *n=2).

time (hours)	mean absorbance (570nm) mean±sem	% of control mean±sem
0	0.629*	100
2	0.629*	100
4	0.615±0.027	97.77±4.29
8	0.599±0.053	95.12±8.42
12	0.423±0.016	67.25±2.54
24	0.399±0.025	63.59±3.98

Table 15.2 Viability of neonatal rat skin in static diffusion cells, assessed by the MTT assay. Viability expressed as a percentage of control at t_0. (mean±sem, n=6, *n=2).

time (hours)	mean absorbance (570nm) mean±sem	% of control mean±sem
0	0.629*	100.00
2	0.636*	101.11
4	0.626±0.015	99.46±2.38
8	0.581±0.026	92.37±4.13
12	0.372±0.040	59.14±6.36
24	0.315±0.011	50.05±1.75

Graph 15.1. Viability of neonatal rat skin in flow-through and static diffusion cells assessed by the MTT assay. Viability expressed as a percentage of control at t_0. Receptor medium was RPMI1640 tissue culture medium containing gentamycin (20μg/ml). Cells were maintained at 32°C for 24 hours. (mean±sem, n=6)

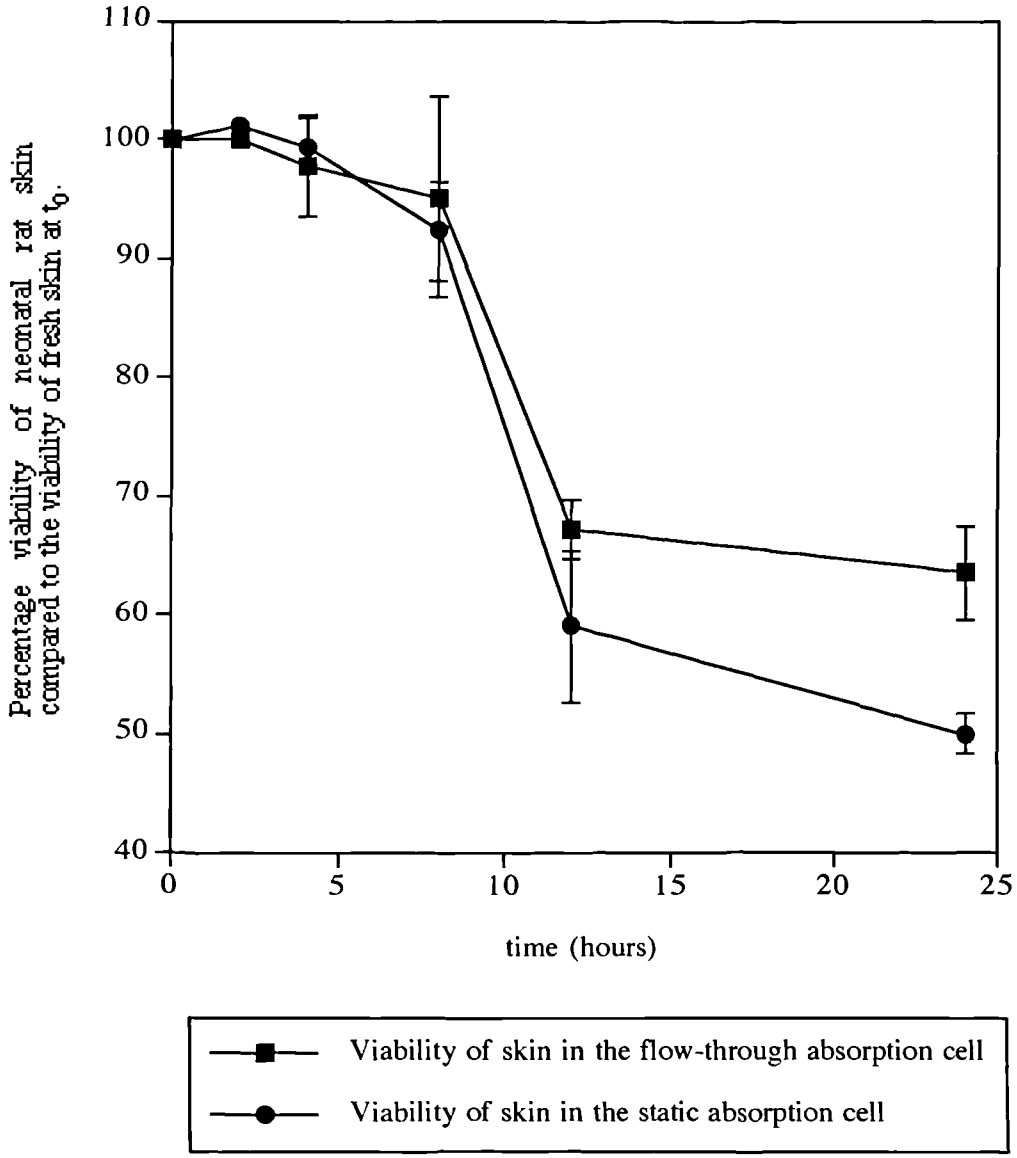

Measurement of levels of glutathione (GSH) in neonatal rat skin in diffusion cells showed a substantial decrease over 24 hours. Differences between the flow-through diffusion cell and the static diffusion cell were significant at all time points ($p<0.01$). By 24 hours, GSH levels in the flow-through diffusion cell had fallen to approximately 25% of fresh skin, whereas GSH levels in the static diffusion cell had fallen to approximately 7%. Analysis of the receptor medium showed no detectable levels of GSH which may have leaked from the skin into the tissue culture medium. Data is found in tables 15.3 and 15.4. Graph 15.2 illustrates the decrease in GSH levels in neonatal rat skin.

Table 15.3 Reduced glutathione (GSH) levels in neonatal rat skin in the flow-through diffusion cell (mean±sem, n=4).

time (hours)	GSH (nmoles/cm^2) (mean±sem, n=4)
0	89.99±3.70
4	86.89±1.96
12	39.89±1.09
24	22.21±1.46

Table 15.4 Reduced glutathione (GSH) levels in neonatal rat skin in the static diffusion cell (mean±sem, n=4).

time (hours)	GSH (nmoles/cm^2) (mean±sem, n=4)
0	89.99±3.70
4	48.22±3.99
12	17.78±1.75
24	6.29±1.49

Graph 15.2 Reduced glutathione levels in neonatal rat skin in flow-through and static diffusion cells (nmoles/cm^2). Receptor medium was RPMI1640 tissue culture medium containing gentamycin (20μg/ml). Cells were maintained at 32°C for 24 hours. (mean±sem, n=4)

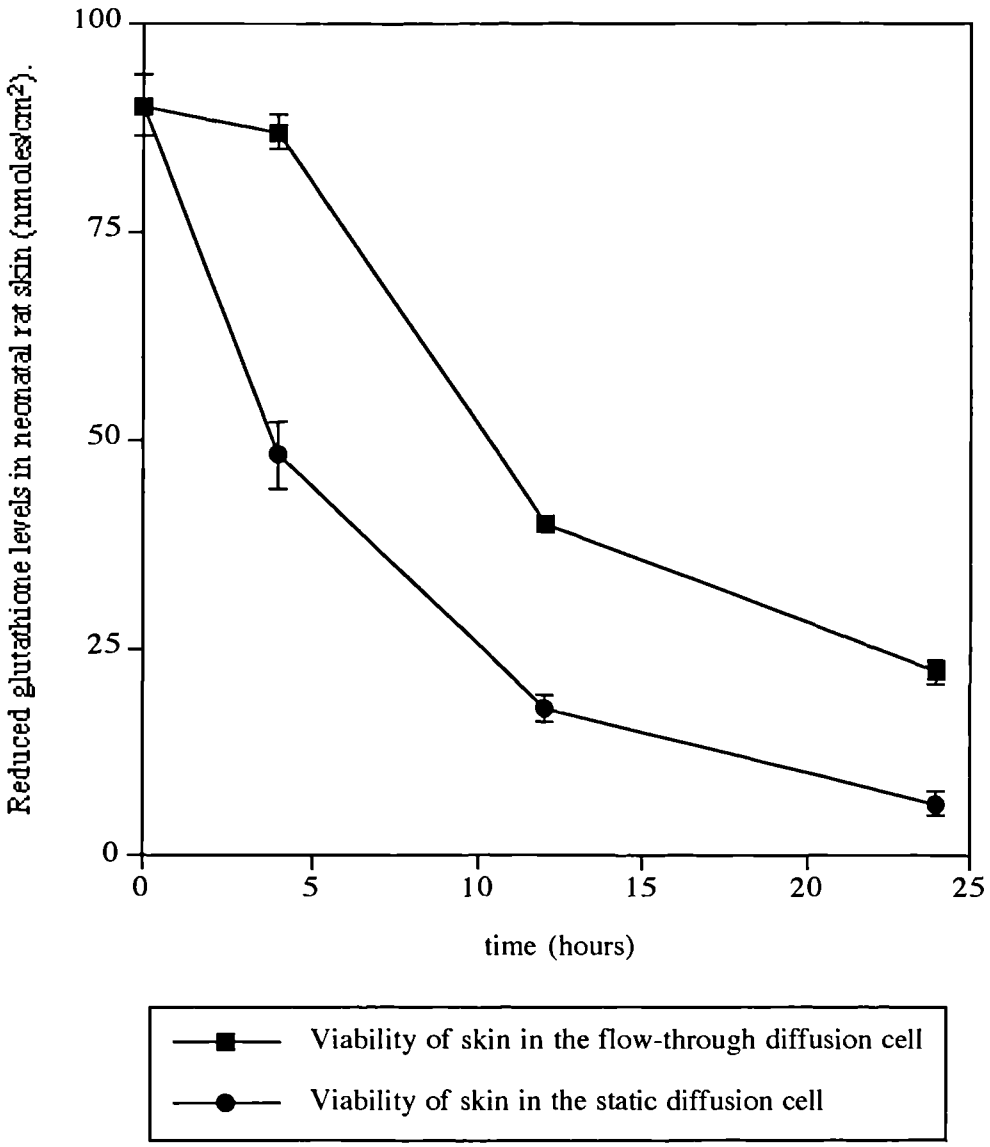

There was no significant difference ($p>0.01$) in skin esterase activity between the flow-through or static diffusion cells over 24 hours. At 12 hours, there was no significant decrease in esterase activity from fresh skin ($p>0.01$). At 24 hours there was a significant difference compared to fresh skin ($p<0.05$), but not between 12 hours and 24 hours ($p>0.01$). The profiles show a high degree of variation. This was due to small samples of tissue, leading to a greater variability in protein recovery after tissue homogenisation. Data are found in tables 15.5 and 15.6. Graph 15.3 illustrates the change in esterase activity.

Table 15.5 Esterase activity in neonatal rat skin in the flow-through diffusion cell, measured with the esterase substrate 4-MUH (mean±sem, n=6, *n=4).

time (hours)	esterase activity (nmoles/min/mg post mitochondrial protein) mean±sem
0	23.78±1.5
4	22.43±2.72
8	19.68±3.6
12	20.14±4.09
24	10.43±5.71*

Table 15.6 Esterase activity in neonatal rat skin in the static diffusion cell, measured with the esterase substrate 4-MUH (mean±sem, n=6, *n=4).

time (hours)	esterase activity (nmoles min mg post mitochondrial protein) mean±sem
0	23.78±1.50
4	21.65±2.90
8	22.75±3.69
12	20.20±3.81
24	11.07±5.57*

Graph 15.3 Esterase activity in neonatal rat skin in flow-through and static diffusion cells (nmoles/min/mg post mitochondrial protein). Receptor medium was RPMI1640 tissue culture medium containing gentamycin (20μg/ml). Cells were maintained at 32°C for 24 hours. (mean±sem, n=6, *n=4).

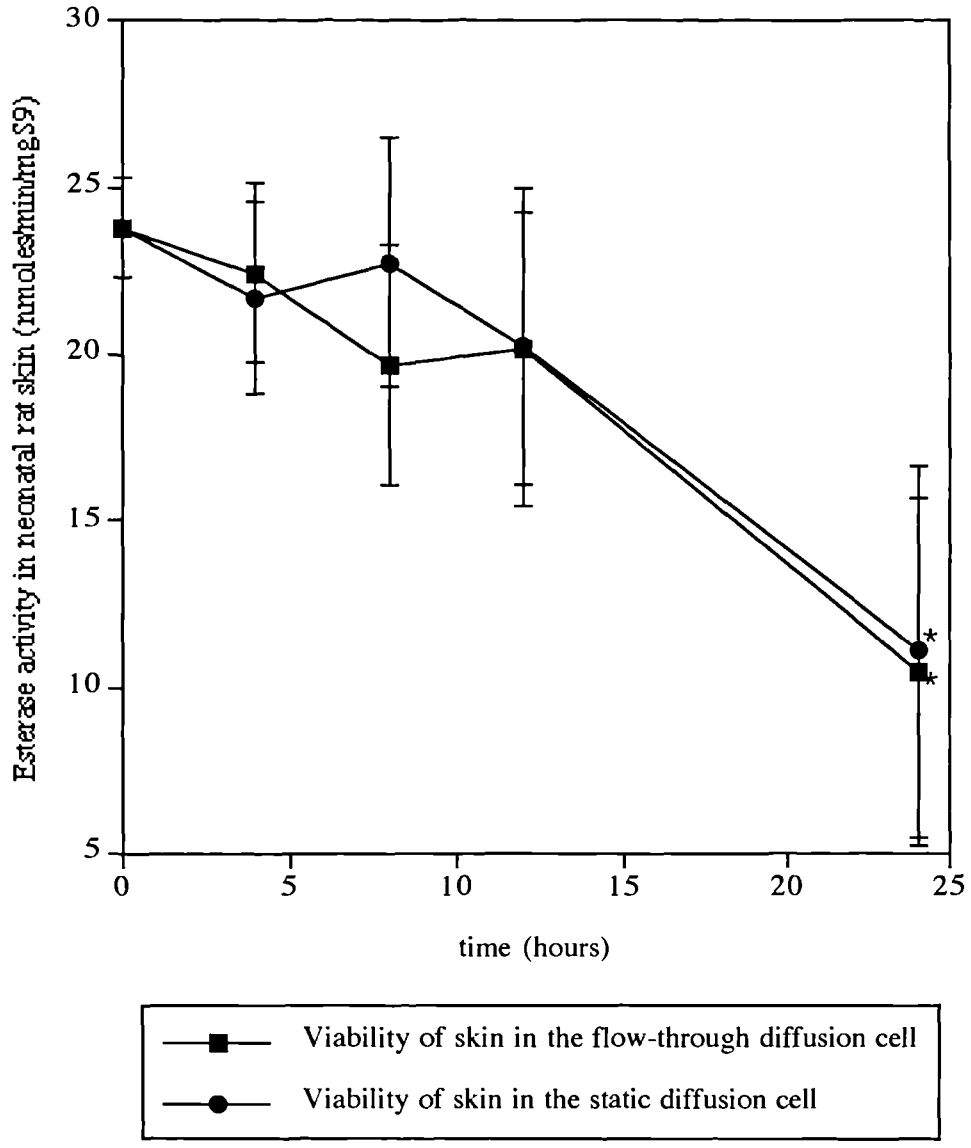

GST activities in neonatal rat skin in both diffusion cell systems appear to be stable over 24 hours. There was also no significant difference between diffusion cell type ($p>0.05$). Data are found in tables 15.7 and 15.8. Graph 15.4 illustrates GST activity in neonatal rat skin.

Table 15.7 Glutathione-S-transferase activity in neonatal rat skin in the flow-through diffusion cell. (mean±sem, n=4).

time (hours)	Glutathione-S-transferase activity (nmoles/min/mg post mitochondrial protein) mean±sem
0	0.052±0.005
4	0.054±0.002
8	0.053±0.004
12	0.056±0.004
24	0.058±0.002

Table 15.8 Glutathione-S-transferase activity in neonatal rat skin in the static diffusion cell (mean±sem, n=4).

time (hours)	Glutathione-S-transferase activity (nmoles min/mg post mitochondrial protein) mean±sem
0	0.052±0.005
4	0.056±0.005
8	0.054±0.006
12	0.054±0.002
24	0.059±0.004

Graph 15.4 Glutathione-S-transferase activity in neonatal rat skin in the flow-through and static call absorption systems (nmoles/min/mg post mitochondrial protein). Receptor medium was RPMI1640 tissue culture medium containing gentamycin (20μg/ml). Cells were maintained at 32°C for 24 hours. (mean±sem, n=4)

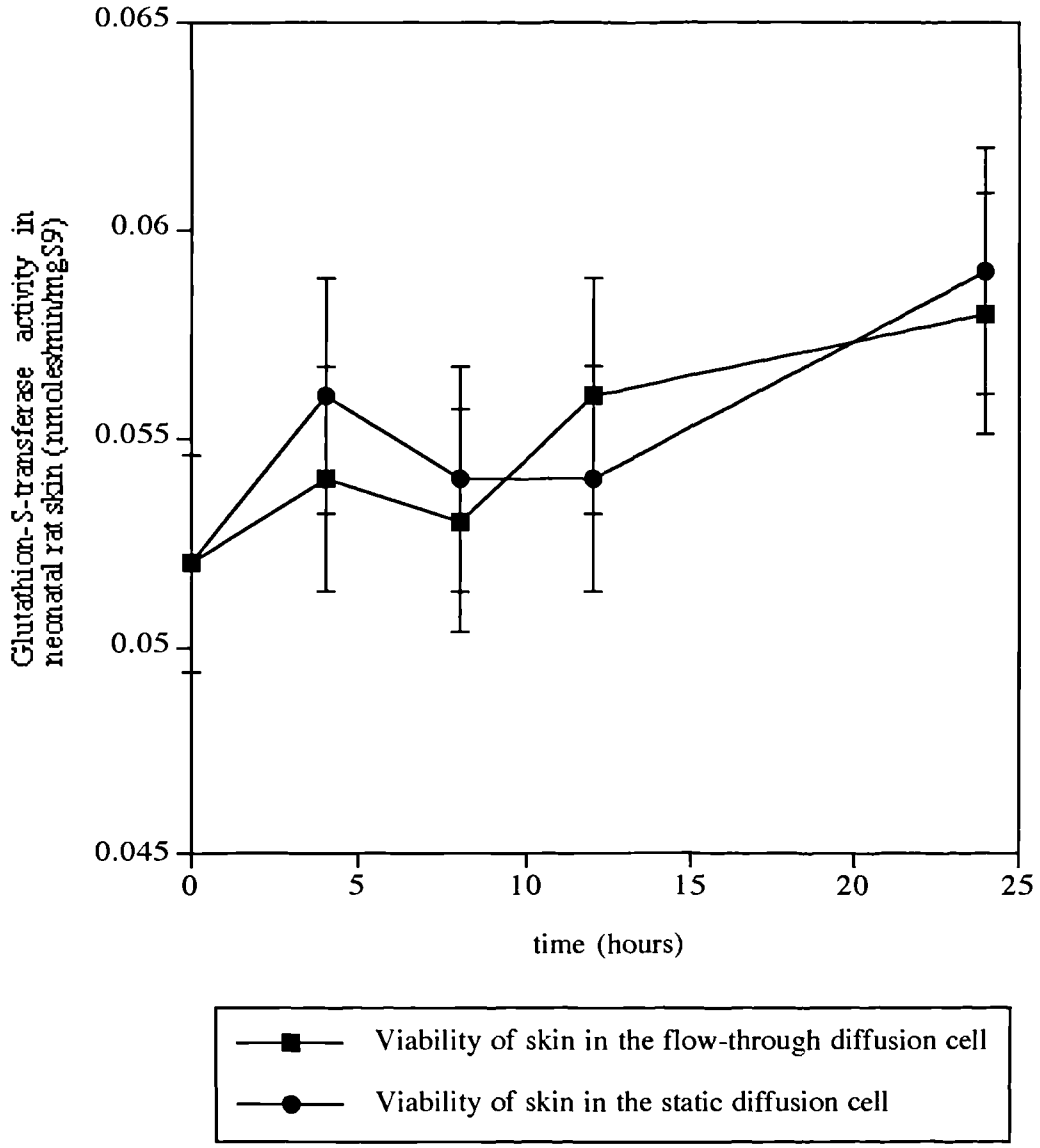

15.3.6 Discussion

The MTT assay measures viability as a function of mitochondrial dehydrogenase activity, an enzyme essential in the cellular energy production. Although there was a decrease in this activity over the 24 hours, the levels were still high, with 50% activity remaining in the skin of the static cells and 64% remaining in the skin of the flow-through cells. The results showed that the flow-through diffusion cell maintained skin viability significantly better than the static diffusion cell ($p<0.01$). This illustrates that viability of skin *in vitro* can be maintained, but this does not demonstrate it's ability to metabolise xenobiotics.

Reduced glutathione levels were measured in skin as it is the cofactor used by GST's in the conjugation of many electrophilic xenobiotics, including DNCB. Levels of GSH decreased substantially over 24 hours, suggesting that GSH is an unstable molecule in skin *in vitro*. Although levels of GSH decreased, it was still present at 24 hours. In the static diffusion cell GSH was at approximately 7% compared to fresh skin. In the flow-through diffusion cell the level was at approximately 25%. Therefore the flow-through system was found to be significantly better at maintaining GSH levels in skin than the static system ($p<0.01$). The levels of oxidised glutathione (GSSG) were not measured. Levels of GSH may therfore have decreased more rapidly in the static cell to the oxidised form.

Esterases, relatively stable enzymes, were measured with the esterase substrate 4MUH. There appeared to be a large decrease in esterase activity over 24 hours, though this may be only due to wide variability between samples and small sample number. Sample numbers were limited because only 12 diffusion cells could be run at any one time. The degree of error in esterase activity at 24 hours meant there was no significant difference compared to activity at 12 hours ($p>0.05$). Therefore the decrease in esterase activity by 24 hours may not be as large as the data indicates. Other studies using keratinocytes have suggested a relative stability of this activity

GST's were measured as an indicator for the potential of skin to metabolise DNCB *in vitro* over 24 hours. There was no significant difference in this enzymes activity over 24 hours in either the flow-through or the static diffusion cells ($p>0.01$). GST's therefore appear to be a robust enzyme in skin.

The flow-through diffusion cell system maintained greater skin viability than the static diffusion cell as indicated by the metabolic marker MTT and levels of GSH ($p<0.01$). This increased viability is maintained due to the continual replenishment of receptor medium beneath the skin. Together with enzyme systems such as esterases and GST's, not only is the skin's viability maintained, but also it's metabolic capacity.

Unfortunately, cytochrome P-450 monooxygenase activity could not be measued in such small samples of skin as used in these experiments. Therefore the stability of these enzymes in the diffusion cells could not be assessed.

15.4 Effect of absorption cell receptor medium on glutathione-S-transferase activities

The viability of skin in the flow-through system is greatly influenced by the choice of receptor medium. The receptor medium must be able to supply the skin with essential nutrients as well as maintain pH and osmotic balance. Various receptor media have previously been investigated by Clark *et al,* (1992). Different metabolic processes within the skin may need different nutritional sustenance. Therefore to determine that RPMI1640 tissue culture medium was suitable, it was compared with the tissue culture medium, Eagles minimum essential medium (MEM), which was found to be the optimal choice by Clark *et al, (*1992). The reduced glutathione level in skin was found to be the most sensitive marker of viability, therefore GSH levels were compared in the flow-through absorption system with RPMI1640 and MEM.

GSH is readily oxidised to the GSSG form. To determine whether an antioxidant in the receptor medium would help maintain GSH levels in the skin, ascorbic acid (100μg/ml) was also added to RPMI1640.

15.4.1 Method

The flow-through system was run for 24 hours with neonatal rat skin as with the previous viability studies. Medium RPMI1640 was freshly prepared as described in chapter 10.2h.

15.4.2 Results

There was no significant difference in reduced glutathione levels in neonatal rat skin when different media were used as receptor medium in the flow-through system ($p>0.01$). Data is found in table 17.9. Graph 15.5 illustrates the effect of different media.

Table 15.9 Effect of receptor medium on reduced glutathione levels in neonatal rat skin in the flow-through diffusion cell over 24 hours. (mean±sem, n=4).

	Receptor medium		
time (hours)	RPMI1640	MEM	RPMI1640 + Ascorbic acid
0	89.99±3.70	91.13±4.00	83.59±8.71
4	86.89±1.96	93.36±7.39	80.92±5.84
12	39.89±1.09	38.59±2.70	38.76±3.48
24	22.21±1.46	19.90±3.25	19.73±1.38

Graph 15.5 Effect of receptor medium on the viability of neonatal rat skin in the flow-through diffusion cell. Medium was set at a flow rate of 1.5ml/h. Cells were maintained at 32°C for 24 hours. (mean±sem, n=4).

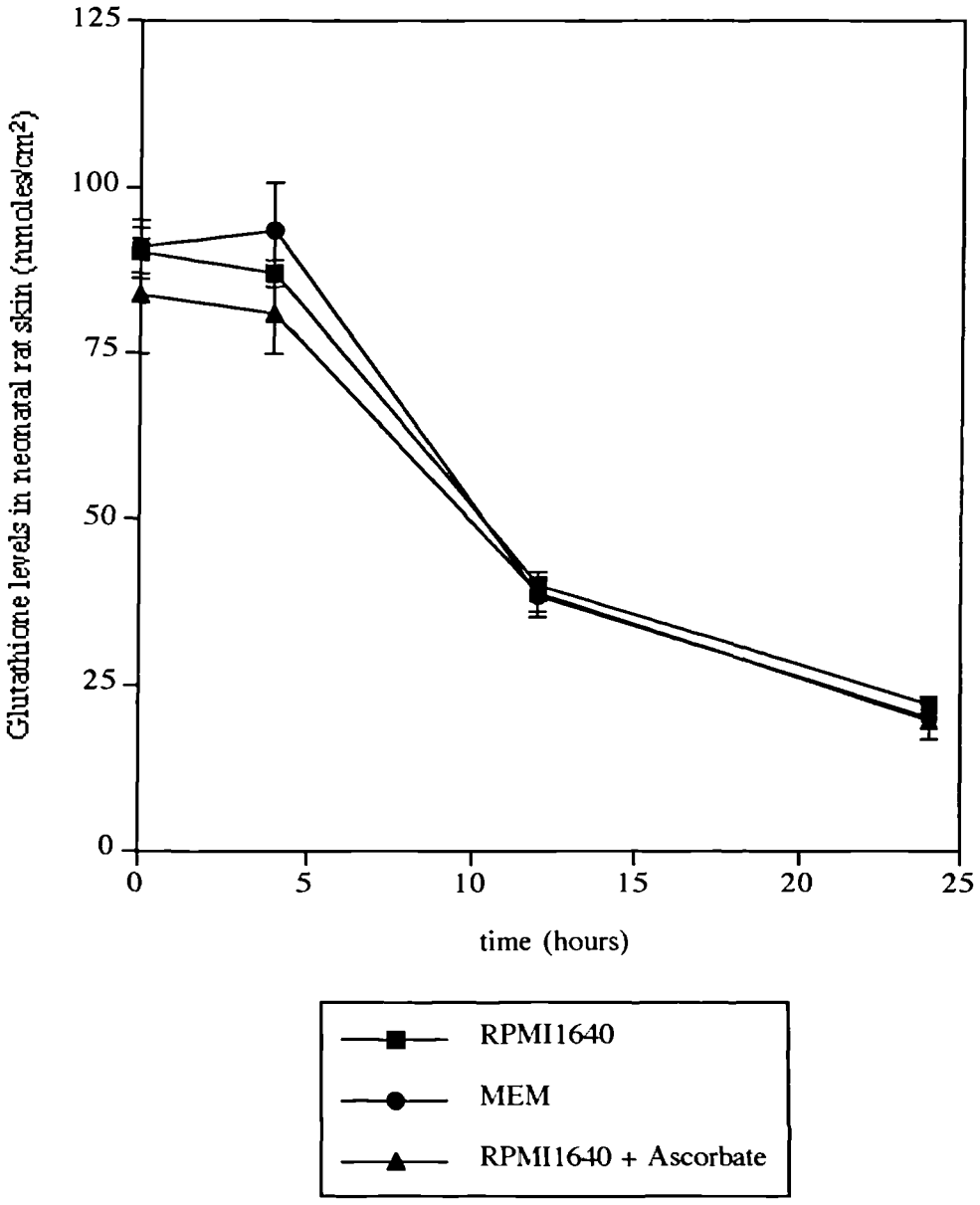

15.4.3 Discussion

RPMI1640 was initially chosen as the medium for *in vitro* absorption studies as it was previously used in preliminary absorption studies with Balb/C mouse skin at Zeneca Central Toxicology Laboratory. It has also been used in skin absorption studies by Van De Sandt, *et al* (1992, 1993). Substitution of the medium with MEM had no significant effect on maintaining GSH levels higher than with RPMI1640. The addition of ascorbic acid (an antioxidant) to RPMI1640 also had no effect on GSH levels. Therefore, because MEM or ascorbic acid had no significant contribution to maintaining skin GSH levels, RPMI1640 was chosen as the receptor medium for further investigative studies.

15.5 Storage of skin prior to absorption studies

The viability of skin declines after being excised from the animal, including it's ability to metabolise xenobiotics. In order to ascertain the optimal conditions for storing freshly excised skin, to maintain it's metabolic activity, skin viability was measured over 24 hours under various storage conditions. It was especially useful to know how to treat fresh skin prior to absorption and metabolism studies, with respect to human skin. Human skin from plastic surgery, when available, is usually obtained late in the afternoon, often after a lengthy operation. Absorption and metabolism studies with human skin are therefore usually started the following morning. By determining the viability of stored skin over 24 hours, a profile of it's ability to metabolise with time could be ascertained. Though human skin would have been the ideal choice to determine optimal storage conditions, it's scarcity meant that animal skin had to be used instead. Data from animal skin could then be used as an indicator of the best storage method.

15.5.1 Method

Neonatal Wistar rats (6 animals) were sacrificed and the skin was excised and cut into discs ($0.5cm^2$) with a cork borer. Discs of skin were maintained in air at 32°C, 20°C and 4°C for 24 hours. Discs were also placed on filter paper soaked with RPMI1640 tissue culture medium pH7.4, containing gentamycin (20μg ml) at 4°C for 24 hours. Uncut skin was placed on medium at 4°C and cut into discs only when it was to be assayed at 24 hours. Viability was assayed by the MTT assay and by measurement of GSH levels.

15.5.2 Results

Viability assessed by the MTT assay, showed that it decreased with time, but more rapidly with the higher the temperature, (table 15.10). When stored on medium at 4°C the loss in viability was approximately 10%. There was no significant difference between cutting the skin into discs or remaining uncut until the time of assay ($p>0.01$). The viability of skin by the MTT assay is illustrated in graph 15.6.

GSH levels in skin decreased dramatically under all conditions within 4 hours except for the uncut skin, (table 15.11). The levels of GSH stabilised after 4 hours and steadily decreased thereafter, illustrated in graph 15.7. The higher the storage temperature, the more dramatic was the loss in GSH. Uncut skin stored on medium at 4°C, maintained its level of GSH for 24 hours.

Loss of esterase activity in skin was proportional to storage temperature, the higher the temperature the greater the decrease in activity (table 15.12). There was no significant difference by 24 hours between skin that was cut and uncut ($p>0.01$). Skin stored on medium at 4°C lost approximately 18% of its activity. This is graphically represented in graph 15.8.

GST activity remained unchanged in all conditions ($p>0.05$), with the exception of 32°C, where activity was completely lost ($p<0.01$) (table 15.13). GST activity in skin at 32°C decreased steadily over the 24 hours of the experiment, graph 15.9. It was noted that at this temperature the discs of skin had dried out and shrunk.

Table 15.10 Viability of skin stored at 32°C, 20°C, 4°C in air and at 4°C on RPMI1640 medium (containing gentamycin 20μg/ml) cut and uncut, as assessed by the MTT assay (mean±sem, n=6). Viability measured by the MTT assay and expressed as a percentage of fresh skin viability at t_0. (mean±sem, n=6).

time (hours)	32°C	20°C	4°C	medium/cut	medium/uncut
0	100.00±2.70	100.00±2.70	100.00±2.70	100.00±2.70	100.00±2.70
2	86.01±2.70	-	96.23±4.95	-	-
4	67.41±3.48	73.07±7.21	94.04±9.21	96.08±5.94	112.87±10.59
8	51.83±5.25	-	83.65±2.70	-	-
12	33.55±3.98	46.02±3.92	64.44±2.86	94.35±4.46	101.31±7.64
24	18.92±1.75	39.50±0.61	55.96±1.27	88.77±6.60	93.56±5.62

Table 15.11 GSH levels in skin stored at 32°C, 20°C, 4°C in air and at 4°C on RPMI1640 medium (containing gentamycin 20μg ml) cut and uncut (nmoles/cm^2). (mean±sem, n=4).

time (hours)	32 C	20°C	4°C	medium/cut	medium/uncut
0	89.99±3.70	89.99±3.70	89.99±3.70	88.71±7.89	88.71±7.89
4	14.85±1.53	33.838±1.50	43.49±2.88	47.56±9.93	95.89±5.44
8	2.63±0.65	16.33±0.94	44.25±2.20	49.49±0.97	86.83±2.41
24	not detectable	5.83±1.20	28.42±2.86	44.08±3.34	88.43±1.32

Table 15.12 Esterase activity in skin stored at 32°C, 20°C, 4°C in air and at 4°C on RPMI1640 medium (containing gentamycin 20μg ml) cut and uncut. (mean±sem, n=6). (nmoles/min/mg post mitochondrial fraction)

time (hours)	32 C	20°C	4°C	medium/cut	medium/uncut
0	23.78±1.50	23.78±1.50	23.78±1.50	23.78±1.50	23.78±1.50
4	18.49±1.80	18.92±0.50	22.55±0.91	22.39±1.82	24.52±0.56
12	12.64±0.82	15.62≠1.68	19.97±1.31	20.26±0.98	21.68±1.01
24	6.93±0.57	11.71±1.14	14.71±1.00	19.71≠1.26	19.64±1.43

Table 15.13 GST activity in skin stored at 32°C, 20°C, 4°C in air and at 4°C on RPMI1640 medium (containing gentamycin 20μg/ml) cut and uncut. (mean±sem, n=6). (nmoles/min/mg post mitochondrial fraction)

time (hours)	32°C	20°C	4°C	medium/cut	medium/uncut
0	0.052±0.005	0.052±0.005	0.052±0.005	0.052±0.005	0.052±0.005
4	0.048±0.003	0.051±0.007	0.051±0.006	0.049±0.004	0.052±0.004
12	0.021±0.012	0.052±0.006	0.048±0.003	0.054±0.002	0.053±0.005
24	not detectable	0.063±0,014	0.057±0.005	0.055±0.001	0.056±0.003

Graph 15.6 Viability of excised neonatal rat skin stored at 32°C, 20°C, 4°Cin air and on RPMI1640 tissue culture medium containing gentamycin (20μg/ml) at 4°C, cut and uncut skin stored on medium at 4°C for 24 hours. Viability measured by the MTT assay and expressed as a percentage of fresh skin viability at t_0. (mean±sem, n=6).

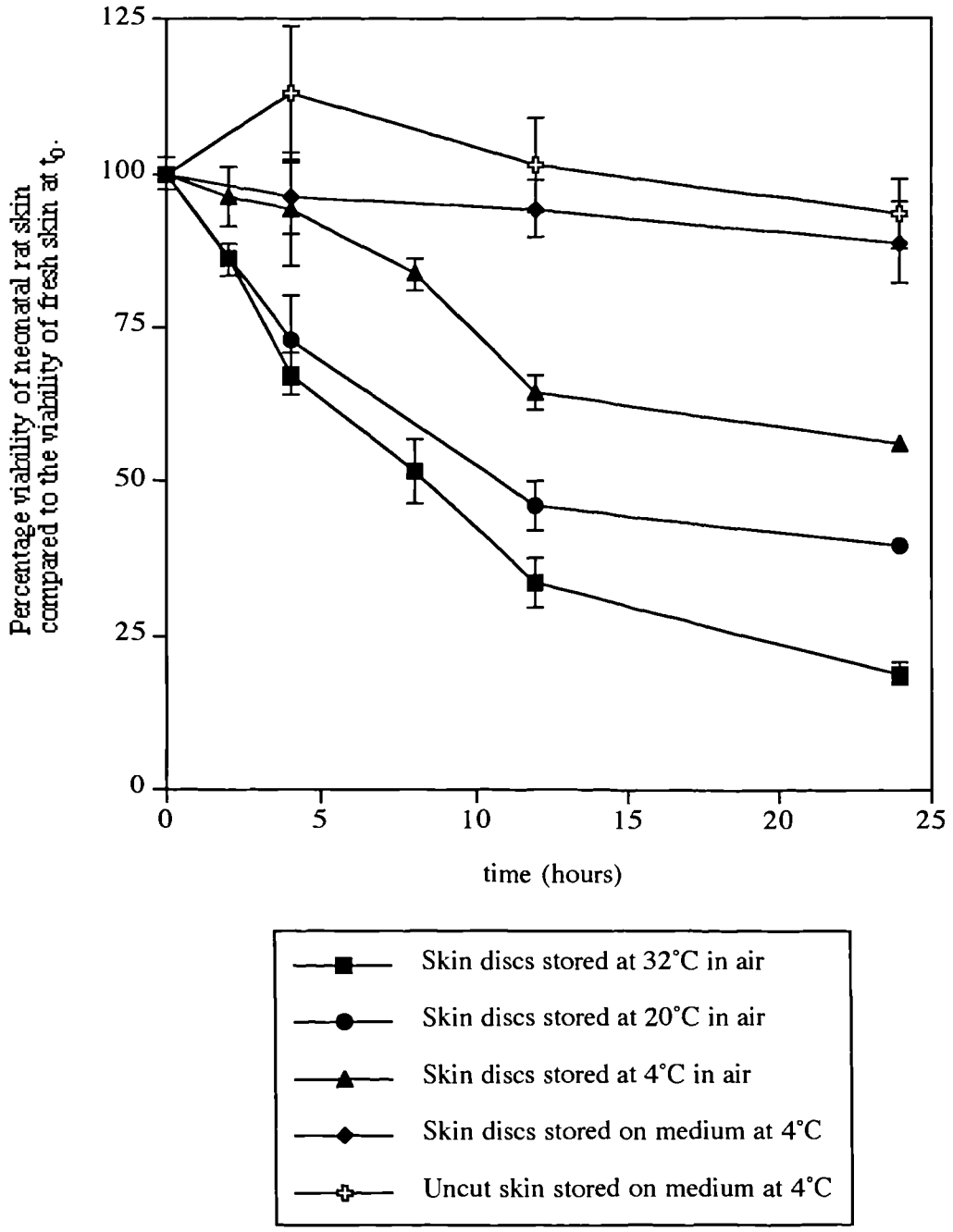

Graph 15.7 Reduced glutathione levels in excised neonatal rat skin stored at 32°C, 20°C, 4°C in air and on RPMI1640 tissue culture medium at 4°C,and uncut skin stored on medium at 4°C for 24 hours. (nmoles/cm^2). (mean±sem, n=4).

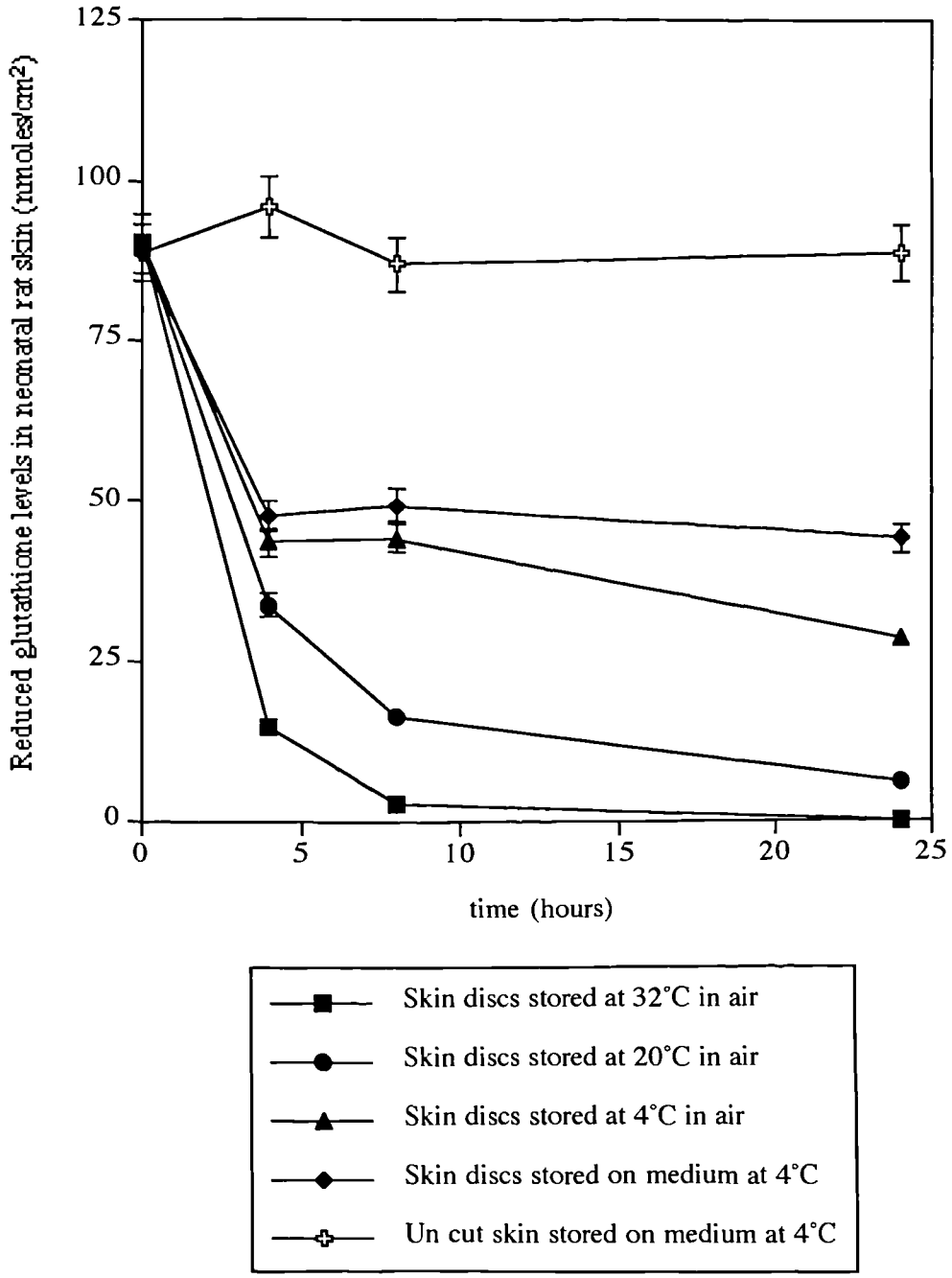

Graph 15.8 Esterase activity in excised neonatal rat skin stored at 32°C, 20°C, 4°C in air and on RPMI1640 tissue culture medium containing gentamycin (20μg/ml) at 4°C,and uncut skin stored on medium at 4°C for 24 hours. Viability measured as (nmoles/min/mg post mitochondrial fraction). (mean±sem, n=6).

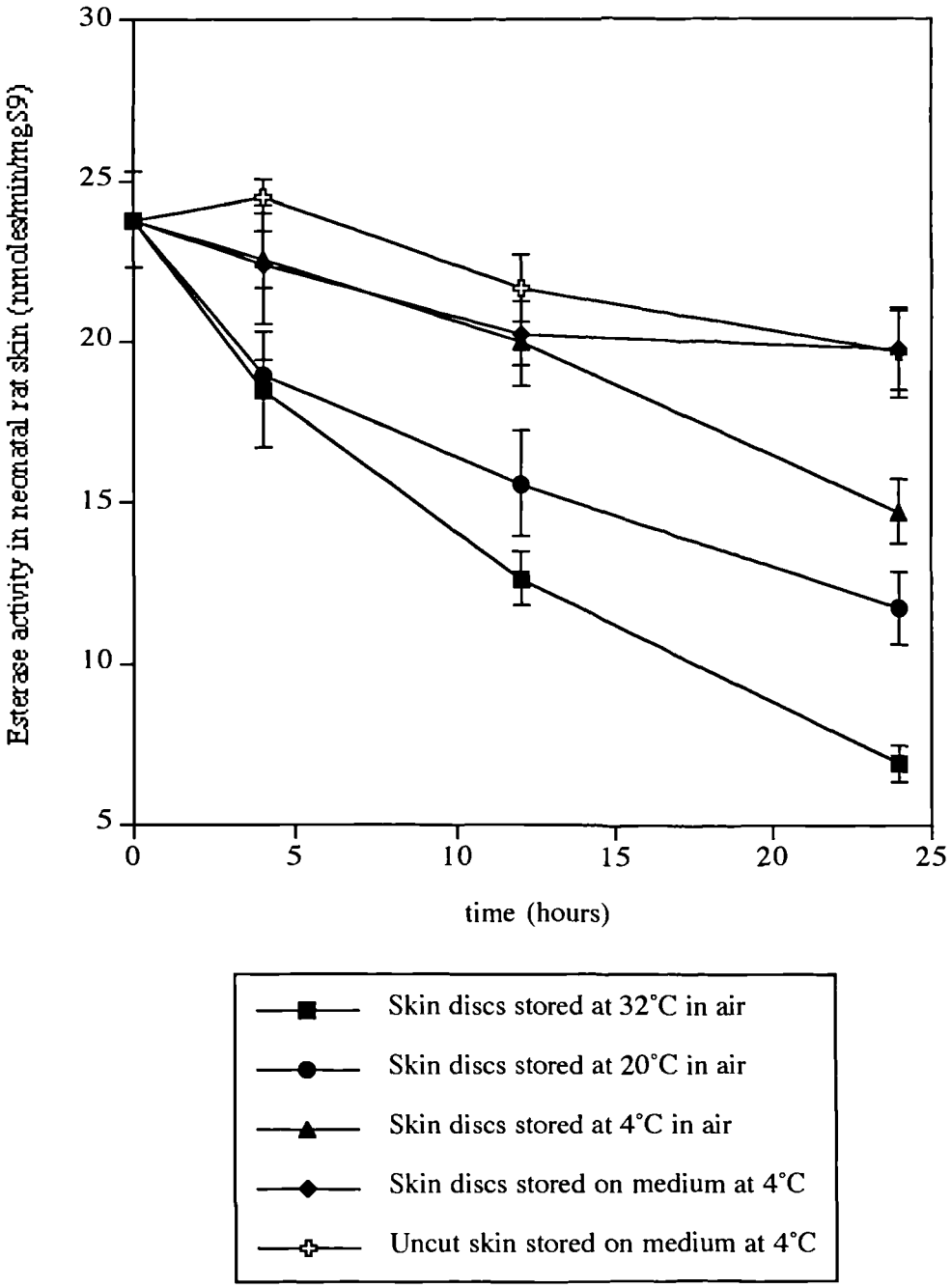

Graph 15.9 GST activity in excised neonatal rat skin stored at 32°C, 20°C, 4°C, on RPMI1640 tissue culture medium containing gentamycin (20μg/ml) at 4°C,and uncut skin stored on medium at 4°C for 24 hours. (nmoles/min/mg post mitochondrial fraction) (mean±sem, n=6).

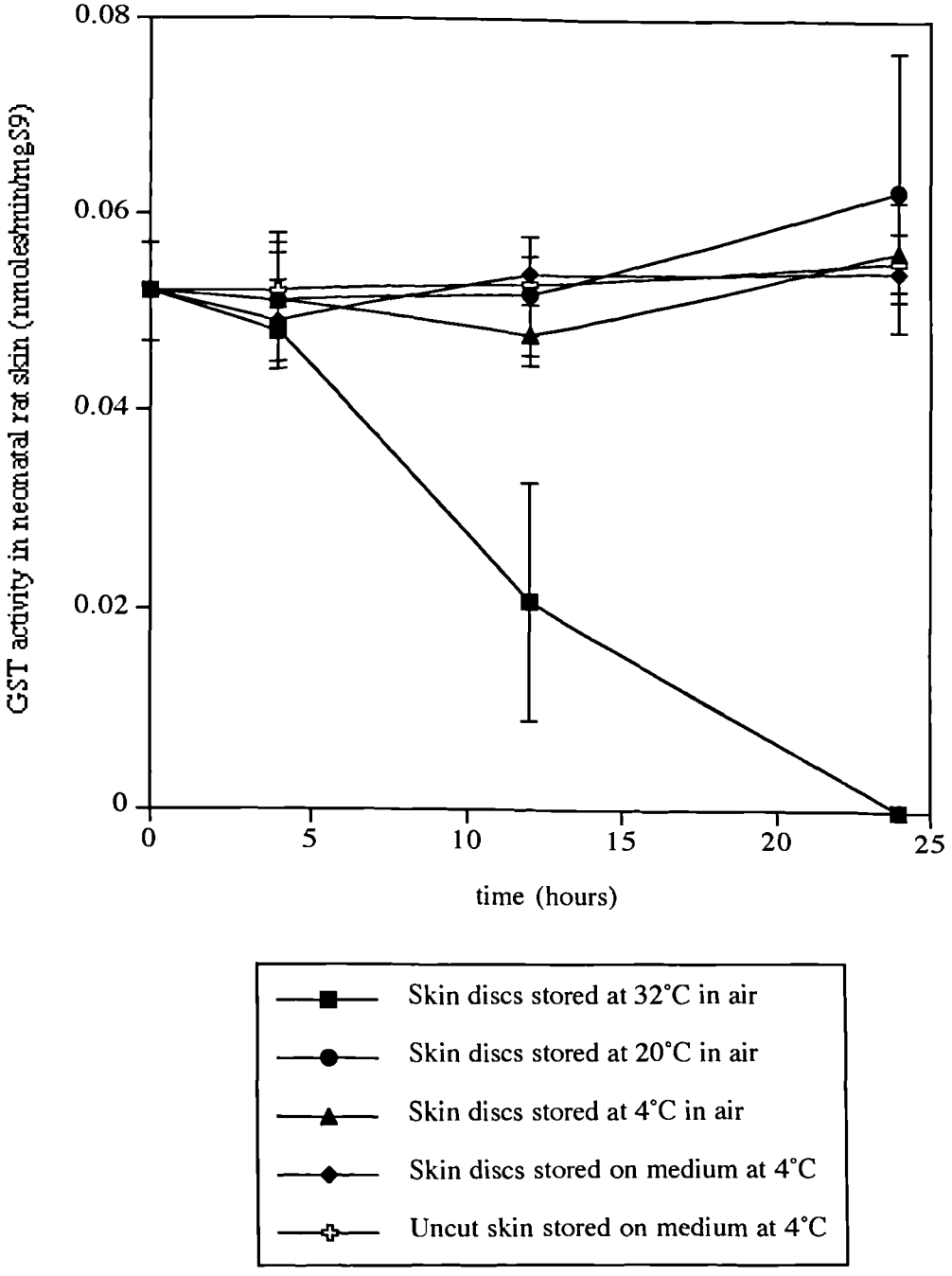

15.5.3 Discussion

The results showed that GST activity remained stable over 24 hours ($p>0.05$), with the exception of 32°C, where activity was lost ($p<0.01$). Other markers of viability showed that excised skin lost metabolic activity rapidly at high temperatures and in the absence of tissue culture medium ($p<0.01$). Skin viability as assessed by its metabolic capacity showed little change when skin was maintained on tissue culture medium at 4°C for 24 hours ($p<0.05$). Enzyme activities also showed no statistical difference between cut and uncut skin ($p>0.05$). However, cutting the skin resulted in a dramatic decrease of reduced glutathione levels ($p<0.01$), whereas no significant decrease was seen in uncut skin. It may be likely that by cutting the skin, GSH is more readily oxidised by exposure of the cut edge of the skin to the atmosphere.

Therefore, the best storage method for excised skin was to place it on filter paper saturated in tissue culture medium and refrigerated at 4°C. By this method nutrients could diffuse through to the skin, tissue degradation is kept to a minimum while still maintaining enzyme activity and the stratum corneum kept dry to avoid epidermal hydration.

15.6 Immunohistochemistry of skin

DNCB is metabolised to the glutathione conjugate by GST's. Therefore, prior to studies examining the percutaneous absorption and metabolism of DNCB through mouse skin *in vitro*, the presence of π class GST's (predominant in mammalian skin, Raza *et al*, (1991)) was investigated in Balb C mouse skin by immunohistochemistry. Staining for GSH in skin was also undertaken by histochemical techniques. Liver was also examined for comparative evaluation.

15.6.1 Method

Balb C mouse skin and liver were excised as described in chapter 10.3. For GST immunohistochemical staining, specimens were placed in a solution of ethanol (95%) and acetic acid (1%) for 3 hours, prior to further processing. Samples for GSH staining were snap frozen in liquid nitrogen.

All staining procedures were undertaken by Dr Sally Wilkins, histologist at Zeneca Central Toxicology Laboratory (CTL), Alderey Park, Cheshire. Immunohistochemical staining of π GST's was achieved by a standard protocol at CTL with antibodies raised against π GST in the Balb/C mouse. Controls were processed in the same manner but without the antibody. Samples were fixed and mounted into wax blocks and sections were cut on a cryostat microtome to 10μm thickness. The sections were mounted onto glass microscope slides and visualised under a light microscope.

Sections were stained for GSH by the method of Smith *et al* (1979). This method is not specific for GSH, but a stain for all thiol groups present in the tissue. By limiting the time of exposure to the dye, the most reactive thiols in the tissue, GSH, will be stained first. Frozen tissue was cut on a cryostat microtome to 10μm thickness and processed immediately. The chemical stain consisted of equal volumes of $FeCl_3$ (2M) and $K_3Fe(CN)_6$ (0.9M) mixed together immediately before staining and the tissue submerged in the stain for 20 seconds at room temperature. Sections were washed in distilled water and dehydrated through graded alcohols and finally in xylene. Sections were mounted in DPX on microscope slides.

15.6.2 Results

Balb C mouse liver sections stained clearly for π GST. The brown staining was most heavy in cells surrounding hepatic blood vessels, but not portal areas (plate 15.1). There was also light staining in all other areas of the liver, including some staining of the blood cells still present in the hepatic vessels. The negatively stained control showed non of these features (plate 15.2). Mouse skin sections were distinctly stained in areas appertaining to the basal layer of the epidermis, hair follicles and sebaceous glands (plate 15.3). The negatively stained control also showed non of these features (plate 15.4).

The stain for glutathione in the liver showed an even distribution throughout the section. The deep blue stain for the thiol could be seen most apparently within the cells of the liver (plate 15.5). Staining in the skin was diffuse and not as clear, although mostly contained to the epidermis, the result was not completely successful. There was no staining of the dermal region of the skin section (plate 16.6).

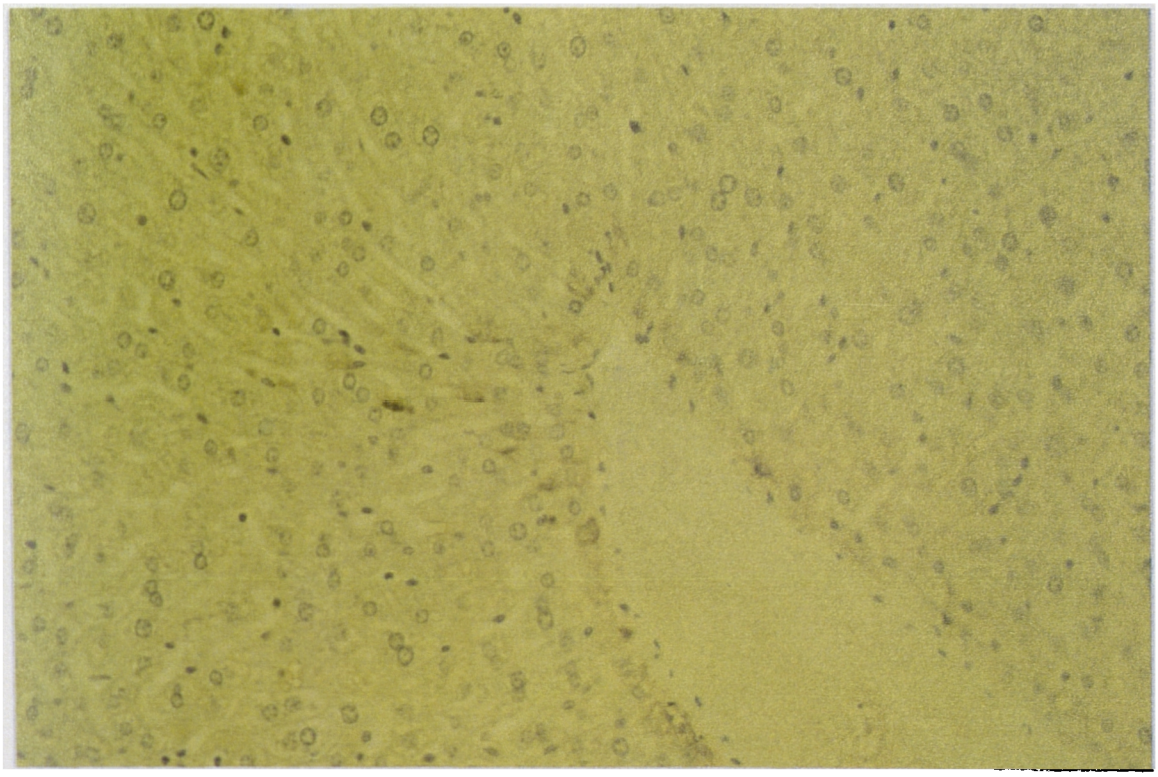

Plate 15.5 Balb/C mouse liver stained for π class glutathione-S-transferase. (x310).

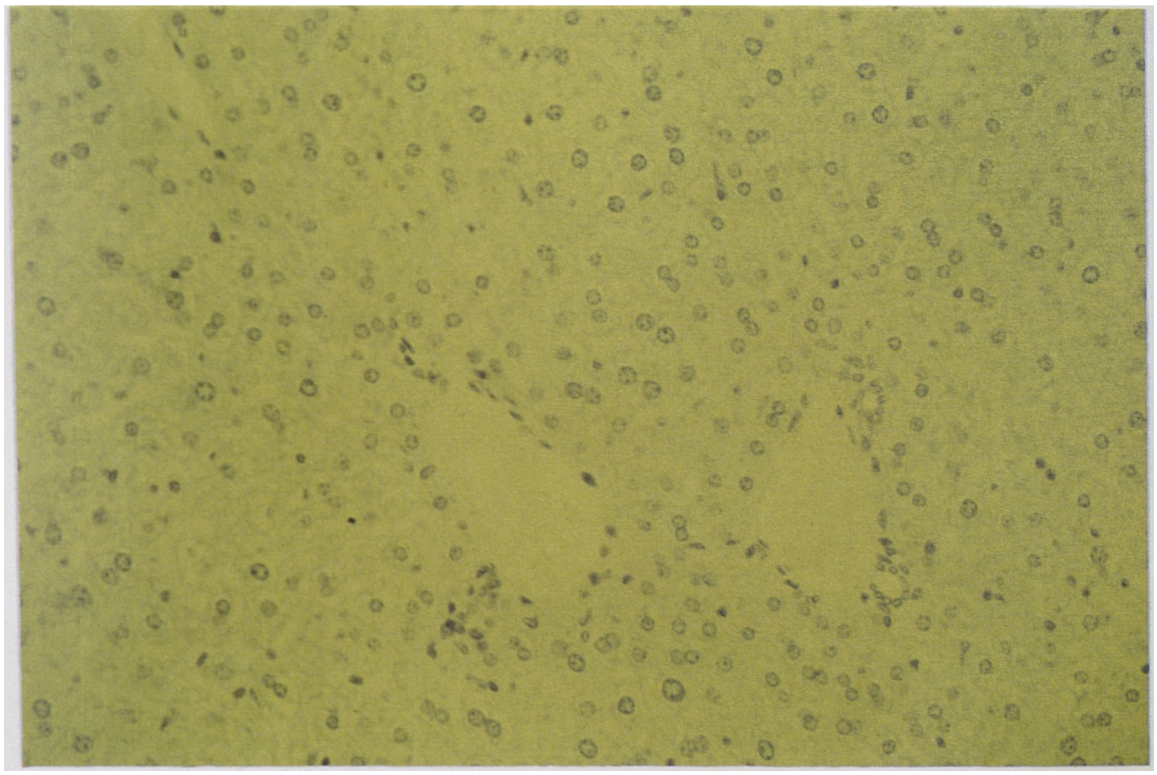

Plate 15.6 Balb/C mouse liver stained for π lass glutathione-S-transferase. (Control, no antigen) (x310).

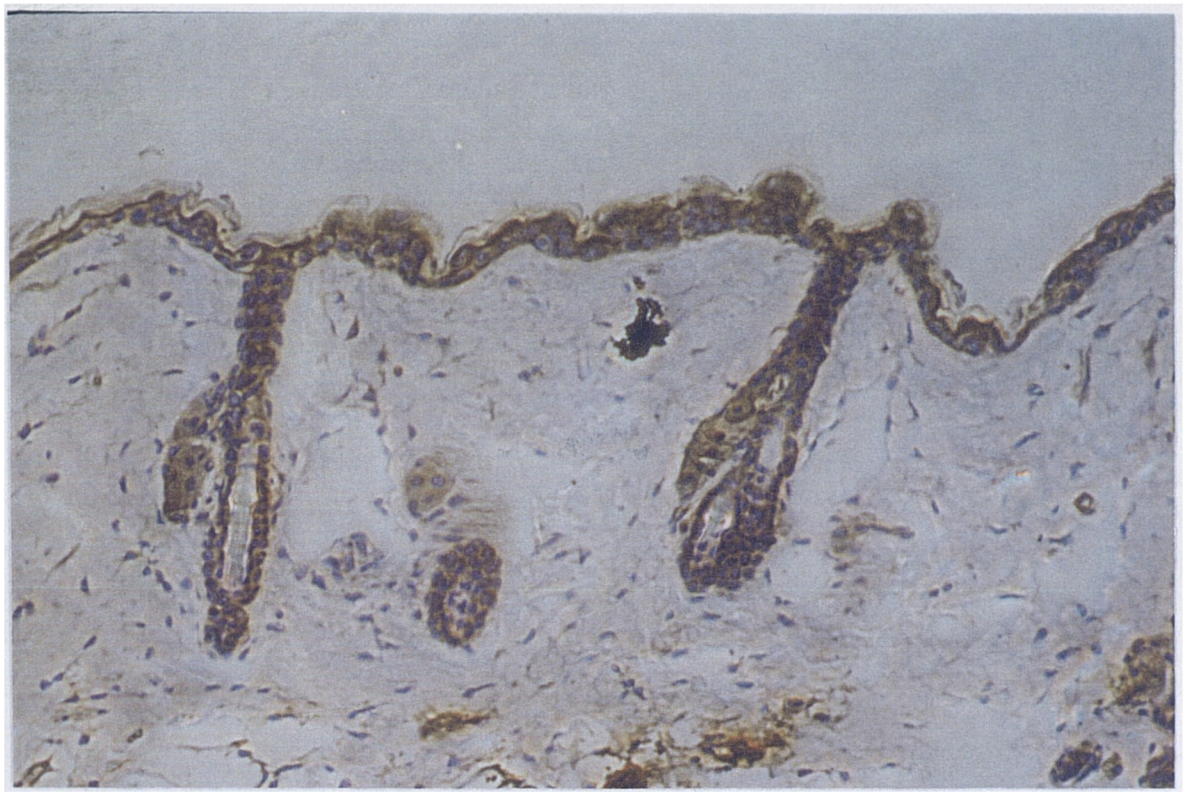

Plate 15.7 Balb/C mouse skin stained for π class glutathione-S-transferase. (x310).

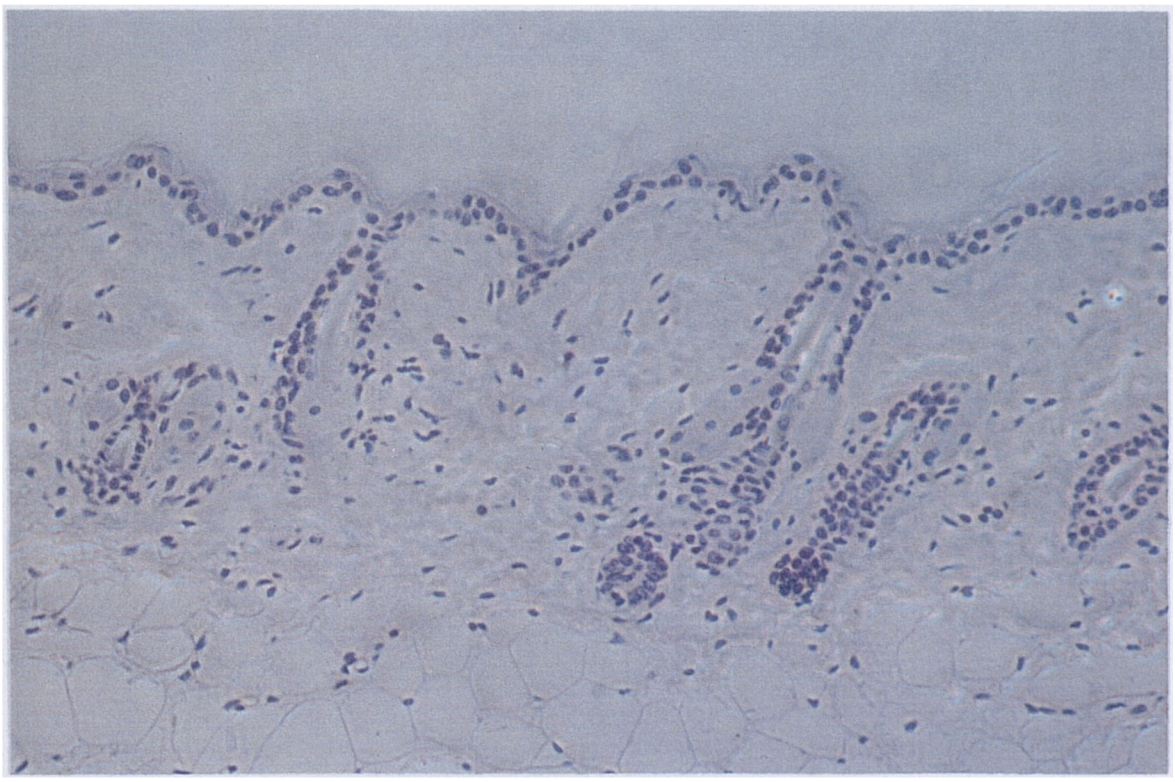

Plate 15.8 Balb/C mouse skin stained for π GST. (Control, no antigen) (x310).

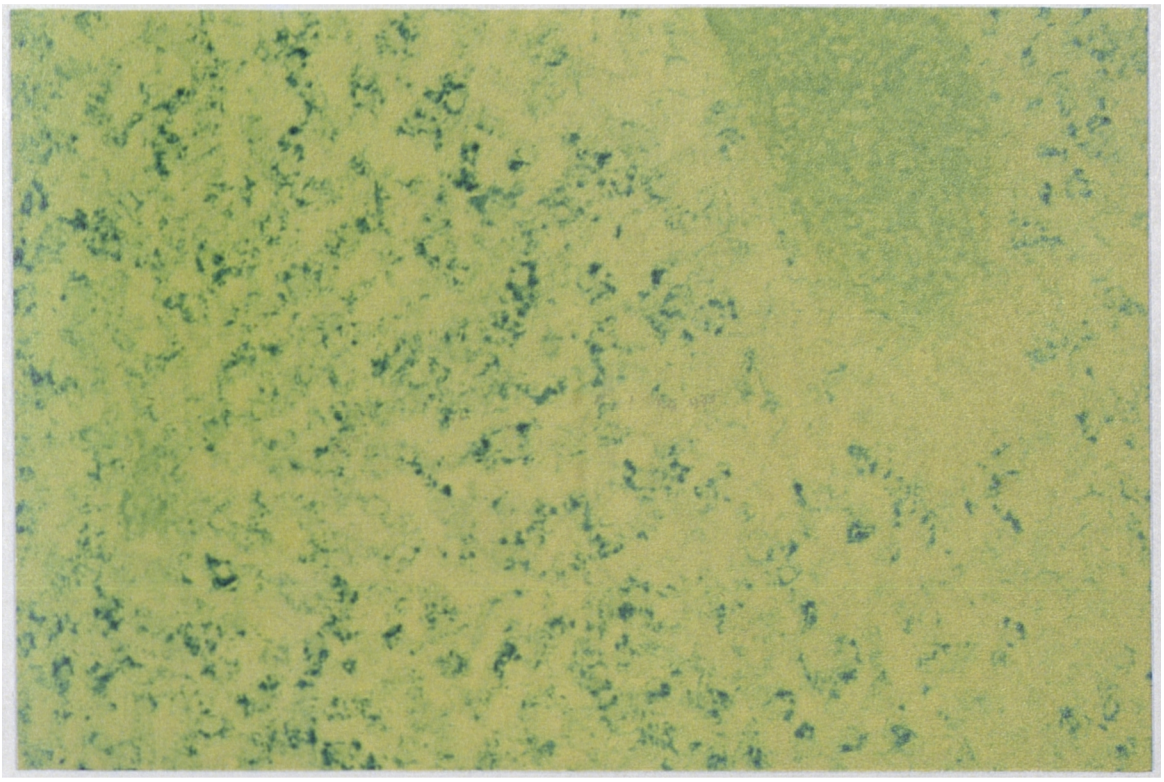

Plate 15.9 Balb/C mouse liver stained for glutathione (x310).

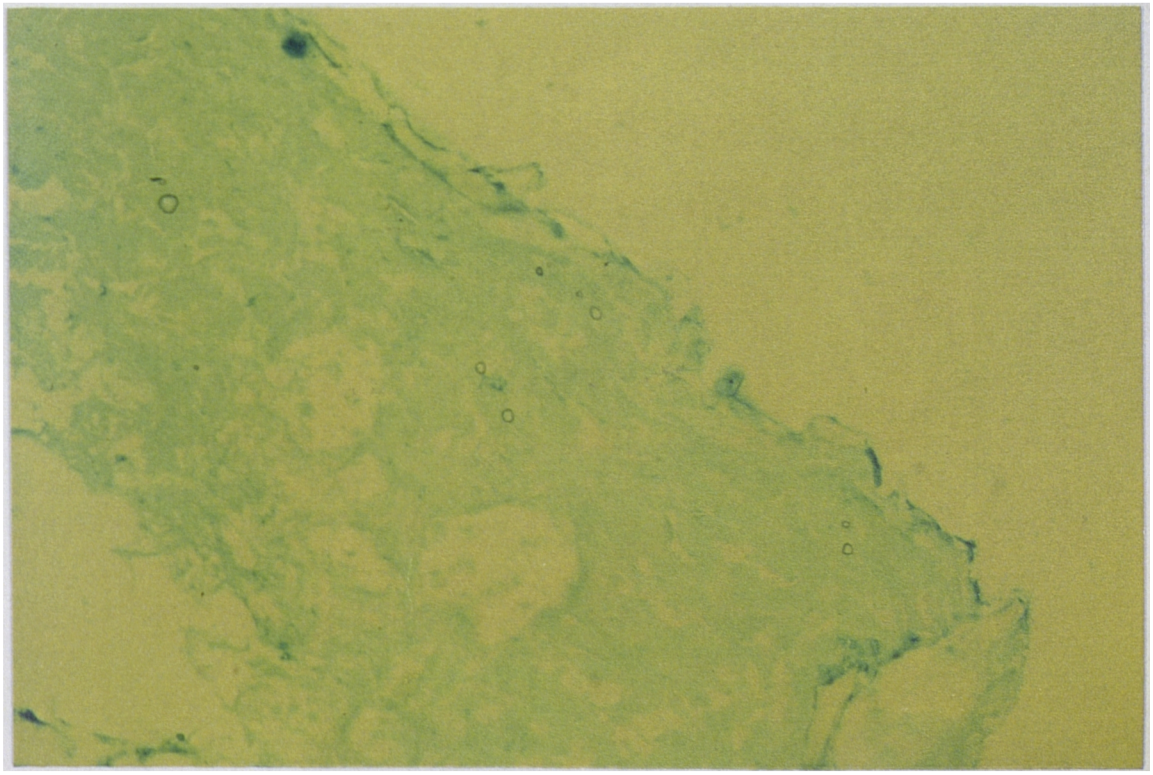

Plate 15.10 Balb/C mouse skin stained for glutathione (x310)..

15.6.3 Discussion

The immunohistochemical study of Balb/C mouse skin revealed localisation of π class GST's consistent with that in the literature, i.e., in the basal layer of the skin and also in areas around the hair follicles and sebaceous glands (Raza *et al*, 1991). It was shown that GST's are present in the skin at the most active site of cell proliferation and differentiation. Rodent skin contains primarily π GST although it is known that some μ isoform is also present. Human skin primarily contains the π isoform with a minor amount of α isoform (Raza and Mukhtar, 1993).

There was very heavy glutathione staining in the epidermal region of the skin section, probably due to over exposure to the histochemical stain, thus, local detail was lost. Nevertheless, the dermal region of the skin was not effected by the stain, therefore glutathione is localised to the epidermal region.

Histology revealed that GST's and to some extent, GSH are located in a one cell thick layer of the skin, the basal layer of the epidermis. Therefore, metabolism of xenobiotics in skin to the glutathione conjugate is localised to this region. During percutaneous absorption, xenobiotics will cross this layer and the amount that can be metabolised will obviously be limited. The capacity of this one layer to metabolise percutaneously absorbed material will be examined in the next chapter.

Chapter 16

In vitro percutaneous absorption and metabolism of dinitrochlorobenzene

In vitro percutaneous absorption and metabolism of dinitrochlorobenzene

16.1 Introduction

The experimental studies discussed in this chapter deal with the *in vitro* percutaneous absorption and metabolism of dinitrochlorobenzene (DNCB). This was investigated with freshly excised skin from mouse, rat, pig and human. The mouse was the first species of interest as it had been previously used in studies investigating the immunological effects of DNCB (Cumberbatch *et al*, 1992b; Kimber *et al*, 1994). Wistar rats were chosen as the second species of interest, as many investigators use rat skin for percutaneous absorption studies. Rat skin at two different ages was assessed, neonatal rat (4 days old) and 26 day old rat. Neonatal rat skin was investigated as it had previously been used in earlier metabolism studies in this thesis. It has little hair, therefore requiring no clipping of the fur and reducing any trauma to the skin. At 26 days old, the roots of the hair in rat skin are at their shortest length relative to the thickness of the epidermis (Dick and Scott, 1990), therefore percutaneous absorption through the hair shaft is minimised. The use of skin from pig ears for absorption studies has attracted interest due to its similarity to human skin and it is ethically acceptable (Dick and Scott, 1992). Lastly, human skin was used for absorption studies. Due to the scarce supply of fresh human skin, only two large samples of abdomen skin were available for this study. One was used to study absorption under unoccluded conditions and the other under occluded conditions. The overall aims were to measure the degree of metabolism of DNCB during percutaneous absorption *in vitro*, to determine the effect of occlusion on absorption and metabolism, and to evaluate species differences.

Two systems were available for studying the percutaneous absorption and metabolism of DNCB through mouse skin *in vitro*. These were the flow-through cell diffusion system and the static cell diffusion system as previously described in chapter 15. As part of a collaborative project with Zeneca Central Toxicology Laboratory (CTL), studies investigating the percutaneous absorption and metabolism of DNCB through Balb/C mouse skin were undertaken at CTL. Both systems have been used at Zeneca Central Toxicology Laboratory and at the University of Newcastle Upon Tyne in the Department of Environmental and Occupational Medicine. Viability studies in the previous chapter have already shown that the flow-through diffusion cell maintains greater viability of skin than the static diffusion cell.

Previous studies at Zeneca Central Toxicology Laboratory, investigating the immunological effects of DNCB with Balb/C mouse have used dermally applied DNCB dissolved in two different vehicles, acetone and propylene glycol (PG) (Heylings *et al*, 1996). Similar formulations were used in these studies. The dose of DNCB applied to the surface of the skin was similar to those applied to the mouse ear in immunological studies (Cumberbatch *et al*, 1992b). At a concentration of 0.5% DNCB in acetone (125μg/cm^2 in a volume of 25μl vehicle), an immunological response was initiated and

detected by the draining lymph node assay (Kimber, 1994). This was therefore the chosen dose to apply to the skin in the absorption studies. Additionally, a lower dose (25μg/cm^2) and a higher dose (500μg/cm^2) were applied to determine the degree of metabolism at different varying doses.

16.2 Separation of DNCB and glutathione conjugate

A method was developed to analyse the diffusion cell receptor medium for DNCB and the glutathione conjugate. The glutathione conjugate is the only metabolite of DNCB referred to in the literature, but it was necessary to examine the receptor medium for the presence of any further metabolites that may have been formed during the percutaneous absorption of DNCB. Due to the small amount of DNCB being used in this study, radiolabelled material was used for greater analytical sensitivity

16.2.1 Method

To assess the receptor medium for DNCB and it's metabolite(s) DNCB (125μg in 25μl acetone) was applied to Balb C mouse skin in the static diffusion cell (12 cells run in parallel). The [^{14}C] DNCB was undiluted radiolabelled compound with a specific activity of 125MBq/mg. The static cells were filled with RPMI1640 medium (containing gentamycin, 20μg/ml) and the study run for 4 hours. Samples of medium were taken and spotted on to TLC plates (25μl). DNCB (0.5%,5μg ml) was spotted (20μl, 0.1μg) and used as a standard. A solution of DNCB (4μg/ml), glutathione (2μg ml) and cytosolic extract from mouse skin (50μg ml) was incubated for 20 minutes and the spotted (25μl) onto the TLC plate. Plates (Whatman reversed phase KC18F) were run with two consecutive solvent systems. Firstly with 1% acetone in chloroform for 50 minutes and secondly with 70% methanol for 30 minutes. DNCB and the glutathione conjugate were visualised under ultraviolet light and glutathione was visualised by spraying the plate with bicinchoninic acid protein reagent (see section 11.1). Plates were then scanned on a Bethroid Automatic TLC-Linear Analyser, gassed with 10% methane in argon.

For separation of DNCB from it's glutathione conjugate from diffusion cell receptor medium samples were collected in glass vials (chosen because DNCB has an affinity for plastic). DNCB was extracted from the medium with iso-hexane (3:10 v v), by shaking vigorously for 2 minutes by hand. The hydrophilic glutathione conjugate remained in the aqueous phase. The separated phases were added to LSC and counted for ^{14}C activity. A standard of DNCB was tested to confirm 100% extraction of the parent compound.

16.2.2 Results

The TLC plate revealed the presence of only one metabolite, (the glutathione conjugate of DNCB), in both the incubation with skin cytosol and receptor medium from the diffusion cells. There was good resolution between DNCB, glutathione and the metabolite. Figure 16.1 illustrates the TLC plate. Analysis of the TLC plates with a linear analyser for radioactivity revealed only two peaks, one for DNCB and the other for the glutathione conjugate, in both the skin cytosol incubation and in the receptor fluid of the diffusion cells

Extractive separation of DNCB and the conjugate for the diffusion cell receptor medium was very efficient. A standard of DNCB (40μg) in RPMI1640 receptor medium (3ml) could be completely extracted into iso-hexane (10ml) (>99% recovery confirmed by TLC).

Figure 16.1 Thin liquid chromatography plate. Track 1, GSH in distilled water. Track 2, DNCB in acetone. Track 3, an incubation of DNCB and GSH in the presence of cytosolic protein from mouse skin. Track 4, diffusion cell receptor medium after application of DNCB to mouse skin *in vitro.*
(□ = GSH, Δ = DNCB, O = glutathione conjugate of DNCB).

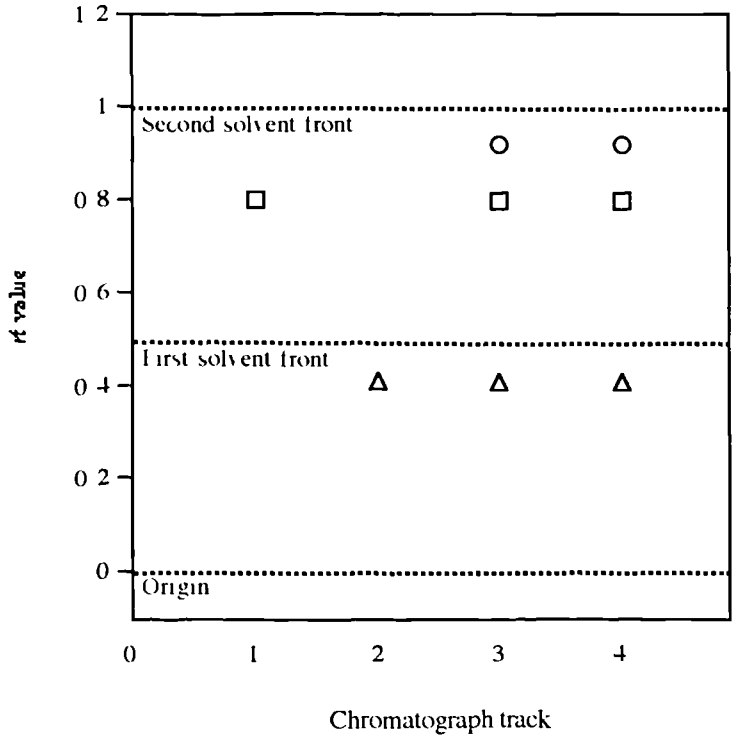

16.2.3 Discussion

Incubation of DNCB with mouse skin cytosolic fraction resulted in the formation of only one metabolite, the DNCB glutathione conjugate. This was confirmed by thin layer chromatography (TLC). Separation of DNCB from the glutathione conjugate was successfully accomplished by

isohexane extraction of the parent compound from the aqueous solution. After percutaneous absorption through Balb/C mouse skin in static diffusion cells for 4 hours, and both DNCB and the metabolite were found in the receptor medium, and could be separated by isohexane extraction. Therefore the extraction method for DNCB separation was used in further studies to investigate percutaneous absorption and metabolism of DNCB through skin *in vitro*.

16.3 Percutaneous absorption and metabolism of DNCB through mouse skin in vitro

16.3.1 Method

The following method was used to investigate the *in vitro* percutaneous absorption and metabolism of DNCB through Balb/C mouse skin *in vitro*. Balb/C mice were all female 7-9 weeks old from Harlan Olac Limited, Shaws farm, Blackworth, Bicester, Oxon. Freshly excised Balb/C mouse skin from twelve animals was mounted full thickness onto twelve flow-through and twelve static diffusion cells as described in chapter 15. The static diffusion cells were filled with RPMI1640 tissue culture medium as described in section 15.2.4. Flow-through cells were connected to peristaltic pump tubing and medium flushed through the system as described in section 15.2.2. Diffusion cells were maintained at 32 C. [^{14}C]-DNCB with a specific activity of 417kBq/mg was dissolved in either acetone or propylene glycol at concentrations of 1mg/ml, 5mg/ml and 20mg/ml and was applied to the surface of the skin at doses of 25, 125 and 500μg/cm^2 in either acetone or propylene glycol vehicle (25μl cm^2). Six cells of each diffusion system were used for DNCB in acetone and six for DNCB in propylene glycol. A thin filter of activated carbon cut into a small disc was placed on top of the donor chamber to capture any evaporated material. Activated carbon filters were cut from cooker hood filters obtained from Galley Matrix. At timed intervals over 24 hours, samples of the receptor medium were collected. DNCB was extracted from the receptor medium using isohexane (3:10 v/v) as previously described, the conjugated DNCB remained in the aqueous phase. The separated isohexane and aqueous phases were then added to liquid scintillation cocktail (LSC) and counted for ^{14}C activity. At the end of the study, the cells were removed and the skin was washed while still in the diffusion cell. Washing consisted of 10x5ml aliquots of 3% Teepol solution (the required volume to remove the surface compound). A sample of this wash (4ml) was added to liquid scintillation cocktail (LSC) for counting. The skin was then removed from the diffusion cell and tape stripped with 6 consecutive strips of "Scotch magic" tape to remove the outer stratum corneum. Tape strips were placed into LSC counting vials with 2ml of Biolute-S, a tissue solubiliser and allowed to dissolve before adding liquid scintillant. The diffusion chamber donor was washed with 5ml of iso-hexane and the washings were added to LSC. Each sample of skin was placed in glass vials with 5ml of distilled water and gently agitated for 24 hours to extract the hydrophilic conjugate. Skin was then placed in 10ml of iso-hexane for 24 hours and gently agitated to extract DNCB. Aqueous and iso-hexane phases were each added to LSC. The skin was finally added to 3ml of Biolute-S and the tissue solubilised, this was facilitated by placing in an oven at 50 $^{\circ}$C. The solubilised tissue was then added

to LSC. Carbon filters were added directly to LSC. All samples were counted on a liquid scintillation counter.

16.3.2 Results

Tables 16.2, 16.3 and 16.4 give the disposition of DNCB not absorbed into the receptor medium at 24 hours after application of 25μg/cm^2, 125μg/cm^2 and 500μg/cm^2 respectively in flow-through and static diffusion cells. Graphs 16.1, 16.2 and 16.3 illustrate the rate of appearance of DNCB and glutathione conjugated DNCB in the receptor medium over 24 hours.

DNCB was well absorbed through intact mouse skin *in vitro* and the degree of absorption was dependent upon the applied dose, vehicle and diffusion cell system used. A maximum of 75% was absorbed with an applied dose of 25μg cm^2 in acetone in the static diffusion cell. At 24 hours, skin integrity in the static diffusion cells appeared to be deteriorating. On removal of the skin from the static diffusion cells, the epidermis easily separated from the dermis. Skin from the flow-through diffusion cells however was still firmly intact. Tissue culture medium of the static diffusion cells became more acidic over the 24 hours, whereas in the flow-through diffusion cells it was continually replenished with fresh medium and pH was maintained at 7.4.

Table 16.1 illustrates the percentage of the applied dose that evaporated for each cell type and vehicle. Evaporation was greater from the acetone vehicle than the PG vehicle at all doses studied ($p<0.01$).

Table 16.1 Percentage of evaporative loss of DNCB from Balb C mouse skin from static diffusion cells and flow through (FT) diffusion cells when dissolved in acetone and propylene glycol vehicles after application at 25μg cm^2, 125μg cm^2 and 500μg cm^2. (mean±sem,n=6).

	% applied dose evaporated	
Applied dose and vehicle	Static cell	FT cell
25μg cm^2 in acetone	12.80±1.76	25.61±2.33
25μg cm^2 in PG	4.63±1.05	12.56±1.23
125μg cm^2 in acetone	10.56±1.56	32.40±2.46
125μg cm^2 in PG	4.87±0.68	10.15±1.40
500μg cm^2 in acetone	6.67±1.10	19.88±2.73
500μg cm^2 in PG	3.58±1.10	8.20±1.62

A surface wash of the skin removed the unabsorbed DNCB which had not been lost by evaporation. Increasing amounts could be removed with increase in application dose. More could be washed from the skin that had been applied in the PG vehicle than the acetone vehicle indicating a slower penetration of DNCB with this vehicle. Washings from the donor cell holding the skin in place showed that material was present underneath the seal, showing that DNCB has diffused laterally across the skin.

Tape strippings from the skin (6 consecutive strippings with "scotch magic" tape) removed the outer layers of the stratum corneum. These were assayed to determine the presence of DNCB which may have been bound to the outer layers of the epidermis. The results showed that no detectable levels of DNCB was found in the stratum corneum in either the static or flow-through diffusion cells or with either the acetone or PG vehicle.

An aqueous extraction of skin dosed with 25μg cm^2 showed no detectable conjugated DNCB. At applied doses of 125 and 500μg cm^2 the aqueous extract did contain some small amounts of conjugated DNCB. The isohexane extract from all three applied doses also led to the recovery of DNCB, which increased with increasing concentration of applied dose. At 500μg/cm^2, high amounts were present in the skin (20-25% of applied dose). Generally, similar level of DNCB and conjugated DNCB were found in skin from the static diffusion cells and the flow-through cells. Further amounts of material was detected in the solubilised tissue, which also increased with increasing the applied dose. It was also shown that statistically higher levels of DNCB applied to skin in the PG vehicle remained in the skin than when DNCB was applied in the acetone vehicle ($p<0.01$). Additionally, at 25μg cm^2 and 125μg cm^2 greater amounts of DNCB remained in the skin in the static diffusion cells than in the flow-through cells ($p<0.01$). At 500μg cm^2, levels were similar, suggesting a level of saturation had been reached.

Both DNCB and conjugated DNCB were found in the receptor medium from both the flow-through diffusion cells and the static diffusion cells of all applied doses. At 25μg/cm^2, using both types of diffusion cells, a majority of the absorbed material found in the receptor medium was conjugated DNCB. With increasing dose, the amount of DNCB absorbed into the receptor medium increased, but the amount of conjugated DNCB in the receptor medium did not. At applied doses of 25μg cm^2 and 125μg cm^2 in acetone, the appearance of DNCB in the receptor medium was faster than the appearance from equally applied doses in the PG vehicle. At 500μg cm^2 the rate of appearance was similar for both vehicles used. Maximum conjugation of the applied dose, which appeared in the receptor fluid, occurred at 4 hours for the acetone vehicle and at 6 hours for the PG vehicle, illustrating a vehicle effect on the rate of penetration. There was no significant difference in the amount of DNCB metabolised to the glutathione conjugate between static and flow-through diffusion cells ($p>0.05$). However, there was a difference between the amount of DNCB absorbed between diffusion cell types, with more of the applied dose being absorbed in the static cell than the flow-through cell at 24 hours ($p<0.01$). Table 16.5 summarises the amount of DNCB absorbed and

metabolised during percutaneous absorption through mouse skin *in vitro* using acetone and propylene glycol vehicles at 24 hours in both static diffusion cells and flow-through diffusion cells. It was also shown that the total amount of absorbed dose in the static cell was greater than with the flow-through cell.

Table 16.5 Amount of DNCB absorbed and metabolised ($\mu g/cm^2$) through mouse skin *in vitro* using acetone (Ac) and propylene glycol (PG) vehicles at 24 hours in both static diffusion cells and flow-through (FT) diffusion cells.(mean±SEM,n=6)

		Amount absorbed at 24 h ($\mu g/cm^2$)					
		25$\mu g/cm^2$ DNCB		125$\mu g/cm^2$ DNCB		500$\mu g/cm^2$ DNCB	
		Ac	PG	Ac	PG	Ac	PG
DNCB	Static cell	7.7±0.4	4.1±0.1	52.6±4.6	26.2±2.5	107.0±15.8	121.8±16.7
DNCB	FT cell	6.2±0.5	4.0±0.3	21.2±1.2	14.0±1.2	32.6±5.6	43.2±4.2
Conjugated	Static cell	11.0±0.6	10.4±0.7	19.0±1.7	19.1±2.5	19.5±2.3	14.6±2.9
Conjugated	FT cell	12.1±0.3	12.3±0.6	25.2±2.7	19.3±2.6	20.1±3.1	15.9±2.9
% Absorbed Static cell		74.8±4.0	58.0±3.2	57.3±5.0	36.2±4.0	25.3±3.6	27.5±3.9
% Absorbed FT cell		73.2±3.2	65.2±3.6	37.1±3.1	26.6±3.0	10.5±1.7	11.8±1.4

Table 16.2 Disposition of DNCB not absorbed into the receptor medium by 24 hours after application of 25μg/cm^2 DNCB in acetone or propylene glycol (PG) to Balb/C mouse skin in the flow-through diffusion cell or static diffusion cell. (mean±sem, n=6 diffusion cells with skin from 6 different animals.

	Flow-through diffusion cells		Static diffusion cells	
Disposition of DNCB not found in the receptor medium	μg/cm^2±sem in acetone	μg/cm^2±sem in PG	μg/cm^2±sem in acetone	μg/cm^2±sem in PG
Evaporated	6.403±0.553	3.140±0.139	3.201±0.317	1.158±0.112
Skin wash	2.130±0.171	3.830±0.549	2.513±0.933	3.965±0.422
Cell donor	0.497±0.144	0.385±0.034	0.190±0.021	0.516±0.133
Tape stripping	0.000±0.000	0.000±0.000	0.000±0.000	0.000±0.000
Skin-aqueous extraction	0.000±0.000	0.000±0.000	0.000±0.000	0.000±0.000
Skin-hexane extraction	0.373±0.125	1.207±0.211	1.858±0.363	1.737±0.264
Skin solubilised	1.691±0.223	3.870±0.683	3.512±0.206	8.210±0.732

Graph 16.1 Absorbed DNCB (squares) and metabolised DNCB (circles) found in the receptor medium over time after application of 25μg cm^2 DNCB in acetone (open symbol) and 25μg/cm^2 DNCB in propylene glycol (closed symbol) to Balb C mouse skin in the flow-through diffusion cell or static diffusion cell (Raw data can be found in appendices 1,2 4 and 5). (mean±sem, n=6).

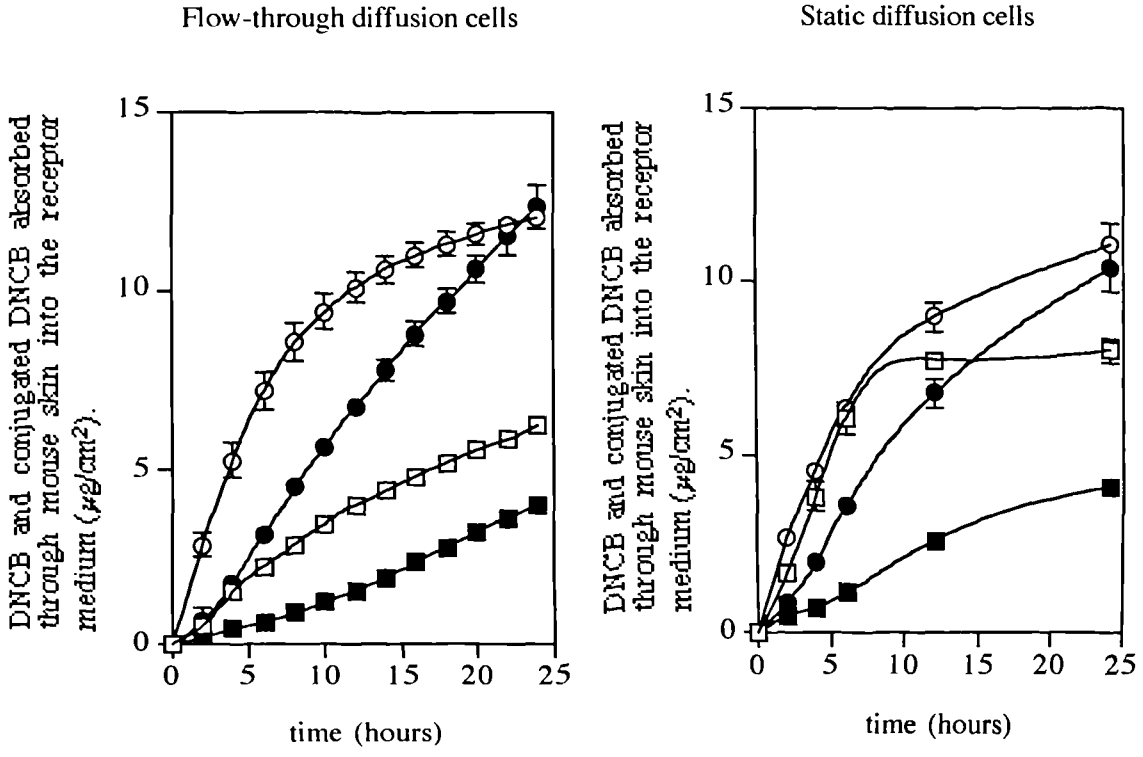

Table 16.3 Disposition of DNCB not absorbed into the receptor medium by 24 hours after application of 125μg/cm^2 DNCB in acetone or propylene glycol (PG) to Balb/C mouse skin in the flow-through diffusion cell or static diffusion cell. (mean±sem, n=6 diffusion cells with skin from 6 different animals.

	Flow-through diffusion cells		Static diffusion cells	
Disposition of DNCB not found in the receptor medium	μg/cm^2±sem in acetone	μg cm^2±sem in PG	μg/cm^2±sem in acetone	μg/cm^2±sem in PG
Evaporated	40.498±3.092	12.688±0.994	13.962±0.970	6.085±0.236
Skin wash	5.125±1.384	7.020±0.656	8.962±0.970	13.793±0.236
Cell donor	0.890±0.359	0.923±0.301	0.573±0.108	1.982±0.368
Tape stripping	0.000±0.000	0.000±0.000	0.000±0.000	0.000±0.000
Skin-aqueous extraction	0.267±0.069	0.368±0.096	1.671±0.295	1.710±0.265
Skin-hexane extraction	4.371±1.018	6.433±1.661	25.770±2.844	24.005±3.005
Skin-solubilised	16.907±2.876	47.393±8.392	38.571±7.099	61.658±17.31

Graph 16.2 Absorbed DNCB (squares) and metabolised DNCB (circles) found in the receptor medium over time after application of 125μg cm^2 DNCB in acetone (open symbol) and 125μg/cm^2 DNCB in propylene glycol (closed symbol) to Balb C mouse skin in the flow-through diffusion cell or static diffusion cell (Raw data can be found in appendices 6,7,11 and 12). (mean±sem, n=6).

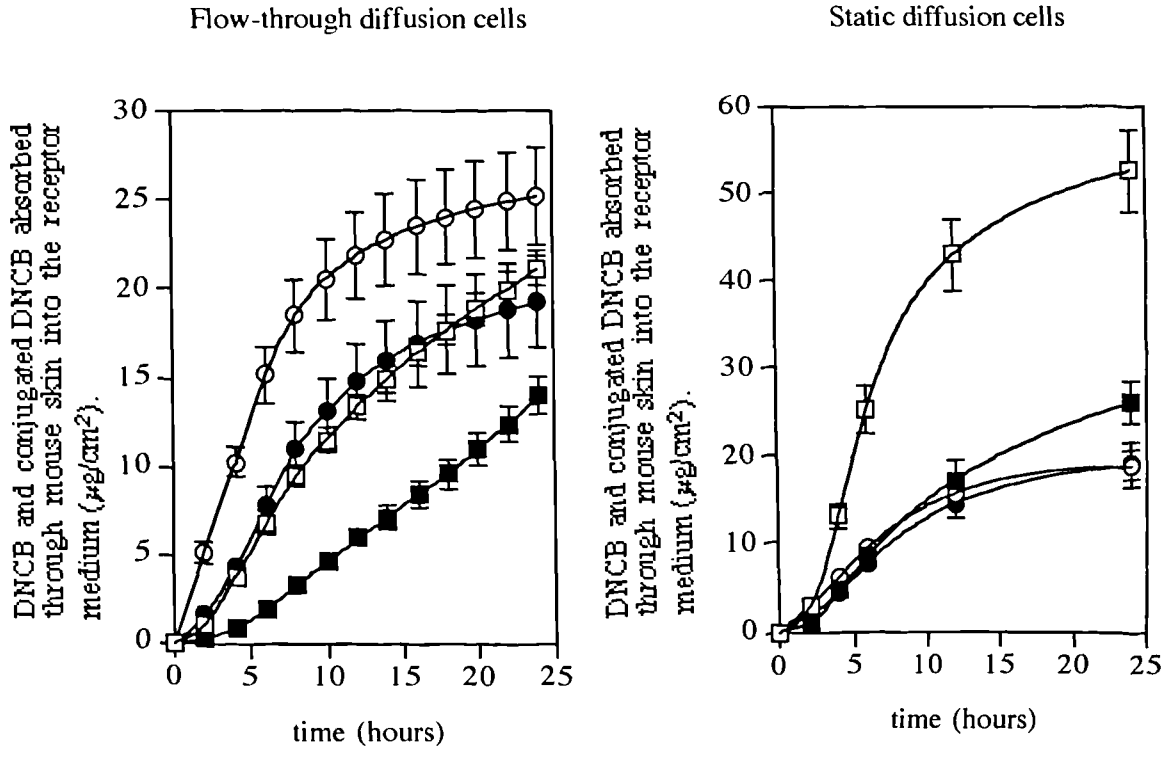

Table 16.4 Disposition of DNCB not absorbed into the receptor medium by 24 hours after application of 500μg/cm^2 DNCB in acetone or propylene glycol (PG) to Balb/C mouse skin in the flow-through diffusion cell or static diffusion cell. (mean±sem, n=6 diffusion cells with skin from 6 different animals.

	Flow-through diffusion cells		Static diffusion cells	
Disposition of DNCB not found in the receptor medium	μg/cm^2±sem in acetone	μg/cm^2±sem in PG	μg/cm^2±sem in acetone	μg/cm^2±sem in PG
Evaporated	99.154±16.71	19.923±2.480	28.337±2.463	17.932±2.480
Skin wash	28.154±2.235	54.030±4.503	60.965±13.89	83.126±4.932
Cell donor	11.090±3.546	3.622±1.060	1.925±0.527	3.622±1.060
Tape stripping	0.000±0.000	0.000±0.000	0.000±0.000	0.000±0.000
Skin aqueous extraction	2.722±0.266	4.412±0.401	4.965±0.354	4.427±0.392
Skin hexane extraction	175.69±17.63	161.63±14.78	164.35±4.843	161.63±14.78
Skin-solubilised	77.280±11.92	101.21±21.09	103.35±4.843	101.21±21.09

Graph 16.3 Absorbed DNCB (squares) and metabolised DNCB (circles) found in the receptor medium over time after application of 500μg cm^2 DNCB in acetone (open symbol) and 500μg/cm^2 DNCB in propylene glycol (closed symbol) to Balb C mouse skin in the flow-through diffusion cell or static diffusion cell (Raw data can be found in appendices 15,16,17 and 18). (mean±sem, n=6).

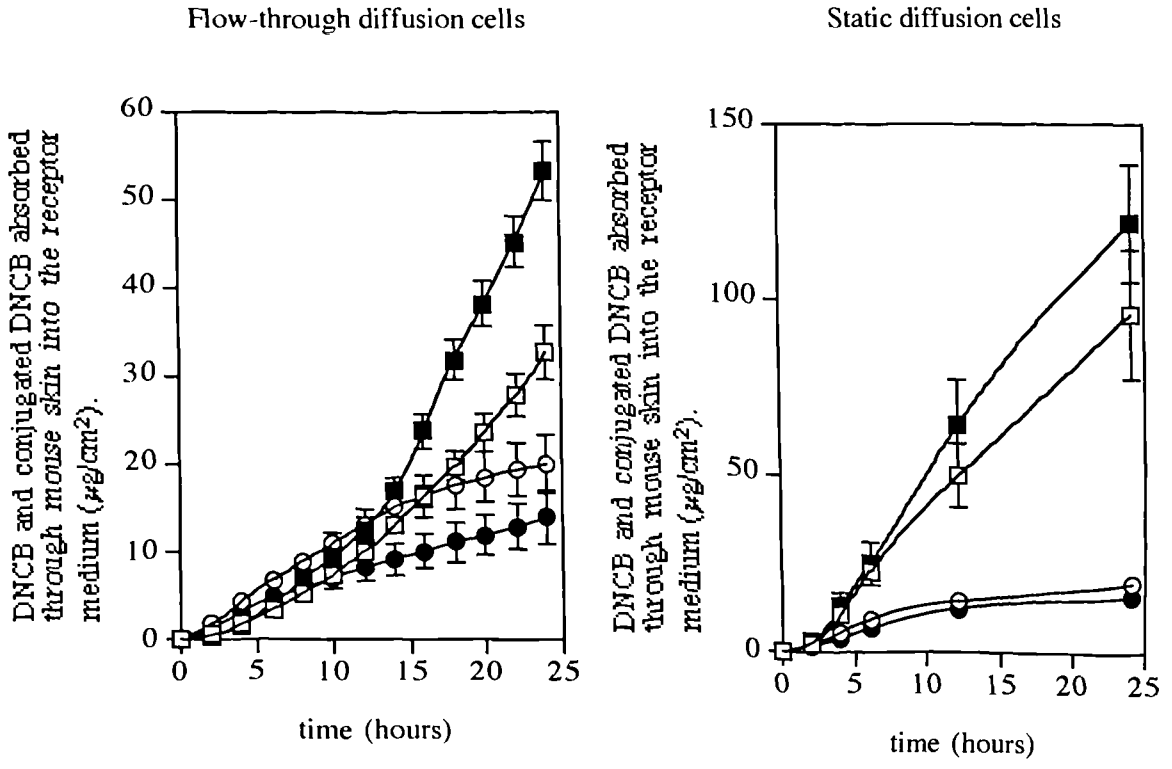

16.3.3 Discussion

Evaporation of DNCB from the skin surface was found to be greater with the acetone vehicle than the PG vehicle. Evaporation of the vehicle could be expected as acetone is the more volatile solvent, and due to the vapour pressure of a very small volume of solvent ($25\mu l/cm^2$) exposed to a very large volume of air. However, the degree of evaporation (approximately 20%) of DNCB from the surface of the skin was unexpected. It was not considered to be a volatile compound, having a boiling point of 315 C. Evaporation was greater from the flow-through cell, possibly due to the differences in donor chamber design, between the two diffusion cell types. The static cell donor chamber has a diameter of 1cm and a depth of 1.2cm, whereas the flow-through cell donor chamber has a diameter of 0.9cm and is flanged to a diameter of 1.6cm in a depth of 0.6cm giving greater airflow above the skin. The effect of material evaporating from the skin may have also influenced the amount of compound penetrating the skin. It must be noted however, that the evaporation of compounds applied to the skin has largely been ignored by other investigators of percutaneous penetration, and the relevance of this is very important to mass balance studies. In these studies, recovery of the applied dose of DNCB was greater than 95%and this would have been very much lower if evaporated material had been ignored. Not only is capturing evaporated material important for the accountability of the applied dose, but is also important for the safety of the investigator. Applied material, especially radiolabelled compounds, could evaporate into the atmosphere of the laboratory and be inhaled.

Material that had not evaporated from the skin, washed from the surface of the skin or was absorbed into the receptor medium had remained within the skin. DNCB was not found in the stratum corneum by tape stripping, but a small amount of DNCB and conjugated DNCB could be extracted from the remaining tissue. After tissue solubilisation, further levels of radioactivity were found to be remaining in the skin. Whether the material in the skin was in the form of DNCB or conjugated DNCB is not known, but was most likely to have been bound to the skin proteins. Protein binding of DNCB has been previously investigated by Schmidt and Read, (1996) and implicated in the role of skin sensitisation.

It was found that at 24 hours the integrity of skin in the static diffusion cells was deteriorating. The epidermis easily separated from the dermis of this skin. Integrity of epidermis of skin from the flow-through remained intact. This may have been a factor caused by the culture medium in the static diffusion cell becoming acidic. DNCB was absorbed through mouse skin to a greater degree in the static diffusion cell system, a factor which may be attributed to a greater loss of tissue integrity as compared to the flow-through system. The flow-through cell was developed for maintaining viability of skin *in vitro*, which does not occur for any great length of time in the static cell. Therefore further studies investigating absorption and metabolism of DNCB through the skin of other species were conducted in the flow-through diffusion cells only.

From these studies it was shown that regardless of which vehicle or diffusion cell system used, the proportion of conjugated DNCB absorbed into the receptor medium was similar. At 25$\mu g/cm^2$, approximately half the applied dose was recovered as conjugate. At 125$\mu g/cm^2$ and 500$\mu g/cm^2$ the amount of DNCB conjugated was around 20$\mu g/cm^2$, suggesting that a limit to the amount of DNCB that could be conjugated had been reached. The rate of absorption, from either acetone of PG vehicles, did not effect the degree of metabolism. Therefore the slower rate of absorption with the PG vehicle did not allow more DNCB to be conjugated as it passed through the metabolically active layer of the skin.

It is therefore shown that levels of glutathione in the skin become saturated and are limiting the glutathione-S-transferase metabolising pathway. Metabolism by cytochrome P450 or esterase pathways is not limited by the need for cofactors, which suggests that the rate of absorption might influence the degree of metabolism via these pathways

16.4 Percutaneous absorption and metabolism of DNCB through mouse skin in the flow-through system under occluded conditions

16.4.1 Method

The method used for investigating the percutaneous absorption and metabolism of DNCB under occluded conditions was similar to that used for unoccluded studies, except that instead of carbon filters above the donor chamber of the diffusion cell, parafilm was used. This study was run with flow-through diffusion cells only, since skin integrity seemed to be compromised in the static diffusion cell. Six female Balb/C mice were sacrificed and the skin clipped of fur and removed. The skin was used to set up 12 flow-through diffusion cells as previously described. DNCB was applied to the surface of the skin in acetone only, and at doses of 25μg/cm^2 for six cells and 125μg/cm^2 for the remaining six cells. Immediately after applying the dose, parafilm was used to cover the donor chamber. Cells were run for 24 hours.

16.4.2 Results

Graph 16.4 illustrates the data for absorption and metabolism of DNCB through mouse skin under unoccluded and occluded conditions.

Graph 16.4 Effect of occlusion on the percutaneous absorption and metabolism of DNCB after application of 25μg cm^2 and 125μg cm^2 to Balb C mouse skin in the flow-through diffusion system. Absorbed DNCB (squares) and metabolised DNCB (circles) found in the receptor medium over time. Unoccluded (open symbol) and occluded (closed symbol). (mean±sem, n=6). Raw data to be found in appendices 3 and 10.

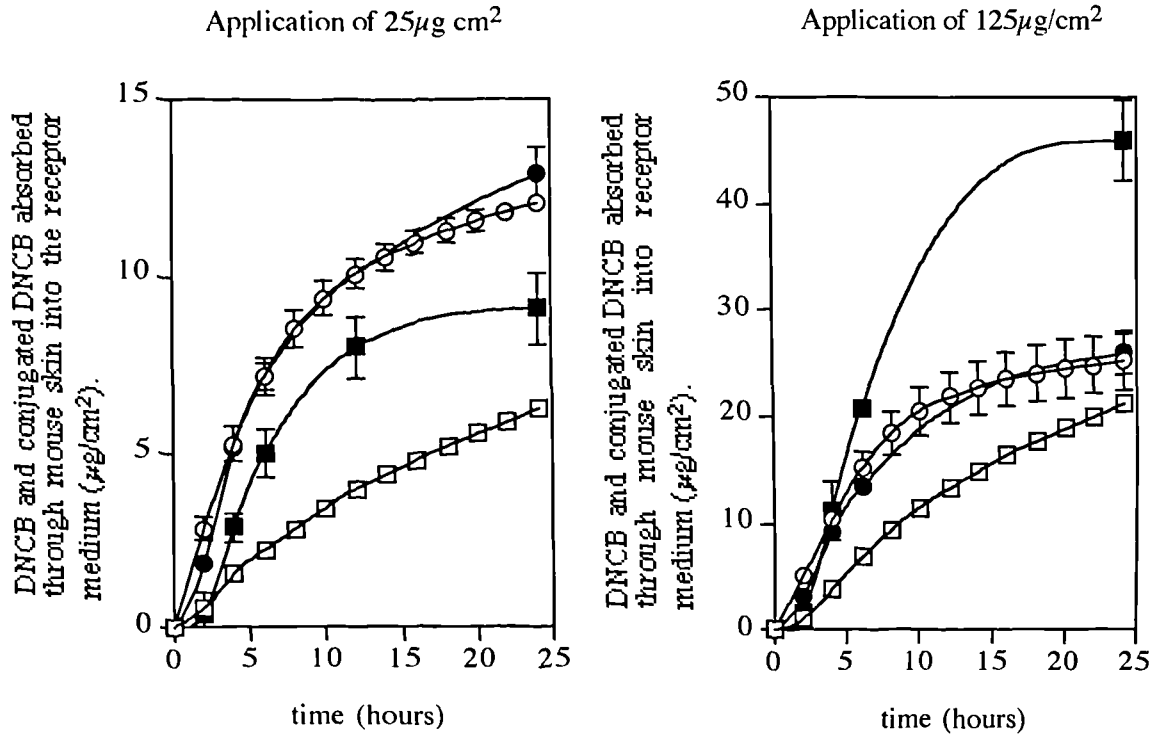

16.4.3 Discussion

Occlusion of diffusion cells resulted in a significantly greater amount of DNCB being absorbed into the receptor medium in 24 hours than when unoccluded ($p<0.01$). The rate at which DNCB was absorbed into the receptor medium was also increased under occlusion. The level of conjugated DNCB found in the receptor medium was however no different under occluded conditions than under unoccluded conditions ($p>0.01$).

Therefore, although occlusion did lead to an increase in the total amount absorbed, it did not lead to an increase in the rate or the level of glutathione conjugation of DNCB during percutaneous absorption through Balb C mouse skin.

16.5 Percutaneous absorption and metabolism of DNCB through the skin of buthionine sulphoximine pretreated mice

To investigate the effect of glutathione depletion on DNCB absorption and metabolism in the skin, the following study was undertaken, whereby mice were depleted of glutathione by BSO administration. Buthionine sulphoximine (BSO) inhibits the synthesis of glutathione (Plummer *et al*, 1981). Balb/C mouse skin was then mounted in diffusion cells and dosed with DNCB dissolved in acetone and propylene glycol at a concentration of 125μg/cm^2.

16.5.1 Method

The following dosing protocol was used to deplete glutathione levels in Balb/C mice. Buthionine sulphoximine was dissolved in saline (80mg/ml) with the aid of 0.1N NaOH (final pH 8.5). Mice (16 animals) were given a single i.p. dose in saline at 1.6g/kg in a dose volume of 20ml/kg. Mice were also given drinking water at 0.2mg/ml ad lib for 24 hours. The control group (8 mice) received saline only. Mice were then sacrificed by cervical dislocation. Skin was removed and mounted in flow-through diffusion cells and static diffusion cells as previously described. DNCB was applied to skin at a dose of 125μg cm^2 in acetone or propylene glycol. Data from control mice were combined with data from the previous experiments using 25μg/cm^2 and 125μg/cm^2 to bring numbers up to 8 for statistical evaluation.

16.5.2 Results

The amount of DNCB and conjugated DNCB in the receptor medium at 24 hours after application of DNCB in acetone was not significantly different ($p>0.01$) between mouse skin from BSO treated mice and through control skin. After application of DNCB in the PG vehicle, the amount of DNCB appearing in the receptor medium from the control skin was significantly lower than the BSO treated mice ($p<0.01$), but the amount of conjugated DNCB appearing in the receptor medium was insignificantly different ($p>0.01$).

In the static diffusion cell, the amount of DNCB in the receptor medium at 24 hours after application in both acetone and PG vehicle was insignificantly different from controls. The amount of conjugated DNCB appearing was however significantly lower by 24 hours ($p<0.01$) but was still similar to controls.

Graph 16.6 Appearance of DNCB (squares) and glutathione conjugated DNCB (circles) through mouse skin in flow-through diffusion cells. Mice pretreated with buthionine sulphoximine (BSO) to deplete glutathione (open symbols) and control mice treated with saline (closed symbols). DNCB applied to skin at a dose of 125μg/cm^2 in acetone and propylene glycol (PG). (mean±sem, n=4 for BSO treated mice, n=8 for control mice). Raw data to be found in appendices 13 and 14.

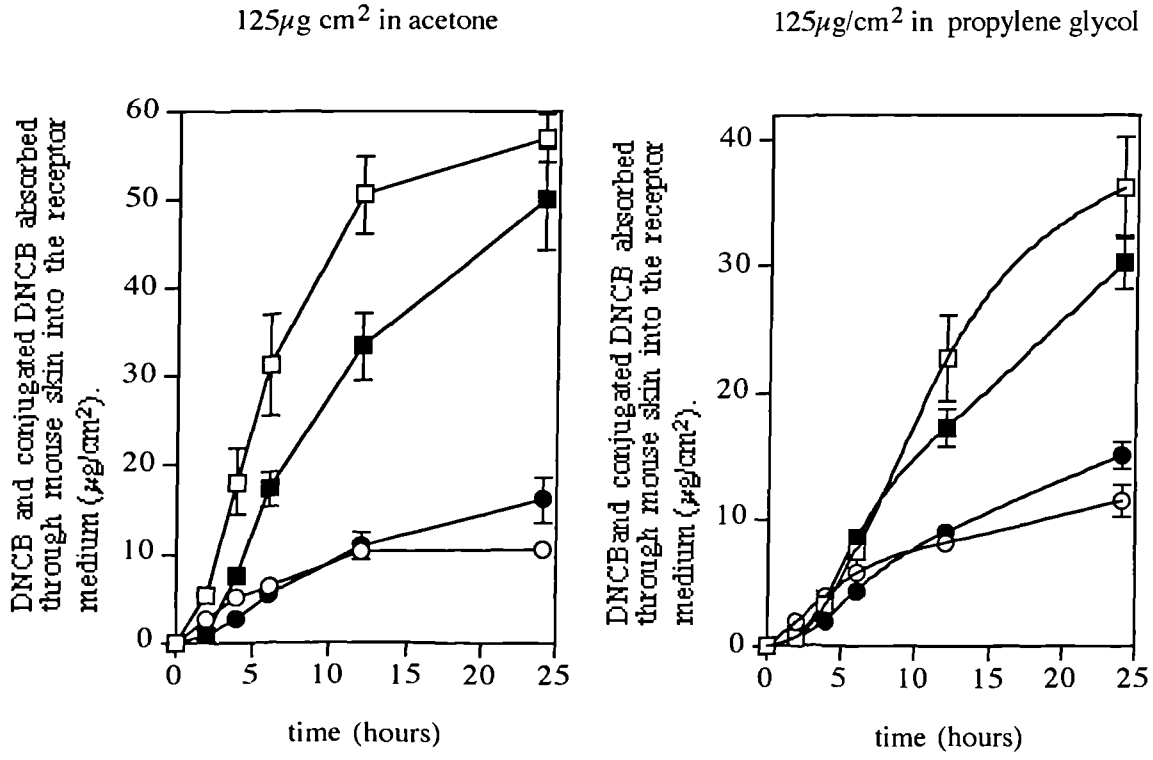

16.5.3 Discussion

The study of the inhibition of the glutathione conjugation of DNCB during absorption through mouse skin, from mice pretreated with the glutathione depleter buthionine sulphoximine was possibly unsuccessful. The degree of metabolism during absorption did not significantly change from control in the flow-through diffusion cell at 24 hours. There was however a difference between control and BSO treated mice in the static cell. Even though in BSO treated mice of DNCB conjugation was lower, the levels for control and BSO treated were still similar and that no marked degree of inhibition of glutathione conjugation was seen.

The reason why inhibition of glutathione conjugation was not accomplished in not clear. It is possible that the regimen employed for BSO pretreatment of the mice, (initially developed for depletion of glutathione in the liver, Plummer *et al*, 1981) did not result in sufficient BSO reaching the skin to deplete the glutathione. Alternatively, glutathione synthesis may have been inhibited, but a pool of glutathione still existed within the skin that maintained its ability for glutathione conjugation. Induction studies *in vivo* did not influence skin metabolism of cytochrome P-450's or esterases, therefore it seems probable that orally and intraperatonial administration of metabolism modulating agents lack access to the skin. What therefore needed to be done was the measurement of glutathione levels in the skin, and to investigate whether topical application of BSO would have depleted glutathione levels.

16.6 Depletion of glutathione in mouse skin in vitro

From the previous studies, it had become clear that glutathione conjugation of DNCB during Percutaneous absorption was limited by the level of glutathione in the skin. The question then asked, was this due to DNCB conjugation utilising all the available glutathione or were the levels of glutathione in skin decreasing due to a decline in skin viability. Therefore levels of glutathione in skin in static diffusion cells following DNCB application were evaluated for glutathione concentration with time and compared to the decrease of glutathione in control skin. The viability of the skin was also assessed to determine any detrimental effects of exposure to acetone or DNCB in acetone. Viability was evaluated by the MTT assay, as previously described in chapter 15.

16.6.1 Method

Balb/C mouse skin from 8 mice was mounted in 16 static diffusion cells as previously described. At timed intervals skin was removed from 4 cells, (2 control and 2 treated with DNCB in acetone) and assayed for glutathione levels. Glutathione was measured by the method described in section 12.7. The experiment was repeated twice to obtain sufficient numbers for statistical evaluation. Additionally, static diffusion cells were mounted with skin and treated three ways. Firstly, the skin was left untreated. Secondly, skin was treated with acetone (25μl) and thirdly, skin was treated with DNCB in acetone (125μg/cm^2). After 6 hours, skins were removed from the static cells and assayed for viability by the MTT assay (see section 15.3.1). Skin was also left on the laboratory bench to act as negative control.

16.6.2 Results

Following application of DNCB in acetone, to skin in the static cells, levels of (GSH) were rapidly depleted and had disappeared by 6 hours. Table 16.5 shows the disappearance of GSH in treated and untreated skin over 12 hours. Graph 16.7 illustrates this data graphically. Glutathione in control skin decreased at a slower rate, with glutathione levels greater than 50%still remaining in the skin after 6 hours.

Table 16.6 Reduced glutathione in mouse skin untreated and treated with 125μg/cm^2 DNCB in acetone in the static cell with RPMI1640 receptor medium. (mean±SEM, n=4) ND=not detectable.

	nmoles GSH/cm^2 skin	
Time (hours)	Untreated	Treated
0	151.2±6.89	-
2	123.05±10.35	18.48±3.26
4	85.76±12.64	5.86±0.87
6	74.80±6.24	ND
12	35.12±5.91	ND

Graph 16.7 Depletion of glutathione levels in control skin (squares) and skin dosed with DNCB (125μg cm^2) in acetone (circles) in the static cell with RPMI receptor medium. (mean±SEM, n=4)

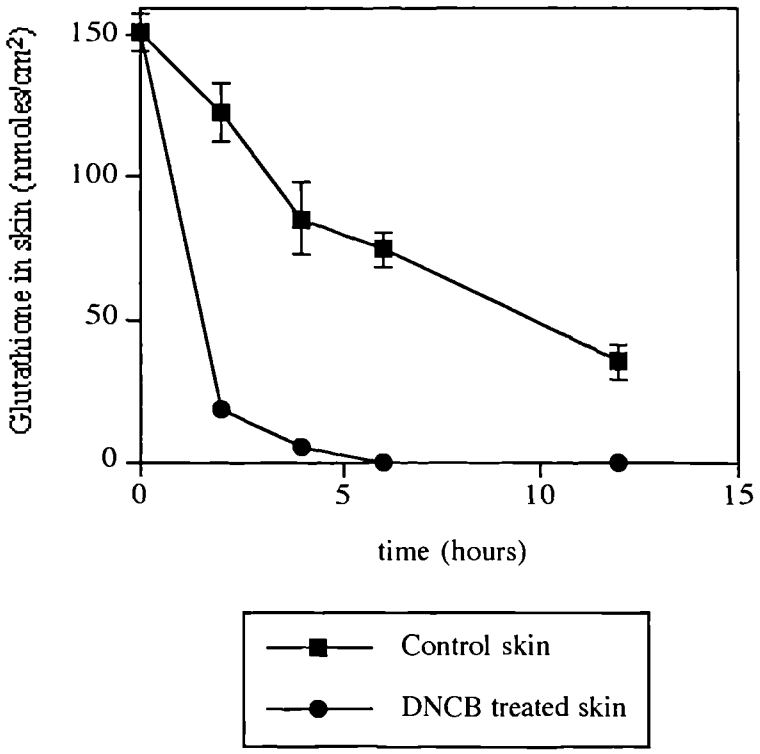

Skin viability in the static cell, as assessed by the MTT assay, showed that skin treated with DNCB in acetone was indistinguishable by 6 hours from controls, (acetone only and untreated skin) ($p>0.01$, evaluated by ANOVA), thus indicating that DNCB in acetone at the applied doses were not detrimental to viability at 6 hours. For a negative control, skin left at room temperature decreased to 30% viability by 6 hours. Table 16.6 shows the percentage viability as compared to fresh skin.

Table 16.7 Viability of skin as assessed by the MTT assay after 6 hours in the static cell, expressed as a percentage of fresh skin. (mean±SEM,n=4)

Skin treatment	% viability of control at 6 h
Untreated	100.00±13.52
acetone treated	99.43±9.20
DNCB treated	98.98±8.18
Skin left on lab bench	31.59±3.07

16.6.3 Discussion

These results indicated that DNCB in acetone did not effect skin viability, and that the rapid depletion of glutathione after application of DNCB was due to its glutathione conjugation.

16.7 Depletion of glutathione in mouse skin by DEM, prior to application of DNCB in vitro

Pretreatment of Balb/C mice with buthionine sulphoximine to deplete glutathione levels was unsuccessful. Therefore an *in vitro* approach was adopted to determine whether glutathione conjugation of DNCB could be prevented by removing the glutathione from the skin before application of DNCB.

16.7.1 Method

Diethyl maleate (DEM), a depleter of reduced glutathione (Plummer *et al*, 1981) was used to remove the glutathione from the skin. Static cells were mounted with Balb/C mouse skin and RPMI1640 medium containing DEM (1mM) was placed in the receptor chamber. Static cells were maintained for 1 hour before application of DNCB in acetone (125μg/cm^2). Samples of receptor medium were taken at timed intervals up to 6 hours and extracted with isohexane. Isohexane and aqueous fractions were then assayed for presence of DNCB and DNCB conjugate respectively.

16.7.2 Results

In the presence of DEM, all the radiolabelled compound in the receptor medium was extracted into isohexane indicating only unchanged DNCB. No DNCB conjugate was found in the remaining receptor medium. This compared to the parallel study in the absence of DEM where 30% of radiolabel in the receptor medium was found as the conjugate. These results were confirmed by TLC.

16.7.3 Discussion

Diethyl maleate was absorbed into the skin where it could successfully deplete glutathione levels. Consequently, glutathione conjugation of DNCB during percutaneous absorption was inhibited. This confirms the importance of endogenous levels of glutathione in skin and its role in glutathione conjugation.

16.8 Percutaneous absorption and metabolism of DNCB through the skin of neonatal rat, 26 day old rat, pig and human

The absorption and metabolism of DNCB was assessed in full thickness neonatal rat skin, dermatomed 26 day old rat skin, dermatomed pig skin and dermatomed human abdomen skin. From studies with mouse skin it was shown that an applied dose of 500μg/cm^2 did not lead to the formation of additional conjugate compared to a dose of 125μg/cm^2. Together with the knowledge that mouse skin had the highest concentration of glutathione of all species examined it was expected that an application of 500μg/cm^2 would not lead to greater levels of metabolism in other species compared to 125μg cm^2. Therefore the 500μg/cm^2 dose was not investigated with rat, pig or human skin. DNCB was dissolved in acetone only, since vehicle effects were not the key interest in these studies. All absorption studies with rat, pig and human were conducted using the flow-through diffusion cells, as this system was shown to maintain greater skin viability. As well as unoccluded conditions, the effect of occlusion was studied.

16.8.1 Method

Full thickness neonatal rat skin, dermatomed 26 day old rat skin, dermatomed pig skin and dermatomed human abdomen skin were mounted in flow-through diffusion cells as previously described. DNCB in acetone was applied to skin at concentrations of 25μg/cm^2 and 125μg/cm^2. Studies were conducted under unoccluded and occluded conditions. Six cells were used for each application, each species of skin and under unocclusion and occlusion.

16.8.2 Results

Table 16.7 details the disposition of unabsorbed DNCB for all species. Similar levels of DNCB evaporated from the surface of the skin from all species under unoccluded conditions ($p<0.01$). Under occluded conditions, DNCB was found on the parafilm forming the occlusion, but this was much less than that which had evaporated from unoccluded cells. Surface wash of all skins removed small amounts of DNCB which were similar for all species, therefore the remainder of the applied dose had been absorbed into the skin.

It could be seen that large amounts of DNCB remained in the skin of neonatal rat and 26 day old rat at the application dose of 125μg cm^2 accounting for 15% of the dose under unoccluded conditions and 24% of the applied dose with occlusion. In pig and human skin, these levels were lower accounting for approximately 6% and 11% of the applied dose under unoccluded and occluded conditions.

Table 16.8 Disposition of unabsorbed DNCB in a) neonatal rat skin, b) 26 day old rat skin, c) pig skin and d) human abdomen skin in flow-through diffusion cells after application of 25μg/cm^2 and 125μg/cm^2 DNCB dissolved in acetone, conducted under unoccluded and occluded conditions. (mean±sem, n=6 individual skins for neonatal and 26 day old rat skin, n=5 individual skins for pig and n=6 samples of the same human skin). Raw data to be found in appendices 19-34.

a)

Disposition of DNCB not found in receptor medium	Application of 25μg DNCB in acetone		Application of 125μg DNCB in acetone	
	μg/cm^2±sem unoccluded	μg/cm^2±sem occluded	μg/cm^2±sem unoccluded	μg/cm^2±sem unoccluded
Evaporated	6.154±0.687	1.581±0.208	54.094±4.301	6.868±1.541
Skin wash	2.397±0.652	2.890±0.929	5.100±0.901	1.479±0.021
Skin-solubilised	3.213±0.439	3.74±0.972	20.128±3.587	28.951±6.607

b)

Disposition of DNCB not found in receptor medium	Application of 25μg DNCB in acetone		Application of 125μg DNCB in acetone	
	μg cm^2±sem unoccluded	μg/cm^2±sem occluded	μg/cm^2±sem unoccluded	μg/cm^2±sem occluded
Evaporated	3.011±0.301	0.891±0.232	18.514±3.479	2.673±0.919
Skin wash	0.922±0.320	1.752±0.301	6.484±2.220	8.097±1.900
Skin-solubilised	1.905±0.358	6.407±1.938	13.182±3.311	29.959±4.234

c)

Disposition of DNCB not found in receptor medium	Application of 25μg DNCB in acetone		Application of 125μg DNCB in acetone	
	μg cm^2±sem unoccluded	μg cm^2±sem occluded	μg/cm^2±sem unoccluded	μg/cm^2±sem occluded
Evaporated	8.491±0.329	0.956±0.383	8.491±0.329	0.956±0.383
Skin wash	2.193±0.122	1.762±0.819	2.193±0.122	1.762±0.819
Skin-solubilised	1.687±0.122	6.055±1.890	1.687±0.122	6.055±1.890

d)

Disposition of DNCB not found in receptor medium	Application of 25μg DNCB in acetone		Application of 125μg DNCB in acetone	
	μg cm^2±sem unoccluded	μg/cm^2±sem occluded	μg/cm^2±sem unoccluded	μg/cm^2±sem occluded
Evaporated	-	2.351±0.632	-	11.344±3.648
Skin wash	0.803±0.203	0.788±0.244	4.108±0.762	3.460±0.768
Skin-solubilised	2.102±0.286	1.913±0.292	7.561±1.801	14.206±2.605

Absorption profiles for DNCB and conjugated DNCB in the receptor medium over time can be found in graph 16.8. A summary of the final amount of DNCB and conjugated DNCB found in the receptor medium at 24 hours can be seen in table 16.8.

DNCB was absorbed through adult rat skin at a far greater rate than the other species investigated and had a much greater rate than neonatal rat skin, which had the lowest DNCB absorption rate. DNCB was reported in the literature to be rapidly absorbed through fuzzy rat skin (Bronaugh *et al*, 1994). Pig and human skin had very similar absorption rates for DNCB at both application concentrations ($p>0.05$).

The rate of glutathione conjugation during percutaneous absorption of DNCB was greatest with mouse skin. Neonatal rat skin had a long lag phase and absorption of DNCB increased after approximately 3 hours. Adult rat skin had no lag phase and conjugation of DNCB to the glutathione conjugate appeared to have reached a maximum by 4 hours. Pig and human skin had very similar profiles for the rate of DNCB conjugation, with the final amount of conjugate formed by pig and human skin at an applied dose of 125μg cm^2 being insignificantly different ($p<0.01$).

Graph 16.8 Absorption and metabolism of DNCB though a) neonatal rat skin, b) 26 day old rat skin, c) pig skin and d) human abdomen skin in the *in vitro* flow-through system, unoccluded and occluded. DNCB was dissolved in acetone and applied to skin at concentrations of 25μg/cm^2 (dotted lines) and 125μg/cm^2 (solid lines). Squares represent DNCB, circles represent conjugated DNCB. Solid symbols represent occluded conditions. Receptor medium was RPMI1640 and set at a flow rate of 1.5ml/h. Cell temperature was maintained at 32°C. (mean±sem, n=6 individual skins for neonatal and 26 day old rats, n=5 individual skins for pig, n=6 samples of the same skin for human). Raw data to be found in appendices 19-34.

a) Neonatal rat skin

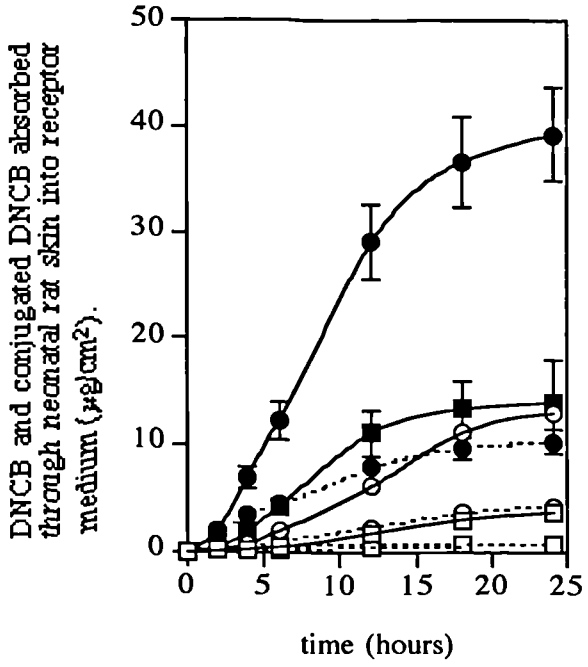

b) 26 day old rat skin

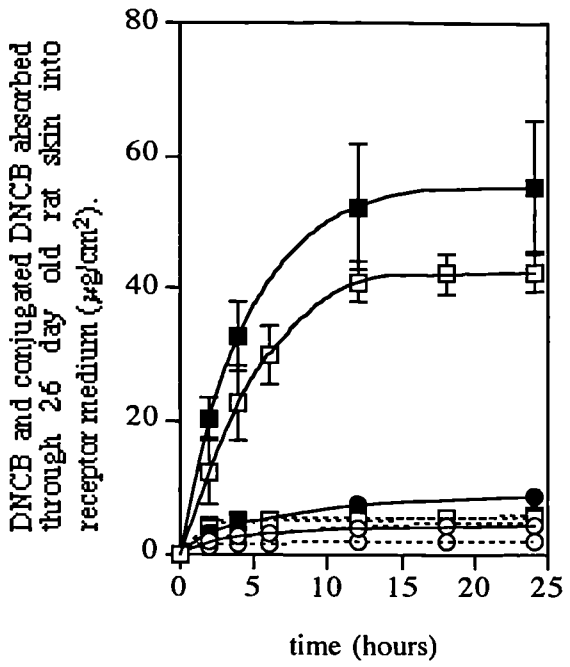

c) Pig skin

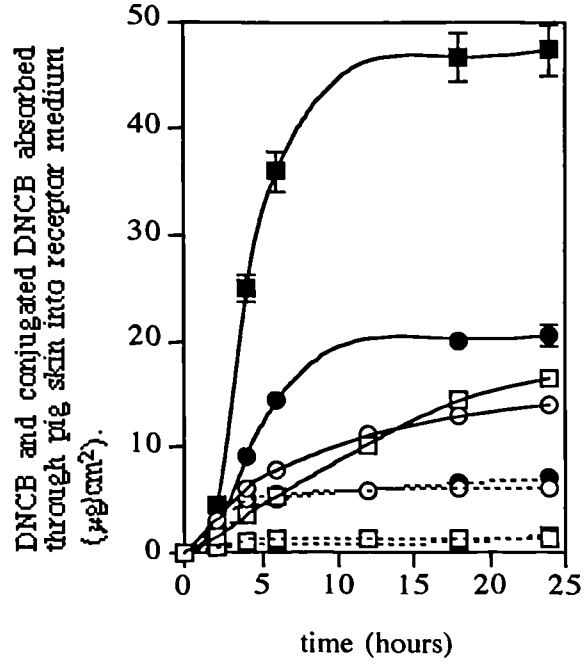

d) Human skin

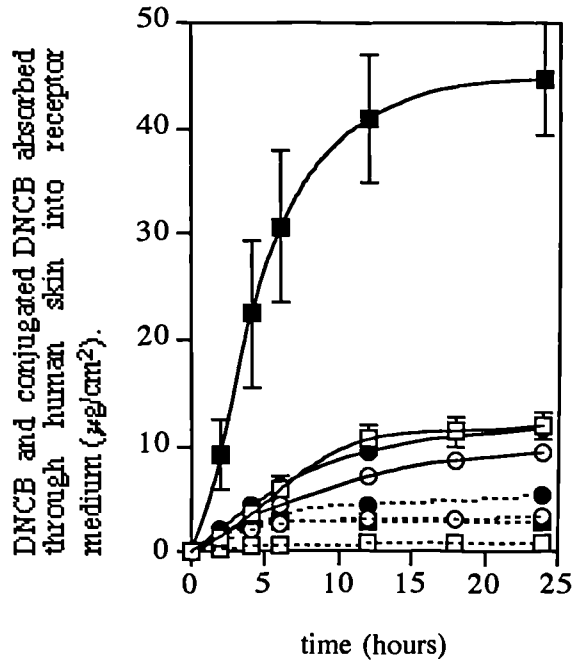

Table 16.9 DNCB and conjugated DNCB absorbed through Balb/C mouse, neonatal Wistar rat, 26 day old Wistar rat, domestic pig and human abdomen skin into the receptor medium under unoccluded and occluded conditions at 24 hours.

		DNCB dosage applied to skin			
		25μg/cm^2		125μg/cm^2	
Species		Unoccluded	Occluded	Unoccluded	Occluded
Balb/C mouse	DNCB	6.192±0.110	9.062±1.017	21.148±0.968	45.984±3.846
	Conjugated DNCB	12.053±0.287	12.844±0.791	25.244±2.744	25.953±1.895
Neonatal Wistar rat	DNCB	0.629±0.027	0.714±0.136	3.706±0.394	14.093±3.850
	Conjugated DNCB	4.267±0.238	10.302±1.119	13.107±0.652	39.321±4.518
26 day old Wistar rat	DNCB	5.393±0.257	5.731±1.066	42.620±3.004	55.418±10.13
	Conjugated DNCB	2.013±0.358	4.732±0.765	4.254±0.290	8.542±1.085
Domestic pig	DNCB	1.389±0.352	2.549±0.727	16.371±3.810	43.357±10.86
	Conjugated DNCB	6.167±0.421	7.011±1.906	13.924±1.920	20.451±1.023
Human	DNCB	0.788±0.328	2.949±0.948	11.882±1.314	44.676±5.179
	Conjugated DNCB	3.299±0.125	5.345±0.356	9.400±0.685	11.592±0.572

16.8.3 Overall discussion of studies with DNCB

The aim of this study was to define the profile of the absorption of DNCB through skin of a range of species *in vitro* and to determine the capacity of skin to metabolise DNCB to the glutathione conjugate using the flow-through diffusion cell system.

The localisation of xenobiotic metabolising enzymes in the basal layer of the epidermis has been reported by many groups including Coomes *et al*, (1983) and Pendlington *et al*, (1994). In these studies, immunohistochemistry of π-GST in mouse skin revealed that the enzyme was localised in the basal layer of the epidermis and the cells lining the hair follicles and sebaceous glands. Therefore the viable basal layer of the epidermis functions as an enzymatic barrier to drugs and xenobiotics. During the percutaneous absorption, DNCB must pass through this layer and therefore exposed to the metabolising enzymes.

The viability of GST enzymes was shown to be stable in neonatal rat skin in the flow-through and static diffusion cells over 24 hours (see chapter 15), though it was shown that the viability of skin was more greatly maintained in the flow-through system by the MTT assay and levels of reduced glutathione. Studies investigating the percutaneous absorption of DNCB were therefore conducted using the flow-through cell so as to give the closest viability possible to *in vivo* skin.

DNCB was metabolised by mouse skin GST's to the glutathione conjugate during percutaneous absorption *in vitro* and the amount of conjugated DNCB formed was independent of diffusion cell type. At applied doses of 125μg/cm^2 and 500μg/cm^2 a limited amount of DNCB was conjugated whereas when a dose of 25μg/cm^2 was applied, there was not enough DNCB to saturate the glutathione in the skin. The rapid depletion of GSH in the skin correlated with the appearance of the conjugate in the receptor medium. It has been shown that DNCB is absorbed through the skin at a rate which is dependent on its vehicle formulation (Heylings *et al*, 1996). This was reflected in these studies where maximum conjugated material was detected at 4 hours when DNCB was dissolved in the acetone vehicle and 6 hours in the PG vehicle. This illustrates the influence the vehicle had on percutaneous penetration, where the PG vehicle takes longer to deliver DNCB to the site of the conjugating enzymes located at the basal layer of the epidermis. The disappearance of conjugating activity was not attributable to a loss of skin viability, as assessed by the MTT assay, but by the limiting amount of glutathione available. The use of diethyl maleate to deplete the available glutathione in the skin showed that no conjugation was possible without it.

Mouse skin had the highest levels of glutathione, but had low GST activity. Absorption and conjugation of DNCB was influenced mainly by skin GSH content. Mouse skin and adult rat skin absorbed DNCB by similar amounts ($p>0.05$), but more of the absorbed DNCB was metabolised in mouse to the glutathione conjugate than in the adult rat skin due to it's higher GSH content. DNCB permeated neonatal rat skin much less than adult rat skin, but because it contained higher levels of GSH than adult rat skin, a far greater proportion of the DNCB was metabolised. Therefore it was seen that GSH content of the skin was a more important factor in the metabolism of DNCB than the GST activity of the skin. The advantage of using intact skin for evaluating the degree of metabolism is clearly shown by these studies. Whereas the use of subcellular fractions requires the addition of excess GSH which does not limit the degree of metabolism and therefore does not indicate the degree of metabolism that can occur in skin *in vivo*.

Human skin (from breast reduction plastic surgery) and pig skin (from ears of domestic pigs) had similar GSH content, but human skin had nearly three times more GST activity. Human skin showed the highest GST activity compared to all the other species examined and human keratinocytes (cells of the basal layer of the epidermis) had even higher activity, showing the concentration of these enzymes with the basal layer of the epidermis. Absorption profiles of DNCB through pig and human skin were very similar and glutathione conjugation of DNCB during percutaneous absorption resulted in similar amounts of metabolism taking place ($p>0.05$).

Occlusion of skin resulted in a greater absorption of DNCB with all species investigated, a result consistent with the effects of occlusion published in the literature (Wurster and Kramar, 1961; Bronaugh *et al*, 1990). This is due to an increase in skin hydration, resulting in greater permeability

of the stratum corneum. Although DNCB absorption was increased, the formation of the glutathione conjugate was not, again due to the limited available glutathione.

As previously stated, DNCB is a skin irritant and sensitiser and causes severe allergic dermatitis. It has been shown that DNCB elicits a faster immune response in vehicles that have a faster initial absorption rate (Heylings *et al*, 1996). It was therefore interesting to determine the role of percutaneous absorption and metabolism of DNCB and conclude whether this bears any relation to the immune response.

Studies with mouse skin in the flow-through diffusion cell showed that after application of DNCB in acetone the rate of the glutathione congugate appearing in the receptor medium slowed down after 4 hours, corrosponding to when most of the available glutathione in the skin had been utilised. Application in a propylene glycol vehicle lead to a slower rate of absorption and maximum levels of the conjugate was not attained until 6 hours. After topical application of DNCB (0.5%) in acetone to Balb C mouse skin an immune reaction is seen which can be followed by the production of interleukin 6 (Il 6). Maximum production of Il-6 occurs 4 hours after application of the dose (Dearman *et al*, 1995). This corrosponds with the time at which maximum levels of glutathione conjugate had appeared in the receptor medium of flow-through cells after application of DNCB in acetone. This therefore might suggest that after all the glutathione levels had been depleted in the skin, the toxicological effects of DNCB were elicited.

The degree of the immune response has been shown to be proportional to the amount of DNCB applied to the skin. At an applied dose of $25\mu g/cm^2$ only a modest response was seen (Cumberbatch *et al*, 1993). It can be postulated that glutathione conjugation of DNCB leads to its detoxification and possibly removes the causative agent of the immune response.

In conclusion, glutathione levels in skin was the main factor influencing DNCB metabolism during percutaneous absorption. Pig skin was a better model for predicting human DNCB absorption and metabolism in the flow-through diffusion cell than rat or mouse skin due to its similar absorption profile and similar levels of glutathione. Therefore pig skin is the best model for human skin in evaluating the toxicological implications of dermally absorbed DNCB.

Section 4

General Discussion

Chapter 17

Discussion

General discussion

The skin is the largest organ of the body whose barrier properties are not completely inpenetratable. A myriad of compounds including drugs, agrochemicals and environmental pollutants can penetrate through the skin and their metabolism may lead to toxic or carcinogenic effects. Even though liver is the main site of metabolism of these substances the potential of the skin to metabolise them cannot be dismissed, especially when it is also the primary route of exposure. Percutaneous absorption is not necessarily an adverse disadvantage, but can be utilised for the dermal administration of drugs, and metabolism may even be of benefit, especially when the skin is the site of medical treatment.

The studies in this thesis have explored the different *in vitro* models for assessing skin xenobiotic metabolism, each with increasing complexity. The models investigated were skin subcellular fractions, cultures of keratinocytes, the living skin equivalent and skin mounted in diffusion cells. This chapter summarises the experimental results obtained and discusses them in relation to each other and with reference to published literature.

The use of *in vitro* methods for assessing skin metabolism allows the skin to be studied independently of other tissues. The requirement for *in vitro* toxicology studies for predicting cutaneous penetration of chemicals has become the driving force into the development of methods for the replacement of *in vivo* studies and the reduction of the number of animals used in research, with the final aim of eliminating the need for animals altogether. Therefore, *in vitro* models must be thoroughly evaluated and validated for their usefulness and to provide data that can be extrapolated to man.

Initial studies concentrated on the use of subcellular fractions for investigations of xenobiotic metabolism. Skin has been a difficult tissue to assess for xenobiotic metabolism using subcellular fractions because of the difficulty in preparing homogenates. The skin requires rough techniques to extract the constituent enzymes, which may lead to some or all enzyme activity being lost. Therefore skin in these studies was frozen in liquid nitrogen and then ground to a powder to help facilitate the homogenisation and reduce the loss of enzyme activity. Also, the use of a dermatome to remove the most active layer of skin from the thicker and much less active dermal layer helps concentrate the active enzymes from the skin. This is particularly useful for human skin, which is invariably tougher to homogenise and contains lower levels of enzyme than animal skin. This simple model lacks the complexities of intact skin, but it does provide valuable information on the skin's potential to metabolise xenobiotics.

Cytochrome P-450 activity (CYP1A1 and CYP2B) was examined in rat, pig and human tissue, and activity measured with the substrates 7-ethoxyresorufin and 7-pentoxyresorufin respectively. Further studies examined the age of the rat and effects of the inducing agents ß-

naphthoflavone and phenobarbital on P450 activities. The activities of cytochrome P450 as determined by ethoxyresorufin-*O*-deethylation (EROD) and pentoxyresorufin-*O*-depentylation (PROD) were determined with freshly prepared microsomal protein to measure activity as close to *in vivo* as possible and to minimise the loss of activity when stored at -70°C. In rat skin, cytochrome P450 activity did not change with age. EROD activity in skin of 26 day old rat was 3.79±1.32pmoles min/mg microsomal protein, while PROD activity was 2.68±0.58pmoles/min/mg microsomal protein. The published literature on the activity of cytochrome P4501A1 in the skin as measured by EROD shows activity varying from 0.1 to 15% to that of specific liver activity (Hotchkiss 1992). There are very few reported P450 activities in the skin using microsomal preparations. Most studies in the literature have used Sprague-Dawley rats and activities quoted have been for example, 3.6±0.3pmoles min mg (Pham *et al*, 1989) which correlates well with activities found in the studies of this thesis. However, other levels of activities quoted are 0.64±0.1pmoles min mg (Khan *et al*, 1989) and Venkatesh *et al*, (1992) reported an activity of 35±3pmoles min mg with CD-1 mouse skin microsomes. Therefore the reported activities vary to a great extent. Faradin (1969) and Mukhtar *et al* (1987) showed hydroxylation of testosterone at the 6ß, 7α and 16α positions, using rat skin. This indicates the presence of cytochrome P4503A and cytochrome P4502C subfamilies. Therefore it is apparent that the skin has the capacity to metabolise with a range of cytochrome P450 isoenzymes. As rat skin has been shown to exhibit varying cytochrome P450 metabolising enzymes and human skin has not, the use of rat skin for determining cytochrome P450 activity may not be a suitable model for human skin. In the studies of this thesis, human EROD and PROD activities in skin microsomes were not detectable. Pig EROD activity was detectable at low levels (0.223±0.057pmoles min mg microsomal protein). Therefore pig skin was a closer model of human skin cytochrome P450 activity than rat skin, which had showed much higher activities.

One of the aims of these studies was to investigate the influence of inducing agents on cytochrome P450 activity in rat skin by pretreatment with the classical inducing agents ß-naphthoflavone and phenobarbital. The results showed that liver activity was induced but skin activity was not. It may have been that the inducing agents did not reach the skin, although studies were not undertaken to investigate this. It may be more appropriate to apply inducing agents topically to promote local induction. Studies with LSE suggest that this is the case. The LSE was found not to possess EROD activity until exposure to 3-methylcholanthrene.

Esterase activities were examined in the cytosolic fraction of skin with 4-methylumbelliferyl heptanoate (4 MUH) as the substrate. Studies showed that 4-MUH was hydrolysed by carboxylesterases in the skin of mouse, rat, pig and human. The age of rat did not influence cytosolic 4-MUH hydrolysis, and activities were not induced by pretreament with ß-naphthoflavone of phenobarbital. Again this may have been contributable to the inducers not reaching the skin. 4-MUH hydrolysis by pig skin cytosol was similar to human skin cytosolic activity, whereas rat and mouse skin cytosolic activities were much higher. Therefore, pig skin was once again shown to be a better model of human skin than rodent skin.

Glutathione-S transferase (GST) activities were measured in rodent, pig and human skin with the substrate dinitrochlorobenzene (DNCB). Human skin contained the highest GST activity of all species examined. Adult rat skin GST activity was higher than in neonatal rat skin. GST activities determined using subcellular fractions require the addition of exogenous reduced glutathione. This does not give a true picture of GST activity in skin, because it provides excess glutathione. Skin has a finite amount of reduced glutathione available which consequently determines the amount of GST metabolism possible. Human skin and pig skin were found to contain low levels of reduced glutathione, whereas rodent skin had higher levels and mouse skin the highest levels in the species examined. This would infer that mouse skin has the greatest capacity for glutathione conjugation, which was later found to be true in the flow-through studies investigating percutaneous absorption and metabolism of DNCB.

Human skin would be the most ideal source of xenobiotic metabolising enzymes, but this is often difficult to obtain, especially fresh. Therefore animal skin is used as it is more readily available. However, animal skin usually exhibits a completely different distribution of enzyme activities which may not necessarily be relevant to human dermal xenobiotic metabolism. Although pig skin exhibited similar enzyme activities to human skin, pig skin may also have metabolic pathways not yet characterised. The main disadvantage of using subcellular fractions is that skin loses it three dimensional structure and the complex mechanism of dermal absorption. Localisation of enzyme systems are also lost while stability of enzymes such as cytochrome P450's are severely impaired.

The next part of the project was to grow keratinocytes in tissue culture and to assess them for their capacity to metabolise xenobiotics in the skin. The use of keratinocytes was one step higher in skin model complexity from subcellular fractions. Keratinocytes were grown from rat skin and from human skin which was obtained from plastic surgery. Development of keratinocyte cell culture was a lengthy process as these cells are difficult to grow, particularly human keratinocytes. The success of their culture depended on supplying the necessary nutritional requirements. The tissue culture of both rat and human keratinocytes was established and cells could be maintained in a defined serum-free medium and utilised for metabolic studies. Human keratinocytes could be passaged to allow a series of experiments to be performed on the same sample, but rat keratinocytes, however, were not successfully passaged due to their sensitivity to trypsin. Inducers and inhibitors were added directly to these cell cultures and the changes in metabolic activity determined. Constitutive cytochrome P450 levels in rat skin subcellular fractions showed that activity in neonatal rat was comparable to the adult rat. The neonatal rat was a more suitable source of keratinocytes than the adult rat because of less contamination from hair follicles and dead squames. Therefore, since P450 activity in neonatal rat was similar to the adult rat, the keratinocytes of neonatal rat were used. Another important consideration of enzymes in skin is their stability. P450 levels were measured against time to determine if they were maintained at physiological levels or if their activity decreased with time. Results showed that P450 activity decreased rapidly in isolated keratinocytes and were not found in subsequent cultures of keratinocytes. Freshly isolated keratinocytes showed an EROD activity of 7.640±0.156pmoles min 10^6 cells. Enzyme levels in subsequent untreated cultures of rat and human

keratinocytes were found to be undetectable, and treatment with ß-naphthoflavone added directly to the cultures yielded unreproducible results. Measurement of esterase and GST activities in cultured keratinocytes were similar to those found in subcellular fractions of skin. Suggesting that these enzymes are more stable and reliably expressed than the cytochrome P450's. However, levels of reduced glutathione in cultured keratinocytes were very low compared with intact skin, illustrating the unstability of this cofactor, required for glutathione conjugation.

To summarise, keratinocytes were not a useful model to study skin xenobiotic metabolism. Cytochrome P450 monooxygenase activity was unstable and quickly lost in freshly isolated cells. Cells cultured as monolayers displayed no cytochrome P450 activity and induction of cytochrome P450 activity by ß-naphthoflavone was not reproducible. Esterase and GST activities were present in keratinocytes, but levels of glutathione were lower than human skin.

The next model for assessing skin xenobiotic metabolism was the living skin equivalent (LSE). This raised the level of model complexity from isolated cells and cultured monolayers to the three dimensional structure of living tissue. The final goal in the development of alternative (*in vitro*) models for cytotoxicity studies is to create an *in vitro* model that enables the extrapolation to *in vivo* results and prediction of the effects of tested substances in humans. An LSE could meet such a requirement in that it has a tissue morphology which correlates well to that of *in vivo* skin. Although the LSE is commercially available, it was too expensive to be used for these studies. Therefore for the purpose of these investigations an LSE was grown from isolated cells. This was a more ambitious model to engineer. Dermal fibroblasts were grown on a porous membrane to form their own matrix suitable for supporting a differentiated epidermis derived from cultured keratinocytes. However, the LSE required long periods of time to produce and the number of metabolic studies using the LSE were not large. Initial studies did show some interesting results, esterase and GST activities were similar to human skin subcellular fractions, but cytochrome P450 activity was not present. Cytochrome P450 activities were induced to measurable levels and esterase and GST activities were also induced. This suggests that enzyme activity is not fully expressed in isolated cells, but is fully expressed in the complete skin structure. Keratinocytes therefore require the presence of a basal membrane and the process of differentiation for xenobiotic metabolism enzymes to be expressed.

The LSE is still not a good model for investigating the percutaneous absorption of xenobiotics, due to its extensive hydration and lack of barrier properties. but it is suitable for investigating the effects of inducing agents on human skin, which cannot be done *in vivo* for ethical reasons.

The most complex skin model was the use of freshly excised skin mounted in flow-through diffusion cells. The flow-through diffusion cell maintained skin viability greater than the static diffusion cell. Over 24 hours, skin in the flow-through cell remained firmly intact, having a tighter epidermal/dermal junction. Viability as assessed by the MTT assay and levels of reduced glutathione were better maintained in the flow-through diffusion cell than the static diffusion cell. Cytochrome

P450 activity could not be measured in skin samples from the flow-through diffusion cells because they were too small. It was shown that cytochrome P450 activity drops off rapidly in freshly isolated skin cells, but can be maintained in the LSE. This suggests that cytochrome P450 activity is possibly present in intact skin, and the flow-through system would help maintain it. The flow-through system utilises intact skin from animals and therefore the skin has all the characteristic properties necessary for investigating percutaneous absorption, therefore being the best *in vitro* model for studying this. The choice of animal skin however, influences the rate of absorption due to the differences in the skin's barrier properties of each species.

Investigations in this project have concentrated on the metabolism of dinitrochlorobenzene (DNCB), a skin sensitiser and a substrate for glutathione-S-transferases. The aim was to define the importance of DNCB metabolism during percutaneous absorption, and relate this to the metabolic capacity of other skin models. As DNCB is a skin irritant and sensitiser, it was interesting to determine the role of DNCB percutaneous absorption and metabolism and conclude whether this could bear any relation to the immune response.

Immunohistochemistry of GST revealed that the enzyme was localised in the basal layer of the epidermis and therefore the viable basal layer of the epidermis functions as an enzymatic barrier to DNCB during percutaneous absorption. It has been shown that DNCB is absorbed through the skin at a rate which is dependent on its vehicle formulation and the degree of immune response is greater with vehicles which have a faster initial absorption rate (Heylings *et al*, 1996).

Viability of GST enzymes was shown to be stable in the flow-through and static diffusion cells over 24 hours. Mouse skin contained low GST activity but it contained the highest levels of reduced glutathione of the species examined. However, the levels of GST's were not the determining factor in glutathione conjugation of DNCB. The level of glutathione conjugation during percutaneous absorption of DNCB was greatest with mouse skin. Adult rat skin had higher GST activity than neonatal rat skin, but neonatal rat skin had higher GSH than adult rat skin. During percutaneous absorption of DNCB, neonatal rat skin metabolised more DNCB to the glutathione conjugate than adult rat skin. It appeared that GSH content of the skin was a more important factor in determining the metabolism of percutaneously absorbed DNCB in the flow-through system than the GST activity of the skin.

Similar absorption profiles were found for the percutaneous absorption of DNCB through human skin and pig skin. They had similar GSH content, but human skin had nearly three times more GST activity. Glutathione conjugation of DNCB during percutaneous absorption resulted in similar amounts of metabolism taking place. Thus showing that limited levels of reduced glutathione limit DNCB conjugation and therefore could influence the degree of the immune response.

Mouse skin showed a maximum rate of DNCB conjugation in 4 hours when applied in an acetone vehicle. Which corresponds to a loss in available glutathione in the skin. DNCB in a propylene glycol vehicle has a slower rate of absorption and the formation of conjugate declined after 6 hours. An immune reaction was seen following application of DNCB in acetone to mouse skin which can be measured by the production of interleukin-6 (Il-6). Maximum production of Il-6 occurs 4 hours after application of the dose (Dearman *et al*, 1995), corresponding with the time at which maximum levels of glutathione conjugate had appeared in the receptor medium in *in vitro* diffusion cells after application of DNCB in acetone. This therefore might suggest that after all the glutathione levels had been depleted in the skin, the toxicological effects of DNCB were elicited.

In conclusion, rodent skin was a poor model for predicting human skin xenobiotic metabolism as it displayed a higher level of cytochrome P-450 monooxygenase and esterase activity than human skin. Mouse skin had higher levels of reduced glutathione. This led to a greater degree of DNCB metabolism during percutaneous absorption in the flow-through diffusion cells, therefore unable to predict human percutaneous absorption and metabolism of DNCB. Pig skin was shown to be a good model of human skin for assessing xenobiotic metabolism and absorption. Pig and human skin showed similar levels of recovery for microsomal and cytosolic protein. Human skin contained no detectable cytochrome P-450 monooxygenase activity. Pig skin exhibited very low cytochrome P-450 monooxygenase activity, whereas rat skin had comparably high levels of activity. 4-MUH hydrolysis by pig and human skin were also similar. Likewise reduced glutathione levels in pig and human skin were similar. During the percutaneous absorption and metabolism of DNCB in flow-through diffusion cells, pig and human skin had similar levels of DNCB and glutathione conjugated DNCB appearing in the tissue culture receptor medium at 24 hours. To summarise, DNCB glutathione conjugation in skin during percutaneous absorption is limited by the levels of glutathione available. Percutaneous absorption of DNCB increases under occluded conditions, but the degree of metabolism does not. Glutathione conjugation of DNCB is suggested to be a detoxification pathway by removing the parent compound DNCB.

The assessment of *in vitro* models for investigating dermal xenobiotic metabolism have shown that with increasing complexity from subcellular fractions, to keratinocytes, to living skin equivalents and finally full intact skin from the animal, the closer you get to predicting the metabolism of dermally exposed compounds.

Chapter 18

Future work

Future research

Several key areas of the research undertaken in this thesis raised questions that require further studies in order to answer them. Therefore the following ideas are proposed as areas of future research.

1. These results have suggested that pig skin is a good model for human skin for percutaneous absorption and metabolism, but limited information is available on pig skin xenobiotic metabolism. There is a need for more compounds to be evaluated in pig skin to determine the full profile of its metabolic capacity, so that this can be extrapolated to human data.

2. The studies showed that 4-MUH was hydrolysed by carboxylesterases, but it has been shown that four or more carboxylesterases are present in human skin (Heymann *et al*, 1993). Characterisation of these carboxylesterases and there involvement in the metabolism of 4-MUH should be defined. This could be done by first purifying carboxylesterases from skin. Then to determinine their activities independently and during percutaneous absorption. Antibodies could be raised against specific isoforms of carboxylesterases and used as specific inhibitors.

3. Only reduced glutathione levels were measured in the skin as attempts to measure oxidised glutathione were inconclusive. The use of bromobimane was unsuitable for the measurement of oxidised glutathione. Therefore an alternative method would need to be used to measure the oxidised form in skin. Oxidised levels of glutathione (GSSG) should be measured to reveal the ratio of reduced to oxidised forms. This would give more information on the oxidative stress of skin *in vitro*.

4. Keratinocytes were successfully grown from human and rat skin. It may also be possible to grow keratinocytes from pig skin, though culture medium may need to be modified. As results indicated, pig skin xenobiotic metabolisng enzymes were similar to human skin. Therefore, pig keratinocytes could potentially be used to model human keratinocytes. Pig skin is more readily available than human skin, and could provide a plentyful source of keratinocytes for metabolism studies. If pig keratinocytes could be grown, then it would also be possible for a pig LSE to be developed.

6. Depletion of reduced glutathione levels in Balb C mouse skin by pretreatment with buthionine sulphoximine (BSO) was unsuccessful. Measurement of the glutathione concentration in skin and liver after dosing could be used to determine whether inhibition is confined to hepatic tissue. Studies into the effect of BSO after topical application may find a greater degree of glutathione inhibition.

7. It was clear from the studies in this thesis that the LSE has greater potential as a model of human skin for the determination of xenobiotic metabolism than isolated cell systems. Derived from cells isolated from human skin, the LSE would also contain enzymes more relevent to man than animal skin models. Therefore the characterisation of xenobiotic metabolising enzymes expressed in the LSE and the determination of their activities is of great inportance in future studies. At present, there is limited information on the use of the LSE for xenobiotic metabolism. Reports in the literature (Slivka *et al*,1993) indicate that metabolic activity of cytochrome P450 is active in the LSE even when they are in culture for several weeks, which makes this model potentially useful for long term studies. For this LSE model to become more widely used, the metabolism of a broad range of compounds needs to be defined.

7. The percutaneous absorption of DNCB in the flow-through diffusion cell has shown the profile of its metabolism with time. DNCB is also a skin irritant and sensitiser and studies could be run in parallel with metabolism to assertain the release of proinflammatory factors such as Il-6 into the receptor medium.

8. For the preparation of microsomes from skin, the tissue was first frozen in liquid nitrogen, then ground to a powder before being homogenised. Microsomal recoveries from skin were low and possessed low enzymatic activity. Therefore an intersting study would be the preparation of microsomal samples from skin for electron microscopy. This would show any detrimental effects during their preparation, indicating if low activity was due to extensive damage to the microsomes.

Section 5

References and Appendices

References

References

Abel and West, (1986). Mechanisms in contact dermatitis. *Chemicl reviews in allergy*, **4**, 339-352.

Ademola, J.I., Wester, R.C., Maibach, H.I., (1993). Absorption and metabolism of 2-chloro-2,6-diethyl-N-(butoxymethy)acetanilide (Butachlor) in human skin in vitro. *Toxicology and applied pharmacology*, **121**, 78-86.

Agarwal, R., Raza, H., Allyn, D.L., Bickers, D.R., Mukhtar, H., (1992). Glutathione S-transferase-dependent conjugation of leukotriene A4-methyl ester to leukotriene C4-methyl ester in mammalian skin. *Biochemical pharmacology*, **44**, 2047-2053.

Aitio, A., (1978). A simple and sensitive assay of 7-ethoxycoumarin deethylation. *Analytical biochemistry*, **85**, 488-491.

Aldridge, W.N., (1953). Serum esterases 2. An enzyme hydrolysing diethyl-p-nitrophenylphosphate (E600) and its identity with the A esterase of mammalia sera. *Biochemical journal*, **53**, 117-124.

Aldridge, W.N., (1989). A-esterases and B-esterases in perspective. *In Enzymes hydrolysing organophosphorous compounds*. Edited by Riener, E., Aldridge, W.N., Hoskin, F.C.G. pp1-14.

Andersson, T., Cederberg, C., Edvardsson, G., Heggdund, A., Lundborg, P., (1990). Effect of omeprazole treatment on diazapam plasma levels in slow versus rapid metabolisers of omprazole. *Clinical pharmacology and therapeutics*, **47**, 79-85.

Awasthi, Y., Sharma, R., Singhal, S.S., (1994). Human glutathione-S-transferases. *International journal of biochemistry*, *26*, 295-308.

Baden, H.P., Kubilus, J., (1983). The growth and differentiation of cultured newborn rat keratinocytes. *Journal of investigative dermatology*, **80**, 124-130.

Barker, J.N.W.N., (1992). The role of keratinocytes in allergic contact dermatitis. *Contact dermatitis*, **26**, 145-148.

Bartek, M.J., Labukle, J.A., Maibach, H.I., (1972). Skin permeability in vivo: comparison in rat, rabbit, pig and man. *Journal of investigative dermatology*, **58**, 114-123.

Barton, S.P., Marks, R., (1981). Changes in suspensions of keratinocytes due to trypsin. *Archives of dermatological research*, **271**, 245-257.

Bell, E., Ivarsson, B., Merrill, C., (1979). Production of a tissue like structure by contraction of collagen lattices by human fibroblasts of different proliferative potential in vitro. *Proceedings of the national acadamy of sciences*, USA, **76**, 1274-1278.

Bell, E., Sher, S., Hull, B., Merrill, C., Rosen, S., Chamson, A., Asselineau, D., Dubertret, L., Coulomb, B., Lapiere, C., Nusgens, B., Neveux, Y., (1983). The reconstitution of living skin. *Journal of investigative dermatology*, **81**, 2s-10s.

Bell, E., Parenteau, N., Gay, R., Nolte, C., Kemp, P., Bilbo, P., Ekstein, B., Johnson, E., (1991). The living skin equivalent: Its manufacture, its organotypic properties and its responses to irritants. *Toxicology in vitro*, **5**, 591-596.

Bergman, F., Segal, R., Rimon, S., (1957). A new type of esterase in hog kidney extract. *Biochemical Journal*, **111**, 67-72.

Bickers, D.R., Kappas, A., Alvares, A.P., (1974). Differences in inducibility of cutaneous and hepatic drug metabolising enzymes and cytochrome P450 by polychlorinated biphenyls and 1,1,1-trichloro-2,2-bis(p-chlorophenyl)ethane (DDT). *Journal of pharmacology and experimental therapeutics*, **188**, 300-309.

Bickers, D.R., Duttachoudhury, T., Mukhtar, H., (1982a). Epidermis: A site of drug metabolism in neonatal rat skin. *Molecular pharmacology*, **21**, 239-247.

Bickers, D.R., Marcelo, C.L., Duttachoudhury, T., Mukhtar, H., (1982b). Studies on microsomal cytochrome P450 monooxygenases and epoxide hydrolase in cultured keratinocytes and intact epidermis from Balb/C mice. *Journal of pharmacology and experimental therapeutics*, **223**, 163-168.

Bickers, D.R., Mukhtar, H., Dutta-Choudury, T., Marcelo, C.L., Voorhees, J.J., (1984). Aryl hydrocarbon hydrolase, epoxide hydrolase and beno[a]pyrene metabolism in human epidermis: comparitive studies in normal subjects and patients with psoriasis. *Journal of investigative dermatology*, **83**, 51-56.

Birkendal-Hansen, H., Hansen, I.L., Nellemann, K., Westergaard, J., (1981). Growth and differentiation of an established rat keratinocyte line in serial culture. *In vitro*, **17**, 553-562.

Blacker, K.L., Olson, E., Vessey, D.A., Boyer, T.D., (1991). Characterisation of glutathione-S-transferases in cultured human keratinocytes. *Journal of investigative drmatology*, **97**, 442-446.

Blank, I.H., Griesener, R.D., Gould, E., (1958). The penetration of an anticholinesterase agent (Sarin) into skin. *Journal of investigative dermatology*, **30**, 187-191.

Boehnlein, J., Sakr, A., Lichtin, J.L., Bronaugh, R.L., (1994). Characterisation of esterase and alcohol dehydrogenase activity in skin. Metabolism of retinyl palmitate to retinol (vitamin A) during percutaneous absorption. *Pharmaceutical research*, **8**, 1155-1159.

Boyce, S.T., Ham, R.G., (1983). Calcium-regulated differentiation of normal human epidermal keratinocytes in chemically defined colonal culture and serum free serial culture. *Journal of investigative dermatology*, **81**, 33s-40s.

Briggaman, R.A., Abele, D.C., Harris, S.R., Wheeler, C.E., (1967). Preparation and characterisation of a visible suspension of postembryonic human epidermal cells. *Journal of investigative dermatology*, **48**, 159-168.

Bronaugh, R.L., Stewart, R.F., Congdon, E.F., (1982). Methods for in vitro percutaneous absorption studies II: Animal models for human skin. *Toxicology and applied pharmacology*, **62**, 481-488.

Bronaugh, R.L., Stewart, R.F., Congdon, E.F., (1983). Differences in permeability of rat skin related to sex and body site. *Journal for the society of cosmetic chemistry*, **34**, 127-135.

Bronaugh, R.L.,Wester, R.C., Bucks, D., Maibach, H.I., (1990). In vivo percutaneous absorption of fragrance ingrediants in monkey and humans. *Food and chemical toxicology*, **28**, 369-373.

Bronaugh, R.L., Roberts, CD., McCoy, J.L., (1994). Dose-response relationship in skin sensitization. *Food and Chemical Toxicology*,.**32**, 113-117.

Bronaugh, R.L., Collier, S.W., Stewart, R.F., (1989). In vitro percutaneous absorption of hydrophobic compounds through viable hairless guinea pig skin. *Toxicologist*, **9**, 241.

Bronaugh, R.L., Collier, S.W., Storm, J.E., Stewart, R.F., (1990). In vitro evaluation of skin absorption and metabolism. *Journal of toxicology*, **8**, 453-467.

Bronaugh, R.L., Collier, S.W., (1991). Preparation of human and animal skin, chapter 1 in *In vitro percutaneous absorption: Principles, fundamentals and applications.* Edited by Bronaugh, R.L., and Maibach, H.I. CRC Press.

Bucks, D., Guy, R., Maibach, H., (1992). Effects of occlusion, chapter 8 in *In vitro percutaneous absorption: Principles, fundamentals and applications.* Edited by Bronaugh, R.L., and Maibach, H.I. CRC Press.

Burke, M.D., Thompson, S., Elcombe, C.R., Halpert, G., Haaparanta, T., Mayer, R.T., (1985). Ethoxy-, pentoxy- and benzyloxyphenoxazones and homologues: A series of substrates to distinguish between different induced cytochromes P450. *Biochemical pharmacology*, **34**, 3337-3345.

Carver, M.P., Riviere, J.E., (1989). Percutaneous absorption and excretion of xenobiotics after topical and intravenous administration to pigs. *Fundamental and applied toxicology*, **13**, 714-722.

Chang, T., Levine, M., Bandiera, S.M., Bellward, G.D., (1992). Selective inhibition of rat hepatic microsomal cytochrome P450 1.Effect of the in vivo administration of cimetidine. *Journal of pharmacology and experimental therapeutics*, **260**, 1441-1449.

Clark, N.W.E., Blain, P.G., Scott, R.C., Williams, F.M., (1991). *Maintenance of skin viability in skin absorption systems*. In *Prediction of percutaneous penetration*, Vol.II. IBC Technical Services, London, pp541-547.

Clark, N.W.E., Scott, R.C., Blain, P.G., Williams, F.M., (1993). Fate of fluazifop butyl in rat and human skin in vitro. *Archives of toxicology*, **67**, 44-48.

Clowes, H.M., Scott, R.C., Heylings, J.R., (1994). Skin absorption: Flow-through or static diffusion cells. *Toxicology in vitro*, **8**, 827-830.

Cohen, S., (1960). Purification of a nerve growing promoting protein from the mouse salivary gland and its neuro-cytotoxic antiserum. *Proceedings of the national academy of sciences, USA*, **46**, 302-311.

Collier, S.W., Sheikh, N.M., Sakr, A., Lichtin, J.L., Stewart, R.F., Bronaugh, R.L., (1989). Maintenance of skin viability during in vitro percutaneous absorption/metabolism studies. *Toxicology ans applied pharmacology*, **99**, 522-533.

Collier, S.W., Storm, J.E., Bronaugh, R.L., (1993). Reduction of azo dyes during in vitro percutaneous absorption. *Toxicology and applied pharmacology*, **118**, 73-79.

Contard, P., Bartel, R.L., Jacobs, L., Perlish, J.S., MacDonald, E.D., Handler, L., Cone, D., Fleischmajer, R., (1993). Culturing keratinocytes and fibroblasts in a three-dimensional mesh results in epidermal differentiation and formation of a basal lamina-anchoring zone. *Journal of investigative dermatology*, **100**, 35-39.

Cook, J.R., Gabriels, J., Patrone, L.M., Rhoads, L.S., Van Buskirk, R.G., (1992). A human epidermal model that can be used in an automated multiple endpoint assay. *ALTA-Alternatives to laboratory animals*, **20**, 313-323.

Coomes, M.W., Norling, A.H., Pohl, R.J., Müller, D., Fouts, J.R., (1983). Foreign compound metabolism by isolated skin cells from the hairless mouse. *Journal of pharmacology and experimental therapeutics*, **225**, 770-777.

Cormier, M., Ledger, P.W., Marty, J.P., Amkraut, A., (1991). In vitro cutaneous biotransformation of propranolol. *Journal of investigative dermatology*, **97**, 447-453.

Cotgreave, I.A., Moldéus, P., (1986). Methodologies for the application of monobromobimane to the silultaneous analysis of soluble and protein thiol components of biological systems. *Journal of biochemical and biophysical methods*, **13**, 231-246.

Cumberbatch, M., Kimber, I., (1992). Dermal tumour necrosis factor a induces dendritic cell migration to draining lymph nodes and possibly one stimulus for Langerhans' cell migration. *Immunology*, **75**, 237-263.(33)

Cumberbatch, M., Gould, S.J., Peters, S.W., Basketter, D.A., Dearman, RJ., Kimber, I., (1992b). Influence of topical exposure to chemical allergens on murine langerhans cells. Comparison of 2,4-dinitrochlorobenzene with trimellitic anhydride. *Journal of Clinical and Laboratory Immunology,* 1992, **37**, 65-81.

D'Amour, M., Charbonneau, M., (1992). Sex related differences in hepatic glutathione conjugation of hexachlorobenzene in rat. *Toxicology and applied pharmacology*, **112**, 229-234.

Dearman, R.J., Holliday, M.R., Corsini, E., Basketter, D.A., (1995). Skin sensitisation is associated with induced changes in cutaneous cytokine expression. *Toxicology letters,* supplement 1/78, 27.

Del Tito, B.J., Mukhtar, H., Bickers, D.R., (1983). Inhibition of epidermal metabolism and DNA binding of benzo[a]pyrene by ellagic acid. *Biochemical and biophysical research communications*, **114**, 388-394.

Dick., I.P., Scott, R.C., (1990). The influence of different strain and age on in vitro rat skin permeability to water and mannitol. *Pharmaceutical research*, **9**, 884-887.

Dick., I.P., Scott, R.C., (1990). The influence of different strain and age on rat skin permeability. *Journal of pharmacy and pharmacology*, **42**, 84P.

Dick., I.P., Scott, R.C., (1992). Pig ears as an in vitro model for human permeability. *Journal of pharmaceuticals and pharmacology*, **44**,640-645.

Donnely, T.A., King, B.D. (1994). Penetration prediction, barrier function and metabolism using an in vitro skin model. In *Prediction of percutaneous penetration*, Vol.III. IBC Technical Services, London.

Draize, J.K., Woodard, G., Cavery, H.O., (1944) Methods for the study of irritation and toxicity of substances applied to the skin and mucous membranes. *Journal of pharmacology and experimental therapeutics*, **82**, 377-390.

Dupuis, D., Rougier, A., Roguet, R., Lotte, C., Kalopissis, G., (1984). In vivo relationship between horny layer reservoir effect and percutaneous absorption in human and rat. *Journal of investigative dermatology*, **82**, 353-357.

Dupuis, D., Rougier, A., Roguet, R., Lotte, C., (1986). The measurement of the stratum corneum reservoir: a simple method to predict the influence of vehicles on in vivo percutaneous absorption. *British journal of dermatology*, **115**, 233-238.

Dykes, P.J., Edwards, M.J., O'Donovan, M.R., Merret, V., Morgan, H.E., Marks, R., (1991). In vitro reconstruction of human skin. The use of skin equivalents as potential indicators of cutaneous toxicity. *Toxicology in vitro*, **5**, 1-8.

Dykes, P.J., Jenner, L.A., Marks, R., (1982). The effect of calcium on the initiation and growth of human epidermal cells. *Archives of dermatological research*, **273**, 225-231.

Eadsforth, C.V., Moser, P., (1983). Assessment of reverse phase chromatographic methods for determining partition coefficients. *Chemosphere*, **12**, 1459-1475.

Elnarson, K., Gustafsson, J.A., Stengerg, A., (1973). Neonatal imprinting of liver microsomal hydroxylation and reduction of steroids. *Journal of biological chemistry*, **284**, 4987-4997.

Elias, P.M., Feingold, K.R., (1992). Lipids and the epidermal water barrier: Metabolism, regulation and pathophysiology. *Seminars in dermatology*, **11**, 176-182.

Enk, A.H., Katz, S.I., (1992). Early molecular events in the induction phase of contact sensitivity. *Procedings of the national acadamy of sciences, USA*, **89**, 1398.

Ernesti, A.M., Swiderek, M., Gay, R., (1992). Absorption and metabolism of topically applied testosterone in an organotypic skin culture. *Skin pharmacology*, **5**, 146-153.

Emmett, I., (1991) Toxic responses of the skin. Chapter 15 in *Toxicology*, Edited by Amdur, M.O., Doull, J., Klaassen, C.D., Pergamon press.

Falaney, C., (1991). Molecular enzymology of the human liver cytosolic sulfotransferases. *Trends in pharmacological sciences*, **12**, 255-259.

Feldman, R.J., Maibach, H.I., (1966). Percutaneous penetration of ^{14}C cortisol in man. *Journal of investigative dermatology*, **44**, 649-651.

Feldman, R.J., Maibach, H.I., (1967). Regional variation in percutaneous penetration of 14C cortisol in man. *Journal of investigative dermatology*, **48**, 181-183.

Feldman, R.J., Maibach, H.I., (1970). Absorption of some organic compounds through the skin in man. *Journal of investigative dermatology*, **54**, 399-404.

Feldman, R.J., Maibach, H.I., (1974). Percutaneous absorption of some pesticides and herbicides in man. *Toxicology and applied pharmacology*, **28**, 126-132.

Fisher, S.M., Viaje, A., Mills, G.D., Slaga, T.J., (1980). Explant methods for epidermal cell culture. *Methods in cell biology*, **21A**, 207-227.

Flowers, M.E.D., Stockschlaeder, M.A.R., Schuenig, F.G., Niederwieser, D., Hackman, R., Miller, D., Storb, R., (1987). Long term transplantation of canine keratinocytes made resistant to G418 through retrovirus mediated gene transfer. *Proceedings of the national acadamy of sciences USA*, **87**, 2349-2353.

Franz, T.J., (1975). On the relevence of *in vitro* data. *Journal of investigative dermatology*, **54**, 190.

Freidmann, P.S., (1981). Disappearance of epidermal Langerhans cells during PUVA therapy. *British journal of dermatology*, **105**, 219-221.

Fuchs, E., (1990). Epidermal differentiation: The bare essentials. *The journal of cell biology*, **111**, 2807-2814.

Fusenig, M.E., Worst, P.K.M., (1975). Mouse epidermal cell culture II. *Experimental cell research*, **93**, 443-457.

Gay, R., Swiderek, M., Nelson, D., Ernesti, A., (1992). The living skin equivalent as a model in vitro for ranking the toxic potential of dermal irritants. *Toxicology in vitro*, **6**, 303-315.

Gilchrest, B.A., Nemore, R.E., Weimstein, R., Macaig, T,. (1981). Demonstration of multiple extracutaneous hormonal influences on epidermal growth through serum free cultivation of human keratinocytes. *Journal of investigative dermatology*, **74**, 306.

Gilchrest, B.A.,(1983). In vitro assessment of keratinocyte ageing. *Journal of investigative dermatology*, **81**, 184s-189s.

Graham, M.J., Williams, F.M., Rawlins, M.D., (1991). Metabolism of aldrin to dieldrin by rat skin following topical application. *Food and chemical toxicology*, **29**, 707-711.

Green, H., Kehinde, O., Thomas, J., (1979). Growth of cultured human epidermal cells into multiple epithelia suitable for grafting. *Proceedings of the national academy of sciences*, USA, **76**, 5665-5668.

Griffith, O.W., Meister, A., (1979). Depletion of murine glutathione after treatment with buthionine sulphoximine. Procedings of the national academy of sciences, USA, **76**, 5606-6511.

Gueniche, A., Ponec, M., (1993). Use of human skin cell cultures for the estimation of potential skin irritants. *Toxicology in vitro*, **7**, 15-24.

Guo, J., Brown, R., Rothwell, C.E., Bernstein, I.A., (1990). Levels of cytochrome P450 mediated aryl hydrocarbon hydroxylase (AHH) are higher in differentiated than in germinative cutaneous keratinocytes. *Journal of investigative dermatology*, **94**, 86-93.

Guy, R.H., Hadgraft, J., (1989). *Structure-activity correlations in percutaneous absorption.* In Percutaneous absorption, Second edition. Edited by Bronaugh, R.L., and Maibach, H.I. Marcel Decker, New York.

Guy, R.H., Mak, V.H.W., Kai, T., Bommannan, D., Potts, R.O., (1990). Percutaneous penetration enhancers: mode of action. In *prediction of percutaneous penetration*, IBC Technical Services, London, pp213-223.

Habig, W.H., Pabst, M.J., Jakoby, W.B., (1974). Glutathione S-transferases. *The journal of biological chemistry*, **249**, 7130-7139.

Harvell, J.D., Tsai, Y.C., Maibach, H.I., Gay, R., Gordon, V.C., Miller, K., Mun, G.C., (1994). An in vivo correlation with three in vitro assys to assess skin irritation potential. *Journal of toxicoligy - cutaneous and occular toxicity*, **13**, 171-183.

Hawley-Nelson, P.S., Sullivan, J.E., Kung, M.,, Hennings, M., Yuspa, S.H., (1980). Optimised conditions for the growth of human epidermal cells in culture. *Journal of investigative dermatology*, **75**, 176-182.

Hewitt, P.G., Hotchkiss, S.A., Caldwell, J., (1992). Comparison of the percutaneous absorption of MbOCA and MDA through rat and human skin in vitro. *Human and Experimental Toxicology*, **11**, 585.

Heylings, J.R., Clowes, H.M., Cumberbatch, M., Dearman, R.J., Fielding, I., Hilton, J., Kimber, I., (1996). Sensitization to 2,4-dinitrochlorobenzene: Influence of vehicle on absorption and lymph node activation. *Toxicology*, **109**, 57-65.

Heymann, E., Hoppe, W., Krüsselmann, A., Tschoetschel, C., (1993). Organophosphate sensitive and insensitive carboxylesterases in human skin. *Chemical and biological interactions*, **87**, 217-226.

Higashi, T., Hiromasa, T., Tamae, A., (1990). Effects of individual mutations in the P450(2C1) activity and their distribution in the patient genome of congenital steroid 21-hydroxylase deficiency. *Journal of biochemistry*, **109**, 638-644.

Higo, N., Hinz, R.Z., Lau, D.T.W., Benet, L.Z., Guy, R.H., (1992). Cutaneous metabolism of nitroglycerin in vitro 1.Homogenised versus intact skin. *Pharmacological research*, **9**, 187-190.

Hoh, A., Maier, K., Dreher, R.M., (1987). Multilayered keratinocyte culture used for in vitro toxicology. *Molecular toxicology*, **1**, 537-546.

Horiguchi, Y., Maruguchi, T., Mauguchi, S., Suzuki, S., Fine, J.D., Leigh, I.M., Yoshiki, T., Ueda, M., Toda, K.I., Issiki, N., Imamura, S., (1994). Ultrastructural and immunohistochemical characterisation of basal cells in three-dimensional culture models of the skin. *Archives of dermatological research*, **286**, 53-61.

Horikosh, T., Balin, A.K., Carter, D.M., (1986). Effect of oxygen on the growth of human epidermal keratinocytes. *Journal of investigative dermatology*, **86**, 424-428.

Hotchkiss, S.A.M., (1992). Skin as a xenobiotic metabolising organ. *Progress in drug metabolism*, **13**, 217-262.

Hotchkiss, S.A.M., Hewitt, P., Caldwell, J., (1993). Percutaneous absorption of 4,4'-methylene-bis-(2-chloroanaline) and 4,4'-methylenedianiline through rat and human skin in vitro. *Toxicology in vitro*, **7**, 141-148.

Hotchkiss, S.A.M., (1994). How thin is your skin. *New scientist*, **1910**, 24-27.

Huckle, K.R., Smith, R.J., Watson, W.P., Wright, A.S., (1986). Comparison of hydrocarbon DNA adducts formed in mouse skin in vivo and in organ culture in vitro following treatment with benzo[a]pyrene. *Carcinogenesis*, **7**, 965-970.

Hueber, F., Schaefer, H., Wepiere, J., (1994). Role of transepidermal and transfollicular routes in percutaneous absorption of steroids: In vitro sudies on human skin. *Skin pharmacology*, **7**, 237-244.

Hughs, M.F., Fisher, H.L., Birnbaum, L.S., Hall, L.L., (1994). Effect of age on in vitro percutaneous absorption of phenols in mice. *Toxicology in vitro*, **8**, 221-227.

Hughs, M.F., Shrivastava, S.P., Fisher, H.L., Hall, L.L., (1993). Comparitive in vitro percutaneous absorption of p-substituted phenols through rat skin using static and flow-through absorption systems. *Toxicology in vitro*, **7**, 221-227.

Hulbert, P.B., Yakubu, S.I., (1982). Monobromobimane: a substrate for the fluorimetric assay of glutathione transferase. *Journal of pharmaceuticals and pharmacology*, **35**, 384-386.

Jepsen, A., MacCallum, D.K., Lillie, J.H., (1980). Fine structure of subcultivated stratified squamous epithelium. *Experimental cell research*, **125**, 140-152.

Jones, C.L., (1994). The biogenesis of underarm odour. *The biochemist*, **Feb/Mar**, 18-20.

Junge, W., (1978). Human microsomal carboxylesterase (EC 3.1.1.1). In *Enzymes in health and disease* edited by Goldberg, D.M., and Wilkinson, J.H., Basel, pp54-58.

Junge, W., (1983). Carboxylesterases, in *Methods of enzymatic analysis*, Volume four, third edition, Bergmeyer. pp2-74.

Kao, J., Patterson, F.K., Hall, J., (1985). Skin penetration and metabolism of topically applied chemicals in six mammalian species, including man: An in vitro study with benzo[a]pyrene and testosterone. *Toxicology and applied pharmacology*, **81**, 502-516.

Kao, J., Hall, J., Helman, G., (1988). In vitro percutaneous absorption in mouse skin: influence of skin appendages. *Toxicology and applied pharmacology*, **94**, 93-103.

Kao, J., Carver, M.P., (1990). Cutaneous metabolism of xenobiotics. *Drug metabolism reviews*, **22**, 363-410.

Kao, J., Carver, M.P., (1991). *Skin metabolism.* In Dermatotoxicology, 4th Edition. Edited by Marzulli, F & Maibach, H.I. Hemisphere press.

Karasek, M.A., (1966). In vitro culture of human skin epithelial cells. *Journal of investigative dermatology*, **47**, 533-540.

Kimber, I., (1993). Epidermal cytokines in contact hypersensitivity: Immunological roles and practicle applications. *Toxicology in vitro*, **7**, 295-298.

Kitano, Y., Okada, N., (1983). Separation of the epidermal shhet by dispase. *British journal of dermatology*, **108**, 555-560.

Klingenburg, M., (1958). Pigments in rat liver microsomes. *Archives of biochemistry and biophysics*, **75**, 379-386.

Koob, M., Dekant, W., (1991). Bioactivation of xenobiotics by formation of toxic glutathione conjugates. *Chemical and biological interactions*, **77**, 107-136.

Kosower, N.S., Kosower, E.M., (1987). Thiol labeling with bromobimanes. *Methods in enzymology*, **143**, 76-84.

Kupper, S., (1989). Mechanisms of cutaneous inflammation. *Archives in dermatology*, **125**, 1406-1412.

Kuroki, T., Hosomi, J., Munakata, K., Onizuka, T., Teraucki, M., Nemoto, N., (1982). Metabolism of benzo[a]pyrene in epidermal keratinocytes and dermal fibroblasts of human and mice with reference to variation among species, individuals and cell types. *Cancer research*, **42**, 1859-1865.

Lavker, R.M., Sun, T., (1982). Heterogeneity in epidermal basal keratinocytes: Morphological and functional correlations. *Science*, **215**, 1239-1241.

Laurer, A.C., Lieb, L.M., Ramachandran, C., Flynn, G.L., Weiner, N.D., (1995). Transfollicular drug delivery. *Pharmaceutical research*, **12**, 179-186.

Leider, M., Bruce, C.M., (1954). *Archives in dermatology*, **69**, 563.

Lenoir, M., Bernard, B.A., Pautrat, G., Darmon, M., Shroot, B., (1988). Outer root sheeth cells of human hair follicles are able to regenerate a fully differentiated epidermis in vitro. *Developmental biology*, **130**, 610-620.

Leo, A., Hansch, C., Elkins, D., (1971). Partition coefficients and their uses. *Chemical reviews*, **71**, 525-616.

Lillie, J.H., MacCallen, D., Jepsen, A., (1980). Fine structure of subcultivated squamous epithelium grown on collagen rafts. *Experimental cell research*, **125**, 153-165.

Lu, A.Y.H., Junk, K.W., Coon, M.J., (1969). Resolution of the cytochrome P450 containing ω-oxidation system of liver microsomes into three components. *Journal of biological chemistry*, **244**, 3714-3721.

MacConaill, M.A., Gurr, E., (1964). The histological properties of rhodanile blue. Irish journal of medical science, 251-258.

Mackness, M.I., Thompson, H.M., Hary, A.R., Walker, C.H., (1987). Distinction between A esterase and arylesterase. *Biochemical journal*, **179**, 293-296.

MacPherson, S.E., Scott, R.C., Williams, F.M., (1991). Fate of carbaryl in skin. *Archives of toxicology*, **65**, 594-596.

MacPherson, S.E., Scott, R.C., Williams, F.M., (1991). Percutaneous absorption and metabolism of aldrin by rat skin in diffusion cells. *Archives of toxicology*, **65**, 599-602.

Maggs, J.L., Kitteringham, N.R., Grabouski, P.S., Park, B.K., (1986). Drug-protein conjugates X. *Biochemical pharmacology*, **35**, 505-513.

Maibach, H.I., Feldman, R.J., (1971). Regional variation in percutaneous penetration in man. *Archives in environmental health*, **23**, 208-211.

Mannervik, B., Castro, V.M., Danielson, V.H., Tahir, M.K., Hansson, J., Ringborg, V., (1987). Expression of class pi glutathione transferase in human malignant melanoma cells. *Carcinogenesis*, **8**, 1929-1932.

Martin, R.J., Denyer, S.P., Hadgraft, J., (1987). Skin metabolism of topically applies compounds. *International journal of pharmaceutics*, **39**, 23-52.

McCracken, N.W., (1992). Role of esterases in the detoxification of pesticides. PhD thesis, University of Newcastle Upon Tyne, U.K.

McCracken, N.W., Blain, P.G., Williams, F.M., (1993a). Human xenobiotic metabolising esterases in liver and blood. *Biochemical pharmacology*, **46**, 1125-1129.

McCracken, N.W., Blain, P.G., Williams, F.M., (1993b). Peripheral esterases in the rat. Effect of classical inducers. *Chemico-biological interactions*, **87**, 183-185.

McCracken, N.W., Blain, P.G., Williams, F.M., (1993c). Nature and role of xenobiotic metabolizing esterases in rat liver, lung, skin and blood. *Biochemical Pharmacology*, **45**, 31-36.

McKenzie, R.C., Sauder, D.N., (1990). The role of keratinocytes cytokines in inflammation and immunology. *Journal of investigative dermatology*, **95**, 105S-107S.

Merk, H.F., (1989). Geriatric dermatopharmacology. *H + G Zeitschrift fur Hautkraunkhheiten*, **11**, 1015-1018.

Meyer, W., Neurand, K., (1976). The distribution of enzymes in the skin of the domestic pig. *Lab animals*, **10**, 237-247.

Meyer, W., Schwarz, R., Neurand, K., (1978). *Current problems in dermatology*, **7**, 39.

Meyer, W., Neurand, K., Radke, B., (1981). *Archives of dermatological research*, **270**, 391.

Meyer, W., Neurand, K., Radke, B., (1982). *Jounal of anatomy*, **134**, 139.

Mint, A., Hotchkiss, S.A.M., Caldwell, J., (1994). Percutaneous absorption of diethyl phthalate through rat and human skin in vitro. *Toxicology in vitro*, **8**, 251-256.

Moloney, S.J., Fromson, J.M., Bridges, J.W., (1982a). The metabolism of 7-ethoxycoumarin and 7-hydroxycoumarin by rat and hairless mouse skin strips. *Biochemical pharmacology*, **31**, 4005-4009.

Moloney, S.J., Fromson, J.M., Bridges, J.W., (1982b). Cytochrome P450 dependent deethylase activity in rat and hairless mouse skin microsomes. *Biochemical pharmacology*, **31**, 4011-4018.

Montagna, W., Yun, J.S., (1963). The skin of the domestic pig. *Journal of investigative dermatology*, **43**, 11-21.

Montagna, W., (1974). *The structure and function of skin*, 3rd edition. New York Academic Press.

Monteiro-Reviere, N.A., Bristol, D.G., Manning, T.O., Rogers, R.A., Riviere, J.E., (1990). Interspecies and ineregional analysis of the comparitive hisologic thickness and laser doppler blood flow measurements at five cutaneous sites in nine species. *Journal of investigative dermatology*, **95**, 582-586.

Moody, R.P., Grayhurst, M., Ritter, L., (1989). Evaluation of the rat tail model for estimating dermal absorption of lindane. *Journal of toxicology and environmental heath*, **28**, 317-326.

Moody, R.P., Nadeau, B., (1993). An automated in vitro dermal absorption procedure: III. In vivo and in vitro comparison with the insect repellent N,N-diethyl-m-toluamide in mouse, rat, guinea pig, pig, human and tissue cultured skin. *Toxicology in vitro*, **7**, 167-176.

Moody, R.P., Nadeau, B., Chu, I., (1994). An automated in vitro dermal absorption procedure: VI. In vivo and in vitro comparison of the organochlorine insecticide DDT in rat, guinea pig, pig, human and tissue cultured skin. *Toxicology in vitro*, **6**, 1225-1232.

Moody, R.P., Nadeau, B., Chu, I., (1994). In vitro dermal absorption of pesticides: V. In vivo and in vitro comparison of the herbicide 2,4-dichlorophenoxyacetic acid in rat, guinea pig, pig and human and tissue cultured skin. *Toxicology in vitro*, **6**, 1219-1224.

Mosmann, T., (1983). Rapid colormetric assay for cellular growth and survival: Application to proliferation and cytotoxic assays. *Journal of immunological methods*, **6**, 55-63.

Moss, T., Howels, D., Blain, P.G., Williams, F.M., (1996). Characteristics of sulphotransferases in human skin. In *Prediction of percutaneous penetration*, Edited by Brain, K.R., James, V.J., Walters, K.A. STS Publishing, Cardiff. **4b**, pp307-310.

Mukhtar, H., Bresnick, E., (1976). Glutathione-S-epoxide transferase in mouse skin and human foreskin. *Journal of investigative dermatology*, **66**, 710-714.

Mukhtar, H., Bickers, D.R., (1981a). Aminopyrine-N-demethylase activity in neonatal rat skin. *Biochemical pharmacology*, **30**, 3257-3260.

Mukhtar, H., Bickers, D.R., (1981b). Comparitive activity of the mixed-function oxidases, epoxide hydrotase and glutathione-S-transferase in liver and skin of the neonatal rat. *Drug metabolism and disposition*, **9**, 311-314.

Mukhtar, H., Bickers, D.R., (1981c). Drug metabolism in skin. *Drug metabolism and disposition*, **9**, 311-314.

Nebert, D.W., Gonzalez, F.J., (1987). P450 genes: Structure, evolution and regulation. *Annual reviews of biochemistry*, **56**, 945-993.

Nebert, D.W., Nelson, D.R., Coon, M.J., Estabrook, R.W., Feyereisen, R., Fujii-kuryama, Y., Gonzalez, F.J., Guengerich, F.P., Gunsalus, I.C., Johnson, E.F., Loper, J.C., Sato, R., Waterman, M.R., Waxman, D.J., (1991). The P-450 superfamily: Update on new sequences. gene mapping and recommended nomenclature. *DNA and cell biology*, **10**, 1-14.

Nelson, D.R., Kamataki, T., Waxman, D.J., Guengerich, F.P., Estabrook, R.W., Feyereisen, R., Gonzalez, F.J., Coon, M.J., Gunsalus, I.C., Gotoh, O., Okuda, K., Nebert, D.W., (1993). The P450 superfamily: Update on new sequences, gene mapping, accession numbers, early trivial names of enzymes, and nomenclature. *DNA and cell biology*, **12**, 1-51.

Nelson, D.R., Koymans, L., Kamataki, T., Stegeman, J.J., Feyereisen, R., Waxman, D.J., Waterman, M.R., Gotoh, O., Coon, M.J., Estabrook, R.W., Gunsalus, I.C., Nebert, D.W., (1996). P450 superfamily: Update on new sequences, gene mapping accession numbers and nomenclature. *Pharmacogenetics*, **6**, 1-42.

Ng, K.M.E., Bronaugh, R.L., Franklin, C.A., Somers, D.A., (1991). Percutaneous absorption/ metabolism of phenanthrene in the hairless guinea pig: Comparison of in vitro and in vivo results. *Fundamental and applied toxiology*, **16**, 517-524.

Nhamburo, P.T., (1990). *Biochemistry*, **29**, 5491-5499.

O'Keefe, E., Battin, T., Payne, R., (1982). Epidermal growth factor in human epidermal cells. Direct demonstration in cultured cells. *Journal of investigative dermatology*, **78**, 482-487.

O'Shaughnessy, J.A., Sultatos, L.G., (1995). Interaction of ethanol and the organphosphorus insecticide parathion. *Biochemical pharmacology*, **11**, 1925-1932.

Parry, G.E., Bunge, A.L., Silcox, G.D., Pershing, L.K., Pershing, D.W., (1990). Percutaneous absorption of benzoic acid across human skin.1. In vitro experiments and mathematical modelling. *Pharmaceutical research*, **7**, 230-236.

Peehl, D.M., Ham, R.G., (1980). Clonal growth of human keratinocytes with small amounts of dialysed serum. *In Vitro*, **16**, 526-538.

Pendlington, R.U., Williams, D.L., Naik, J.T., Sharman, R.K., (1994). Distribution of xenobiotic metabolising enzymes in skin. *Toxicology in vitro*, **8**, 525-527.

Peters, M.M.C.G., Walters, D.G., Van Omman, B., Van Bladeren, P.J., Lake, B.G., (1991) Effects of inducers of cytochrome P450 on the metabolism of [3-14C] coumarin by rat hepatic microsomes. *Xenobiotica*, **21**, 500-514.

Pham, M., Magdalou, J., Totis, M., Fournel-Gigleux, S., Siest, G., Hammock, B.D., (1989). Characterisation of distinct forms of cytochromes P450, epoxide metabolising enzymes and UDP-glucoronosyltransferases in rat skin. *Biochemical pharmacology*, **38**, 2187-2194.

Pham, M., Magdalou, J., Siest, G., Lenoir, M., Bernard, B.A., Jamoulle, J., Shroot, B., (1990). Reconstituted epidermis: A novel model for the study of drug metabolism in human epidermis. *Journal of investigative dermatology*, **94**, 749-752.

Pickett, C.B., Telakowski-Hopkins, C.A., Ding, G.J.F., Argengright, L., Lu, A.Y.H., (1984). Rat liver glutathione-S-transferase: Complete nucleotide sequence of a glutathione-S-transferase mRNA and the regulation of the Ya, Yb and Yc mRNAs by 3-methylcholanthrene and phenobarbital. *Journal of biological chemistry*, **259**, 5182-5188.

Pinkis, H., Mehregan, A.H., (1981). Norman structure of skin, chapter 2 in *A guide to dermatohistopathology*, third edition, New York press.

Pittlekow, M.R., Scott, R.E., (1987). New techniques for the in vitro culture of human skin keratinocytes and perspectives on their use for grafting of patients with extensive burns. *Mayo clinic proceedings*, **61**, 771-777.

Plummer, J.L., Smith, B.R., Sies, H., Bend, J.R., (1981). Chemical depletion of glutathione in vivo. *Methods in enzymology*, **77**, 50-63.

Ponec, M., (1991). Reconstruction of human epidermis on de-epidermized demis. Expression of differentiation-specific protein markers and lipid composition. *Toxicology in vitro*, **5**, 597-606.

Potts, R.O., Francoeur, M.L., (1991). The influence of stratum corneum morphology on water permeability. Journal of investigative dermatology, 96, 495-499.

Potts, R.O., Bommannan, B., Guy, R.H., (1992). Percutaneous absorption. *In Pharmacology of the skin*, Edited by Mukhtar, H., CRC Press, pp13-27.
Potts, R.O., Guy, R.H., (1992). Predicting skin permeability. *Pharmaceutical research*, **9**, 663-669.

Prunieras, M., Regnier, M., Woodley, D., (1983). Methods for cultivation of keratinocytes with an air-liquid interface. *Journal of investigative dermatology*, **81**, 28s-33s.

Raffali, F., Rougier, A., Roguet, R., (1994). Measurement and modulation of cytochrome P450 dependent enzyme activity in cultured human keratinocytes. *Skin pharmacology*, **7**, 345-354.

Raza, H., Yogesh, C., Awasthi, M., Zaim, T., Eckert, R.L., Mukhtar, H., (1991). Glutathione S-transferases in human and rodent skin: Multiple forms and species-specific expression. *Journal of investigative dermatology*, **96**, 463-467.

Raza, H., Agarwal, R., Bickers, D.R., Mukhtar, H., (1992). Purification and molecular characterisation of ß-naphthoflavone-inducible cytochrome P450 from rat epidermis. *Journal of investigative dermatology*, **98**, 233-240.

Raza, H., Mukhtar, H., (1993). Differences in inducibility of cytochrome P450 1A1 monooxygenases and glutathione-S-transferases in cutaneous and extracutaneous tissues after topical and parental administration of ß-naphthoflavone to rats. *International journal of biochemistry*, **25**, 1511-1516.

Régnier, M., Pruniéras, M., Woodley, D., (1981) Growth and differntiation of adult human epidermal cells on dermal substrates. *Frontiers of matrix biology*, **9**, 4-35.

Reifenrath, W.G., Kemppainen, P.K., (1991). Skin storage conditions, chapter 9 in *In vitro percutaneous absorption: Principles, fundamentals and applications.* Edited by Bronaugh, R.L., and Maibach, H.I. CRC Press.

Reiners, J.J, Cantu, A.R., Pavone, A., (1990). Modulation of constitutive cytochrome P450 expression in vivo and in vitro in murine keratinocytes as a function of differentiation and extracellular Ca++ concentration. *Procedings of the national academy of sciences, USA*, **87**, 1825-1829.

Rettie, A.E., Williams, F.M., Rawlins, M.D., (1986). Substrate specificity of mouse skin mixed function oxidase system. *Xenobiotica*, **16**, 205-211.

Rettie, A.E., Williams, F.M., Rawlins, M.D., Mayers, R.T., Burke, M.D., (1986). Major differences between lung, skin and liver in the microsomal metabolism of homologous series of resorufin and coumarin ethers. *Biochemical pharmacology*, **35**, 3495-3500.

Rheinwald, J.G., Green, H., (1975). Serial cultivation of strains of human epidermal keratinocytes; the formation of keratinizing colonies from single cells. *Cell*, **6**, 331-334.

Rheinwald, J.G., (1980). Serial cultivation of normal human epidermal keratinocytes. *Methods in cell biology*, **21A**, 229-254.

Robine-Leon, S., Appay, M.D., Chavalier, G., Zweibaum, A., (1981). Proliferation, differentiation and maturation of mouse epidermal keratinocyte cell line. *Experimental cell research*, **133**, 273-284.

Roguet, R., Cohen, C., Dossou, K.G., Rougier, A., (1994). Episkin, a reconstituted human epidermis for assessing in vitro the irritancy of topically applied compounds. *Toxicology in vitro*, **8**, 283-291.

Roguet, R., Cotovio, J., Rougier, A., Kremers, P., Leclaire, J., (1994). Measurement and induction of cytochrome P450 dependent enzyme activities in a reconstituted human epidermis.

Roskos, K.V., Maibach, H.I., Guy, R.H., (1989). The effect of ageing on percutaneous absorption in man. *Journal of pharmacokinetics and biopharmaceutics*, **17**, 617-630.

Rougier, A., Dupuis, D., Lotte, C., Roguet, R., Schaefer, H., (1983). In vivo correlation between stratum corneum reservoir function and percutaneous absorption. *Journal of investigative dermatology*, **81**, 275-278.

Rougier, A., Dupuis, D., Lotte, C., Roguet, R.,(1985). The measurement of the stratum corneum reservoir. A predictive method for in vivo percutaneous absorption studies: Influence of application time. *Journal of investigative dermatology*, **84**, 66-68.

Rougier, A., Lotte, C., Corcuff, P., Maibach, H.I., (1988). Relationship between skin permeability and corneocyte size according to anatomic site, age and sex in man. *Journal for the society of cosmetic chemistry*, **39**, 15-26.

Schaffer, H., Jamoulle, J.C., (1988). Skin pharmacokinetics. *International journal of dermatology*, **27**, 351-359.

Schmidt, R.J., Read, D.C., (1996). An electrochemical approach to the study of prohapten activation: A possible nitroreductase model. *Prediction of percutaneous penetration*, Edited by Brain, K.R., James, V.J., Walters, K.A. STS Publishing, Cardiff. **4b**, 222-226.

Scott, R.C., Walker, M., Dugard, P.H., (1986). In vitro percutaneous absorption experiments: A technique for the production of intact epidermal membranes from rat skin. *Journal of the society of cosmetic chemistry*, **37**, 35-41.

Scott, R.C., Corrigan, M.A., Smith, F., Mason, H., (1991). The influence of skin structure on permeability: an intersite and interspecies comparison with hydrophobic penetrants. *Journal of investigative dermatology*, **96**, 921-925.

Shaefer, H., (1993). Penetration and pecutaneous absorption of topical retanoids. A review. *Skin pharmacology*, **6**, 17-23.

Shah, P.V., Fisher, H.L., Sumler, M.R., (1987). Comparison of the penetration of 14 pesticides through the skin of young and adult rats. *Journal of toxicology and environmental health*, **21**, 3553-366.

Shipley, G.D., Pittlekow, M.R., (1987). Control of growth and differentiation in vitro of human keratinocytes cultured in serum-free medium. *Archives of dermatology*, **123**, 1541a-1544a.

Singhal, S.S., Saxena, M., Awasthi, S., Mukhtar, H., Zaidi, S.I.A., Ahmed, H., Awasthi, Y.C., (1993). Glutathione S-transferases of human skin: qualitative and quantitative differences in men and women. *Biochimica et biophysica acta*, **1163**, 266-272.

Slivka, S.R., (1992). Testosterone metabolism in an in vitro skin model. *Cell biology and toxicology*, **8**, 267-276.

Slivka, S.R., Landeen, L.K., Zeigler, F., Zimber, M.P., Bartel, R.L., (1993). Characterisation, barrier function, and drug metabolism of an in vitro skin model. *Journal of investigative dermatology*, **100**, 40-46.

Smith, H.F.,(1962). *American Industrial Hygeine Assossiation Journal*, **23**, 95.

Smith, P.K., Krohn, R.I., Hermanson, G.T., Mallia, A.K., Gartner, F.H., Provenzano, M.D., Fujimoto, F.K., Goeke, N.M., Olsen, B.J., Klenk, D.C., (1985). Measurement of protein using bicinchoninic acid. *Analytical chemistry*, **150**, 76-85.

Soucek, P., Gut, I., (1992). Cytochrome P450 in rats: structures, functions and properties and relevent human forms. *Xenobiotica*, **22**, 83-103.

Stadler, R., Detmar, M., Stephenek, K., Bangemann, C., Orfanos, C.E., (1989). A rapid fluorimetric assay for the determination of keratinocyte proliferation in vitro. *Journal of investigative dermatology*, **93**, 532-534.

Steinstrasser, I., Merkle, H.P., (1995). Dermal metabolism of topically applied drugs: Pathways and models reconsidered. *Pharmaceutica acta helvetiae*, **70**, 3-24.

Storm, J.E., Collier, S.W., Stewart, R.F., Bronaugh, R.L., (1990). Metabolism of xenobiotics during percutaneous penetration: Role of absorption rate and cutaneous enzyme activity. *Fundamental and applied toxicology*, **15**, 132-141.

Summer, K., Göggelmann, W., (1980). 1-Chloro-2,4-dinitrobenzene depletes glutathione in rat skin and is mutagenic in Salmonella typhimurium. *Mutation research*, **77**, 91-93.

Swabrick, J., Lee, G., Brom, J., (1982). Drug permeation through human skin.1. Effect of storage conditions on skin. *Journal of investigative dermatology*, **78**, 63-66.

Talmadge, J.E., Bowersox, O., Tribble, H., Lee, S.H., Shepard, H.M., Liggitt, D., (1987). Toxicity of tumour necrosis factors synergistic with gamma interferon and can be reduced with cyclooxygenase inhibitors. *American journal of pathology*, **128**, 410-425.

Theall, G., Eisinger, M., Gunberger, D., (1981). Metabolism of benzo[a]pyrene and DNA adduct formation in cultured human epidermal keratinocytes. *Carcinogenesis*, **2**, 581-587.

Thody, A., (1995). Epidermal melanocytes: Their regulation and role in the skin pigmentation. *European journal of dermatology*, **5**, 558-565.

Tsao, M.C., Walthall, B.J., Ham, R.G., (1982). Clonal growth of normal human epidermal keratinocytes in a defined medium. *Journal of cell physiology*, **110**, 219-229.

Van Berzooijen, C.F.A., (1984). Influence of age related changes in rodent liver morphology and physiology on drug metabolism - a review. *Mechanisms of ageing and development*, **25**, 1-22.

Van Bladeren, P.J., Van Ommen, B., (1991). The inhibition of glutathione S-transferases: Mechanisms, toxic cosequenses and therapeutic benifits. *Pharmacology and therapeutics*, **51**, 35-46.

Van De Sandt, J.J.M., Rutten, A.A.J.J.L., Van Ommen, B., (1993). Species specific cutaneous biotransformation of the pesticide propoxur during percutaneous absorption in vitro. *Toxicology and applied pharmacology*, **123**, 144-150.

Vaughan, F.L., Kass, L.L., Vamen, J.A., (1981). Requirement of hydrocortisone and insulin for extended proliferation and passage of rat keratinocytes. *In vitro*, **11**, 941-946.

Vecchini, F., Michel, S., (1994). Importance of cytochrome P450 for the development of new drug concepts in the skin. *European journal of dermatology*, **4**, 583-588.

Vellom, D.C., Radic, Z., Li, Y., Pickering, N.A., Camp, S., Taylor, P., (1993). Amino acid residues controlling acetylcholinesterase and butylcholinesterase specificity. *Biochemistry*, **32**, 12-17.

Vessey, D.A., Lee, K., (1993). Inactivation of enzymes of the glutathione antioxidants system by treatment of cultured human keratinocytes with peroxides. *Journal of investigative dermatology*, **100**, 829-833.

Venkatesh, K., Levi, P.E., Inman, A.O., Monteiro-Riviere, N.A., Misra, R., Hodgson, E., (1992). Enzymatic and immunohistochemical studies on the role of cytochrome P450 and the flavin-containing monooxygenase of mouse skin in the metabolism of pesticides and other xenobiotics. *Pesticide biochemistry and pharmacology*, **43**, 53-66.

Walter, K., Kurz, H., (1988). Binding of drugs to human skin: influencing factors and the role of tissue lipids. *Journal of pharmacy and pharmacology*, **40**, 689-693.

Watson, W.P., Smith, R.J., Huckle, K.R., Wright, A.S., (1988). Human organ culture techniques for the detection and evaluation of genotoxic agents. *IARC Sci. Publ*, **89**, 384-388.

Watt, F.M., Green, H., (1982). Stratification and terminal differentiation of cultured epidermal cells. *Nature*, **295**, 434-436.

Watt, F.M., (1988). Epidermal stem cells in culture. *Journal of cellular science, supplement*, **10**, 85.

Wester, R.C., Maibach, H.I., (1982). Percutaneous absorption of drugs. *Clinical pharmacokinetics*, **23**, 253-266.

Wester, R.C., Maibach, H.I., (1983). Cutaneous pharmacokinetics: 10 steps to percutaneous absorption.. *Drug metabolism reviews*, **14**, 169-205.

Wester, R.C., Maibach, H.I., Sedik, L., Melendres, J., Dizio, S., Wade, M., (1991). In vitro percutaneous absorption of cadmium from water and soil into human skin. *Fundamental and applied toxicology*, **19**, 1-5.

Wester, R.C., Sedik, L., Melendres, J., Logan, F., Maibach, H.I., Russell, I., (1993). Percutaneous absorption of diazinon in humans. *Food and chemical toxicology*, **31**, 569-572.

Wilce, M.C.J., Parker, M.W., (1994). Structure and function of glutathione S-transferases. *Biochimica et biophysica acta*, **1205**, 1-18.

Williams, D., Woodhouse, K., (1995a). The relationship between age and cutaneous aryl hydrocarbon hydroxylase (AHH) activity. *Age and ageing*, **24**, 213-216.

Williams, D., Woodhouse, K., (1995b). Age related changes in NADPH cytochrome *c* reductase activity in mouse skin and liver microsomes. *Archives of gerontology and geriatrics*, **21**, 191-197.

Williams, F.M., Rettie, A.E., Rawlins, M.D., (1985). Aldrin metabolism in the skin. *Human toxicology*, **4**, 108.

Williams, R.T. (1975). Interspecies variations in the metabolism of xenobiotics. *Biochemistry society transactions*, **2**, 359-377.

Wolf, J., (1934). Die innere stuckter der zellen des stratum desquamans der menschlichen epidermis. *Z. Mikroscop. Anat. Forsch*, **46**, 170-202.

Wong, K.O., Tan, A.Y.H., Lim, B.G., Wong, K.P., (1993). Sulfate conjugation of minoxidil in rat skin. *Biochemical pharmacology*, **45**, 1180-1182.
Wood, E.J., Raxworthy, M.J., (1994). In vitro reconstruction of human skin. *The biochemist*, **Feb/Mar**, 3-7.

Woodhouse, K.W., Williams, F.M., Mutch, E., Wright, P., James, O.F.W., Rawlins, M.D., (1983). The effect of alcoholic cirrhosis on the activities of microsomal alsrin epoxidase, 7-ethoxycoumarin *O*-deethylase and epoxide hydrolase, and on the concentrations of reduced glutathione in human liver. *British journal of pharmacology*, **15**, 667-672.

Yuspa, S.H., Morgan, D.L., Walker, R.J., Bates, R.R., (1970). The growth of fetal mouse skin in cell culture and transplantation to F1 mice. *Journal of investigative dermatology*, **55**, 379-389.

Zeigler, D.H., (1990). Flavin containing monooxygenases: enzymes adapted for multisubstrate specificity. *Trends in pharmacological sciences*, **11**, 321-324.

Appendices

Appendix 1

Absorption of dinitrochlorobenzene

Species . . . . . Balb C Mouse Absorption system . . . . . Flow-through

Dose and vehicle . . . . . 25μg cm^2 in acetone (25μl/cm^2) Occlusion . . . . . no

Material absorbed into the receptor fluid. mean ± SD, sem (n=6), n is for 6 individual skins.						
Time (hours)	DNCB (μg cm^2)	SD	sem	Conjugated DNCB (μg/cm^2)	SD	sem
2	0.569	0.089	0.037	2.851	0.749	0.306
4	1.515	0.220	0.089	5.252	1.164	0.475
6	2.245	0.278	0,114	7.201	1.304	0.532
8	2.852	0.257	0.105	8.559	1.217	0.497
10	3.452	0.234	0.095	9.406	1.125	0.495
12	3.982	0.246	0.100	10.094	0.969	0.396
14	4.395	0.229	0.094	10.620	0.907	0.370
16	4.813	0.227	0.093	10.986	0.839	0.343
18	5.188	0.217	0.089	11.317	0.779	0.318
20	5.532	0.236	0.096	11.584	0.743	0.303
22	5.826	0.272	0.111	11.812	0.721	0.295
24	6.192	0.271	0.110	12.053	0.703	0.287

Disposition of remaining material after 24 hours mean ± SD, sem (n=6), n is for 6 individual skins.			
	DNCBμg cm^2	SD	sem
Wash	2.130	0.419	0.171
Filter	6.403	1.354	0.553
Donor cell	0.497	0.353	0.144
Tape strip	0.000	0.000	0.000
Skin-Biolute S fraction	1.691	0.547	0.223
Skin-Hexane fraction	0.373	0.306	0.125
Skin-Aqueous fraction	0.000	0.000	0.000
Total in skin	2.064	0.744	0.304

Appendix 2

Absorption of dinitrochlorobenzene

Species . . . . . Balb/C Mouse Absorption system . . . . . Flow-through

Dose and vehicle . . . . . 25μg/cm^2 in propylene glycol(25μl/cm^2) Occlusion . . . . . no

Material absorbed into the receptor fluid. mean ± SD, sem (n=6), n is for 6 individual skins.						
Time (hours)	DNCB (μg cm^2)	SD	sem	Conjugated DNCB (μg/cm^2)	SD	sem
2	0.218	0.019	0.008	0.676	0.99	0.41
4	0.448	0.037	0.015	1.752	0.204	0.083
6	0.647	0.037	0.015	3.123	0.364	0.149
8	0.895	0.041	0.017	4.467	0.509	0.208
10	1.216	0.074	0.030	5.649	0.615	0.251
12	1.565	0.128	0.052	6.748	0.738	0.301
14	1.943	0.164	0.067	7.812	0.796	0.325
16	2.332	0.208	0.085	8.823	0.797	0.325
18	2.771	0.257	0.105	9.719	0.866	0.353
20	3.204	0.286	0.117	10.597	0.983	0.401
22	3.596	0.335	0.137	11.474	1.195	0.488
24	3.964	0.362	0.148	12.326	1.435	0.586

Disposition of remaining material after 24 hours mean ± SD, sem (n=6), n is for 6 individual skins.			
	DNCBμg cm^2	SD	sem
Wash	3.830	1.344	0.549
Filter	3.140	0.340	0.139
Donor cell	0.385	0.092	0.034
Tape strip	0.000	0.000	0.000
Skin Biolute S fraction	3.870	1.674	0.683
Skin Hexane fraction	1.207	0.501	0.211
Skin-Aqueous fraction	0.000	0.000	0.000
Total in skin	5.077	2.166	0.884

Appendix 3

Absorption of dinitrochlorobenzene

Species . . . . . Balb/c mouse Absorption system . . . . . Flow-through

Dose and vehicle . . . . . 25μg/cm^2 in acetone (25μl/cm^2) Occlusion . . . . . yes

Material absorbed into the receptor fluid. mean ± SD, sem (n=6), n is for 6 individual skins.						
Time (hours)	DNCB (μg/cm^2)	SD	sem	Conjugated DNCB (μg/cm^2)	SD	sem
2	0.406	1.406	0.574	1.812	0.250	0.102
4	2.876	1.047	0.427	5.156	0.609	0.249
6	5.000	1.718	0.707	7.188	0.922	0.376
12	-	-	-	-	-	-
[illegible]		-	-	-	-	-
24	9.062	2.484	1.014	12.844	1.938	0.791

Disposition of remaining material after 24 hours mean ± SD, sem (n=6), n is for 6 individual skins.			
	DNCBμg cm^2	SD	sem
Parafilm	0.375	0.266	0.108
Wash	0.109	0.094	0.038
Skin-Biolute S fraction	7.094	3.703	1.512

Appendix 4

Absorption of dinitrochlorobenzene

Species . . . . . Balb/C Mouse Absorption system . . . . . Static

Dose and vehicle . . . . . 25μg/cm^2 in acetone(25μl/cm^2) Occlusion . . . . . no

Material absorbed into the receptor fluid. mean ± SD, sem (n=6), n is for 6 individual skins.						
Time (hours)	DNCB (μg/cm^2)	SD	sem	Conjugated DNCB (μg/cm^2)	SD	sem
2	1.681	0.507	0.207	2.618	0.403	0.165
4	3.813	0.980	0.400	4.573	0.421	0.172
6	6.056	1.110	0.454	6.391	0.661	0.269
12	7.449	0.681	0.278	8.964	0.974	0.398
24	7.691	0.848	0.346	11.013	1.572	0.642

Disposition of remaining material after 24 hours mean ± SD, sem (n=6), n is for 6 individual skins.			
	DNCBμg cm^2	SD	sem
Wash	2.513	0.244	0.099
Filter	3.201	0.777	0.317
Donor cell	0.190	0.051	0.021
Tape strip	0.000	0.000	0.000
Skin Biolute S fraction	3.512	0.506	0.206
Skin-Hexane fraction	1.858	0.889	0.363
Skin-Aqueous fraction	0.000	0.000	0.000
Total in skin	5.370	1.352	0.552

Appendix 5

Absorption of dinitrochlorobenzene

Species . . . . . Balb/C Mouse Absorption system . . . . . Static

Dose and vehicle . . . . . 25μg/cm^2 in propylene glycol(25μl/cm^2) Occlusion . . . . . no

Material absorbed into the receptor fluid. mean ± SD, sem (n=6), n is for 6 individual skins.						
Time (hours)	DNCB (μg/cm^2)	SD	sem	Conjugated DNCB (μg/cm^2)	SD	sem
2	0.477	0.094	0.038	0.873	0.166	0.068
4	0.702	0.169	0.069	1.976	0.413	0.168
6	1.124	0.247	0.101	3.540	0.599	0.245
12	2.597	0.489	0.199	6.775	1.182	0.408
24	4.114	0.234	0.096	10.347	1.662	0.679

Disposition of remaining material after 24 hours mean ± SD, sem (n=6), n is for 6 individual skins.			
	DNCBμg/cm^2	SD	sem
Wash	3.965	1.033	0.422
Filter	1.158	0.275	0.112
Donor cell	0.516	0.327	0.133
Tape strip	0.000	0.000	0.000
Skin-Biolute S fraction	8.210	1.793	0.732
Skin-Hexane fraction	1.737	0.647	0.264
Skin-Aqueous fraction	0.000	0.000	0.000
Total in skin	9.947	2.049	0.836

Appendix 6

Absorption of dinitrochlorobenzene

Species . . . . . Balb/C Mouse Absorption system . . . . . Flow-through

Dose and vehicle . . . . . 125μg/cm^2 in acetone (25μl/cm^2) Occlusion . . . . . no

Material absorbed into the receptor fluid. mean ± SD, sem (n=6), n is for 6 individual skins.						
Time (hours)	DNCB (μg/cm^2)	SD	sem	Conjugated DNCB (μg/cm^2)	SD	sem
2	1.031	0.365	0.149	5.114	1.609	0.657
4	3.792	1.429	0.584	10.287	2.142	0.875
6	6.804	1.624	0.663	15.160	3.745	1.529
8	9.497	1.592	0.649	18.489	4.848	1.979
10	11.528	1.662	0.678	20.539	5.529	2.257
12	13.366	1.723	0.704	21.891	5.923	2.418
14	14.935	1.796	0.733	22.806	6.211	2.535
16	16.393	1.910	0.779	23.481	6.390	2.609
18	17.684	2.039	0.833	24.056	6.526	2.664
20	18.875	2.149	0.877	24.494	6.603	2.696
22	19.984	2.291	0.935	24.868	6.659	2.719
24	21.148	2.372	0.968	25.244	6.702	2.744

Disposition of remaining material after 24 hours mean ± SD, sem (n=6), n is for 6 individual skins.			
	DNCBμg/cm^2	SD	sem
Wash	5.125	3.389	1.384
Filter	40.498	7.573	3.092
Donor cell	0.890	0.881	0.359
Tape strip	0.000	0.000	0.000
Skin-Biolute S fraction	16.907	7.044	2.876
Skin-Hexane fraction	4.371	2.498	1.018
Skin-Aqueous fraction	0.267	0.164	0.069
Total in skin	21.545	9.694	3.958

Appendix 7

Absorption of dinitrochlorobenzene

Species . . . . . Balb/C Mouse Absorption system . . . . . Flow-through

Dose and vehicle . . . . . 125μg/cm^2 in propylene glycol(25μl/cm^2) Occlusion . . . . . no

Material absorbed into the receptor fluid. mean ± SD, sem (n=6), n is for 6 individual skins.						
Time (hours)	DNCB (μg/cm^2)	SD	sem	Conjugated DNCB (μg/cm^2)	SD	sem
2	0.230	0.024	0.009	1.558	0.436	0.178
4	0.888	0.179	0.073	4.357	1.279	0.522
6	1.963	0.425	0.174	7.885	2.496	1.019
8	3.307	0.749	0.306	10.960	3.696	1.509
10	4.590	1.048	0.428	13.067	4.549	1.857
12	5.941	1.329	0.543	14.777	5.196	2.121
14	7.137	1.576	0.643	15.992	5.643	2.304
16	8.395	1.818	0.742	16.936	5.903	2.412
18	9.622	2.031	0.829	17.706	6.129	2.502
20	11.003	2.259	0.922	18.261	6.263	2.557
22	12.400	2.447	0.999	18.809	6.383	2.606
24	14.001	2.697	1.101	19.325	6.427	2.624

Disposition of remaining material after 24 hours mean ± SD, sem (n=6), n is for 6 individual skins.			
	DNCBμg/cm^2	SD	sem
Wash	7.020	1.606	0.656
Filter	12.688	2.435	0.994
Donor cell	0.923	0.738	0.301
Tape strip	0.000	0.000	0.000
Skin-Biolute S fraction	47.393	20.556	8.392
Skin-Hexane fraction	6.433	4.069	1.661
Skin-Aqueous fraction	0.368	0.236	0.096
Total in skin	54.194	21.734	8.873

Appendix 8

Absorption of dinitrochlorobenzene

Species . . . . . Balb/C Mouse Absorption system . . . . . Flow-through

Dose and vehicle . . . . . 125μg/cm^2 in acetone(25μl/cm^2) Occlusion . . . . . no

Study with mice pretreated with buthionine sulfoximine (BSO).

Material absorbed into the receptor fluid.								
BSO treated mice mean ± SD, sem (n=4), n is for 4 individual skins.							control mice mean of 2	
Time (hours)	DNCB μg/cm^2	SD	sem	Conjugated DNCB μg/cm^2	SD	sem	DNCB μg/cm^2	conjugated DNCB μg/cm^2
2	0.941	0.304	0.152	2.974	0.662	0.311	0.828	3.852
4	3.260	0.834	0.417	6.078	1.084	0.542	3.503	7.071
6	6.512	1.711	0.856	9.053	1.903	0.952	6.233	9.602
8	9.683	2.181	1.091	11.561	2.819	1.409	8.674	11.296
10	12.193	2.473	1.236	13.528	3.752	1.876	10.905	12.571
12	14.363	2.811	1.405	15.083	4.487	2.242	12.851	13.566
14	16.162	3.000	1.500	16.427	5.094	2.547	14.403	14.463
16	17.783	3.112	1.558	17.656	5.597	2.798	15.883	15.264
18	19.183	3.225	1.612	18.773	6.069	3.035	17.053	15.925
20	20.507	3.214	1.607	19.837	6.474	3.237	18.219	15.589
22	21.653	3.101	1.551	21.061	7.038	3.519	19.114	17.509
24	22.762	3.043	1.521	22.256	7.621	3.811	19.897	18.534

Disposition of remaining material after 24 hours				
	BSO treated mice mean ± SD, sem (n=6)			Control mice mean of 2
	DNCB μg/cm^2	SD	sem	DNCB μg/cm^2
Wash	3.155	0.589	0.295	2.745
Filter	36.788	3.979	1.994	33.83
Donor cell	0.655	0.410	0.205	0.905
Tape strip	0.000	0.000	0.000	0.000
Skin-Biolute S fraction	13.920	3.938	1.969	9.810
Skin-Hexane fraction	4.193	3.521	1.760	1.255
Skin-Aqueous fraction	0.000	0.000	0.000	0.000
Total in skin	18.113	7.426	3.713	11.065

Appendix 9

Absorption of dinitrochlorobenzene

Species . . . . . Balb/C Mouse Absorption system . . . . . Flow-through

Dose and vehicle . . . . . 125μg/cm^2 in propylene glycol(25μl/cm^2) Occlusion . . . . . no

Study with mice pretreated with buthionine sulfoximine (BSO).

Material absorbed into the receptor fluid.								
BSO treated mice mean ± SD, sem (n=4), n is for 4 individual skins.							control mice mean of 2	
Time (hours)	DNCB μg/cm^2	SD	sem	Conjugated DNCB μg/cm^2	SD	sem	DNCB μg/cm^2	conjugated DNCB μg/cm^2
2	0.310	0.089	0.45	1.200	1.001	0.500	0.213	0.525
4	0.971	0.337	0.169	2.772	1.344	0.672	0.612	1.759
6	2.222	0.688	0.344	4.219	1.753	0.876	1.361	3.012
8	3.959	0.916	0.458	5.905	1.925	0.962	2.339	3.954
10	5.159	1.272	0.636	7.790	1.782	0.891	3.568	5.275
12	8.578	0.906	0.453	9.927	1.614	0.807	5.147	6.771
14	10.954	1.055	0.528	12.243	3.119	1.559	7.803	8.830
16	13.511	1.380	0.690	14.821	6.160	3.080	8.275	11.210
18	15.936	1.800	0.900	17.534	9.801	4.901	10.078	13.554
20	18.341	2.261	1.130	20.138	13.106	6.553	12.005	15.859
22	20.489	2.541	1.270	22.602	15.895	7.947	13.645	18.091
24	22.465	2.851	1.426	24.884	18.209	9.104	14.818	20.400

Disposition of remaining material after 24 hours				
	BSO treated mice mean ± SD, sem (n=6)			Control mice mean of 2
	DNCB μg/cm^2	SD	sem	DNCB μg/cm^2
Wash	9.238	2.763	1.381	4.045
Filter	10.26	2.733	1.367	8.395
Donor cell	1.142	0.506	0.253	0.310
Tape strip	0.000	0.000	0.000	0.000
Skin-Biolute S fraction	24.122	8.264	4.132	18.105
Skin-Hexane fraction	6.797	4.814	2.407	15.195
Skin-Aqueous fraction	0.000	0.000	0000	0.000
Total in skin	30.920	7.977	3.989	33.300

Appendix 10

Absorption of dinitrochlorobenzene

Species . . . . . Balb/C mouse Absorption system . . . . . Flow-through

Dose and vehicle . . . . . 125μg/cm^2 in acetone (25μl/cm^2) Occlusion . . . . . yes

Material absorbed into the receptor fluid. mean ± SD, sem (n=6), n is for 6 individual skins.						
Time (hours)	DNCB (μg/cm^2)	SD	sem	Conjugated DNCB (μg/cm^2)	SD	sem
2	1.578	1.406	0.574	3.156	0.344	0.140
4	11.219	6.828	2.787	9.218	1.328	0.542
6	20.750	1.063	0.434	13.437	2.094	0.855
12	-	-	-	-	-	-
[illegible]	-	-	-	-	-	-
24	45.984	9.422	3.846	25.953	4.641	1.895

Disposition of remaining material after 24 hours mean ± SD, sem (n=6), n is for 6 individual skins.			
	DNCBμg/cm^2	SD	sem
Parafilm	2.875	1.188	0.485
Wash	0.296	0.125	0.051
Skin-Biolute S fraction	24.750	5.828	2.379

Appendix 11

Absorption of dinitrochlorobenzene

Species . . . . . Balb/C Mouse Absorption system . . . . . Static

Dose and vehicle . . . . . 125μg/cm^2 in acetone(25μl/cm^2) Occlusion . . . . . no

Material absorbed into the receptor fluid. mean ± SD, sem (n=6), n is for 6 individual skins.						
Time (hours)	DNCB (μg/cm^2)	SD	sem	Conjugated DNCB (μg/cm^2)	SD	sem
2	2.818	1.083	0.442	2.869	0.601	0.245
4	13.090	3.272	1.336	6.259	0.624	0.255
6	25.254	6.486	2.648	9.509	1.038	0.424
12	42.958	10.199	4.164	15.719	2.816	1.149
24	52.636	11.283	4.606	19.004	4.283	1.748

Disposition of remaining material after 24 hours mean ± SD, sem (n=6), n is for 6 individual skins.			
	DNCBμg cm^2	SD	sem
Wash	8.962	2.377	0.970
Filter	13.205	3.056	1.248
Donor cell	0.573	0.266	0.108
Tape strip	0.000	0.000	0.000
Skin-Biolute S fraction	38.571	17.391	7.099
Skin-Hexane fraction	25.77	6.966	2.844
Skin-Aqueous fraction	1.671	0.723	0.295
Total in skin	66.012	18.358	7.495

Appendix 12

Absorption of dinitrochlorobenzene

Species . . . . . Balb/C Mouse Absorption system . . . . . Static

Dose and vehicle . . . . . 125μg/cm^2 in propylene glycol(25μl/cm^2) Occlusion . . . . . no

Material absorbed into the receptor fluid. mean ± SD, sem (n=6), n is for 6 individual skins.						
Time (hours)	DNCB (μg/cm^2)	SD	sem	Conjugated DNCB (μg/cm^2)	SD	sem
2	1.058	0.494	0.202	1.869	0.526	0.215
4	4.616	2.075	0.847	4.548	0.991	0.405
6	8.652	2.984	1.218	7.830	2.261	0.923
12	17.239	5.366	2.191	14.517	4.332	1.769
24	26.189	6.152	2.512	19.077	6.076	2.480

Disposition of remaining material after 24 hours mean ± SD, sem (n=6), n is for 6 individual skins.			
	DNCBμg/cm^2	SD	sem
Wash	13.793	4.001	1.633
Filter	6.085	0.578	0.236
Donor cell	1.982	0.902	0.368
Tape strip	0.000	0.000	0.000
Skin-Biolute S fraction	61.658	42.391	17.306
Skin-Hexane fraction	24.005	7.362	3.005
Skin-Aqueous fraction	1.710	0.649	0.265
Total in skin	87.373	43.226	17.647

Appendix 13

Absorption of dinitrochlorobenzene

Species . . . . . Balb/C Mouse Absorption system . . . . . Static

Dose and vehicle . . . . . 125μg/cm^2 in acetone(25μl/cm^2) Occlusion . . . . . no

Study with mice pretreated with buthionine sulfoximine (BSO).

Material absorbed into the receptor fluid.								
BSO treated mice mean ± SD, sem (n=4), n is for 4 individual skins.							control mice mean of 2	
Time (hours)	DNCB μg/cm^2	SD	sem	Conjugated DNCB μg/cm^2	SD	sem	DNCB μg/cm^2	conjugated DNCB μg/cm^2
2	5.456	1.633	0.827	2.678	0.209	0.104	2.016	2.737
4	18.078	7.538	3.769	4.906	0.502	0.251	7.473	5.798
6	31.244	11.402	5.702	6.347	0.491	0.246	16.473	7.903
12	50.588	8.879	4.439	10.038	1.799	0.899	40.094	14.629
24	57.025	6.609	2.804	10.509	0.216	0.108	45.634	15.765

Disposition of remaining material after 24 hours				
	BSO treated mice mean ± SD, sem (n=6)			Control mice mean of 2
	DNCB μg/cm^2	SD	sem	DNCB μg/cm^2
Wash	4.838	1.455	0.727	4.045
Filter	10.180	2.964	1.482	8.395
Donor cell	0.295	0.044	0.022	0.310
Tape strip	0.000	0.000	0.000	0.000
Skin-Biolute S fraction	31.525	6.095	3.048	18.105
Skin-Hexane fraction	24.552	3.674	1.838	15.195
Skin-Aqueous fraction	0.000	0.000	0.000	0.000
Total in skin	55.975	5.566	2.783	33.300

Appendix 14

Absorption of dinitrochlorobenzene

Species . . . . . Balb/C Mouse Absorption system . . . . . Static

Dose and vehicle . . . . . 125μg/cm^2 in propylene glycol(25μl/cm^2) Occlusion . . . . . no

Study with mice pretreated with buthionine sulfoximine (BSO).

Material absorbed into the receptor fluid.								
BSO treated mice mean ± SD, sem (n=4), n is for 4 individual skins.							control mice mean of 2	
Time (hours)	DNCB μg/cm^2	SD	sem	Conjugated DNCB μg cm^2	SD	sem	DNCB μg/cm^2	conjugated DNCB μg/cm^2
2	0.725	0.234	0.117	1.886	0.275	0.137	0.616	0.843
4	3.168	1.596	0.798	3.854	0.432	0.216	1.997	2.823
6	7.514	2.618	1.309	5.632	0.708	0.354	5.722	4.371
12	22.715	6.842	3.421	8.117	0.174	0.087	16.789	7.006
24	36.115	8.048	4.024	11.461	2.568	1.284	30.516	13.785

Disposition of remaining material after 24 hours				
	BSO treated mice mean ± SD, sem (n=6)			Control mice mean of 2
	DNCB μg cm^2	SD	sem	DNCB μg/cm^2
Wash	19.035	6.546	3.273	17.400
Filter	5.243	2.368	1.184	4.150
Donor cell	3.083	2.663	1.331	1.530
Tape strip	0.000	0.000	0.000	0.000
Skin-Biolute S fraction	41.005	10.015	5.007	75.730
Skin-Hexane fraction	29.887	8.598	4.299	15.545
Skin-Aqueous fraction	0.000	0.000	0.000	0.000
Total in skin	70.885	3.662	10831	91.275

Appendix 15

Absorption of dinitrochlorobenzene

Species . . . . . Balb/C Mouse Absorption system . . . . . Flow-through

Dose and vehicle . . . . . 500μg/cm^2 in acetone (25μl/cm^2) Occlusion . . . . . no

Material absorbed into the receptor fluid. mean ± SD, sem (n=5), n is for 5 individual skins.						
Time (hours)	DNCB (μg/cm^2)	SD	sem	Conjugated DNCB (μg/cm^2)	SD	sem
2	0.507	0.129	0.057	1.725	0.731	0.327
4	1.735	0.485	0.217	4.279	1.485	0.664
6	3.345	0.917	0.409	6.745	2.026	0.906
8	5.266	1.280	0.572	8.882	2.499	1.118
10	7.358	1.626	0.727	10.877	3.069	1.372
12	9.949	1.972	0.882	13.107	3.939	1.762
14	13.063	2.368	1.059	14.998	4.790	2.142
16	16.337	2.961	1.324	16.430	5.489	2.455
18	19.767	3.678	1.645	17.559	6.006	2.686
20	23.683	4.577	2.047	18.498	6.394	2.859
22	27.819	5.365	2.520	19.323	6.669	2.983
24	32.573	6.734	3.011	20.121	6.894	3.083

Disposition of remaining material after 24 hours mean ± SD, sem (n=5), n is for 5 individual skins.			
	DNCBμg/cm^2	SD	sem
Wash	28.154	4.997	2.235
Filter	99.380	37.364	16.709
Donor cell	11.090	7.930	3.546
Tape strip	0.000	0.000	0.000
Skin Biolute S fraction	77.280	26.654	11.92
Skin-Hexane fraction	175.690	39.420	17.629
Skin-Aqueous fraction	2.722	0.596	0.266
Total in skin	255.692	22.415	10.024

Appendix 16

Absorption of dinitrochlorobenzene

Species . . . . . Balb/C Mouse Absorption system . . . . . Flow-through

Dose and vehicle . . . . . 500μg/cm^2 in propylene glycol(25μl/cm^2) Occlusion . . . . . no

Material absorbed into the receptor fluid. mean ± SD, sem (n=6), n is for 6 individual skins.						
Time (hours)	DNCB (μg/cm^2)	SD	sem	Conjugated DNCB (μg/cm^2)	SD	sem
2	0.415	0.119	0.049	1.209	0.501	0.205
4	1.654	0.450	0.184	3.165	1.144	0.467
6	4.042	1.429	0.584	4.712	1.911	0.780
8	6.867	2.325	0.949	5.911	2.566	1.048
10	10.348	3.078	1.257	7.008	3.227	1.317
12	12.479	3.437	1.403	8.193	3.875	1.582
14	14.942	4.047	1.652	9.215	4.424	1.806
16	25.826	4.945	2.020	10.143	4.885	1.994
18	31.906	5.618	2.294	11.063	5.344	2.182
20	38.258	6.211	2.536	11.928	5.820	2.376
22	45.204	7.079	2.865	12.828	6.355	2.594
24	53.253	7.902	3.226	13.860	7.051	2.879

Disposition of remaining material after 24 hours mean ± SD, sem (n=6), n is for 6 individual skins.			
	DNCBμg/cm^2	SD	sem
Wash	54.030	11.029	4.503
Filter	19.923	6.075	2.480
Donor cell	3.622	2.598	1.060
Tape strip	0.000	0.000	0.000
Skin-Biolute S fraction	101.207	51.647	21.085
Skin-Hexane fraction	161.625	36.212	14.783
Skin-Aqueous fraction	4.412	0.982	0.401
Total in skin	267.244	32.639	13.325

Appendix 17

Absorption of dinitrochlorobenzene

Species . . . . . Balb/C Mouse Absorption system . . . . . Static

Dose and vehicle . . . . . 500μg/cm^2 in acetone(25μl/cm^2) Occlusion . . . . . no

Material absorbed into the receptor fluid. mean ± SD, sem (n=6), n is for 6 individual skins.						
Time (hours)	DNCB (μg/cm^2)	SD	sem	Conjugated DNCB (μg/cm^2)	SD	sem
2	2.514	1.319	0.539	2.329	0.684	0.279
4	10.733	6.312	2.577	5.573	1.574	0.643
6	22.794	10.076	4.114	9.460	2.193	0.895
12	49.860	22.761	9.292	14.491	2.386	0.974
24	96.309	44.623	18.217	19.489	5.563	2.271

Disposition of remaining material after 24 hours mean + SD, sem (n=6), n is for 6 individual skins.			
	DNCBμg cm^2	SD	sem
Wash	60.965	34.018	13.888
Filter	28.337	6.032	2.463
Donor cell	1.925	1.289	0.527
Tape strip	0.000	0.000	0.000
Skin-Biolute S fraction	103.218	45.058	18.395
Skin-Hexane fraction	164.350	11.863	4.843
Skin-Aqueous fraction	4.965	0.867	0.354
Total in skin	272.533	51.510	21.029

Appendix 18

Absorption of dinitrochlorobenzene

Species . . . . . Balb/C Mouse Absorption system . . . . . Static

Dose and vehicle . . . . . 500μg/cm^2 in propylene glycol(25μl/cm^2) Occlusion . . . . . no

Material absorbed into the receptor fluid. mean ± SD, sem (n=6), n is for 6 individual skins.						
Time (hours)	DNCB (μg/cm^2)	SD	sem	Conjugated DNCB (μg/cm^2)	SD	sem
2	2.945	2.563	1.047	1.833	0.932	0.381
4	12.685	9.706	3.963	3.967	1.687	0.689
6	25.016	14.839	6.058	6.856	2.661	1.086
12	64.143	32.431	13.240	12.523	5.406	2.207
24	121.773	40.85	16.675	15.569	7.212	2.944

Disposition of remaining material after 24 hours mean ± SD, sem (n=6), n is for 6 individual skins.			
	DNCBμg cm^2	SD	sem
Wash	53.126	12.079	4.932
Filter	17.932	6.075	2.480
Donor cell	3.622	2.596	1.060
Tape strip	0.000	0.000	0.000
Skin-Biolute S fraction	101.207	51.647	21.085
Skin-Hexane fraction	161.625	36.212	14.783
Skin-Aqueous fraction	4.427	0.960	0.392
Total in skin	267.259	16.348	6.674

Appendix 19

Absorption of dinitrochlorobenzene

Species . . . . . neonatal Wistar rat Absorption system . . . . . Flow-through

Dose and vehicle . . . . . 25μg/cm^2 in acetone (25μl/cm^2) Occlusion . . . . . no

Material absorbed into the receptor fluid. mean ± SD, sem (n=6), n is for 6 individual skins.						
Time (hours)	DNCB (μg/cm^2)	SD	sem	Conjugated DNCB (μg/cm^2)	SD	sem
2	0.034	0.017	0.007	0.085	0.051	0.021
4	0.085	0.017	0.007	0.340	0.153	0.016
6	0.153	0.034	0.013	0.884	0.204	0.020
12	0.357	0.051	0.021	2.261	0.323	0.136
18	0.527	0.068	0.027	3.621	0.493	0.204
24	0.629	0.068	0.027	4.267	0.561	0.238

Disposition of remaining material after 24 hours mean ± SD, sem (n=6), n is for 6 individual skins.			
	DNCBμg/cm^2	SD	sem
Filter	6.154	1.683	0.687
Wash	2.397	1.598	0.652
Skin Biolute S fraction	3.213	1.139	0.465

Appendix 20

Absorption of dinitrochlorobenzene

Species . . . . . neonatal Wistar rat Absorption system . . . . . Flow-through

Dose and vehicle . . . . . 25μg/cm^2 in acetone (25μl/cm^2) Occlusion . . . . . yes

Material absorbed into the receptor fluid. mean ± SD, sem (n=6), n is for 6 individual skins.						
Time (hours)	DNCB (μg/cm^2)	SD	sem	Conjugated DNCB (μg/cm^2)	SD	sem
2	0.119	0.034	0.014	1.530	0.476	0.194
4	0.306	0.119	0.012	3.434	0.986	0.403
6	0.425	0.170	0.016	4.437	1.207	0.493
12	0.629	0.306	0.119	7.871	2.108	0.861
18	0.697	0.340	0.136	9.707	2.516	1.027
24	0.714	0.340	0.136	10.302	2.720	1.119

Disposition of remaining material after 24 hours mean ± SD, sem (n=6), n is for 6 individual skins.			
	DNCBμg/cm^2	SD	sem
Parafilm	1.581	0.510	0.208
Wash	2.890	2.278	0.929
Skin Biolute S fraction	3.740	2.380	0.972

Appendix 21

Absorption of dinitrochlorobenzene

Species . . . . . neonatal Wistar rat Absorption system . . . . . Flow-through

Dose and vehicle . . . . . 125μg/cm^2 in acetone (25μl/cm^2) Occlusion . . . . . no

Material absorbed into the receptor fluid. mean ± SD, sem (n=6), n is for 6 individual skins.						
Time (hours)	DNCB (μg/cm^2)	SD	sem	Conjugated DNCB (μg/cm^2)	SD	sem
2	0.034	0.017	0.007	0.153	0.085	0.035
4	0.119	0.034	0.014	0.612	0.272	0.111
6	0.391	0.119	0.049	1.853	0.544	0.222
12	1.666	0.408	0.167	6.069	0..680	0.278
18	3.006	1.020	0.416	11.186	1.547	0.632
24	3.706	0.969	0.394	13.107	1.598	0.652

Disposition of remaining material after 24 hours mean ± SD, sem (n=6), n is for 6 individual skins.			
	DNCBμg/cm^2	SD	sem
Filter	54.094	10.557	4.301
Wash	5.100	2.210	0.901
Skin Biolute S fraction	20.128	8.806	3.587

Appendix 22

Absorption of dinitrochlorobenzene

Species . . . . . neonatal Wistar rat Absorption system . . . . . Flow-through

Dose and vehicle . . . . . 125μg/cm^2 in acetone (25μl/cm^2) Occlusion . . . . . yes

Material absorbed into the receptor fluid. mean ± SD, sem (n=6), n is for 6 individual skins.						
Time (hours)	DNCB (μg/cm^2)	SD	sem	Conjugated DNCB (μg/cm^2)	SD	sem
2	0.255	0.102	0.042	2.023	0.306	0.125
4	1.853	1.139	0.465	7.004	2.533	1.034
6	4.250	2.431	0.992	12.198	4.505	1.839
12	11.135	5.423	2.218	29.019	8.636	3.526
18	13.413	6.273	2.561	36.686	10.659	4.352
24	14.093	6.545	3.850	39.321	11.067	4.518

Disposition of remaining material after 24 hours mean ± SD, sem (n=6), n is for 6 individual skins.			
	DNCBμg/cm^2	SD	sem
Parafilm	6.868	3.774	1.541
Wash	1.479	0.0.51	0.021
Skin-Biolute S fraction	28.951	16.184	6.607

Appendix 23

Absorption of dinitrochlorobenzene

Species . . . . . Wistar rat (26 days old) Absorption system . . . . . Flow-through

Dose and vehicle . . . . . 25μg/cm^2 in acetone (25μl/cm^2) Occlusion . . . . . no

Material absorbed into the receptor fluid. mean ± SD, sem (n=6), n is for 6 individual skins.						
Time (hours)	DNCB (μg/cm^2)	SD	sem	Conjugated DNCB (μg/cm^2)	SD	sem
2	3.764	0.353	0.144	1.137	0.154	0.063
4	4.763	0.522	0.213	1.413	0.215	0.088
6	4.947	0.615	0.251	1.552	0.261	0.107
12	5.193	0.645	0.263	1.936	0.737	0.301
[illegible]	[illegible]	0.630	0.257	2.013	0.876	0.358
24	5.393	0.630	0.257	2.013	0.876	0.358

Disposition of remaining material after 24 hours mean ± SD, sem (n=6), n is for 6 individual skins.			
	DNCBμg cm^2	SD	sem
Filter	3.011	0.737	0.301
Wash	0.922	0.784	0.320
Skin-Biolute S fraction	1.905	0.876	0.358

Appendix 24

Absorption of dinitrochlorobenzene

Species . . . . . Wistar rat (26 days old) Absorption system . . . . . Flow-through

Dose and vehicle . . . . . 25μg/cm^2 in acetone (25μl/cm^2) Occlusion . . . . . yes

Material absorbed into the receptor fluid. mean ± SD, sem (n=6), n is for 6 individual skins.						
Time (hours)	DNCB (μg cm^2)	SD	sem	Conjugated DNCB (μg/cm^2)	SD	sem
2	4.394	1.214	0.496	2.089	0.446	0.182
4	5.070	1.629	0.665	2.643	0.722	0.294
6	-	-	-	-	-	-
12	5.485	1.905	0.778	4.071	1.643	0.671
18	-	-	-	-	-	-
24	5.731	2.612	1.066	4.732	1.874	0.765

Disposition of remaining material after 24 hours mean ± SD, sem (n=6), n is for 6 individual skins.			
	DNCBμg/cm^2	SD	sem
Parafilm	0.891	0.568	0.232
Wash	1.752	0.737	0.301
Skin-Biolute S fraction	6.407	4.747	1.938

Appendix 25

Absorption of dinitrochlorobenzene

Species . . . . . Wistar rat (26 days old) Absorption system . . . . . Flow-through

Dose and vehicle . . . . . 125μg/cm^2 in acetone (25μl/cm^2) Occlusion . . . . . no

Material absorbed into the receptor fluid. mean ± SD, sem (n=4), n is for 4 individual skins.						
Time (hours)	DNCB (μg cm^2)	SD	sem	Conjugated DNCB (μg/cm^2)	SD	sem
2	12.353	9.987	4.994	1.767	0.369	0.185
4	22.785	11.016	5.508	2.597	0.369	0.185
6	30.083	9.142	4.571	3.073	0.353	0.177
12	41.099	6.146	3.073	3.912	0.568	0.284
18	42.49	6.007	3.004	4.254	0.580	0.290
24	42.62	6.007	3.004	4.254	0.580	0.290

Disposition of remaining material after 24 hours mean ± SD, sem (n=4), n is for 4 individual skins.			
	DNCBμg/cm^2	SD	sem
Filter	18.514	6.959	3.479
Wash	6.484	4.440	2.220
Skin-Biolute S fraction	13.182	6.622	3.311

Appendix 26

Absorption of dinitrochlorobenzene

Species . . . . . Wistar rat (26 days old) Absorption system . . . . . Flow-through

Dose and vehicle . . . . . 125μg/cm^2 in acetone (25μl/cm^2) Occlusion . . . . . yes

Material absorbed into the receptor fluid. mean ± SD, sem (n=6), n is for 6 individual skins.						
Time (hours)	DNCB (μg/cm^2)	SD	sem	Conjugated DNCB (μg/cm^2)	SD	sem
2	20.526	7.313	2.986	3.149	0.722	0.295
4	32.941	12.737	5.199	4.486	1.306	0.533
6	-	-	-	-	-	-
12	52.438	22.893	9.346	7.390	1.536	0.627
18	-	-	-	-	-	-
24	55.418	24.567	10.129	8.542	2.658	1.085

Disposition of remaining material after 24 hours mean ± SD, sem (n=6), n is for 6 individual skins.			
	DNCBμg/cm^2	SD	sem
Parafilm	2.673	2.228	0.919
Wash	8.097	4.655	1.900
Skin Biolute S fraction	29.959	10.371	4.234

Appendix 27

Absorption of dinitrochlorobenzene

Species . . . . . Domestic pig Absorption system . . . . . Flow-through

Dose and vehicle . . . . . 25μg/cm^2 in acetone (25μl/cm^2) Occlusion . . . . . no

Material absorbed into the receptor fluid. mean ± SD, sem (n=5), n is for 5 individual skins.						
Time (hours)	DNCB (μg/cm^2)	SD	sem	Conjugated DNCB (μg/cm^2)	SD	sem
2	0.562	0.431	0.176	2.774	1.012	0.413
4	1.143	0.731	0.298	4.967	1.143	1.223
6	1.293	0.862	0.352	5.529	1.068	0.436
12	1.368	0.862	0.352	5.923	0.596	0.390
18	1.385	0.862	0.352	6.111	1.012	0.413
24	1.389	0.862	0.352	6.167	1.031	0.421

Disposition of remaining material after 24 hours mean ± SD, sem (n=5), n is for 5 individual skins.			
	DNCBμg cm^2	SD	sem
Filter	8.491	0.806	0.329
Wash	2.193	1.087	0.444
Skin-Biolute S fraction	1.687	0.299	0.122

Appendix 28

Absorption of dinitrochlorobenzene

Species . . . . . Domestic pig Absorption system . . . . . Flow-through

Dose and vehicle . . . . . 25μg/cm^2 in acetone (25μl/cm^2) Occlusion . . . . . yes

Material absorbed into the receptor fluid. mean ± SD, sem (n=6), n is for 6 individual skins.						
Time (hours)	DNCB (μg/cm^2)	SD	sem	Conjugated DNCB (μg/cm^2)	SD	sem
2	0.412	0.675	0.275	1.443	0.806	0.329
4	0.787	1.143	0.467	4.105	2.774	1.133
6	0.862	1.259	0.513	5.061	3.243	1.324
12	-	-	-	-	-	-
18	0.993	1.368	0.559	6.542	4.161	1.699
24	2.549	1.781	0.727	7.011	4.668	1.906

Disposition of remaining material after 24 hours mean ± SD, sem (n=6), n is for 6 individual skins.			
	DNCBμg/cm^2	SD	sem
Parafilm	0.956	0.932	0.383
Wash	1.762	2.006	0.819
Skin Biolute S fraction	6.055	4.630	1.890

Appendix 29

Absorption of dinitrochlorobenzene

Species . . . . . Domestic pig Absorption system . . . . . Flow-through

Dose and vehicle . . . . . 125μg/cm^2 in acetone (25μl/cm^2) Occlusion . . . . . no

Material absorbed into the receptor fluid. mean ± SD, sem (n=5), n is for 5 individual skins.						
Time (hours)	DNCB (μg/cm^2)	SD	sem	Conjugated DNCB (μg/cm^2)	SD	sem
2	1.425	2.118	0.865	3.093	1.575	0.643
4	3.505	4.461	1.821	6.148	1.987	0.811
6	5.286	5.923	2.418	7.798	2.137	0.872
12	1.158	8.723	3.459	10.985	2.830	1.156
18	14.265	9.204	3.757	12.803	2.999	1.224
24	16.371	9.335	3.810	13.924	4.703	1.920

Disposition of remaining material after 24 hours mean ± SD, sem (n=5), n is for 5 individual skins.			
	DNCBμg/cm^2	SD	sem
Filter	44.631	9.709	3.964
Wash	12.522	5.361	2.189
Skin-Biolute S fraction	18.014	8.229	3.359

Appendix 30

Absorption of dinitrochlorobenzene

Species . . . . . Domestic pig Absorption system . . . . . Flow-through

Dose and vehicle . . . . . 125μg/cm^2 in acetone (25μl/cm^2) Occlusion . . . . . yes

Material absorbed into the receptor fluid. mean ± SD, sem (n=5), n is for 5 individual skins.						
Time (hours)	DNCB (μg cm^2)	SD	sem	Conjugated DNCB (μg/cm^2)	SD	sem
2	4.443	6.804	3.043	2.324	1.443	0.645
4	25.024	26.562	11.879	9.148	2.587	1.157
6	35.953	27.068	12.105	14.302	2.081	0.931
12	-	-	-	-	-	-
18	42.626	24.462	10.939	19.045	2.081	0.931
24	43.357	24.275	10.856	20.451	2.287	1.023

Disposition of remaining material after 24 hours mean ± SD, sem (n=5), n is for 5 individual skins.			
	DNCBμg/cm^2	SD	sem
Parafilm	2.812	3.130	1.399
Wash	5.155	5.192	2.322
Skin Biolute S fraction	41.164	5.379	2.406

Appendix 31

Absorption of dinitrochlorobenzene

Species . . . . . Human (Abdomen, female) Absorption system . . . . . Flow-through

Dose and vehicle . . . . . 25μg/cm^2 in acetone (25μl/cm^2) Occlusion . . . . . no

Material absorbed into the receptor fluid. mean ± SD, sem (n=6), n is for 6 cells.						
Time (hours)	DNCB (μg cm^2)	SD	sem	Conjugated DNCB (μg/cm^2)	SD	sem
2	0.277	0.365	0.149	0.964	0.146	0.059
4	0.569	0.701	0.286	2.088	0.175	0.072
6	0.657	0.774	0.316	2.643	0.204	0.083
12	0.701	0.788	0.322	2.993	0.263	0.107
18	0.759	0.788	0.322	3.139	0.292	0.119
24	0.788	0.803	0.328	3.299	0.307	0.125

Disposition of remaining material after 24 hours mean ± SD, sem (n=6), n is for 6 cells.			
	DNCBμg/cm^2	SD	sem
Filter	-	-	-
Wash	0.803	0.496	0.203
Skin Biolute S fraction	2.102	0.701	0.286

Appendix 32

Absorption of dinitrochlorobenzene

Species . . . . . Human (Abdomen, female) Absorption system . . . . . Flow-through

Dose and vehicle . . . . . 25μg/cm^2 in acetone (25μl/cm^2) Occlusion . . . . . yes

Material absorbed into the receptor fluid. mean ± SD, sem (n=6), n is for 6 cells.						
Time (hours)	DNCB (μg cm^2)	SD	sem	Conjugated DNCB (μg/cm^2)	SD	sem
2	1.591	1.971	0.805	1.431	0.365	0.149
4	2.497	2.292	0.936	2.511	0.701	0.286
6	2.789	2.321	0.948	3.446	0.628	0.256
12	2.920	2.321	0.948	4.438	0.657	0.268
18	-	-	-	-	-	-
24	2.949	2.321	0.948	5.343	0.919	0.356

Disposition of remaining material after 24 hours mean ± SD, sem (n=6), n is for 6 cells.			
	DNCBμg/cm^2	SD	sem
Parafilm	2.351	1.548	0.632
Wash	0.788	0.599	0.244
Skin-Biolute S fraction	1.913	0.715	0.292

Appendix 33

Absorption of dinitrochlorobenzene

Species . . . . . Human (Abdomen, female) Absorption system . . . . . Flow-through

Dose and vehicle . . . . . 125μg/cm^2 in acetone (25μl/cm^2) Occlusion . . . . . no

Material absorbed into the receptor fluid. mean ± SD, sem (n=6), n is for 6 cells.						
Time (hours)	DNCB (μg/cm^2)	SD	sem	Conjugated DNCB (μg/cm^2)	SD	sem
2	1.431	2.453	1.001	1.299	0.336	0.137
4	3.475	2.920	1.192	3.241	0.175	0.072
6	5.825	3.051	1.246	4.380	0.277	0.113
12	10.599	3.475	1.419	7.125	0.847	0.346
18	11.359	3.460	1.413	8.658	1.402	0.572
24	11.882	3.218	1.314	9.400	1.679	0.685

Disposition of remaining material after 24 hours mean ± SD, sem (n=6), n is for 6 cells			
	DNCBμg/cm^2	SD	sem
Filter	-	-	-
Wash	4.108	1.865	0.762
Skin Biolute S fraction	7.561	4.412	1.801

Appendix 34

Absorption of dinitrochlorobenzene

Species . . . . . Human (Abdomen, female) Absorption system . . . . . Flow-through

Dose and vehicle . . . . . 125μg/cm^2 in acetone (25μl/cm^2) Occlusion . . . . . yes

Material absorbed into the receptor fluid. mean ± SD, sem (n=6), n is for 6 cells.						
Time (hours)	DNCB (μg cm^2)	SD	sem	Conjugated DNCB (μg/cm^2)	SD	sem
2	9.213	8.030	3.278	2.146	0.715	0.292
4	22.382	16.863	6.884	4.234	1.124	0.459
6	30.66	17.359	7.087	6.132	1.358	0.554
12	40.895	14.615	5.966	9.446	1.153	0.471
18	-	-	-	-	-	-
24	44.676	12.687	5.179	11.592	1.402	0.572

Disposition of remaining material after 24 hours mean ± SD, sem (n=6), n is for 6 cells.			
	DNCBμg/cm^2	SD	sem
Parafilm	11.344	8.935	3.648
Wash	3.460	1.883	0.768
Skin Biolute S fraction	14.206	6.380	2.605